



# **Development of Functionalized Polymers using Bis(phenoxyimine)titanium and alpha-Diimine Nickel(II) Catalysts for the Production of New Polyolefin Architectures**

by Amelia Marie Anderson

---

This thesis/dissertation document has been electronically approved by the following individuals:

Coates, Geoffrey (Chairperson)

Collum, David B (Minor Member)

Wolczanski, Peter Thomas (Minor Member)

DEVELOPMENT OF FUNCTIONALIZED POLYMERS USING  
BIS(PHENOXYIMINE)TITANIUM AND  $\alpha$ -DIIMINE NICKEL(II) CATALYSTS  
FOR THE PRODUCTION OF NEW POLYOLEFIN ARCHITECTURES

A Dissertation

Presented to the Faculty of the Graduate School  
of Cornell University

In Partial Fulfillment of the Requirements for the Degree of  
Doctor of Philosophy

by

Amelia Marie Anderson

August 2010

© 2010 Amelia Marie Anderson

DEVELOPMENT OF FUNCTIONALIZED POLYMERS USING  
BIS(PHENOXYIMINE)TITANIUM AND  $\alpha$ -DIIMINE NICKEL(II) CATALYSTS  
FOR THE PRODUCTION OF NEW POLYOLEFIN ARCHITECTURES

Amelia Marie Anderson, Ph.D.

Cornell University 2010

Decades of research in the area of metal-catalyzed olefin polymerization, since the initial discoveries by Ziegler and Natta in the 1950s, has led to the development of a wide variety of transition metal catalysts as well as numerous polymer architectures. Although early work in the field focused on heterogeneous catalysis, Kaminsky's discovery of the scavenger/activator methylaluminoxane in 1980 facilitated a renaissance in the area of homogeneous catalysts. Today, many commercial polyolefin materials are still limited to linear homopolymers, random copolymers, or blends thereof. Therefore, our efforts have focused on the end-functionalization and random incorporation of polar functional groups into polyolefins to produce polymers with improved properties and more complex architectures than traditional linear polymers.

Initial work in this area focused on the development of well-defined long-chain branched polymers from end-functionalized polypropylene. Although many star polymers have been produced using anionic, cationic and radical methods, semicrystalline polypropylene materials with similar structures from coordination-insertion polymerization were not known. Using a non-living bis(phenoxyimine)titanium catalyst, allyl-terminated syndiotactic polypropylene was produced and utilized in the production of alcohol-, azide- and amine-terminated polymers. These end-functionalized macromolecules were employed in the synthesis of a variety of well-defined branched polymers including star, miktoarm star and H-

polymers. In an effort to produce branched polyolefin materials with high molecular weight, a norbornene-terminated polymer was synthesized from the allyl-terminated syndiotactic polypropylene. Using ring-opening metathesis polymerization, a number of high molecular weight polypropylene comb polymers were produced. All of the branched, syndiotactic polypropylene materials were analyzed further in an effort to related branching with observed polymer properties.

To produce polyolefins with improved properties, a series of random copolymers derived from propylene and a polar, hydrogen bonding monomer were produced using Ni(II)  $\alpha$ -diimine catalysts. By varying the reaction temperature, hydrogen bonding polypropylene materials with a range of microstructures were produced. At high reaction temperatures, regioirregular, amorphous polypropylene was obtained, whereas, decreasing reaction temperature lead to highly regioregular, isotactic polypropylene. Utilizing the living nature of the Ni(II)  $\alpha$ -diimine catalysts, a series of triblock copolymers containing hydrogen bonding moieties in the midblock were also produced. The mechanical properties of all materials were investigated and generally observed to improve upon incorporation of small amounts (~1%) of the ureidopyrimidinone. For the branched and hydrogen bonding polymer reported herein, functionalization of polypropylene allowed for the synthesis of new polyolefin architectures.

## BIOGRAPHICAL SKETCH

Amelia Marie Anderson was born on October 31<sup>st</sup>, 1982 in Olivia, MN to Rob and Linda Anderson. She was raised in the booming metropolis of Renville, MN (population = 1,323) with her older sister and two older brothers. Amelia attended elementary, middle and high school in the Belview Danube Renville Sacred Heart (BDRSH) school district. Even at a young age, Amelia enjoyed all of her science and math classes, however, junior year of high school was when she became particularly fascinated with chemistry. Amelia's chemistry teacher, Mr. Sinner, deserves a lot of credit for fostering her love of chemistry. She particularly enjoyed his chemistry songs including "What's a mole?" and "The Stoichiometry Blues". Amelia graduated first in her class from Renville County West High School, formerly BDRSH, in 2001.

Amelia began her college career in the fall of 2001 at Hamline University as chemistry major. Although her course work was thoroughly enjoyable, Amelia needed to explore whether or not a career in the lab was right for her. In the summer of 2003, she was accepted into the National Science Foundation Summer Research Program in Solid State Chemistry. As a part of the program, she traveled to Clemson University for a week-long tutorial on solid-state chemistry. Following the symposium, she worked as an undergraduate research assistant at the University of Minnesota in the lab of Dr. Michael Ward working on the synthesis of oligothiophenes for organic semiconductors. Amelia continued her research in Dr. Ward's group through the spring of 2005 as a part of the University of Minnesota MRESC REU program as well as for Hamline University senior research credit.

Amelia graduated from Hamline University in the spring of 2005 and moved to Ithaca, NY later that summer to begin her graduate studies at Cornell University. In late 2005, she joined the research group of Professor Geoffrey W. Coates and began working on the development of new polyolefin materials. Specifically, Amelia was

charged with the task of synthesizing a variety of different polyolefin materials bearing polar functional groups for the production of advanced polymer architectures. Through this work, she collaborated with Professor Rufina Alamo at the Florida State University to study the effects of polyolefin structure on polymer rheology. After finishing at Cornell University in July 2010, Amelia will head back to the Midwest to begin her career as an Assistant Professor of Chemistry at Ohio Northern University.

*Dedicated to my parents.*

## ACKNOWLEDGMENTS

A number of people were instrumental in my success and survival over the last five years. Certainly top of the list is my advisor, Dr. Geoffrey Coates. In addition to providing me with the resources necessary to explore the field of olefin polymerization, he was a constant source of knowledge as well as new and interesting ideas. I appreciate all of his advice and guidance and would not be moving on to my new career without his support. I must also thank Dr. Peter Wolczanski and Dr. David Collum for serving on my committee. They were both a source of interesting and insightful questions during my candidacy exam, which definitely contributed to my development as a chemist. Dr. Roger Loring also deserves my gratitude for supervising my work as a general chemistry teaching assistant and for writing countless letters of recommendation. In addition, I must also thank the rest of the faculty and staff of Department of Chemistry and Chemical Biology for providing a supportive research environment.

Several different groups deserve acknowledgement for their generous funding support over the years. First, I must thank the Department of Chemistry and Chemical Biology for supporting me as a teaching assistant during my first two years as a graduate student. Both the Mitsubishi Chemical Company and the Infinuem Corporation must also be thanked for their support at different points during my time at Cornell. Finally and most importantly, I would like to thank the National Science Foundation for their support through the Grant Opportunities for Academic Liaisons with Industry (GOALI) program. Through this opportunity, beneficial collaborations were established with Dr. Rufina Alamo of Florida State University and her students Carolina Ruiz and Syed Abdullah as well as Dr. Julie Kornfield of the California Institute of Technology and her student Iman Hajimorad.

I have to thank all of the wonderful people who I worked with over the years in the Coates groups. Dr. Greg Domski and Dr. Jeff Rose were both crucial in my development as a chemist in my formative years in the group. In addition to being a wealth of knowledge, Jeff and Greg were both great lab mates. I definitely cannot thoroughly express my appreciation for the guidance of both of these fantastic scientists. When Jeff and Greg left S. T. Olin 562 forever, it was Dr. Joe Edson who was put up with all of my questions. Joe was always a source of great ideas and I was lucky to have such an intelligent colleague and friend in the group.

There are a number of other Coates' group members who deserve my thanks for their support and friendship for the past five years. Hisashi Ohtaki has been a fantastic lab mate over the last two years. I could not have asked for a more considerate or thoughtful person to share my lab space. Nick Robertson was always there to put a positive spin on things when I needed it. In addition to being an excellent addition to 562 for the last few months of my graduate career, I have to thank Dr. Kevin Noonan for proofreading and correcting almost my entire thesis. Because of this, I will have to forgive him for beating me in the "eyewash station battle of 2010". I also have to thank Syed "Taz" Ahmed for being a good coffee buddy the last couple years. He was always a great person to talk with when I needed to vent. Both Dr. Brian Long and Pasquale Iacono also have to be thanked for being supportive and helpful olefin subgroup members.

While at Cornell, I was lucky enough to meet my fiancée, Brad Wile. I can without a doubt say that my last three years of graduate school would not have been nearly as enjoyable without him. Brad's weekend visits were always my favorite part of the week and definitely gave me something to look forward to. In addition to being fun to hang out with, Brad was always around with shoulder to cry on when I needed it. I certainly would not be where I am today without his love and support.

Last but certainly not least, I have to thank my mom and dad for being the best parents anyone could ever want. I feel very fortunate to have two of the most caring and loving people for parents. They have always been my biggest supporters and have been there for me with encouraging words whenever I needed it. I know that I would not be the person that I am today without them and could never thank them enough for everything they done for me over the years.

## TABLE OF CONTENTS

BIOGRAPHICAL SKETCH.....	iii
DEDICATION.....	v
ACKNOWLEDGEMENTS.....	vi
LIST OF FIGURES .....	xiv
LIST OF SCHEMES.....	xx
LIST OF TABLES.....	xxiii

<b>Chapter 1</b> Living Transition Metal Catalyzed Polymerization: Polyolefin Synthesis and New Polymer Architectures .....	1
1.1 Introduction .....	2
1.2 Living Olefin Polymerization.....	4
1.2.1 Poly(1-hexene).....	4
1.2.2 Polypropylene .....	5
1.2.3 Polyethylene.....	6
1.2.4 Polyolefins from Conjugated Dienes, Cyclic Olefins and Polar Monomers.....	7
1.2.5 Criteria for Living Polymerization.....	8
1.3 Early Metal Olefin Polymerization Catalysts.....	9
1.3.1 Vanadium Acetylacetonate Catalysts.....	9
1.3.2 Metallocene and Half-Metallocene Catalysts.....	12
1.3.3 Monocyclopentadienyl-Amido Catalysts .....	15
1.3.4 Monocyclopentadienylzirconium Amidinate Catalysts .....	20
1.3.5 Catalysts Bearing Diamido Ligands.....	27
1.3.6 Catalysts Bearing Diamido Ligands with Neutral Donors.....	29

1.3.7 Amine-phenolate Titanium and Zirconium Catalysts .....	31
1.3.8 Titanium Catalysts Bearing Tridentate Aminodiols.....	36
1.3.9 Titanium Catalysts for Styrene Polymerization.....	37
1.3.10 Bis(phenoxyimine)titanium Catalysts .....	38
1.3.11 Bis(phenoxyketimine)titanium Catalysts.....	48
1.3.12 Bis(pyrrolide-imine)titanium Catalysts .....	51
1.3.13 Bis(indolide-imine)titanium Catalysts.....	53
1.3.14 Bis(enaminoketonato)titanium Catalysts.....	53
1.3.15 Bis(phosphanylphenoxy)titanium Catalysts.....	56
1.3.16 Catalysts Supported by $sp^2$ and $sp^3$ Carbon Donors.....	58
1.3.17 Aminopyridinatozirconium Catalysts.....	60
1.3.18 Tris(pyrazolyl)borate Catalysts.....	61
1.3.19 Bis(dimethylamidopyridine)zirconium Catalysts .....	62
1.4 Non-Group 4 Early Metal Polymerization Catalysts.....	62
1.5 Rare-Earth Metal Catalysts .....	66
1.6 Late Metal Olefin Polymerization Catalysts .....	68
1.6.1 Nickel and Palladium $\alpha$ -Diimine Catalysts .....	68
1.6.2 Nickel $\alpha$ -Keto- $\beta$ -Diimine Catalysts .....	86
1.6.3 Other Nickel Catalysts.....	88
1.6.4 Other Palladium Catalysts .....	91
1.6.5 Monocyclopentadienyl Cobalt Catalysts.....	92
1.7 Outlook and Summary .....	
References.....	95

<b>Chapter 2</b>	Synthesis and Functionalization of Allyl-Terminated Syndiotactic Polypropylene.....	111
2.1	Introduction .....	112
2.2	Results and Discussion.....	118
2.2.1	Propylene Polymerization with <b>2.2</b> /MAO .....	118
2.2.2	Synthesis of Dibromo-Terminated <i>s</i> PP .....	119
2.2.3	Synthesis and Ring Opening of Epoxide-Terminated <i>s</i> PP .....	120
2.2.4	Synthesis of Hydroxyl-Terminated <i>s</i> PP .....	122
2.2.5	Reaction of Hydroxyl-Terminated <i>s</i> PP with Acid Chlorides ..	125
2.2.6	Synthesis of Tosyl-Terminated <i>s</i> PP .....	127
2.2.7	Synthesis of Azide-Terminated <i>s</i> PP .....	128
2.2.8	Click Chemistry and Azide-Terminated <i>s</i> PP .....	131
2.2.9	Synthesis of Amine-Terminated <i>s</i> PP .....	132
2.2.10	Reaction of Amine-Terminated <i>s</i> PP with Acid Chlorides.....	133
2.3	Conclusions .....	135
2.4	Experimental .....	135
	References.....	143
<b>Chapter 3</b>	Synthesis of Star, Miktoarm Star and H-Polymers from Allyl-Terminated Syndiotactic Polypropylene.....	150
3.1	Introduction .....	151
3.2	Results and Discussion.....	158
3.2.1	Synthesis of Star Polymers with Ester Functional Groups.....	158
3.2.2	Synthesis of Star Polymers with Triazole Functional Groups.	163
3.2.3	Synthesis of Star Polymers with Amide Functional Groups ...	168

3.2.4 Synthesis of <i>sPP-block</i> -PEG.....	172
3.2.5 Synthesis of <i>sPP-block</i> -PEG- <i>block-sPP</i> .....	177
3.2.6 Synthesis of ( <i>sPP</i> ) <sub>2</sub> - <i>block</i> -PEG .....	180
3.2.7 Synthesis of ( <i>sPP</i> ) <sub>2</sub> - <i>block</i> -PEG- <i>block</i> -( <i>sPP</i> ) <sub>2</sub> .....	184
3.3 Conclusions .....	188
3.4 Experimental .....	188
References.....	198

## **Chapter 4** Synthesis and Ring Opening Polymerization of Norbornene-

Terminated Syndiotactic Polypropylene.....	204
4.1 Introduction .....	205
4.2 Results and Discussion.....	210
4.2.1 Synthesis of <i>sPP</i> Macromonomer .....	210
4.2.2 Ruthenium catalyst screening for metathesis polymerization .	217
4.2.3 Polymerization of Norbornene-Terminated <i>sPP</i> with <b>4.3</b> .....	219
4.2.4 Metathesis polymerization with varied catalyst loadings.....	224
4.3 Conclusions .....	229
4.4 Experimental .....	230
References.....	235

## **Chapter 5** Polymerization of Propylene and Ureidopyrimidinone-Functionalized

Olefins using Ni(II) $\alpha$ -Diimine Catalysts.....	243
5.1 Introduction .....	244
5.2 Results and Discussion.....	247

5.2.1 Homopolymerization of Propylene with <b>5.2</b> and <b>5.3</b> .....	247
5.2.2 Propylene and UP <sub>alkene</sub> Copolymerization with <b>5.2</b> /Et <sub>2</sub> AlCl....	252
5.2.3 Propylene and UP <sub>alkene</sub> Copolymerization with <b>5.3</b> /Et <sub>2</sub> AlCl ..	258
5.2.4 Mechanical Testing of Copolymers .....	263
5.2.5 Triblock Copolymer Synthesis and Mechanical Testing.....	267
5.3 Conclusions .....	274
5.4 Experimental .....	274
References.....	278

## LIST OF FIGURES

1.1	Homopolymers of higher $\alpha$ -olefins.....	5
1.2	Polypropylene microstructures.....	6
1.3	Polyethylene morphologies.....	6
1.4	Polymers derived from 1,5-hexadiene polymerization.....	7
1.5	Cyclic olefin homopolymers and copolymers.....	8
1.6	Vanadium catalysts for living olefin polymerization .....	10
1.7	Metallocene-based catalysts for living olefin polymerization .....	13
1.8	Titanium, zirconium and hafnium olefin polymerization catalysts.....	14
1.9	Zirconocene catalysts for living ethylene/norbornene polymerization .....	15
1.10	Monocyclopentadienyl-amido catalyst precursors for living olefin polymerization.....	16
1.11	Monocyclopentadienyl-amido catalyst precursors with increased steric bulk.	18
1.12	Monocyclopentadienyl amidinate catalysts for olefin polymerization.....	21
1.13	Monocyclopentadienyl amidinate catalysts with varying steric bulk.....	22
1.14	Mono- and bimetallic monocyclopentadienyl amidinate complexes.....	26
1.15	Titanium and zirconium complexes bearing diamido ligands .....	28
1.16	Olefin polymerization precatalysts bearing diamido ligands with neutral donors .....	30
1.17	Titanium and zirconium complexes bearing [ONNO] and [ONO] ligands.....	32
1.18	Titanium complexes bearing [ONOO] ligands .....	33
1.19	Titanium and zirconium complexes bearing [ONNO] ligands with increased steric bulk.....	35
1.20	Aminodiol titanium and zirconium complexes.....	37
1.21	Titanium precatalysts for styrene homopolymerization.....	38
1.22	Early bis(phenoxyimine)titanium complexes .....	39

1.23	Bis(phenoxyimine)titanium complexes with varying fluorination patterns ....	41
1.24	Bis(phenoxyimine)titanium complexes with varying substitution patterns ....	42
1.25	Heteroligated bis(phenoxyimine)titanium catalysts .....	43
1.26	Bis(phenoxyimine)titanium complexes with varying substituents .....	45
1.27	Bis(phenoxyketimine)titanium complexes .....	49
1.28	Bis(phenoxyketimine)titanium complexes with varying substituents .....	50
1.29	Bis(pyrrolide-imine)titanium and bis(indolide-imine)titanium complexes.....	52
1.30	Bis(enaminoketonato)titanium catalysts for living olefin polymerization.....	54
1.31	Bis(phosphanylphenoxy)titanium precatalysts for living olefin polymerization.....	57
1.32	Pyridylamidohafnium complexes.....	58
1.33	Hafnium and zirconium precatalysts for living olefin polymerization.....	60
1.34	Aminopyridinatozirconium catalysts.....	61
1.35	Tris(pyrazolyl)borate and bis(dimethylamidopyridine)zirconium olefin polymerization catalysts .....	62
1.36	Non-group 4 early metal olefin polymerization catalysts.....	63
1.37	Vanadium and yttrium polymerization catalysts.....	64
1.38	Group 5 olefin polymerization catalysts.....	65
1.39	Non-group 4 olefin polymerization catalysts.....	66
1.40	Rare-earth metal olefin polymerization catalysts.....	67
1.41	Nickel $\alpha$ -diimine precatalysts for olefin polymerization.....	69
1.42	Nickel $\alpha$ -diimine olefin polymerization catalysts.....	70
1.43	Nickel and palladium olefin polymerization precatalysts.....	71
1.44	Palladium precatalysts for olefin polymerization.....	72
1.45	Nickel $\alpha$ -diimine catalysts derived from cumyl-based ligands .....	76
1.46	Nickel $\alpha$ -diimine precatalyst for olefin polymerization.....	77

1.47	Nickel complexes bearing fluorinated cyclophane ligands .....	78
1.48	POSS supported palladium complex .....	80
1.49	Trinuclear palladium olefin polymerization catalyst.....	81
1.50	Palladium catalysts for olefin polymerization.....	86
1.51	Nickel $\alpha$ -keto- $\beta$ -diimine olefin polymerization catalysts.....	87
1.52	Nickel precatalysts for olefin polymerization.....	89
1.53	Palladium and cobalt precatalysts for olefin polymerization.....	92
2.1	Chemical structures of propylene/polar olefin random copolymer and end-functionalized polypropylene.....	112
2.2	Living and non-living bis(phenoxyimine)titanium catalysts .....	116
2.3	$^1\text{H}$ NMR spectra of <i>sPP</i> -CH <sub>2</sub> CH=CH <sub>2</sub> , <i>sPP</i> -CH <sub>2</sub> CHBrCH <sub>2</sub> Br and <i>sPP</i> -CH <sub>2</sub> CH(O)CH <sub>2</sub> .....	120
2.4	$^1\text{H}$ NMR spectra of <i>sPP</i> -CH <sub>2</sub> CH(OH)CH <sub>2</sub> OH, <i>sPP</i> -CH <sub>2</sub> CH(OH)CH <sub>3</sub> , <i>sPP</i> -(CH <sub>2</sub> ) <sub>3</sub> OH.....	122
2.5	$^1\text{H}$ NMR spectra of <i>sPP</i> -(CH <sub>2</sub> ) <sub>3</sub> OCOC <sub>6</sub> H <sub>5</sub> and <i>sPP</i> -(CH <sub>2</sub> ) <sub>3</sub> OCOCH=CH <sub>2</sub> ...	127
2.6	$^1\text{H}$ NMR spectra of <i>sPP</i> -(CH <sub>2</sub> ) <sub>3</sub> OTs, <i>sPP</i> -(CH <sub>2</sub> ) <sub>3</sub> N <sub>3</sub> and <i>sPP</i> -(CH <sub>2</sub> ) <sub>3</sub> C <sub>2</sub> HN <sub>3</sub> C <sub>6</sub> H <sub>5</sub> .....	130
2.7	IR spectrum of tosyl-terminated syndiotactic polypropylene.....	130
2.8	IR spectrum of azide-terminated syndiotactic polypropylene .....	131
2.9	$^1\text{H}$ NMR spectra of <i>sPP</i> -(CH <sub>2</sub> ) <sub>3</sub> NH <sub>2</sub> and <i>sPP</i> -(CH <sub>2</sub> ) <sub>3</sub> NHCOC <sub>6</sub> H <sub>5</sub> .....	134
2.10	IR spectrum of amine-terminated syndiotactic polypropylene.....	134
3.1	Representative structures of star, miktoarm star and h-polymers .....	151
3.2	Schematic representation of HDPE and LDPE.....	152
3.3	<i>sPP</i> -(CH <sub>2</sub> ) <sub>3</sub> OCOC <sub>6</sub> H <sub>5</sub> (one-arm), ( <i>sPP</i> -(CH <sub>2</sub> ) <sub>3</sub> OCO) <sub>2</sub> C <sub>6</sub> H <sub>4</sub> (two-arms) and ( <i>sPP</i> -(CH <sub>2</sub> ) <sub>3</sub> OCO) <sub>3</sub> C <sub>6</sub> H <sub>3</sub> (three-arms) $^1\text{H}$ NMR spectra .....	161

3.4	GPC chromatogram of $sPP-(CH_2)_3OH$ (one-arm), $(sPP-(CH_2)_3OCO)_2C_6H_4$ (two-arms) and $(sPP-(CH_2)_3OCO)_3C_6H_3$ (three-arms) .....	162
3.5	$sPP-(CH_2)_3C_2HN_3C_6H_5$ (one-arm), $(sPP-(CH_2)_3C_2HN_3)_2C_6H_4$ (two-arm) and $(sPP-(CH_2)_3C_2HN_3)_3C_6H_3$ (three-arm) $^1H$ NMR spectra.....	166
3.6	$sPP-(CH_2)_3C_2HN_3C_6H_5$ and $(sPP-(CH_2)_3C_2HN_3)_3C_6H_3$ GPC chromatogram	167
3.7	$sPP-(CH_2)_3NHCOC_6H_5$ (one-arm), $(sPP-(CH_2)_3NHCO)_2C_6H_5$ (two-arms) and $(sPP-(CH_2)_3NHCO)_3C_6H_3$ (three-arms) $^1H$ NMR spectra. ....	169
3.8	$sPP-(CH_2)_3NHCOC_6H_5$ (one-arm), $(sPP-(CH_2)_3NHCO)_2C_6H_4$ (two-arms) and $(sPP-(CH_2)_3NHCO)_3C_6H_3$ (three-arms) GPC chromatogram.....	171
3.9	$^1H$ NMR spectra of end-functionalized PEG and $sPP-block-PEG$ .....	176
3.10	$sPP-(CH_2)_3N_3$ and $sPP-block-PEG$ GPC chromatogram .....	176
3.11	$^1H$ NMR spectra of end-functionalized PEG and $sPP-block-PEG-block-sPP$	178
3.12	$sPP-(CH_2)_3N_3$ and $sPP-block-PEG-block-sPP$ GPC chromatogram .....	178
3.13	$^1H$ NMR spectra of end-functionalized PEG and $(sPP)_2-block-PEG$ .....	182
3.14	$sPP-(CH_2)_3N_3$ and $(sPP)_2-block-PEG$ GPC chromatogram .....	183
3.15	$sPP-(CH_2)_3N_3$ and $(sPP)_2-block-PEG-block-(sPP)_2$ GPC chromatogram.....	185
3.16	$^1H$ NMR spectra of end-functionalized PEG and $(sPP)_2-block-PEG-block-(sPP)_2$ .....	186
3.17	DSC thermogram of PEG bearing two trifunctional coupling agents.....	187
3.18	DSC thermogram of azide-terminated syndiotactic polypropylene.....	187
3.19	DSC thermogram of $(sPP)_2-block-PEG-block-(sPP)_2$ .....	188
4.1	Representative structure of linear, long-chain branched and comb polymers	205
4.2	$^1H$ NMR spectrum of $sPP$ -allyl produced with <b>4.1</b> .....	212
4.3	$^{13}C\{^1H\}$ NMR spectrum of MM-3600 .....	212
4.4	$^{13}C\{^1H\}$ NMR spectrum of MM-5600 .....	213
4.5	$^1H$ NMR spectra of $sPP$ -allyl, $sPP$ -hydroxyl and $sPP$ -norbornene .....	213

4.6	<sup>1</sup> H NMR spectrum of <i>s</i> PP-hydroxyl .....	215
4.7	<sup>1</sup> H NMR spectrum of <i>s</i> PP-norbornene .....	216
4.8	Grubbs' olefin metathesis polymerization catalysts for poly(macromonomer) preparation .....	217
4.9	GPC chromatogram of ROMP polymerization of <i>exo</i> -MM-3600 using <b>4.3</b> after 3, 10 and 120 minutes.....	220
4.10	<sup>1</sup> H NMR spectra of poly( <i>exo</i> -MM-3600) produced with <b>4.3</b> after 3, 10 and 120 minutes.....	221
4.11	<sup>1</sup> H NMR spectrum of poly( <i>exo</i> -MM-3600).....	222
4.12	GPC chromatogram of <i>exo</i> -MM-5600 and poly( <i>exo</i> -MM-5600) produced using <b>4.3</b> with 50:1 and 200:1 catalyst loadings.....	224
4.13	GPC chromatogram of <i>exo</i> -MM-3600 and poly( <i>exo</i> -MM-3600) produced using <b>4.3</b> with 50:1 and 200:1 [MM] <sub>0</sub> : $\{Ru\}$ .....	225
4.14	Differential scanning calorimetry thermogram of poly( <i>exo</i> -MM-3600).....	227
4.15	Differential scanning calorimetry thermogram of <i>exo</i> -MM-3600 .....	227
4.16	Differential scanning calorimetry thermogram of poly( <i>exo</i> -MM-5600).....	228
4.17	Differential scanning calorimetry thermogram of <i>exo</i> -MM-5600 .....	228
5.1	$\alpha$ -Diimine Ni(II) olefin polymerization precatalysts .....	244
5.2	<sup>1</sup> H NMR spectra of polypropylene produced with <b>5.2</b> /Et <sub>2</sub> AlCl .....	255
5.3	<sup>13</sup> C{ <sup>1</sup> H} NMR spectra of polypropylene produced with <b>5.2</b> /Et <sub>2</sub> AlCl .....	256
5.4	<sup>1</sup> H NMR spectrum of poly(propylene- <i>co</i> -UP) produced at 0 °C using <b>5.2</b> /Et <sub>2</sub> AlCl.....	257
5.5	<sup>1</sup> H NMR spectra of UP <sub>alkene</sub> and poly(propylene- <i>co</i> -UP) produced at 0 °C ..	257
5.6	<sup>1</sup> H NMR spectra of polypropylene produced with <b>5.3</b> /Et <sub>2</sub> AlCl.....	260
5.7	<sup>13</sup> C{ <sup>1</sup> H} NMR spectra of polypropylene produced with <b>5.3</b> /Et <sub>2</sub> AlCl.....	261

5.8	Tensile stress at break vs tensile strain at break of polypropylene produced with <b>5.2</b> /Et <sub>2</sub> AlCl .....	264
5.9	Tensile stress at break vs tensile strain at break of polypropylene produced with <b>5.3</b> /Et <sub>2</sub> AlCl .....	265
5.10	Tensile stress at break vs tensile strain at break of polypropylene produced with <b>5.3</b> /Et <sub>2</sub> AlCl at -60 °C .....	265
5.11	<sup>1</sup> H NMR spectrum of triblock copolymer produced at -60 to 0 to -60 °C with <b>5.3</b> /Et <sub>2</sub> AlCl .....	269
5.12	<sup>1</sup> H NMR spectra of triblock copolymer produced at -60 to -20 to -60 °C with <b>5.3</b> /Et <sub>2</sub> AlCl .....	270
5.13	<sup>13</sup> C{ <sup>1</sup> H} NMR spectrum of triblock copolymer produced at -60 to 0 to -60 °C with <b>5.3</b> /Et <sub>2</sub> AlCl .....	270
5.14	<sup>13</sup> C{ <sup>1</sup> H} NMR spectrum of triblock copolymer produced at -60 to -20 to -60 °C with <b>5.3</b> /Et <sub>2</sub> AlCl .....	271
5.15	Differential scanning calorimetry thermogram of triblock copolymer produced at -60 to 0 to -60 °C with <b>5.3</b> /Et <sub>2</sub> AlCl .....	271
5.16	Differential scanning calorimetry thermogram of triblock copolymer produced at -60 to -20 to -60 °C with <b>5.3</b> /Et <sub>2</sub> AlCl .....	272
5.17	Tensile stress at break vs tensile strain at break of triblock copolymers produced with <b>5.3</b> /Et <sub>2</sub> AlCl .....	272

## LIST OF SCHEMES

1.1	Propagation and chain transfer mechanisms in transition-metal catalyzed olefin polymerization.....	3
1.2	End-functionalized polypropylene from vanadium-based catalysts.....	11
1.3	Synthesis of <i>sPP-block-aPP</i> using solvent polarity to control tacticity.....	17
1.4	Catalytic synthesis of block copolymers from norbornene and propylene....	19
1.5	Degenerative group transfer polymerization employing <b>21b</b> .....	24
1.6	Synthesis of propylene-based block copolymers using <b>21b</b> .....	25
1.7	Synthesis of ethylene/cyclopentene block copolymers using <b>50</b> .....	46
1.8	Polymerization of 1,5-hexadiene using <b>50</b> .....	47
1.9	Synthesis of propylene/1,5-hexadiene block copolymers.....	48
1.10	Synthesis of ethylene/norbornene block copolymers .....	52
1.11	Synthesis of ethylene/dicyclopentadiene block copolymers.....	56
1.12	Formation of a telechelic initiator for ethylene polymerization.....	68
1.13	$\omega,1$ and $\omega,2$ -enchainment of 1-hexene .....	71
1.14	Synthesis of 1-octene/propylene triblock copolymers using <b>98</b> .....	73
1.15	Synthesis of propylene-based block copolymers using <b>102</b> .....	75
1.16	Synthesis of telechelic polyethylene .....	79
1.17	Graft copolymer synthesis using living insertion and ATRP .....	82
1.18	Synthesis of PE- <i>block</i> -poly( <i>n</i> -butyl acrylate) and polystyrene diblock copolymers.....	83
1.19	Synthesis of poly(E- <i>co</i> -P) combs .....	84
1.20	Polymerization of dienes using <b>114</b> /NaBArF <sub>4</sub> and <b>97</b> /MMAO .....	85
1.21	Synthesis of ethylene/5-norbornen-2-yl acetate block copolymers .....	90
1.22	Synthesis of PE- <i>graft</i> -PMMA copolymers using <b>121c</b> and ATRP .....	91

2.1	Synthesis of end-functionalized polypropylene through living polymerization with vanadium followed by quenching with electrophiles.....	113
2.2	Catalytic production of end-functionalized polyethylene using neodymium and <i>n</i> -butyloctylmagnesium .....	114
2.3	Chain release processes following 1,2- or 2,1-propylene insertions.....	115
2.4	Synthesis of allyl-terminated syndiotactic polypropylene from a non-living bis(phenoxyimine)titanium complex.....	117
2.5	Synthesis of <i>s</i> PP-CH <sub>2</sub> CHBrCH <sub>2</sub> Br and <i>s</i> PP-CH <sub>2</sub> CH(O)CH <sub>2</sub> from <i>s</i> PP-CH <sub>2</sub> CH=CH <sub>2</sub> .....	119
2.6	Ring opening of <i>s</i> PP-CH <sub>2</sub> CH(O)CH <sub>2</sub> under acidic and basic conditions.....	121
2.7	Hydroboration/oxidation of <i>s</i> PP-CH <sub>2</sub> CH=CH <sub>2</sub> .....	123
2.8	Reaction of <i>s</i> PP-(CH <sub>2</sub> ) <sub>3</sub> OH with acid chlorides.....	126
2.9	Reaction of hydroxyl-terminated polypropylene with tosyl chloride to produce tosyl- and chloro-terminated polypropylene.....	128
2.10	Synthesis of azide-terminated polypropylene from tosyl- and chloro-terminated polypropylene.....	129
2.11	Click reaction of <i>s</i> PP-(CH <sub>2</sub> ) <sub>3</sub> N <sub>3</sub> with phenyl acetylene.....	132
2.12	Reduction of <i>s</i> PP-(CH <sub>2</sub> ) <sub>3</sub> N <sub>3</sub> to <i>s</i> PP-(CH <sub>2</sub> ) <sub>3</sub> NH <sub>2</sub> using LiAlH <sub>4</sub> .....	133
2.13	Reaction of <i>s</i> PP-(CH <sub>2</sub> ) <sub>3</sub> NH <sub>2</sub> with benzoyl chloride .....	133
3.1	General star polymer synthesis methods .....	153
3.2	Synthesis of polyethylene and atactic polypropylene using anionic polymerization/hydrogenation of butadiene and 2-methyl-1,3-pentadiene...155	
3.3	“Click” reactions in organic chemistry.....	157
3.4	( <i>s</i> PP-(CH <sub>2</sub> ) <sub>3</sub> OCO) <sub>2</sub> C <sub>6</sub> H <sub>4</sub> (two-arms) and ( <i>s</i> PP-(CH <sub>2</sub> ) <sub>3</sub> OCO) <sub>3</sub> C <sub>6</sub> H <sub>3</sub> (three-arms) synthesis.....	160

3.5	Synthesis of ( <i>s</i> PP-(CH <sub>2</sub> ) <sub>3</sub> C <sub>2</sub> HN <sub>3</sub> ) <sub>2</sub> C <sub>6</sub> H <sub>4</sub> (two-arms) and ( <i>s</i> PP-(CH <sub>2</sub> ) <sub>3</sub> C <sub>2</sub> HN <sub>3</sub> ) <sub>3</sub> C <sub>6</sub> H <sub>3</sub> (three-arms) polymers.....	165
3.6	Synthesis of ( <i>s</i> PP-(CH <sub>2</sub> ) <sub>3</sub> NHCO) <sub>2</sub> C <sub>6</sub> H <sub>4</sub> (two-arms) and ( <i>s</i> PP-(CH <sub>2</sub> ) <sub>3</sub> NHCO) <sub>3</sub> C <sub>6</sub> H <sub>3</sub> (three-arms) polymers.....	170
3.7	Synthesis of a difunctional coupling agent.....	173
3.8	Synthesis of an end-functionalized PEG and <i>s</i> PP- <i>block</i> -PEG.....	174
3.9	Synthesis of an end-functionalized PEG and <i>s</i> PP- <i>block</i> -PEG- <i>block</i> - <i>s</i> PP ....	177
3.10	Synthesis of a trifunctional coupling agent.....	180
3.11	Synthesis of an end-functionalized PEG and ( <i>s</i> PP) <sub>2</sub> - <i>block</i> -PEG.....	182
3.12	Synthesis of an end-functionalized PEG and ( <i>s</i> PP) <sub>2</sub> - <i>block</i> -PEG- <i>block</i> -( <i>s</i> PP) <sub>2</sub> .....	184
4.1	Olefin polymerization chain-transfer pathways.....	208
4.2	Synthesis of allyl-terminated syndiotactic polypropylene using non-living bis(phenoxyimine)titanium catalysts.....	209
4.3	Synthesis of norbornene-terminated syndiotactic polypropylene.....	215
4.4	Ring-opening metathesis polymerization (ROMP) of norbornene-terminated syndiotactic polypropylene.....	219
5.1	Propylene polymerization using <b>5.2</b> or <b>5.3</b> /MAO.....	245
5.2	Hydrogen bonding in 2-ureido-4[1H]-pyrimidinones.....	246
5.3	Mechanism of defect formation in isotactic polypropylene.....	250
5.4	Copolymerization propylene and UP <sub>alkene</sub> with <b>5.2</b> or <b>5.3</b> /Et <sub>2</sub> AlCl.....	253
5.5	Synthesis of triblock copolymers using <b>5.3</b> /Et <sub>2</sub> AlCl.....	268

## LIST OF TABLES

2.1	Optimization of the <i>s</i> PP-CH <sub>2</sub> CH=CH <sub>2</sub> oxidation following hydroboration with 9-BBN.....	124
3.1	Syndiotactic polypropylene with ester functionality characterization .....	162
3.2	Syndiotactic polypropylene with triazole functionality characterization.....	166
3.3	Syndiotactic polypropylene with amide functionality characterization .....	171
3.4	Characterization of di- and triblock copolymers containing <i>s</i> PP and PEG ...	175
3.5	Characterization of miktoarm and h-polymers containing <i>s</i> PP and PEG.....	183
4.1	Syndiotactic polypropylene macromonomer characterization.....	211
4.2	Metathesis polymerization of <i>exo</i> -MM-3600 at 60 °C.....	218
4.3	Metathesis polymerization of <i>exo</i> -MM-3600 with <b>4.3</b> at 60 °C .....	220
4.4	Polymerization of <i>exo</i> -MM-3600 and <i>exo</i> -MM-5600 with <b>4.3</b> .....	223
5.1	Propylene polymerization with <b>5.2</b> and <b>5.3</b> /MMAO-3A.....	251
5.2	Polymerization of propylene and UP <sub>alkene</sub> with <b>5.2</b> /Et <sub>2</sub> AlCl.....	254
5.3	Polymerization of propylene and UP <sub>alkene</sub> with <b>5.3</b> /Et <sub>2</sub> AlCl.....	262
5.4	Mechanical testing of polypropylene produced using <b>5.2</b> and <b>5.3</b> .....	266
5.5	Block copolymer synthesis using <b>5.3</b> /Et <sub>2</sub> AlCl.....	273

# **Chapter 1**

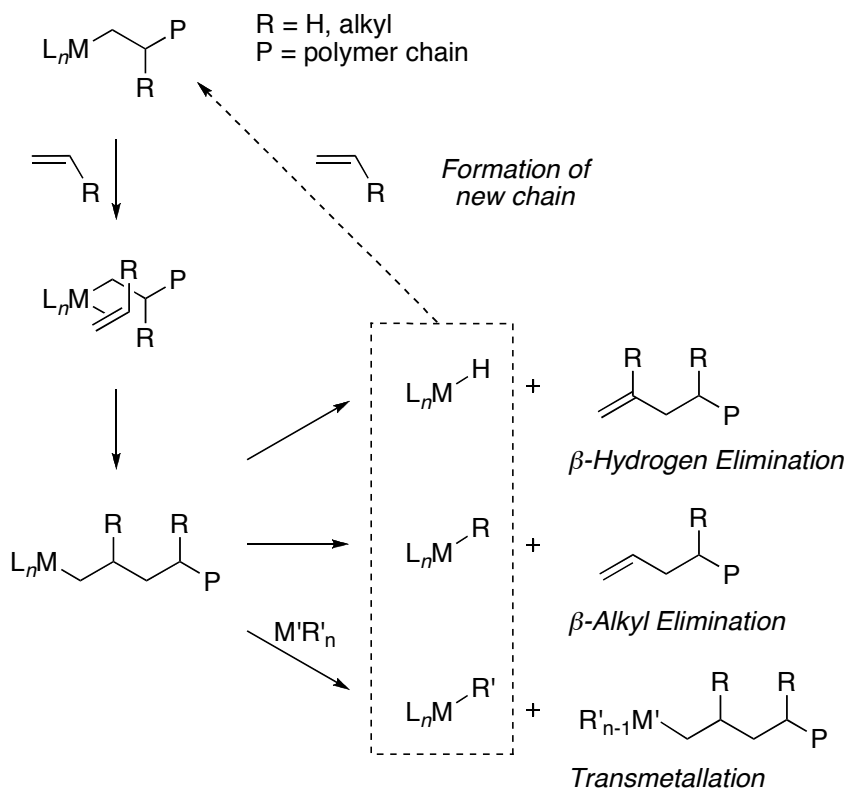
Living Transition Metal Catalyzed Polymerization:  
Polyolefin Synthesis and New Polymer Architectures

## 1.1 Introduction

One of the ultimate challenges in polymer chemistry is the development of new synthetic methods for the polymerization of a wide range of monomers with well-defined stereochemistry<sup>1</sup> while controlling molecular weight and molecular weight distribution.<sup>2-4</sup> Over the last half century, a primary goal of synthetic polymer chemistry has been the development of chain-growth polymerization methods that enable consecutive enchainment of monomer units without termination. Known as living polymerizations,<sup>5</sup> these systems allow precise molecular weight control as well as the synthesis of a wide array of polymer architectures.<sup>6</sup> Additionally, living polymerization methods allow the synthesis of end-functionalized polymers in addition to the creation of virtually limitless types of new materials from a basic set of monomers.

Today, polyolefins are by far the largest volume class and most important commercial synthetic polymers.<sup>7</sup> Since the initial discoveries of Ziegler<sup>8</sup> and Natta,<sup>9</sup> remarkable advances have been reported concerning the control of comonomer incorporation as well as dramatic improvements in activity. Homogeneous olefin polymerization catalysts now exist that are unparalleled in all of polymer chemistry concerning the detailed control of macromolecular stereochemistry.<sup>10</sup> However, olefin polymerization catalysts have traditionally been inferior to their other chain-growth counterparts in one respect. While extraordinary advances in living/controlled polymerization have been discovered using anionic,<sup>11</sup> cationic,<sup>12,13</sup> and radical-based polymerization,<sup>14-18</sup> until very recently there existed a comparative lack of living olefin polymerization systems. The main reason for this is that alkene polymerization catalysts often undergo irreversible chain transfer to metal alkyls and  $\beta$ -elimination reactions that result in the initiation of new polymer chains by the catalyst (Scheme 1.1). However, systems are now available that have acceptable rates of propagation

with negligible rates of termination that allow the truly living polymerization of alkenes such that block copolymer synthesis is now possible.



**Scheme 1.1.** Propagation and chain transfer mechanisms in transition-metal catalyzed olefin polymerization.

By far, the most important application of living olefin polymerization is the production of block copolymers, which is typically achieved via sequential monomer addition furnishing a variety of new materials. Physical blends, or random copolymers often give rise to materials whose properties are intermediate between those of the respective homopolymers. Block copolymers, on the other hand, often furnish materials whose mechanical properties are superior to the sum of their parts. This unique behavior is due to microphase separation of the different segments of the block copolymer into discrete domains which give rise to otherwise unattainable

morphologies.<sup>19,20</sup> One of the most highly sought goals in the field of olefin polymerization is the synthesis of block copolymers containing isotactic polypropylene (*i*PP) domains that are envisioned to possess material properties of great industrial importance. For example diblock copolymers containing *i*PP segments may serve as compatibilizers in blends containing isotactic polypropylene (*i*PP) homopolymers.<sup>21</sup> One of the most actively pursued block copolymer structures are those with “hard” or semicrystalline end blocks (e.g. PE, *i*PP, *s*PP) and amorphous midblocks (e.g. *a*PP, poly(E-*co*-P)); triblock copolymers of this type have been shown to behave as thermoplastic elastomers.<sup>22-29</sup>

This review is a comprehensive account of living alkene polymerization systems with special attention paid to systems developed in the past couple of years focusing on the polymer types and architectures as in our previous reviews.<sup>2-4</sup> This review will primarily focus on living polymerization of terminal-alkenes with some coverage of non-conjugated dienes and cyclic olefins.

## **1.2 Living Olefin Polymerization**

### **1.2.1 Poly(1-hexene)**

One of the most commonly employed monomers for detailed studies of living olefin polymerization is 1-hexene due to the fact that it is an easily handled liquid, and molecular weight determination of its polymers are easily accomplished at or slightly above room temperature employing low boiling GPC eluents (Figure 1.1). However, due to their poor mechanical properties, poly(1-hexene) (PH) and homopolymers derived from higher  $\alpha$ -olefins (with the exception of poly(4-methyl-1-pentene)) are of little commercial significance. One application of amorphous poly( $\alpha$ -olefin)s are as impact strength modifiers when blended with polypropylenes.<sup>7</sup>

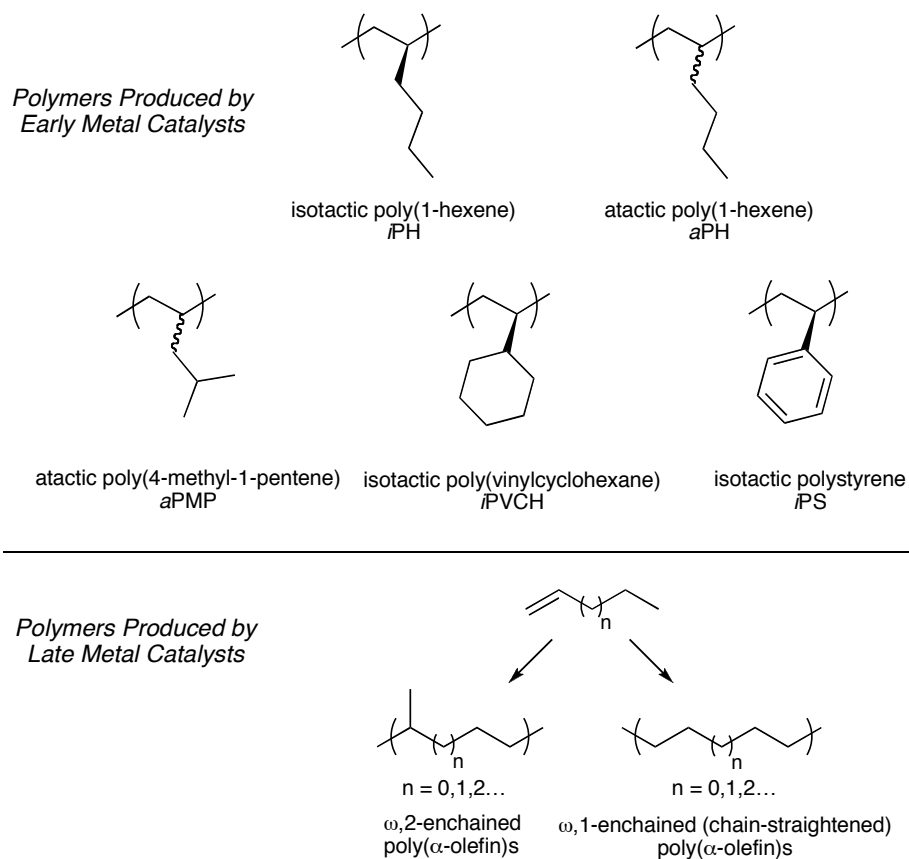


**Figure 1.1.** Homopolymers of higher  $\alpha$ -olefins.

### 1.2.2 Polypropylene

While poly(1-hexene) is an amorphous material regardless of the level of tacticity, polypropylene can range from amorphous to semi-crystalline due to the variability in the level of tacticity. The bulk properties of the polymer are intimately related to its tacticity, with atactic polypropylene (*a*PP; Figure 1.2) being an amorphous material with limited industrial uses (e.g. adhesives, sealants, and caulks) and syndiotactic polypropylene (*s*PP) and isotactic polypropylene (*i*PP) being semicrystalline materials with relatively high  $T_m$  values of  $\sim 150$  °C and  $\sim 165$  °C respectively. The lower crystallinity and the fact that only a very few syndiospecific propylene polymerization catalysts have been discovered to date have limited the

commercial impact of *s*PP. On the other hand, numerous catalysts, both heterogeneous and homogeneous, are capable of isospecific propylene polymerization. When combined with *i*PP's highly desirable mechanical properties (durability, chemical resistance, and stiffness), it is obvious why the vast majority of industrially produced polypropylenes are of the isotactic variety.<sup>30</sup>

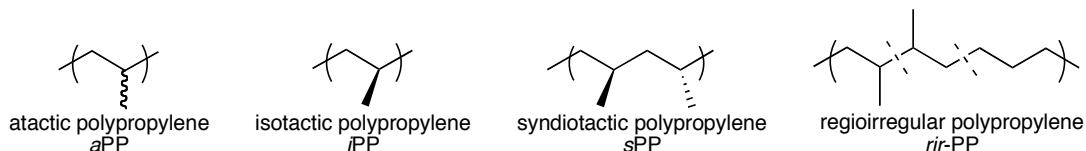


**Figure 1.2.** Polypropylene microstructures.

### 1.2.3 Polyethylene

In addition to *i*PP, polyethylene (PE) represents another commercially important material. The annual production of PE worldwide is in excess of 80 billion pounds.<sup>31</sup> Considering the simplicity of ethylene, the range of different polymer architectures derived from it is truly intriguing (Figure 1.3). The properties of PEs vary greatly depending on the polymer's microstructure (i.e. branched or linear) from high density plastics with relatively high melting points (linear PE:  $T_m \sim 135$  °C), to low density, branched material with  $T_m$  as low as 105 °C. The mechanism by which ethylene is polymerized will ultimately determine the microstructure and therefore the properties of the resultant PE. While most early transition metal olefin polymerization catalysts furnish linear PE, late metal catalysts based on nickel or palladium typically give rise to branched structures.<sup>21</sup>

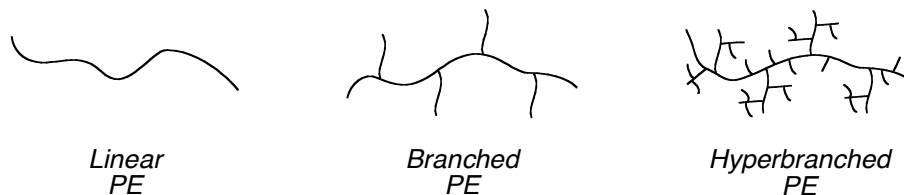


**Figure 1.3.** Polyethylene morphologies.

### 1.2.4 Polyolefins from Conjugated Dienes, Cyclic Olefins, and Polar Monomers

Beyond simple  $\alpha$ -olefins, the polymers obtained from both non-conjugated dienes and cyclic olefins provided materials with desirable properties. Non-conjugated dienes are versatile monomers in that they can furnish polymers with a variety of microstructures depending on the mechanism by which they are polymerized. For example, 1,5-hexadiene can be cyclopolymerized to furnish a polymer with methylene-1,3-cyclopentane (MCP) units (Figure 1.4). Depending on the selectivity of the ring closing reaction, *cis*- or *trans*-rings may be formed. Polymers containing mostly *cis*-rings exhibit higher  $T_m$  values than those with mostly *trans*-rings (e.g. for poly(methylene-1,3-cyclopentane) (PMCP) having > 90% *cis*-ring content the  $T_m$  is 189 °C whereas those containing 82% *trans*-rings exhibit  $T_m$  is 102 °C.<sup>32,33</sup> Polymerization of 1,5-hexadiene can also lead to vinyl-tetramethylene (VTM) units, which may serve as a synthetic handle by which polymer functionalization can be achieved.<sup>34</sup>

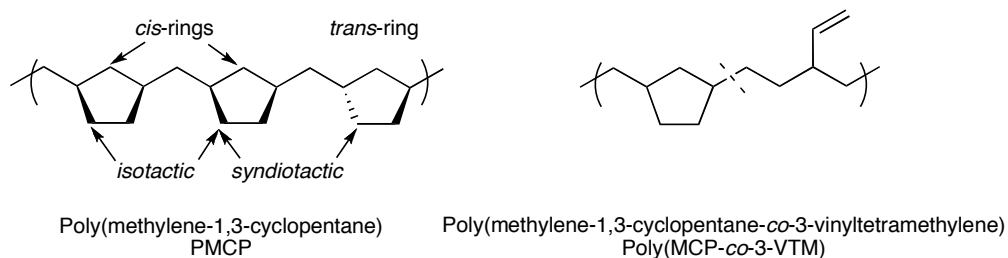


**Figure 1.4.** Polymers derived from 1,5-hexadiene polymerization.

Similarly, homopolymers of cyclic olefins (e.g. polycyclopentene, polynorbornene (PNB), Figure 1.5) are characterized by extremely high melting points and low solubility in most organic solvents. Taken together, these properties of cyclic olefin homopolymers make them difficult to process and therefore commercially insignificant. However, upon incorporation into copolymers with  $\alpha$ -olefins, materials

with desirable properties can be obtained. The copolymers typically exhibit high chemical resistance, good optical properties, and facile processability.<sup>35</sup> In addition to simple hydrocarbon systems, copolymers of polar monomers with olefins are attractive due to enhanced physical properties such as biocompatibility and ease of processing.<sup>36</sup>

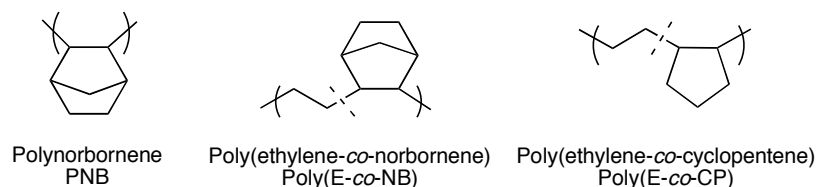


**Figure 1.5.** Cyclic olefin homopolymers and copolymers.

### 1.2.5 Criteria for Living Polymerization

The homopolymerization of the aforementioned alkenes will be discussed in order of early metal to late metal catalyzed polymerizations with special emphasis paid to block copolymers and new polymer architectures. Note that in this review, we refer to living species for alkene polymerization as catalysts, not initiators, to emphasize the fundamental catalytic event of monomer enchainment, not polymer chain formation. There are seven generally accepted criteria for a living polymerization: (1) polymerization proceeds to complete monomer conversion, and chain growth continues upon further monomer addition; (2) number average molecular weight ( $M_n$ ) of the polymer increases linearly as a function of conversion; (3) the number of active centers remains constant for the duration of the polymerization; (4) molecular weight can be precisely controlled through stoichiometry; (5) polymers display narrow molecular weight distributions, described quantitatively by the ratio of the weight average molecular weight to the number average molecular weight ( $M_w/M_n \sim 1$ ); (6) block copolymers can be prepared by sequential monomer addition; and (7)

end-functionalized polymers can be synthesized.<sup>37</sup> Few polymerization systems, whether ionic, radical, or metal mediated, that are claimed to proceed by a living mechanism have been shown to meet all of these criteria. This review will therefore include all systems that claim living alkene polymerization, providing that a number of the key criteria have been met.

### 1.3 Early Metal Olefin Polymerization Catalysts

#### 1.3.1 Vanadium Acetylacetonate Catalysts

In the 1960s, Natta and co-workers discovered that activation of  $VCl_4$  with  $Et_2AlCl$  at  $-78\text{ }^\circ\text{C}$  in the presence of propylene furnished syndio-enriched polypropylene. Linear growth of molecular weight over time for a period of 25 hours was observed.<sup>38</sup> In a subsequent report, the polypropylenes produced by  $VCl_4/Et_2AlCl$  were shown to possess very narrow molecular weight distributions ( $M_w/M_n = 1.4 - 1.9$ ).<sup>39</sup>

The first example of a truly living alkene polymerization catalyst was reported by Doi in 1979.<sup>40,41</sup> Activation of  $V(\text{acac})_3$  (**1**, Figure 1.6) with  $Et_2AlCl$  in the presence of propylene at temperatures  $\leq -65\text{ }^\circ\text{C}$  furnished syndio-enriched PP ( $[r] = 0.81$ ) exhibiting narrow molecular weight distributions ( $M_w/M_n = 1.07 - 1.18$ ) and  $M_n$  as high as 100,000 g/mol. A linear increase in  $M_n$  over the course of 15 hours was additionally observed. Initially, only about 4% of vanadium centers were shown to be active, however, addition of anisole to the polymerization lead to a 3-fold increase in the number of active vanadium centers.<sup>42</sup> Utilizing the living nature of **1**/ $Et_2AlCl$ , Doi and co-workers were able to synthesize block copolymers of propylene and ethylene.<sup>43</sup> Specifically, a *sPP-block-poly(E-co-P)-block-sPP* triblock copolymer was synthesized via sequential monomer addition and exhibited a narrow molecular weight distribution ( $M_w/M_n = 1.24$ ) with  $M_n = 94,000$  g/mol and a propylene content of 70 mol%.

By replacing the acetylacetonate ligands of **1** with 2-methyl-1,3-butanedionato ligands (**2**, Figure 1.6), Doi and co-workers found that nearly all of the vanadium centers were active for polymerization with essentially the same degree of syndioselectivity as **1**/Et<sub>2</sub>AlCl.<sup>44</sup> In addition, the living character of propylene polymerization by **2**/Et<sub>2</sub>AlCl was maintained up to -40 °C (*M<sub>w</sub>*/*M<sub>n</sub>* as low as 1.4).<sup>45,46</sup> Copolymerization of propylene and ethylene by **2**/Et<sub>2</sub>AlCl was also shown to be living.<sup>47</sup>

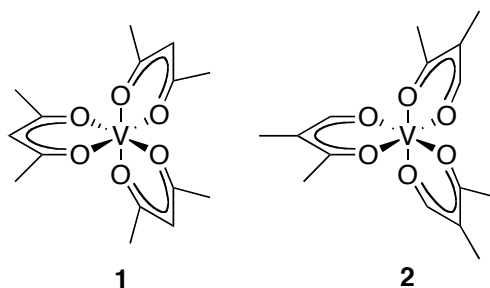
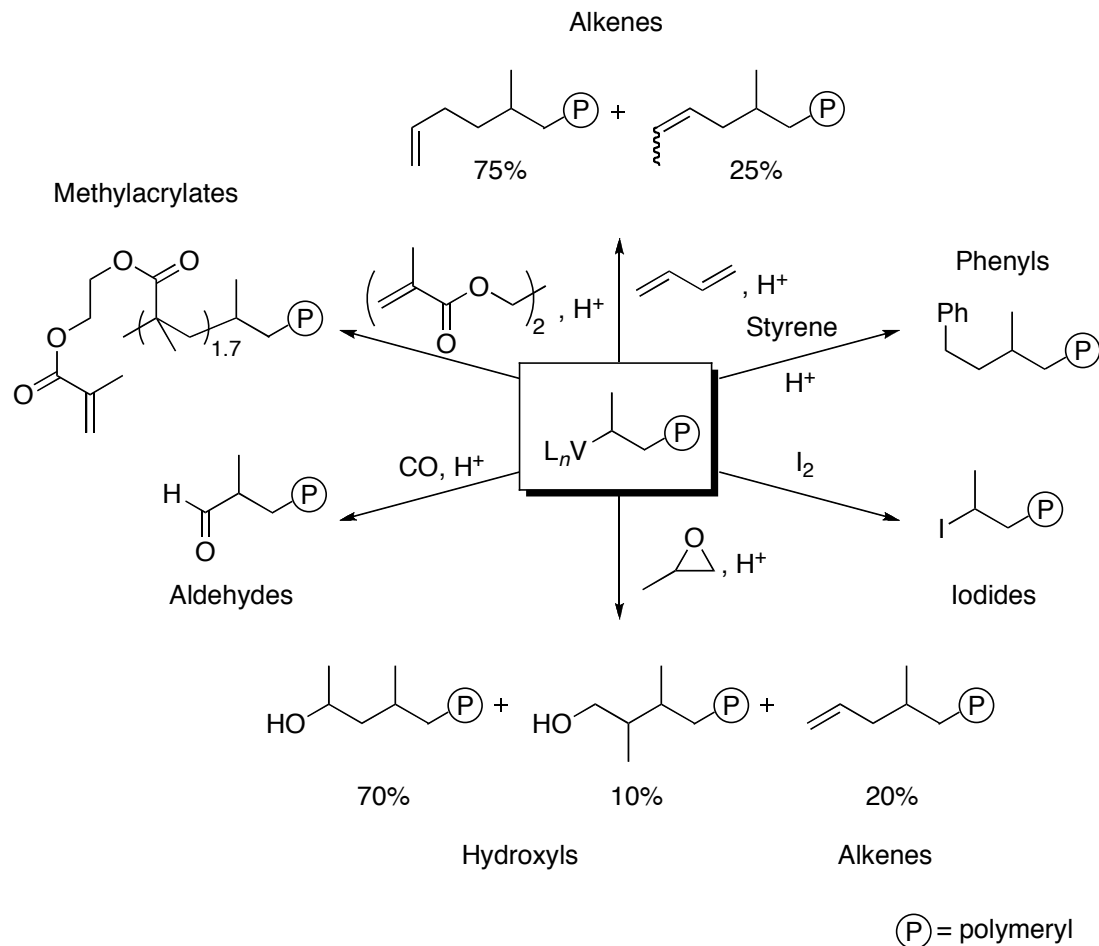


**Figure 1.6.** Vanadium catalysts for living olefin polymerization.

An important application of living olefin polymerization is in the synthesis of end-functionalized polymers, which is typically achieved by reaction of the living chain end with an electrophile. The vanadium-based living olefin polymerization catalysts discovered by Doi and co-workers proved to be particularly amenable to this application.<sup>48-52</sup> The structures of end-functionalized sPPs prepared in this manner are summarized in Scheme 1.2.

Furthermore, one of the most challenging goals in polymer synthesis is the incorporation of polar monomers due to the limited ability of many catalysts to tolerate polar functionalities. In 1983, Doi reported the use of **1**/Et<sub>2</sub>AlCl (Figure 1.6) for the synthesis of a series of PP-*block*-poly(tetrahydrofuran) AB-type diblock copolymers by quenching a living propylene polymerization with iodine and using the iodide-terminated PP to initiate cationic polymerization of THF.<sup>48</sup> Catalyst **1**/Et<sub>2</sub>AlCl

has also been used to synthesize PP-*block*-PMMA (PMMA = poly(methylmethacrylate)).<sup>53</sup> At -78 °C, 1/Et<sub>2</sub>AlCl was used to polymerize propylene to which methyl methacrylate (MMA) was then added. The MMA polymerization, which was proposed to proceed via a radical mechanism, was conducted at 25 °C to form the diblock copolymer.



**Scheme 1.2.** End-functionalized polypropylene from vanadium-based catalysts.

In addition to exhibiting living behavior for propylene polymerization, vanadium acetylacetonate complexes (Figure 1.6) have also been shown to be living for 1,5-hexadiene polymerization as well as for 1,5-hexadiene/propylene copolymerization.<sup>54</sup> At -78 °C, 1/Et<sub>2</sub>AlCl polymerized 1,5-hexadiene to produce a low

molecular weight polymer ( $M_n = 6,600$  g/mol,  $M_w/M_n = 1.4$ ) that contained a mixture of MCP and VTM units in a 54:46 ratio. The distribution of these two units varied in 1,5-hexadiene-propylene random copolymers as a function of 1,5-hexadiene incorporation.

### 1.3.2 Metallocene and Unbridged Half-Metallocene Catalysts

Since the discovery of their catalytic activity, Group 4 metallocene complexes have found extensive use as olefin polymerization catalysts.<sup>1</sup> Due to their high propensity toward termination via chain-transfer (e.g.  $\beta$ -H elimination/transfer, transfer to alkylaluminum species) there have been few examples of living olefin polymerization using metallocene-based catalysts. However, several groups have shown that by employing well-defined boron-based activators<sup>55</sup> at low reaction temperatures these termination pathways can be suppressed. For example, Fukui reported the living polymerization of 1-hexene with a *rac*-(Et)Ind<sub>2</sub>ZrMe<sub>2</sub> (**3**, Figure 1.7) activated with B(C<sub>6</sub>F<sub>5</sub>)<sub>3</sub> at -78 °C in which Al(*n*Oct)<sub>3</sub> was used as a scavenging agent to furnish isotactic poly(1-hexene)s with narrow molecular weight distributions ( $M_w/M_n = 1.22 - 1.29$ ).<sup>56</sup> While the molecular weights were relatively low ( $M_n \leq 5,400$  g/mol), the  $M_n$  was shown to increase linearly with reaction time. In 2009, Potamitis and co-workers reported the polymerization of higher  $\alpha$ -olefins with a  $C_s$ -symmetric metallocene catalyst (**4**, Figure 1.7).<sup>57</sup> Upon activation with [B(C<sub>6</sub>F<sub>5</sub>)<sub>4</sub>][Me<sub>2</sub>NHPh] at 0 °C, **4** produced polymers of higher  $\alpha$ -olefins (1-hexene, 1-octene, 1-decene, 1-tetradecene, 1-hexadecene) with narrow molecular weight distributions ( $M_w/M_n < 1.5$ ).

Upon evaluation of an unbridged half-metallocene complex bearing a phenoxide donor, Nomura and Fudo demonstrated that **5** (Figure 1.7) was also capable of polymerizing 1-hexene in a living fashion.<sup>58</sup> When activated with [Ph<sub>3</sub>C][B(C<sub>6</sub>F<sub>5</sub>)<sub>4</sub>] in the presence of Al(*i*Bu)<sub>3</sub> at -30 °C, **5** furnished poly(1-hexene)s with narrow

polydispersities ( $M_w/M_n = 1.27 - 1.64$ ) and high molecular weight ( $M_n$  up to 1,865,000 g/mol). The  $M_n$  was shown to increase linearly with turn over number (TON).

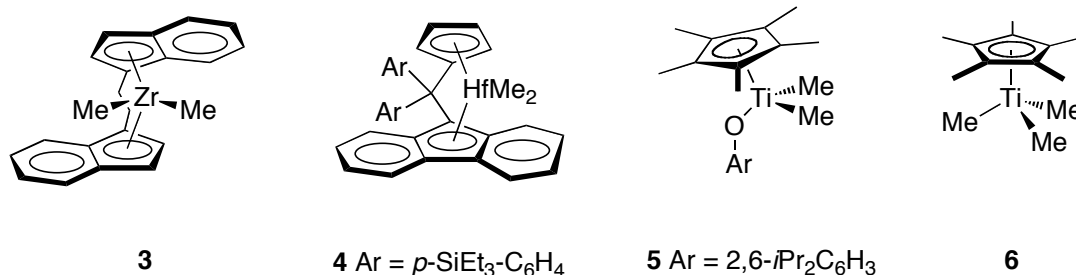


**Figure 1.7.** Metallocene-based catalysts for living olefin polymerization.

In addition to 1-hexene, living metallocene catalysts have been reported for propylene polymerization. Bochmann and co-workers reported that **6** (Figure 1.7) activated with  $\text{B}(\text{C}_6\text{F}_5)_3$  at  $-20\text{ }^\circ\text{C}$  produces atactic, high molecular weight PP that exhibits elastomeric properties with  $M_w = 1,103,000\text{ g/mol}$  and  $M_w/M_n = 1.4$ .<sup>59</sup> From analysis of the GPC trace for this sample, it was estimated that 48% of the polymer was composed of PP with a narrow molecular weight distribution ( $M_w/M_n = 1.10$ ). The polymerization also showed a linear increase in molecular weight with time.

Utilizing a zirconocene catalysts, Fukui and co-workers have reported that **7** (Figure 1.8) activated with  $\text{B}(\text{C}_6\text{F}_5)_3$  at  $-78\text{ }^\circ\text{C}$  in the presence of  $\text{Al}(n\text{Oct})_3$  produces PP with  $M_w/M_n \leq 1.15$  ( $M_n = 9,400 - 27,300\text{ g/mol}$ ).<sup>56</sup> The polymerization shows a linear increase in  $M_n$  with time and it was later reported that quenching the polymerization with CO resulted in aldehyde-functionalized polymer chains.<sup>60,61</sup> Additionally, the hafnium analogue (**8**, Figure 1.8) was shown to be living at  $-50\text{ }^\circ\text{C}$ . Fukui and co-workers were also able to show that iso-enriched PP ( $[mm] = 0.42$ ) could be formed from a mixed catalyst system **7**/ $\text{B}(\text{C}_6\text{F}_5)_3$ /**9** at  $-50\text{ }^\circ\text{C}$ .<sup>62</sup> Over 26 hours, the polymerization exhibits a linear increase in  $M_n$  with time and  $M_n$  up to 17,600 g/mol ( $M_w/M_n = 1.29 - 1.41$ ).

In 1991, Hlatky and Turner reported on the synthesis of diblock copolymers of ethylene and propylene using a hafnocene catalyst.<sup>63</sup> Activation of  $\text{Cp}_2\text{HfMe}_2$  (**8**, Figure 1.8) with  $[\text{PhNMe}_2\text{H}][\text{B}(\text{C}_6\text{F}_5)_4]$  in the presence of propylene furnishes atactic PP. At 0 °C, the rate of termination via  $\beta$ -H transfer was slow enough to allow for the synthesis of *aPP-block*-PE via sequential monomer addition. Both orders of monomer addition (ethylene followed by propylene and propylene followed by ethylene) were successful in furnishing a polymeric product that contained a majority (50 – 60 %) of diblock material isolated by hexanes extraction.

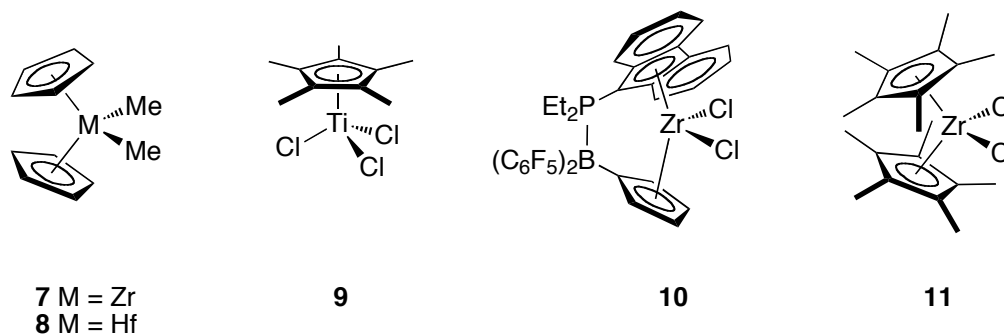


**Figure 1.8.** Titanium, zirconium and hafnium olefin polymerization catalysts.

In a subsequent report by Fukui and co-workers, the synthesis of *aPP-block*-poly(*E-co*-P) diblock copolymers using **7**, **8**, and  $\text{Cp}_2^*\text{HfMe}_2$  activated with  $\text{B}(\text{C}_6\text{F}_3)_3$  and employing  $\text{Al}(n\text{Oct})_3$  as a scavenger was achieved through sequential monomer addition at low temperatures ( $T_{\text{rxn}} = -78$  °C for **7** and  $\text{Cp}_2^*\text{HfMe}_2$ ;  $T_{\text{rxn}} = -50$  °C for **7**).<sup>61</sup> The resultant polymers exhibited narrow molecular weight distributions ( $M_w/M_n = 1.07 - 1.30$ ) and  $M_n = 71,000 - 155,000$  g/mol with propylene contents between 65 – 75 mol%.

Starzewski and co-workers have reported a metallocene with the existence of donor and acceptor groups in the sandwich structure (**10**, Figure 1.8) that generates elastomeric PP in a syndiospecific fashion ( $[rr] = 0.52$ ) upon activation with MAO at

-8 to -6 °C.<sup>64</sup> While the PDIs are somewhat broad ( $M_w/M_n = 1.5 - 1.6$ ,  $M_n$  up to 531,000 g/mol), the  $M_n$  was shown to increase linearly with time over 1 hr. The system was also shown to be living for ethylene and propylene copolymerization.

In addition to 1-hexene and propylene, metallocene catalysts have been identified for the living polymerization of ethylene. Employing  $Cp_2^*ZrCl_2/MAO$  (**11**, Figure 1.8), Chen and co-workers polymerized ethylene in a quasi-living fashion at 60 °C.<sup>65</sup> Over the course of twenty minutes, polymer molecular weight increased ( $M_n = 1,300 - 4,400$  g/mol) while molecular weight distributions remained relatively narrow ( $M_w/M_n = 1.4 - 1.7$ ). The quasi-living behavior of **11** compared to the non-living behavior exhibited by **7**/MAO for ethylene polymerization is attributed to the increased steric bulk around the active site, which suppresses  $\beta$ -H elimination and transfer reactions.

Finally, while investigating cyclic olefin polymerization, Tritto and co-workers have shown that *rac*-Et(Ind)<sub>2</sub>ZrCl<sub>2</sub>/MAO (**12**), 90 % *rac*/10 % *meso*-Et(4,7-Me<sub>2</sub>Ind)<sub>2</sub>ZrCl<sub>2</sub> (**13**), and *rac*-H<sub>2</sub>C(3-*t*BuInd)<sub>2</sub>ZrCl<sub>2</sub>/MAO (**14**) exhibit quasi-living behavior for ethylene-norbornene copolymerization (Figure 1.9).<sup>66,67</sup>

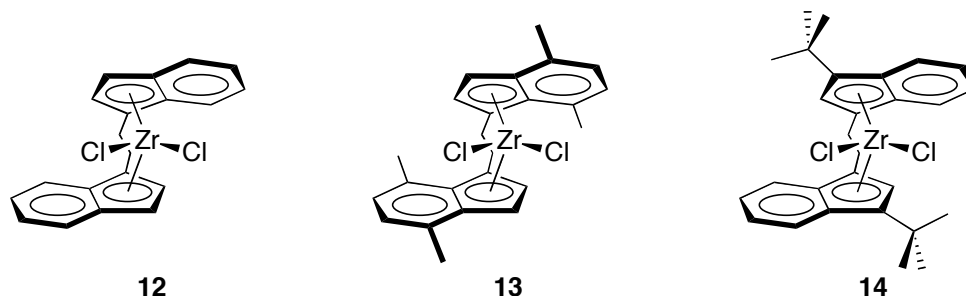
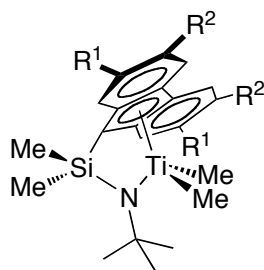


**Figure 1.9.** Zirconocene catalysts for living ethylene/norbornene polymerization.

### 1.3.3 Catalysts Bearing Monocyclopentadienyl-amido Ligands

In spite of the large number of metallocene-based polymerization catalysts, there remain relatively few examples of living systems. Titanium complexes bearing a

linked monocyclopentadienyl-amido ligand, such as **15** (Figure 1.10), have been shown to polymerize 1-hexene in a living fashion when activated with  $B(C_6F_5)_3$  in the presence of  $Al(nOct)_3$  at  $-50\text{ }^\circ\text{C}$ .<sup>68</sup> The poly(1-hexene) formed was syndio-enriched ( $[rr] = 0.49$ ) with  $M_n$  up to 26,000 g/mol and  $M_w/M_n = 1.07 - 1.12$ . A linear relationship between  $M_n$  and polymer yield was also demonstrated. In a subsequent report,  $\mathbf{15}/(B(C_6F_5)_3/Al(nOct)_3)$  was also shown to polymerize 1-octene and 1-butene in a living fashion.<sup>69</sup>

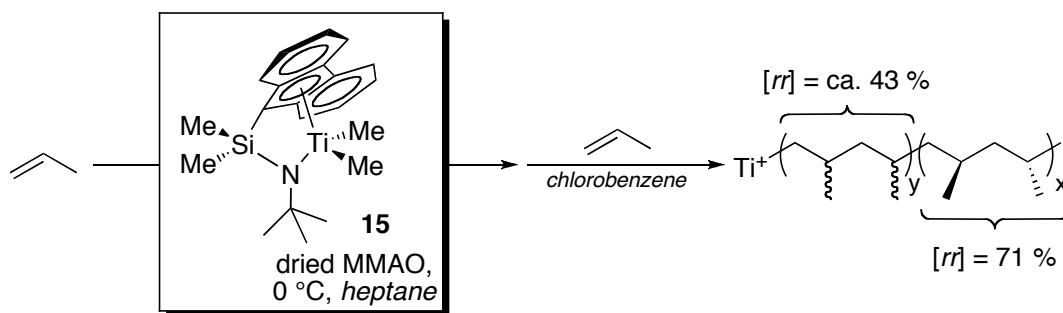


- 15**  $R^1 = R^2 = H$   
**16**  $R^1 = tBu, R^2 = H$   
**17**  $R^1 = H, R^2 = tBu$   
**18**  $R^1, R^2 = -CMe_2CH_2CH_2CMe_2-$

**Figure 1.10.** Monocyclopentadienyl-amido catalyst precursors for living olefin polymerization.

In addition to living 1-hexene polymerization, **15** (Figure 1.10) upon activation with  $B(C_6F_5)_3$  in the presence of  $Al(nOct)_3$  can also produce syndio-enriched PP ( $[rr] \sim 0.49$ ) at  $-50\text{ }^\circ\text{C}$  in living fashion.<sup>68</sup> Subsequent studies showed that when activated with “dried” MAO (dMAO) (free of trimethylaluminum), **15** could polymerize propylene at  $0\text{ }^\circ\text{C}$  producing PP with a higher degree of syndiotacticity ( $[rr] \sim 0.63$ ) and with a relatively narrow molecular weight distribution ( $M_w/M_n = 1.22$ ,  $M_n = 157,000\text{ g/mol}$ ).<sup>70</sup> Shiono and co-workers also demonstrated significant solvent effects on the tacticity of the resulting PP.<sup>71</sup> For example, polymerization of propylene with **15**/dMAO in heptane at  $0\text{ }^\circ\text{C}$  results in polymer with higher tacticity than when the reaction is carried out in toluene ( $[rr] = 0.73$  vs. 0.60) or chlorobenzene ( $[rr] = 0.42$ ).

Utilizing these solvent effects, Shiono and co-workers cleverly prepared stereoblock copolymers of propylene containing *s*PP and *a*PP segments (Scheme 1.3) by initial polymerization in heptane followed by addition of more propylene and chlorobenzene.<sup>72</sup> The resultant *s*PP-*block*-*a*PP had  $M_n = 94,700$  g/mol with a narrow PDI ( $M_w/M_n = 1.27$ ). Shiono and co-workers have also described similar effects of the tacticity of PP generated from **15**/dMMAO under varying propylene pressures.<sup>73</sup> At low pressure (0.2 atm) atactic PP is furnished, but at higher pressure (1 atm) syndiotactic PP is generated. A *s*PP-*block*-*a*PP copolymer and *s*PP-*block*-*a*PP-*block*-*s*PP copolymer were synthesized by varying propylene pressure over the course of the polymerization.



**Scheme 1.3.** Synthesis of *s*PP-*block*-*a*PP using solvent polarity to control tacticity.

Shiono and co-workers also examined structural variants of **15** (**16** and **17**, Figure 1.10) by introducing *tert*-butyl substituents into the fluorenyl ligand framework.<sup>74</sup> When activated with dried MMAO (dMMAO) at 0 °C, **16** produced *s*PP ( $[rr] \sim 0.83$ ). While the molecular weight distribution was somewhat broad ( $M_w/M_n = 1.68$ ,  $M_n = 202,000$  g/mol), a two-stage sequential polymerization of 0.63 g of propylene revealed a nearly doubling of molecular weight than was obtained from a single-stage polymerization. Catalyst **17**/dMMAO furnished polymer with even higher tacticity ( $[rr] \sim 0.93$ ) and lower molecular weight distribution ( $M_w/M_n = 1.45$ ). After

further expanding the sterics about the fluorenyl, **18**/dMMAO (Figure 1.10) was utilized in the production of polypropylene with decreased syndioselectivity ( $[rr] \sim 0.45$ ) compared to the polymer obtained from **17**/dMMAO.<sup>75</sup> While molecular weights ( $M_n = 44,000 - 150,000$  g/mol) increased with polymer yield, molecular weight distributions were broadened ( $M_w/M_n = 2.91 - 4.61$ ). Although some characteristics of a living polymerization were exhibited, a two-stage sequential polymerization resulted in polypropylene which was nearly identical to that obtained from the single-stage polymerization. Further increasing the steric bulk of the fluorenyl ligand from **17** to **18** resulted in a loss of both living character and syndioselectivity for the polymerization of propylene. Employing an indenyl-based ligand, **19**/dMAO (Figure 1.11) at 0 °C affords iso-enriched PP ( $[mm] = 0.40$ ) with quasi-living behavior.<sup>76</sup> Later, Dare and co-workers reported that a similar complex **20**/MAO (Figure 1.11) furnished PP at 0 °C that was syndio-enriched ( $[rr] = 0.56$ ) and exhibited a somewhat narrow PDI ( $M_w/M_n = 1.37$ ,  $M_n = 108,000$  g/mol).<sup>77</sup>

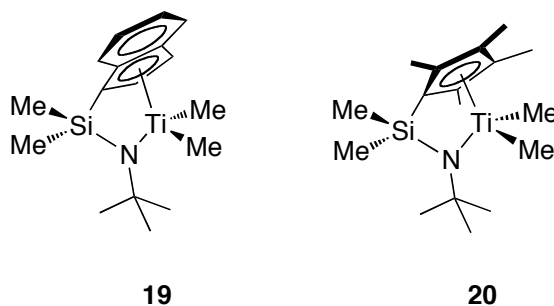


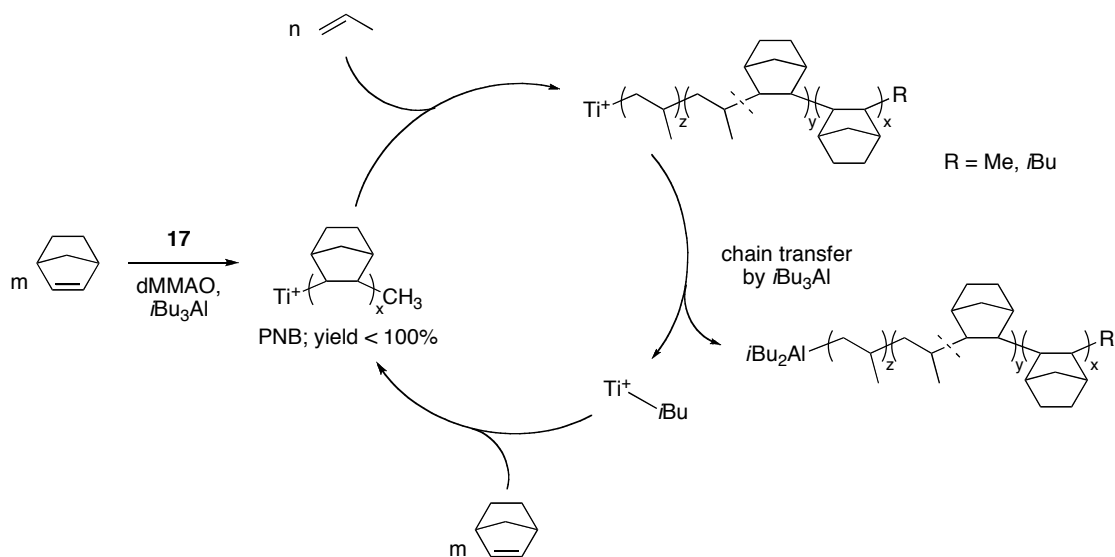
**Figure 1.11.** Monocyclopentadienyl-amido catalyst precursors with increased steric bulk.

In addition to linear  $\alpha$ -olefins, Shino and co-workers reported that **15**/MAO (Figure 1.10) catalyzed the living copolymerization of ethylene and norbornene. For example, at 0 °C **15**/MAO can furnish poly(*E-co*-NB) with 53 mol% norbornene and  $M_n = 78,000$  g/mol with  $M_w/M_n = 1.16$ .<sup>78</sup> Furthermore, a linear increase in  $M_n$  with

reaction time was observed for this system. When activated with MAO at 40 °C, a similar compound, **20** (Figure 1.11), also provided ethylene-norbornene copolymers with fairly narrow PDIs ( $M_w/M_n = 1.21 - 1.27$ ).<sup>79</sup>

Shiono and co-workers also reported the living copolymerization of propylene and norbornene with **15**/dMAO to produce copolymers with very high  $T_g$  values (249 °C) and narrow molecular weight distributions ( $M_w/M_n = 1.16$ ).<sup>80</sup> In a later report, the copolymerization of higher  $\alpha$ -olefins (1-hexene, 1-octene, and 1-decene) with norbornene by **15**/MAO was reported, however, molecular weight distributions were somewhat broadened ( $M_w/M_n = 1.36 - 1.72$ ).<sup>81</sup>

Furthermore, activation of **17** (Figure 1.10) with dMMAO containing 0.4 mol % of triisobutylaluminum (TIBA) in the presence of norbornene catalyzed living polymerization at 20 °C.<sup>82</sup> The molecular weight distributions obtained were narrow ( $M_w/M_n = 1.07 - 1.08$ ). A two-stage reaction was shown to increase the molecular weight of the second-step by double that of the first step when each was carried to quantitative conversion.



**Scheme 1.4.** Catalytic synthesis of block copolymers from norbornene and propylene.

In addition, Shiono and co-workers were able to show in 2006 that **17**/MAO could also copolymerize propylene and norbornene in a living fashion to form random and block copolymers.<sup>83</sup> For example, three *sPP-block-poly(P-co-NB)* diblock copolymers were synthesized through sequential monomer addition that had similar molecular weights ( $M_n \sim 20,000$  g/mol,  $M_w/M_n = 1.21 - 1.32$ ). Shiono and co-workers were able to show that **17**/dMMAO containing 1.8 mol% TIBA could furnish PNB-*block-poly(P-co-NB)-block-PP* triblock copolymers in a catalytic fashion.<sup>82</sup> The successive addition of norbornene and propylene before complete consumption of norbornene gives PNB-*block-poly(P-co-NB)-block-PP* terminated with a Ti-PP bond, which can be exchanged with TIBA. Repeated addition of norbornene and propylene gives a catalytic synthesis of the triblock copolymers in this system (Scheme 1.4).

### 1.3.4 Monocyclopentadienylzirconium Amidinate Catalysts

In 2000, Sita and Jayaratne reported monocyclopentadienyl acetamidinate zirconium dimethyl compounds that exhibited living polymerization behavior at temperatures between -10 and 0 °C.<sup>84</sup> At 0 °C, **21a**/[PhNMe<sub>2</sub>H][B(C<sub>6</sub>F<sub>5</sub>)<sub>4</sub>] (Figure 1.12) formed atactic poly(1-hexene) with a narrow polydispersity ( $M_w/M_n = 1.10$ ) and lack of olefinic resonances in <sup>13</sup>C and <sup>1</sup>H NMR spectra. The C<sub>1</sub>-symmetric complex, **21b**, when activated in an identical manner at -10 °C furnished highly isotactic poly(1-hexene) ( $[mmmm] > 0.95$ ) with a narrow molecular weight distribution ( $M_w/M_n = 1.03 - 1.13$ ). The molecular weight was shown to increase linearly with conversion. This was the first report of a Ziegler-Natta polymerization catalyst that was both living and highly isospecific for  $\alpha$ -olefin polymerization. Covalently attaching **21b** to a crosslinked PS support was also shown to furnish a living and isoselective 1-hexene polymerization catalyst (**22**, Figure 1.12).<sup>85</sup> The hafnium congener of **21b** (**23a**, Figure

1.12) and its diisobutyl analogue (**23b**) were also shown to be living and isospecific 1-hexene polymerization catalysts albeit with a rate ca. 60 times slower than **21b**.<sup>86</sup>

As discussed above, **21b**/[PhNMe<sub>2</sub>H][B(C<sub>6</sub>F<sub>5</sub>)<sub>4</sub>] polymerizes 1-hexene in a living manner to produce highly isotactic poly(1-hexene). However, when a sub-stoichiometric amount of the borate is used (e.g. [PhNMe<sub>2</sub>H][B(C<sub>6</sub>F<sub>5</sub>)<sub>4</sub>] : [**21b**] = 0.5), the resulting polymer is considerably less isotactic with a *[mm]* content of approximately 45 – 50% resulting from degenerative-transfer polymerization (Scheme

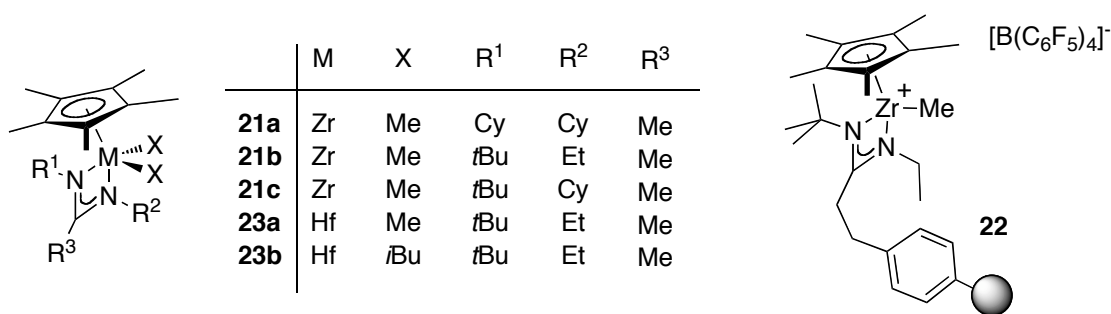


**Figure 1.12.** Monocyclopentadienyl amidinate catalysts for olefin polymerization.

1.5), which will be discussed in detail in the following section. This system has been employed to make a diblock poly( $\alpha$ -olefin) sample.<sup>87</sup> Initially, **21b** was activated with 0.5 equivalent of [PhNMe<sub>2</sub>H][B(C<sub>6</sub>F<sub>5</sub>)<sub>4</sub>] and used to polymerize 1-hexene resulting in the formation of an atactic poly(1-hexene) block. After 2 hours, 1-octene was added along with an additional 0.5 equivalent of the borate leading to the growth of an isotactic poly(1-octene) block. GPC analysis revealed clean formation of the *a*PH-*block-i*-poly(1-octene) diblock copolymer with  $M_n = 12,400$  g/mol and  $M_w/M_n = 1.04$ .

Upon replacing the Cp\* moiety with the less sterically demanding Cp ligand, Sita and co-workers were able to greatly increase the 1-hexene polymerization activity for this class of catalysts.<sup>88</sup> When activated with [PhNMe<sub>2</sub>H][B(C<sub>6</sub>F<sub>5</sub>)<sub>4</sub>] at -10 °C, compounds **24a-c** (Figure 1.13) furnished atactic poly(1-hexene)s with narrow

molecular weight distributions ( $M_w/M_n = 1.03 - 1.10$ ), however, a decrease in enantiofacial selectivity was also observed. The more open environment of the active site did impart the ability to polymerize the more challenging vinylcyclohexane. Upon activation with  $[\text{PhNMe}_2\text{H}][\text{B}(\text{C}_6\text{F}_5)_4]$  at  $-10\text{ }^\circ\text{C}$ , **24a,b** furnished highly isotactic poly(vinylcyclohexane)s ( $[mmmm] = 0.95$ ) with narrow polydispersities ( $M_w/M_n = 1.04 - 1.10$ ). The authors postulate that the high degree of isoselectivity displayed is likely the result of chain-end control. Exploiting the living nature of **24c**/ $[\text{Ph}_3\text{C}][\text{B}(\text{C}_6\text{F}_5)_4]$  for 1-hexene and vinylcyclohexane (VCH) polymerization, a triblock copolymer of isotactic poly(vinylcyclohexane)-*block*-atactic-poly(1-hexene)-*block*-isotactic-poly(vinylcyclohexane) was prepared via sequential monomer addition.<sup>88</sup> The triblock copolymer exhibited a narrow polydispersity ( $M_w/M_n = 1.08$ ) and  $M_n = 24,400\text{ g/mol}$  with a vinylcyclohexane content of 33 mol%.

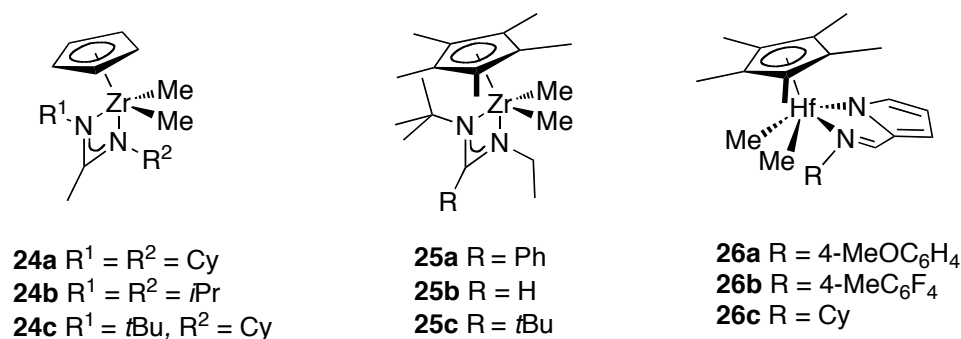


**Figure 1.13.** Monocyclopentadienyl amidinate catalysts with varying steric bulk.

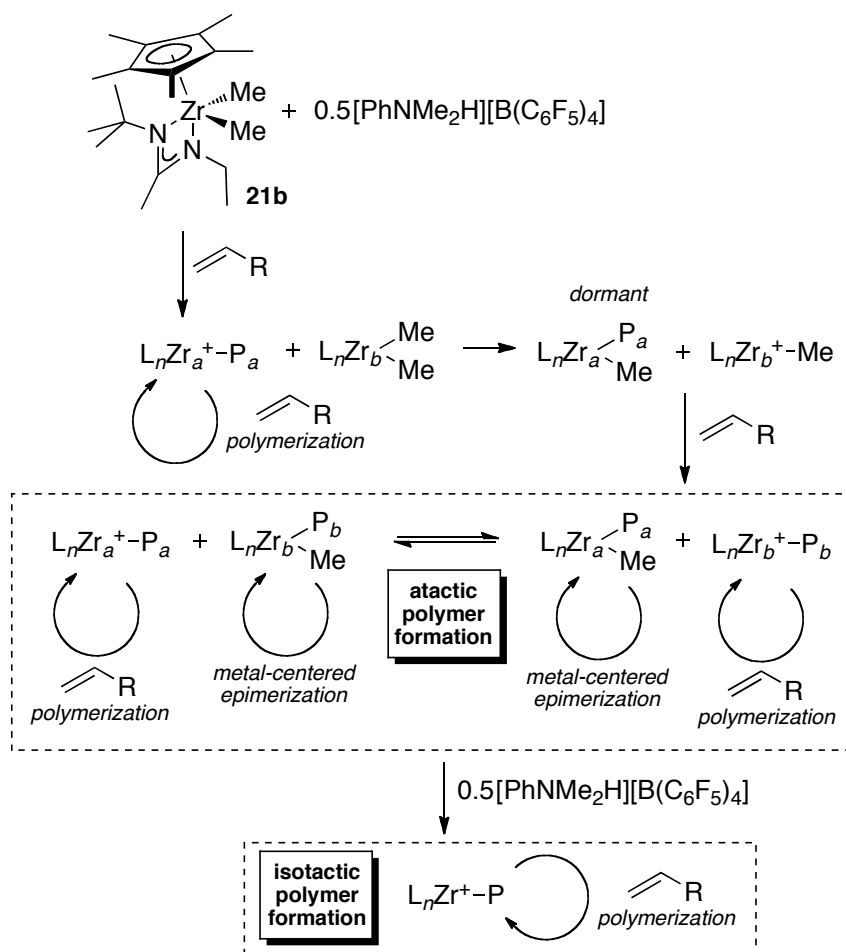
In 2004, the effect of further structural elaboration of the amidinate ligand framework on polymerization behavior was reported.<sup>89</sup> Specifically, altering the identity of the distal  $R^3$  substituent (Figure 1.13) led to dramatic effects on both the living character and stereospecificity of 1-hexene polymerization. At  $-10\text{ }^\circ\text{C}$ , polymerization of 1-hexene by **25a** or **25b** ( $R^3 = \text{Ph}$  or  $\text{H}$ )/ $[\text{PhNMe}_2\text{H}][\text{B}(\text{C}_6\text{F}_5)_4]$  furnished polymer with a significantly lower degree of isotacticity than the poly(1-

hexene) produced by **21b**/[PhNMe<sub>2</sub>H][B(C<sub>6</sub>F<sub>5</sub>)<sub>4</sub>], and in the case of **25b**, the polymerization is no longer living. Furthermore, **25c** (R<sup>3</sup> = *t*Bu)/[PhNMe<sub>2</sub>H][B(C<sub>6</sub>F<sub>5</sub>)<sub>4</sub>] was found to be completely inactive for polymerization. The loss in stereocontrol of **25a** was attributed to a “buttressing effect” by which the *t*Bu and Et groups were “pushed” forward toward the active site leading to a lack of steric discrimination at the metal center for olefin coordination. The decrease in stereoselectivity of **25b** was attributed to a low barrier to metal-centered epimerization relative to **21b**.

Interested in further varying the amidinate portion of the catalyst, Mashima and co-workers recently reported the synthesis and 1-hexene polymerization behavior of Cp\* hafnium dimethyl complexes bearing an iminopyrrolyl ligand.<sup>90</sup> At 0 °C or below, compounds **26a-c**/[Ph<sub>3</sub>C][B(C<sub>6</sub>F<sub>5</sub>)<sub>4</sub>] (Figure 1.13) polymerized 1-hexene to furnish polymers with narrow molecular weight distributions ( $M_w/M_n = 1.07 - 1.12$ ) and  $M_n = 9,000 - 36,100$  g/mol. The poly(1-hexene)s were all significantly isoenriched with the highest level of isotacticity ( $[mmmm] = 0.90$ ) being obtained from **26b** at -20 °C. The polymerization of 1-hexene with **26a** exhibited a linear dependence of  $M_n$  versus time at -20 and 0 °C.

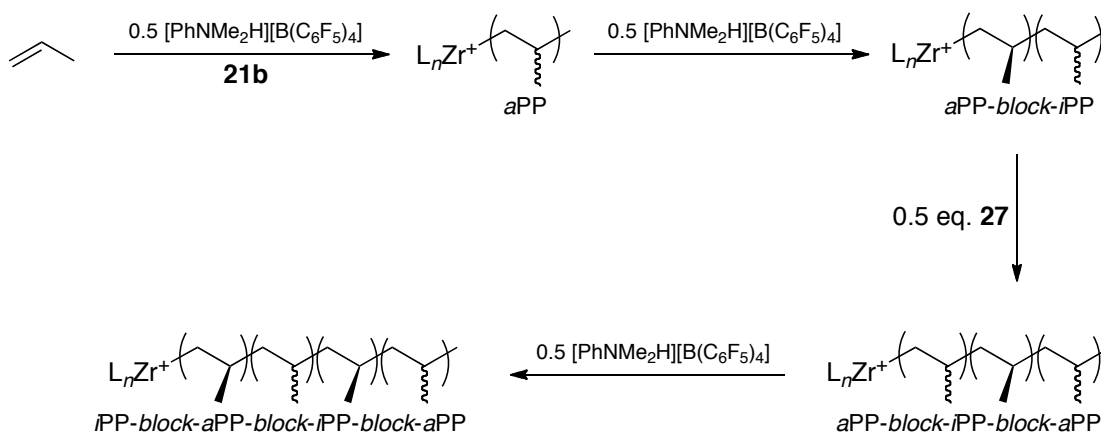
In addition to living 1-hexene polymerization, Sita and co-workers have shown that **21b** activated with [PhNMe<sub>2</sub>H][B(C<sub>6</sub>F<sub>5</sub>)<sub>4</sub>] in a stoichiometric ratio furnished highly isotactic PP ( $[mmmm] = 0.71$ ) in a living fashion ( $M_w/M_n \leq 1.20$ ).<sup>26</sup> Interestingly, activation with 0.5 equivalents of [PhNMe<sub>2</sub>H][B(C<sub>6</sub>F<sub>5</sub>)<sub>4</sub>] resulted in the production of atactic PP where the  $M_n$  was also shown to increase linearly with time ( $M_w/M_n \sim 1.05$ ). A degenerative-transfer (DT) polymerization that proceeds through a rapid and reversible methyl group transfer between the cationic (active) and neutral (dormant) zirconium centers was considered as the mechanism for this living system (Scheme 1.5).<sup>87</sup> Additionally, the methyl-polymeryl dormant species can undergo

epimerization that is faster than propagation. Thus, through a combination of methyl group transfer and epimerization at dormant sites, each occurring faster than propagation, stereocontrol is greatly diminished leading to an atactic microstructure. However, upon addition of a second 0.5 equivalent of  $[\text{PhNMe}_2\text{H}][\text{B}(\text{C}_6\text{F}_5)_4]$ , all Zr species become active for polymerization thereby “turning off” DT and initiating isospecific polymerization, which can advantageously be used for the production of block copolymers. Later, Sita and co-workers synthesized stereogradient PP by initial polymerization under DT polymerization conditions followed by slow introduction of  $[\text{PhNMe}_2\text{H}][\text{B}(\text{C}_6\text{F}_5)_4]$  to 100% activation.<sup>91</sup>



**Scheme 1.5.** Degenerative group transfer polymerization employing **21b**.

The living degenerative transfer system that was employed by Sita and co-workers to make block copolymers from 1-hexene and 1-octene was also applied to propylene polymerization.<sup>26</sup> Formation of a PP diblock copolymer with **21b**/[PhNMe<sub>2</sub>H][B(C<sub>6</sub>F<sub>5</sub>)<sub>4</sub>] was accomplished by initial activation with 0.5 equivalents of [PhNMe<sub>2</sub>H][B(C<sub>6</sub>F<sub>5</sub>)<sub>4</sub>] furnishing an atactic PP segment followed by complete activation with another 0.5 equivalents of [PhNMe<sub>2</sub>H][B(C<sub>6</sub>F<sub>5</sub>)<sub>4</sub>] to furnish the *a*PP-*block-i*PP. It was found that related complex **27** could effectively reinvoke degenerative-transfer by *irreversibly* transferring a methyl group to the active polymerization species. In addition to synthesizing an *a*PP-*block-i*PP diblock copolymer, an *a*PP-*block-i*PP-*block-a*PP triblock and an *a*PP-*block-i*PP-*block-a*PP-*block-i*PP tetrablock sample were formed (Scheme 1.6). The polymers had very similar molecular weights ( $M_n = 164,200 - 172,400$  g/mol,  $M_w/M_n = 1.19$ ). Testing of the tensile properties of the block copolymers showed good elastomeric behavior. For example, the triblock copolymer displayed an elongation to break of 1530%, the highest of the three samples.



**Scheme 1.6.** Synthesis of propylene-based block copolymers using **21b**.

Sita and co-workers also prepared bimetallic analogues of **21b** to investigate further the effects of DT polymerization (**28a-c**, Figure 1.14).<sup>92</sup> Upon activation with 2 equivalents of  $[\text{PhNMe}_2\text{H}][\text{B}(\text{C}_6\text{F}_5)_4]$  at  $-10\text{ }^\circ\text{C}$ , compounds **28a-c** were all found to be living and isoselective for propylene polymerization ( $M_n$  up to 50,000 g/mol,  $M_w/M_n = 1.1 - 1.2$ ), with the degree of stereoselectivity decreasing as the two metal centers are brought closer together. Activation under sub-stoichiometric conditions led to living DT polymerization. Under these conditions, the frequency of  $[mr]$  stereoerrors in the PP decrease as the two metal centers are brought closer together resulting from an increased barrier to metal-centered epimerization of the dormant site. A linear increase in  $M_n$  with time was observed for **28a** under sub-stoichiometric activation conditions to further illustrate the living behavior of the system.

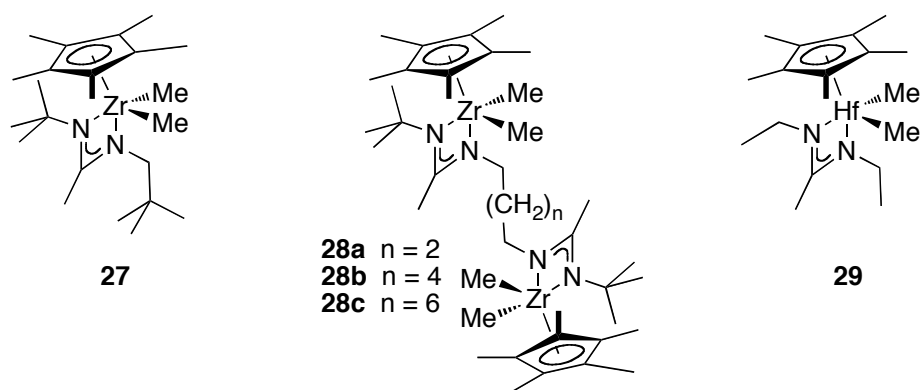


**Figure 1.14.** Mono- and bimetallic monocyclopentadienyl amidinate complexes.

Sita and co-workers have also reported a modified amidinate hafnium catalyst (**29**, Figure 1.14) that furnished atactic PP of high molecular weight ( $M_n = 137,000$  g/mol,  $M_w/M_n = 1.12$ ) upon activation with one equivalent of  $[\text{PhNMe}_2\text{H}][\text{B}(\text{C}_6\text{F}_5)_4]$  at  $-10\text{ }^\circ\text{C}$ .<sup>93</sup>  $M_n$  of up to 830,000 g/mol could be obtained with this system, however significant broadening of the PDI was observed ( $M_w/M_n = 2.43$ ). Furthermore, this system demonstrated the first example of living coordinative chain-transfer

polymerization (CCTP)<sup>94</sup> of propylene with diethyl zinc. It was further used for the living CCTP of ethylene, 1-hexene, 1-octene, and 1,5-hexadiene in addition to living CCTP copolymerization of ethylene with the aforementioned higher  $\alpha$ -olefins.<sup>95</sup>

In addition to simple  $\alpha$ -olefins such propylene, Sita and co-workers showed that **21a-c**/[PhNMe<sub>2</sub>H][B(C<sub>6</sub>F<sub>5</sub>)<sub>4</sub>] (Figure 1.12) were active for the cyclopolymerization of 1,5-hexadiene at -10 °C.<sup>96</sup> The polymers produced possessed  $\geq$  98 % MCP units, and exhibited narrow polydispersities ( $M_w/M_n = 1.03 - 1.09$ ). The selectivity of ring-closure was ubiquitously *trans*; the stereoselectivity increasing with increasing steric bulk of the amidinate ligand (**21a**: % *trans* = 64; **21c**: % *trans* = 82).

Utilizing the living behavior of **21b**/[PhNMe<sub>2</sub>H][B(C<sub>6</sub>F<sub>5</sub>)<sub>4</sub>], Sita and co-workers were able to prepare diblock and triblock copolymers of 1-hexene and 1,5-hexadiene.<sup>96</sup> At -10 °C, isotactic poly(1-hexene)-*block*-PMCP and isotactic-poly(1-hexene)-*block*-PMCP-*block*-poly(1-hexene) were obtained from **21b**/[PhNMe<sub>2</sub>H][B(C<sub>6</sub>F<sub>5</sub>)<sub>4</sub>] through sequential monomer addition. The diblock copolymer possessed  $M_w/M_n = 1.05$  and  $M_n = 22,800$  g/mol with  $T_m = 91$  °C. The triblock copolymer had  $M_w/M_n = 1.10$ ,  $M_n = 30,900$  g/mol, and  $T_m = 79$  °C. Atomic force microscopy (AFM) revealed that microphase separation of the crystalline PMCP and amorphous poly(1-hexene) had occurred.

### 1.3.5 Catalysts Bearing Diamido Ligands

While Group 4 metallocene-based olefin polymerization catalysts have dominated the field of homogenous olefin polymerization catalysis since the late 1950s,<sup>1</sup> the development of complexes bearing non-Cp ligands as potential olefin polymerization catalysts has become a rapidly expanding area over the last 15 years.<sup>97,98</sup> McConville and Scollard reported that titanium complexes bearing diamide ligands, compounds **30a,b** (Figure 1.15), polymerized 1-hexene, 1-octene, and 1-

decene to high molecular weight ( $M_n = 121,500 - 164,200$  g/mol) and narrow polydispersity index (PDI) ( $M_w/M_n = 1.07$ ) upon activation with  $B(C_6F_5)_3$  at room temperature.<sup>99</sup> Polymerization of 1-hexene by **30b**/ $B(C_6F_5)_3$  exhibited a linear increase of  $M_n$  with time. Later, Kim and co-workers reported the living polymerization of 1-hexene catalyzed by a structurally similar zirconium diamide with an ethylene bridging unit (**31**).<sup>100</sup> When activated with  $B(C_6F_5)_3$  at  $-10$  °C, **31** (Figure 1.15) furnished poly(1-hexene)s with  $M_n =$  ca. 30,000 – 175,000 g/mol and  $M_w/M_n = 1.18 - 1.27$ . It was also shown that the  $M_n$  increased linearly with increasing monomer loading. Utilizing sequential monomer addition, Kim and co-workers prepared a block copolymer of 1-hexene and 1-octene.<sup>100</sup> The polymer produced at 0 °C possessed a narrow polydispersity ( $M_w/M_n = 1.21$ ) and a  $M_n = 108,730$  g/mol.

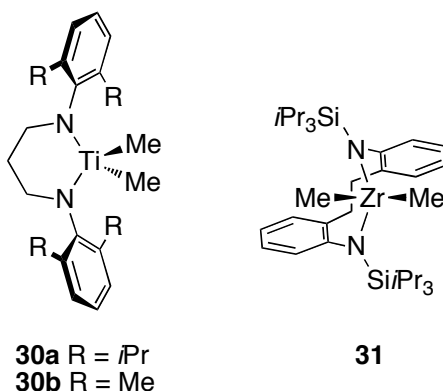


**Figure 1.15.** Titanium and zirconium complexes bearing diamido ligands.

In 2002, Shiono and co-workers reported that upon activation with dMMAO at 0 °C, McConville's dimethyldiamidotitanium complex (**30a**, Figure 1.15) was capable of polymerizing propylene in a living manner.<sup>101</sup> The PPs obtained from **30a**/dMMAO were atactic and displayed narrow molecular weight distributions ( $M_w/M_n =$  ca. 1.16 – 1.3). The  $M_n$  was shown to increase linearly with polymerization time from 10 – 25 minutes ( $M_n$  up to ca. 30,000 g/mol). In later reports, Shiono and co-workers discussed

the effects of supported MMAOs on the propylene polymerization behavior of **30a**.<sup>102-105</sup> Three different supports for MMAO were investigated: SiO<sub>2</sub>, Al<sub>2</sub>O<sub>3</sub>, and MgO. Regardless of the support, polymerization of propylene by **30a**/supported MMAO at 0 °C exhibited a linear increase of  $M_n$  with time

### 1.3.6 Catalysts Bearing Diamido Ligands with Neutral Donors

Interested in investigating the effects of neutral donors on the diamido olefin polymerization systems, Schrock and co-workers synthesized tridentate diamido group IV complexes bearing a central oxygen donor. The authors postulated the neutral donor would enhance stability of the corresponding cationic alkyl active species.<sup>106,107</sup> At 0 °C, **32a**/[PhNMe<sub>2</sub>H][B(C<sub>6</sub>F<sub>5</sub>)<sub>4</sub>] (Figure 1.16), furnished atactic poly(1-hexene) (*aPH*) with  $M_n = \text{ca. } 4,000 - 40,000 \text{ g/mol}$  and  $M_w/M_n = 1.02 - 1.14$ . A linear increase in  $M_n$  with monomer conversion was observed. Upon activation with [PhNMe<sub>2</sub>H][B(C<sub>6</sub>F<sub>5</sub>)<sub>4</sub>], the titanium congener (**32b**) decomposed to unidentifiable species, which were not active for 1-hexene polymerization. The analogous hafnium complex (**32c**) furnished poly(1-hexene) with broadened molecular weight distribution ( $M_w/M_n = 1.19 - 1.53$ ) and anomalous  $M_n$ -values when activated with [PhNMe<sub>2</sub>H][B(C<sub>6</sub>F<sub>5</sub>)<sub>4</sub>].

Schrock and co-workers developed a second class of catalysts bearing diamidopyridine ligands that were shown to be effective living olefin polymerization catalysts.<sup>108</sup> The diamidopyridine zirconium complexes **33a,b** (Figure 1.16) when activated with [Ph<sub>3</sub>C][B(C<sub>6</sub>F<sub>5</sub>)<sub>4</sub>] produce poly(1-hexene)s with narrow polydispersities ( $M_w/M_n < 1.08$ ). The identity of the alkyl group bound to zirconium was shown to greatly affect the polymerization behavior. Upon activation, **33a** reacts with 1-hexene to a significant extent by 2,1-insertion into the initial Zr-Me bond to give a 3-heptyl complex that undergoes  $\beta$ -H elimination to yield 2-heptenes. Only a fraction that

undergoes 1,2-insertion gives a stable propagating species. No 2,1-insertion into the Zr-*i*Bu bond is observed upon activation of **33b** giving rise to a relatively well-behaved polymerization system in which  $M_n$  values are three times higher than those expected based on the assumption of one polymer chain per metal center ( $M_n^{\text{theo}}$ ). At 0 °C, the diisobutyl hafnium analogue (**34**) was shown to polymerize 1-hexene in a living fashion upon activation with  $[\text{Ph}_3\text{C}][\text{B}(\text{C}_6\text{F}_5)_4]$  to furnish poly(1-hexene)s with  $M_w/M_n = 1.02 - 1.05$  and  $M_n = 10,000 - 50,000$  g/mol that matches  $M_n^{\text{theo}}$ .<sup>109,110</sup> The apparent difference in polymerization behavior is attributed to greater stability toward  $\beta$ -H elimination in this system. Upon replacing the mesityl groups with 2,6- $\text{C}_6\text{H}_3\text{Cl}_2$  within the ligand framework of **34**, Schrock and co-workers found that the living character of 1-hexene polymerization catalyzed by **35**/ $[\text{Ph}_3\text{C}][\text{B}(\text{C}_6\text{F}_3)_4]$  was slightly diminished with evidence of  $\beta$ -H elimination.<sup>111</sup> Despite the fact that  $\beta$ -H elimination was observed, the resultant polymers still displayed narrow polydispersities ( $M_w/M_n = 1.01 - 1.05$ ) and the  $M_n$  values were about 90 % of those expected.

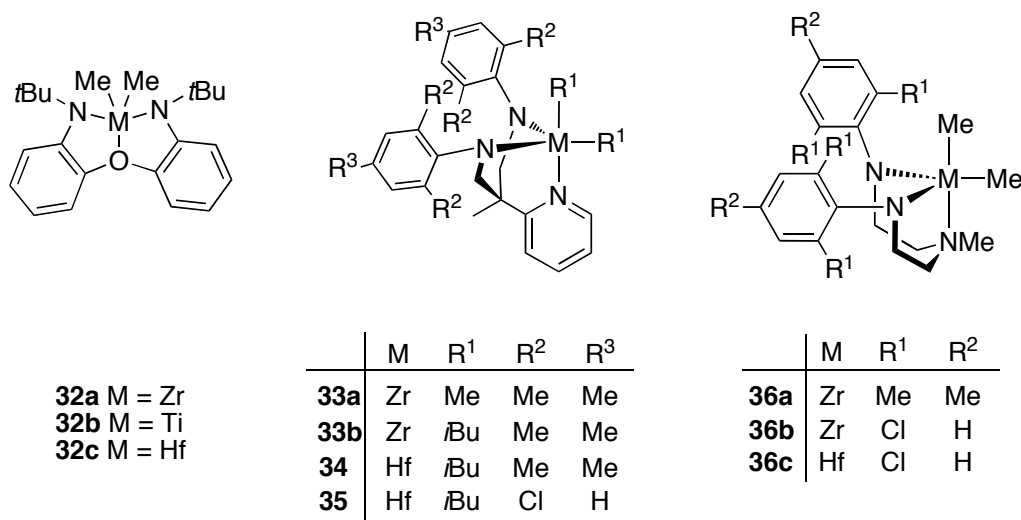


**Figure 1.16.** Olefin polymerization precatalysts bearing diamido ligands with neutral donors.

The diamidoamine complexes of zirconium and hafnium are a third class of compounds for olefin polymerization introduced by Schrock and co-workers.<sup>112-114</sup> When activated with  $[\text{Ph}_3\text{C}][\text{B}(\text{C}_6\text{F}_5)_4]$ , **36a** ( $\text{R}^1 = \text{R}^2 = \text{Me}$ , Figure 1.16) was shown to be active for 1-hexene polymerization furnishing poly(1-hexene)s that possessed  $M_w/M_n = 1.1 - 2.1$  and  $M_n = 19,200 - 45,000$  g/mol that deviated from the expected values.<sup>112</sup> Later studies showed that **36a** undergoes deactivation via an intramolecular C-H activation of the *ortho*-Me on the mesityl group upon methide abstraction. Replacing the *ortho*-Me with *ortho*-Cl (**36b**) and subsequent activation with  $[\text{PhNMe}_2\text{H}][\text{B}(\text{C}_6\text{F}_5)_4]$  at 0 °C gives rise to a catalyst that is living for 1-hexene polymerization.<sup>113</sup> The resultant polymer exhibited narrow polydispersities ( $M_w/M_n = 1.01 - 1.04$ ) and  $M_n$  values that were in good agreement with  $M_n^{\text{theo}}$ . Utilizing  $[\text{Ph}_3\text{C}][\text{B}(\text{C}_6\text{F}_5)_4]$  or  $\text{B}(\text{C}_6\text{F}_5)_3$  as an activator, the hafnium analogue of **36b** (**36c**) exhibited significant termination via  $\beta$ -H elimination.<sup>114</sup>

### 1.3.7 Amine-phenolate Titanium and Zirconium Catalysts

In 2000, Kol and co-workers reported the synthesis and subsequent olefin polymerization behavior of a titanium complex bearing an amine bis(phenolate) ligand which incorporated an additional amino side-arm donor (**37a**, Figure 1.17).<sup>115</sup> When activated with  $\text{B}(\text{C}_6\text{F}_5)_3$  at room temperature, **37a** furnished atactic poly(1-hexene)s with narrow molecular distributions ( $M_w/M_n = 1.09 - 1.18$ ) and the  $M_n$  was shown to increase linearly with time. Upon omission of the amino side-arm donor (**38**), only low molecular weight poly(1-hexene) ( $M_n = \text{ca. } 2,000$  g/mol) with  $M_w/M_n = 1.92 - 2.43$  was obtained. However, replacing the bulky *t*Bu groups with sterically less demanding chlorides (**37b**) allowed the living polymerization of 4-methyl-1-pentene to furnish atactic poly(4-methyl-1-pentene).<sup>116</sup>

Kol and co-workers also reported in 2000 the synthesis and polymerization behavior of the  $C_2$ -symmetric, ethylene-bridged zirconium analogue (**39a**, Figure 1.17) of **37a**.<sup>117</sup> At room temperature, **39a**/ $B(C_6F_5)_3$  furnished highly isotactic poly(1-hexene) and poly(1-octene). The poly(1-hexene)s exhibited narrow polydispersities ( $M_w/M_n = 1.11 - 1.15$ ) with  $M_n = \text{ca. } 4,000 - 12,000 \text{ g/mol}$ ; the  $M_n$  was shown to increase linearly with monomer consumption. Reducing the substituent size on the phenoxide moiety (**39b**) resulted in atactic poly(1-hexene) with a broadened molecular weight distribution ( $M_w/M_n = 1.57$ ). In a subsequent report, it was shown that replacing the *ortho*- and *para*-*tert*-butyl substituents of **39a** with chlorides (**39c**) resulted in greatly diminished living behavior.<sup>118</sup> Importantly, the titanium congener (**39d**) and the analogous 2,4-dibromophenol-bearing complex (**39e**) polymerized 1-hexene in a living manner for a period of 40 to 75 minutes when activated with  $B(C_6F_5)_3$ . The poly(1-hexene)s exhibited extremely high molecular weights ( $M_n$  up to 1,750,000 g/mol,  $M_w/M_n \leq 1.2$ ) and moderate degrees of isotacticity (**39d**:  $[mm] = 0.60$ , **39e**:  $[mm] = 0.80$ ).

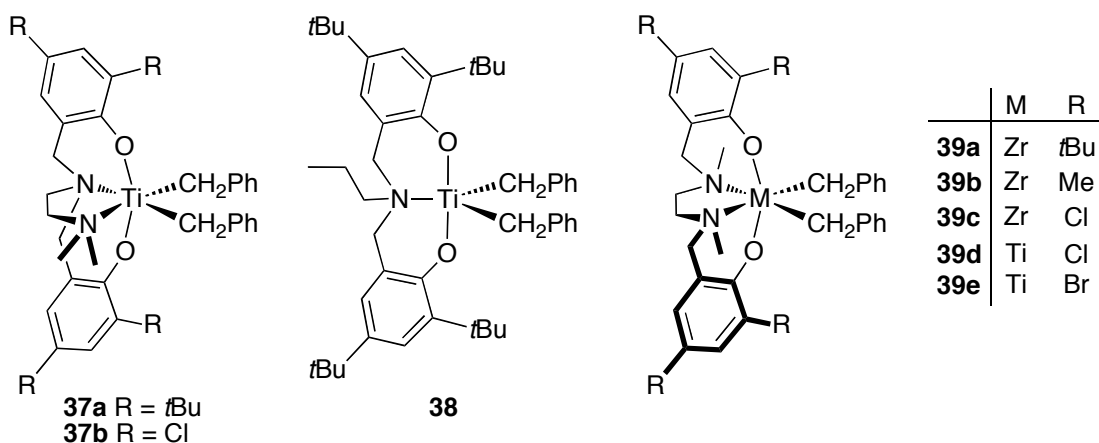


**Figure 1.17.** Titanium and zirconium complexes bearing [ONNO] and [ONO] ligands.

A third class of novel olefin polymerization catalysts featuring [ONOO] Group 4 metal complexes bearing a methoxy side-arm donor (**40**) was introduced by Kol and co-workers in 2001.<sup>119</sup> At room temperature, **40**/ $B(C_6F_5)_3$  (Figure 1.18) furnished poly(1-hexene)s with narrow polydispersities ( $M_w/M_n = 1.07 - 1.12$ ) and high molecular weights ( $M_n$  up to 445,000 g/mol). A linear increase in  $M_n$  with increasing reaction time was observed for up to 31 hours. The living character of the polymerization was maintained upon heating to 65 °C for one hour as evidenced by the narrow polydispersity of the resultant polymer ( $M_w/M_n = 1.30$ ). Kol and co-workers were able to apply this catalyst system to the synthesis of block copolymers of 1-hexene and 1-octene.<sup>119,120</sup> Using **40**/ $B(C_6F_5)_3$  a block copolymer of 1-hexene and 1-octene was prepared via sequential monomer addition where each domain had an atactic microstructure. The polymer possessed a narrow molecular weight distribution ( $M_w/M_n = 1.2$ ) and a  $M_n = 11,600$  g/mol. Further modification of the catalyst system through introduction of the 2,4-dimethyl or 2,4-dichloro phenoxide moiety led to a loss of living character.<sup>121</sup> Additionally, the zirconium and hafnium analogues of **40** were also shown to deviated from living behavior ( $M_w/M_n = 1.4 - 3.0$ ).<sup>122</sup>

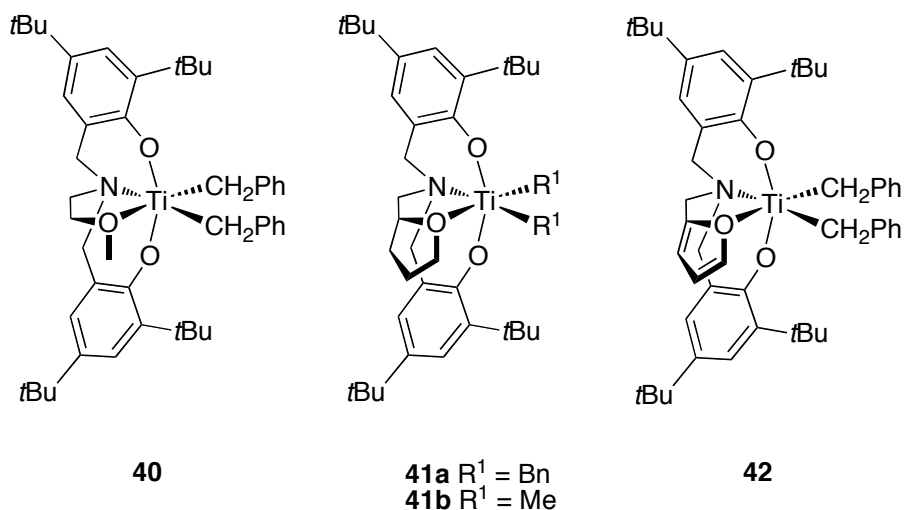


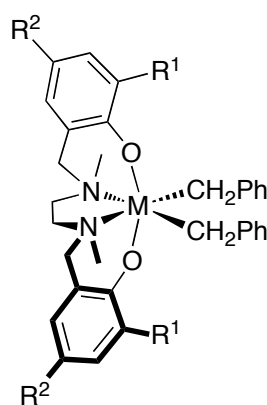
**Figure 1.18.** Titanium complexes bearing [ONOO] ligands.

The effect of the neutral oxygen donor's identity on the polymerization behavior of the [ONOO] titanium complexes has also been investigated. Substituting the methoxy donor of **40** with a THF-moiety (**41a**, Figure 1.18) lead to similar polymerization results, however, replacing the benzyl ligands with methyl ligands (**41b**) results in a dramatic increase in the duration of the living period for up to 6 days at room temperature upon activation with  $B(C_6F_5)_3$ . The resultant atactic poly(1-hexene) had a  $M_n$  up to 816,000 g/mol and  $M_w/M_n = 1.04 - 1.12$ .<sup>120</sup> The extremely long-lived catalyst generated from **41a** was used to prepare a block copolymer of 1-hexene and 1-octene through sequential monomer addition to furnish poly(1-hexene)-*block*-poly(1-octene). The block copolymer had  $M_n = 34,000$  g/mol while maintaining the low  $M_w/M_n = 1.16$ .

Further modification of the system through introduction of a furan donor (**42**, Figure 1.18) into the ligand framework led to a ten-fold increase in polymerization activity relative to **41a**/ $B(C_6F_5)_3$  furnishing poly(1-hexene)s of high molecular weight ( $M_n$  up to 500,000 g/mol,  $M_w/M_n \leq 1.37$ ).<sup>123</sup> The increase in activity of **42**/ $B(C_6F_5)_3$  resulted in diminished living character of the 1-hexene polymerization exhibiting a linear increase in  $M_n$  over the course of only two hours.

In addition to 1-hexene, Busico and co-workers have investigated the propylene polymerization behavior of Kol's octahedral [ONNO] zirconium complexes **39a,b** (Figure 1.17).<sup>124</sup> In contrast to the living 1-hexene polymerization observed for **39a**/ $B(C_6F_5)_3$ , the polypropylenes produced by **39a** and **39b**/[PhNMe<sub>2</sub>H][B(C<sub>6</sub>F<sub>5</sub>)<sub>4</sub>]/Al(*i*Bu)<sub>3</sub> showed evidence of termination via chain transfer to Al and  $\beta$ -H transfer to monomer. Utilizing Kol's diamino bis(phenolate)zirconium catalyst (**39a**), Busico and co-workers reported the preparation of a diblock copolymer of *i*PP and PE under "quasi-living" conditions in 2003.<sup>125</sup> Using **39a**/[PhNMe<sub>2</sub>H][B(C<sub>6</sub>F<sub>5</sub>)<sub>4</sub>] with 2,6-di-*tert*-butylphenol modified

Al(*i*Bu)<sub>3</sub> as scavenger, a diblock copolymer of ethylene and propylene was prepared by sequential monomer addition of ethylene (1.5 minutes) and propylene (20 minutes). The resultant copolymer possessed a narrow polydispersity ( $M_w/M_n$  as low as 1.2 when  $M_n = 6,500$  g/mol). Characterization of the copolymer by <sup>13</sup>C NMR spectroscopy and DSC was consistent with a block structure. These results represented the first synthesis of an *i*PP-*block*-PE copolymer via sequential monomer addition at polymerization durations greater than one minute.



	M	R <sup>1</sup>	R <sup>2</sup>
<b>43a</b>	Zr	1-adamantyl	Me
<b>43b</b>	Zr	cumyl	Me
<b>44a</b>	Hf	1-adamantyl	Me
<b>44b</b>	Hf	cumyl	Me

**Figure 1.19.** Titanium and zirconium complexes bearing [ONNO] ligands with increased steric bulk.

In a subsequent report, Busico and co-workers reported that modification of the ligand framework resulted in the controlled polymerization of propylene with this class of catalysts.<sup>126</sup> By installing bulky 1-adamantyl (**43a**) or cumyl (**43b**) substituents at the *ortho*-position of the phenol moiety (Figure 1.19), PPs with narrow molecular weight distributions were obtained ( $M_w/M_n = 1.2 - 1.6$ ) under the same activation procedure. For **43a**/[PhNMe<sub>2</sub>H][B(C<sub>6</sub>F<sub>5</sub>)<sub>4</sub>]/Al(*i*Bu)<sub>3</sub>, a linear increase of  $M_n$  with time is observed over the course of three hours, however, after three hours

resonances consistent with terminal vinylidene groups were apparent in the  $^{13}\text{C}$  NMR spectrum. Chain transfer to aluminum was suppressed by the addition of 2,6-di-*tert*-butylphenol. The PP formed by **43a**/[PhNMe<sub>2</sub>H][B(C<sub>6</sub>F<sub>5</sub>)<sub>4</sub>]/Al(*i*Bu)<sub>3</sub> was highly isotactic ( $[mmmm] = 0.985$ ,  $T_m = 151$  °C). Utilizing sequential monomer addition of ethylene and propylene, **43a**/[PhNMe<sub>2</sub>H][B(C<sub>6</sub>F<sub>5</sub>)<sub>3</sub>] with 2,6-di-*tert*-butylphenol modified Al(*i*Bu)<sub>3</sub> as a scavenger were employed in the synthesis of a diblock copolymer. The resultant *i*PP-*block*-PE displayed higher molecular weight ( $M_n = 22,000$  g/mol,  $M_w/M_n = 1.3$ ) and  $T_m$  of the *i*PP block (152 °C) than analogous block copolymer obtained from **39a**.<sup>126</sup>

In 2009, Busico and co-workers reported the polymerization behavior of **44a,b** (Figure 1.19), the hafnium analogues of **43a,b**, which were both found to be living for the polymerization of ethylene and propylene.<sup>127</sup> Following activation with MAO and 2,6-di-*tert*-butylphenol in the presence of propylene, **44b** produced isotactic polypropylene ( $[mmmm] = 0.970$ ) with increasing molecular weight ( $M_n = 6,200 - 13,900$  g/mol) over the course of 9 hours while maintaining narrow molecular weight distributions ( $M_w/M_n = 1.3 - 1.5$ ). In addition to propylene, **44b**/MAO/2,6-di-*tert*-butylphenol was found to be living for the polymerization of ethylene over the course of 4 hours, a significant improvement relative to **43a**. Utilizing this improved living behavior, **44b**/MAO/2,6-di-*tert*-butylphenol was used to prepare a triblock copolymer. The resultant *i*PP-*block*-poly(ethylene-*co*-propylene)-*block*-*i*PP possessed narrow polydispersity ( $M_w/M_n = 1.2$ ,  $M_n = 22,000$  g/mol) while maintaining a high  $T_m$  (143 °C).

### 1.3.8 Titanium Catalysts Bearing Tridentate Aminodiol Ligands

The importance of neutral donors in the ligand framework of living olefin polymerization catalysts was also demonstrated recently by Sundararajan and co-

workers.<sup>128,129</sup> In 2002, the authors reported titanium dichloride complexes of tridentate aminodiols ligands (*rac* and *meso*-**45**, Figure 1.20) treated with MAO furnished poly(1-hexene)s possessing relatively narrow polydispersities ( $M_w/M_n = 1.07 - 2.9$ ) with a range of tacticities depending on the symmetry of the catalyst precursor.<sup>128</sup> Incorporation of a pendent methoxy donor into the aminodiols ligand framework gave rise to catalysts that were capable of living 1-hexene polymerization.<sup>129</sup> At temperatures between  $-10 - 30$  °C both **46a**/MAO and **46c**/MAO furnished poly(1-hexene)s with low polydispersities ( $M_w/M_n = 1.06 - 1.11$ ) and  $M_n = 73,000 - 424,000$  g/mol. The highest degree of isotacticity ( $[mmmm] = 0.85$ ) was obtained for polymer produced by **46a** at  $-10$  °C. Additionally, a linear dependence of  $M_n$  on reaction time was observed at  $-10$  °C. The zirconium congeners of **46a** and **46c** (**46b** and **46d**, Figure 1.20) have been prepared by Sudhakar and upon activation with MAO gave similar results for 1-hexene polymerization.<sup>130</sup> A linear relationship between  $M_n$  and reaction time was observed at  $28$  °C.

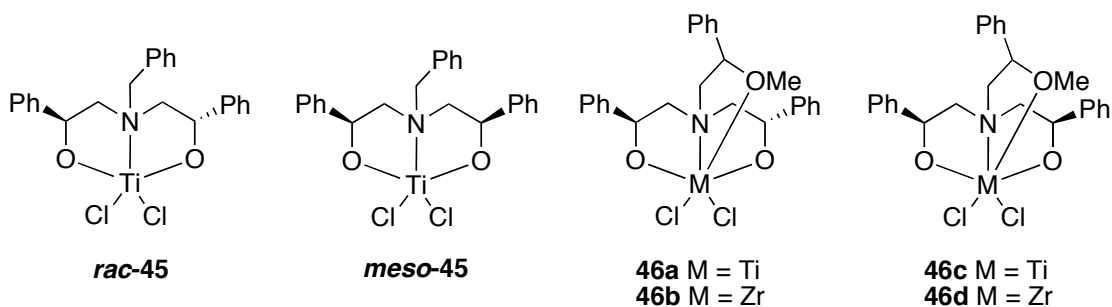


**Figure 1.20.** Aminodiols titanium and zirconium complexes.

### 1.3.9 Titanium Catalysts for Styrene Homo- and Copolymerization

As opposed to other homopolymers of higher  $\alpha$ -olefins, polystyrene has found extensive use as a commodity material. Recently Okuda and co-workers have demonstrated the first report of living and isospecific polymerization of styrene with a

series of titanium complexes bearing tetradentate [OSSO] bis(phenolate) ligands.<sup>131</sup> When activated with [PhNMe<sub>2</sub>H][B(C<sub>6</sub>F<sub>5</sub>)<sub>4</sub>] in the presence of Al(*n*Oct)<sub>3</sub> at 25 °C, **47** (Figure 1.21) produced highly isotactic polystyrene (*i*PS) ( $[mm] > 0.95$ ) with narrow molecular weight distributions ( $M_w/M_n = 1.08 - 1.27$ ) and  $M_n = 18,300 - 106,100$  g/mol. The  $M_n$  was shown to increase as a linear function of the conversion.

Nomura and Zhang reported on the living copolymerization of ethylene and styrene using a cyclopentadienyl(ketimide)titanium(IV) complex (**48**, Figure 1.21) in 2005.<sup>132</sup> Upon activation with MAO at 25 °C, **48** furnished poly(ethylene-*co*-styrene) with narrow polydispersities ( $M_w/M_n = 1.14 - 1.36$ ) and  $M_n = 53,000 - 173,000$  g/mol. The  $M_n$  was shown to increase linearly with time. Interestingly, **48**/MAO exhibited non-living behavior for styrene and ethylene homopolymerizations despite the living behavior observed for the copolymerization of the two monomers.

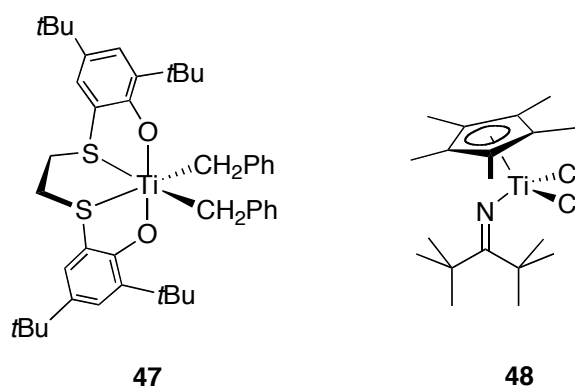


**Figure 1.21.** Titanium precatalysts for styrene homopolymerization.

### 1.3.10 Bis(phenoxyimine)titanium Catalysts

In 1999, Fujita and co-workers reported on a class of Group IV complexes bearing chelating phenoxyimine ligands, including **49a** (Figure 1.22). When activated with MAO, these complexes showed extremely high activity for ethylene polymerization.<sup>133-135</sup> Interested in the development of catalysts that could produce

stereoregular polymers, Coates and co-workers used a pooled combinatorial approach to screen Mitsui-type complexes for propylene polymerization behavior. Despite the  $C_2$ -symmetry of the catalyst precursor, **49b**/MAO furnished syndiotactic PP ( $[r] = 0.94$ ) resulting from a chain-end control mechanism.<sup>136</sup> Later, several studies revealed an unusual 2,1-insertion mechanism.<sup>137-139</sup> In addition, calculations on the system have supported a ligand isomerization event that interconverts the  $\Lambda$  and  $\Delta$  isomers of the active species between consecutive insertions, causing an alternation between *si* and *re* coordination of propylene which leads to syndiotactic polymer formation.<sup>140-142</sup>

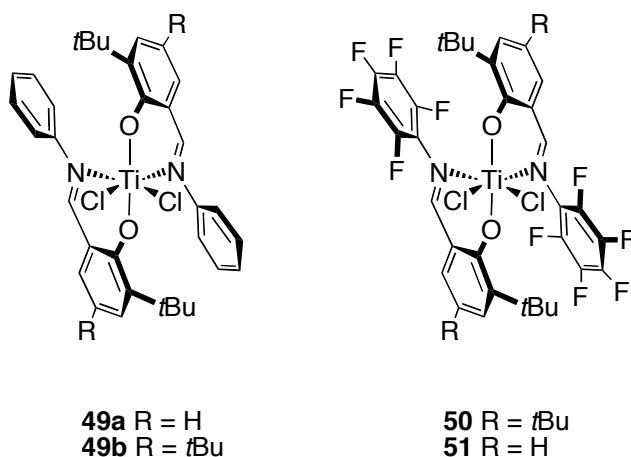


**Figure 1.22.** Early bis(phenoxyimine)titanium complexes.

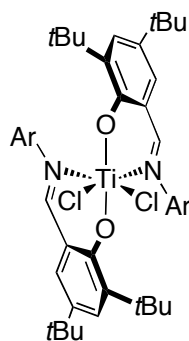
It was later found that the incorporation of fluorinated *N*-aryl moieties into the bis(phenoxyimine) ligand framework could provide catalyst precursors for the syndiotactic and living polymerization of propylene. At 0 °C, **50**/MAO (Figure 1.22) produced highly syndiotactic PP ( $[rrrr] = 0.96$ ) which had a peak melting temperature of 148 °C.<sup>143</sup> The polymerization exhibited a linear increase in  $M_n$  with PP yield while polydispersities remained narrow ( $M_w/M_n \leq 1.11$ ) for  $M_n$  up to 100,000 g/mol. It was also shown that **50**/MAO could copolymerize ethylene and propylene in a living fashion by cleanly synthesizing a monodisperse PP-*block*-poly(E-*co*-P) sample

( $M_w/M_n = 1.12$ ,  $M_n = 145,100$  g/mol). Utilizing the living nature of **50**/MAO, a *sPP-block-poly(E-co-P)* diblock copolymer of high molecular weight ( $M_n = 145,100$  g/mol,  $M_w/M_n = 1.12$ ) was prepared through sequential monomer addition.<sup>143</sup> Several studies on the physical properties of *sPP-block-poly(E-co-P)* diblock copolymers made using **50**/MAO have been conducted including those involving the morphology,<sup>144</sup> thermodynamic behavior, and self-assembly<sup>145</sup> of the materials. In subsequent work, the addition of a third block was employed in the formation of a *sPP-block-poly(E-co-P)-block-sPP* triblock copolymer.<sup>27</sup> TEM revealed that the polymer exhibited a microphase-separated morphology with *sPP* cylinders in a poly(*E-co-P*) matrix. Tensile testing revealed a strain to break of about 550%.

Fujita and co-workers independently reported that **51**/MAO was also living and syndioselective ( $[rr] = 87\%$ ) for propylene polymerization at room temperature, producing polymer with  $M_n = 28,500 - 108,000$  g/mol and  $M_w/M_n = 1.07 - 1.14$ .<sup>146</sup> Living ethylene/propylene copolymerization and block copolymer formation has also been demonstrated with **51**/MAO.<sup>147</sup> Exploiting this living behavior, *sPP-block-poly(E-co-P)*, *PE-block-sPP*, and *PE-block-poly(E-co-P)-block-sPP* have been prepared through sequential monomer addition.<sup>148,149</sup> Furthermore, employing a supported cocatalyst with **51** has also shown characteristics of living behavior. Polypropylene formed using **51**/MgCl<sub>2</sub>/*i*-Bu<sub>*n*</sub>Al(OCH<sub>2</sub>CH(Et)(CH<sub>2</sub>)<sub>3</sub>CH<sub>3</sub>)<sub>3-*n*</sub> had narrow PDIs ( $M_w/M_n = 1.09 - 1.17$ ,  $M_n = 53,000 - 132,000$  g/mol) and the polymerization exhibited a linear increase in  $M_n$  with reaction time.<sup>150</sup>

Studies on the effect of the fluorination pattern of the *N*-aryl ring revealed that complexes bearing the 2,4-di-*tert*-butyl phenoxide moiety require at least one *ortho* fluorine on the *N*-aryl ring to exhibit living propylene polymerization behavior.<sup>151,152</sup> As the amount of fluorination of the *N*-aryl moiety is decreased from the perfluoro complex **50** to the monofluoro complex **52a** (Figure 1.23), activities and tacticities for

propylene polymerization also decreased while the polydispersities remain consistently low ( $M_w/M_n \leq 1.11$ ,  $M_n$  up to 28,900 g/mol) upon MAO activation. Installing a trifluoromethyl group at the *para*-position of the *N*-aryl moiety (**52e**, Figure 1.23) led to an increase in activity of approximately 1.5 times that of **50**/MAO with similar tacticity ( $[rrrr] = 0.91$ ).<sup>153</sup> Interestingly, complexes related to **52a-c** where the *para*-substituent of the phenoxide moiety is H, produced amorphous PP upon MAO activation. These samples gave bimodal GPC traces each composed of a narrow peak ( $M_w/M_n \leq 1.10$ ) and a broad peak ( $M_w/M_n = 4.19 - 14.9$ ).<sup>154</sup>



- 52a** Ar = 2-FC<sub>6</sub>H<sub>4</sub>  
**52b** Ar = 2,6-F<sub>2</sub>C<sub>6</sub>H<sub>3</sub>  
**52c** Ar = 2,4,6-F<sub>3</sub>C<sub>6</sub>H<sub>2</sub>  
**52d** Ar = 2,3,5,6-F<sub>4</sub>C<sub>6</sub>H  
**52e** Ar = 2,3,5,6-F<sub>4</sub>-4-CF<sub>3</sub>-C<sub>6</sub>

**Figure 1.23.** Bis(phenoxyimine)titanium complexes with varying fluorination patterns.

Modification of the *ortho* substituents on the phenolate ring has yielded a number of new complexes. Of note, a complex bearing a *ortho*-phenolate trimethylsilyl group, **53** (Figure 1.24), has been shown to produce *s*PP with very high melting temperatures ( $T_m$  up to 156 °C) in a living fashion.<sup>155</sup> Changing the aforementioned *ortho* position to a larger triethylsilyl group (**54a**) gave similar results as **53** with lower activity.<sup>156</sup> Decreasing sterics through employment of a methyl (**54b**) or isopropyl (**54c**) group in the *ortho* position resulted in a substantial loss of

stereocontrol producing amorphous PP that exhibited fairly narrow polydispersities ( $M_w/M_n \sim 1.2$ ).

Further modifications to both the phenoxide and *N*-aryl moieties, relative to **50** have also been made. For example, **55** (Figure 1.24) contains a 2,6-F<sub>2</sub>C<sub>6</sub>H<sub>3</sub> *N*-aryl moiety and iodine substituents on the phenolate ring. When activated with MAO at 25 °C, **55** was reported to produce amorphous PP which exhibited a narrow molecular weight distribution ( $M_w/M_n = 1.17$ ,  $M_n = 200,000$  g/mol).<sup>157,158</sup> Furthermore, complexes **56a,b** employ 3,5-difluorophenyl *N*-aryl groups and substituents smaller than *tert*-butyl in the *ortho* position of the phenoxide moiety. Both **56a,b**/MAO were shown to furnish amorphous PP ( $[r_{rrrr}] \leq 0.48$ ) with narrow molecular weight distributions ( $M_w/M_n = 1.13 - 1.16$ ,  $M_n$  up to 240,000 g/mol).<sup>159</sup> This finding was surprising in that both complexes lack *ortho* fluorines on the *N*-aryl moiety.

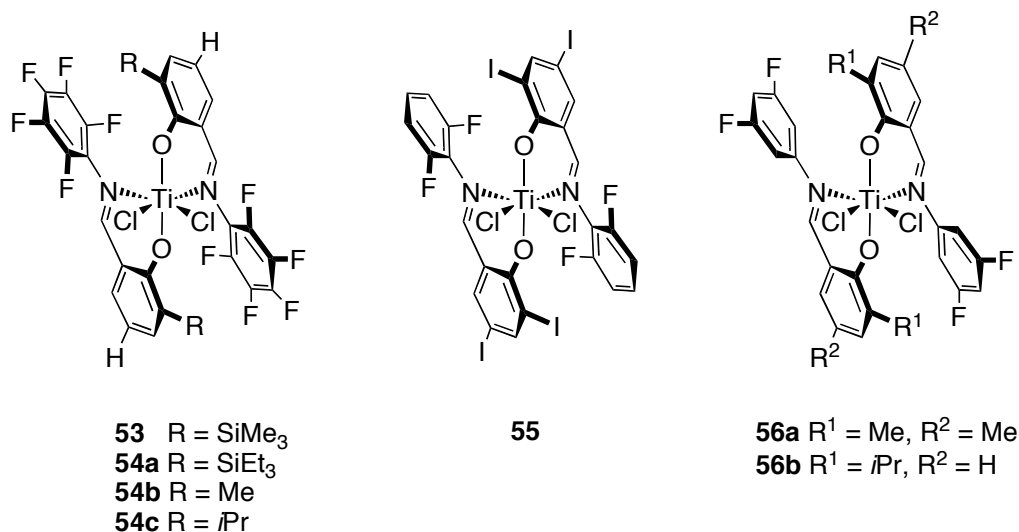


**Figure 1.24.** Bis(phenoxyimine)titanium complexes with varying substitution patterns.

In a final variation to the bis(phenoxyimine) complexes, two different phenoxyimine ligands were coordinated to one titanium center. Using gel permeation chromatography as a combinatorial screening method, a number of heteroligated

phenoxyimine complexes bearing one non-living (*ortho*-non-fluorinated ligand) and one living ligand (*ortho*-fluorinated ligand) displayed superior activities over their homoligated counterparts.<sup>152</sup> For example, PP produced with **49b**/MAO (Figure 1.22) exhibited a broad PDI ( $M_w/M_n = 1.41$ ) and a turn-over frequency (TOF) of 42 h<sup>-1</sup> while **50**/MAO exhibited a narrow PDI ( $M_w/M_n = 1.06$ ) and a TOF of 221 h<sup>-1</sup>. However, the heteroligated catalyst **57**/MAO (Figure 1.25) produced PP with  $M_n = 70,170$  g/mol and  $M_w/M_n = 1.16$  and exhibited a TOF of 760 h<sup>-1</sup>. Additionally, syndiotactic polymer ( $[rrrr] = 0.91$ ) was formed with this heteroligated catalyst.

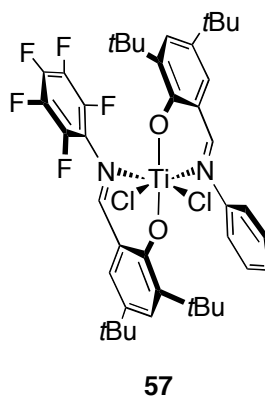


**Figure 1.25.** Heteroligated bis(phenoxyimine)titanium catalyst.

Many of the same titanium bis(phenoxyimine) catalysts used for living propylene polymerization have also been reported for the living polymerization of ethylene. In 2001, Fujita and co-workers found that activation of **51** with MAO at 25 °C (Figure 1.22) furnished linear PE with high molecular weight and narrow molecular weight distribution ( $M_n = 412,000$  g/mol,  $M_w/M_n = 1.13$ ).<sup>160</sup> Furthermore, polymerizations at 25 and 50 °C exhibited a linear increase in  $M_n$  with reaction time. It was later reported that addition of an equimolar amount of functionalized  $\alpha$ -olefin,  $H_2C=CH(CH_2)_n-Y$  ( $Y = OAlMe_2$ ,  $n = 4$  and  $Y = OSiMe_3$ ,  $n = 9$ ), to **51**/MAO and subsequent living ethylene polymerization furnished hydroxyl terminated PEs upon

acidic workup.<sup>161</sup> This strategy was also successful for the production of hydroxyl-terminated syndiotactic PP from **51**/MAO. Furthermore, addition of the aforementioned functionalized  $\alpha$ -olefins as a chain end capping agent furnished telechelic syndiotactic PPs bearing hydroxyl groups at both chain ends upon acidic workup.

While bis(phenoxyimine) titanium complexes can provide highly syndiotactic PP, copolymers that incorporate PE blocks have also been synthesized with these catalysts. Using **51**/MAO (Figure 1.22) a PE-*block*-poly(E-*co*-P) diblock and a PE-*block*-poly(E-*co*-P)-*block*-PE triblock copolymer have been synthesized through sequential monomer addition.<sup>148</sup> A PE-*block*-poly(E-*co*-P) diblock copolymer was also synthesized using **55**/MAO (Figure 1.24).<sup>157,162</sup> While the molecular weight of the polymer was quite high with  $M_n = 2,000,000$  g/mol, the molecular weight distribution was fairly broad ( $M_w/M_n = 1.60$ ).

Some of the early titanium bis(phenoxyimine) catalysts have also been used for living ethylene polymerization. In 2003, Coates and co-workers reported that **49b** when activated with MAO at 50 °C polymerized ethylene to produce polyethylene with  $M_w/M_n = 1.10$  and  $M_n = 44,500$  g/mol.<sup>163</sup> In 2004, Ivanchev *et al.* reported a near-linear increase in  $M_v$  with time for the polymerization of ethylene with **49a**/MAO at 30 °C.<sup>164</sup> In later work on the same system, Fujita and co-workers found that molecular weight distributions were low at a reaction time of one minute ( $M_w/M_n = 1.12$ ,  $M_n = 52,000$  g/mol) while the PDI broadened significantly at reaction times of just five minutes ( $M_w/M_n = 1.61$ ,  $M_n = 170,000$  g/mol).<sup>165</sup> Other, related complexes were synthesized and screened for ethylene polymerization. Complexes **58a,b**/MAO (Figure 1.26) showed a near-linear increase in  $M_v$  with times up to about 20 minutes.<sup>166</sup>

To investigate the effect of the substituent at the *ortho* position of the phenoxide moiety, complexes **54b,c** and **59a,b** (Figures 1.24 and 1.26) were screened for ethylene polymerization.<sup>167</sup> When activated with MAO at 25 °C, each complex produced PE with a narrow molecular weight distribution ( $M_w/M_n = 1.05 - 1.16$ ,  $M_n$  up to 75,000 g/mol), however reaction times were kept to one minute. While all the catalysts were living, activities were about an order of magnitude less than **51**/MAO. Having shown that **51**, **54b**, **59a,b** /MAO were living for ethylene polymerization, Fujita and co-workers investigated the ability of these catalysts to produce ethylene/ $\alpha$ -olefin copolymers in a living fashion.<sup>167</sup> Copolymerizations with ethylene and either 1-hexene, 1-octene, or 1-decene were carried out with each catalyst at 25 °C. In all cases, polymers with narrow molecular weight distributions were obtained ( $M_w/M_n \leq 1.22$ ). As the steric bulk of the *ortho* substituent decreased, increased  $\alpha$ -olefin incorporation was observed. A series of PE-*block*-poly(E-*co*-1-hexene) samples was produced using **54b**/MAO via sequential monomer addition. Molecular weight distributions for the block copolymers were generally low ( $M_w/M_n = 1.11 - 1.31$  for  $M_n$  up to 121,000 g/mol) and 1-hexene contents of up to 28.9 mol% were estimated.

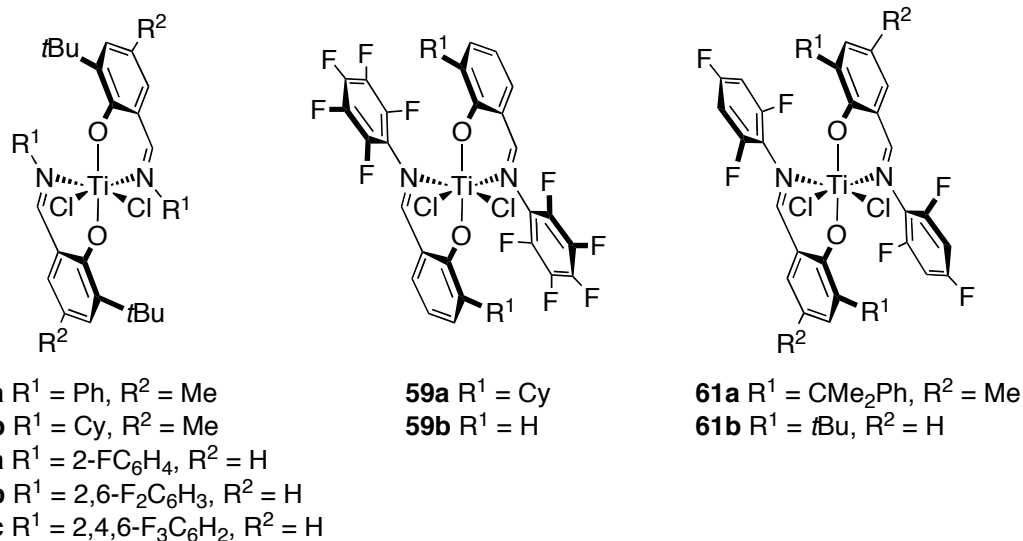
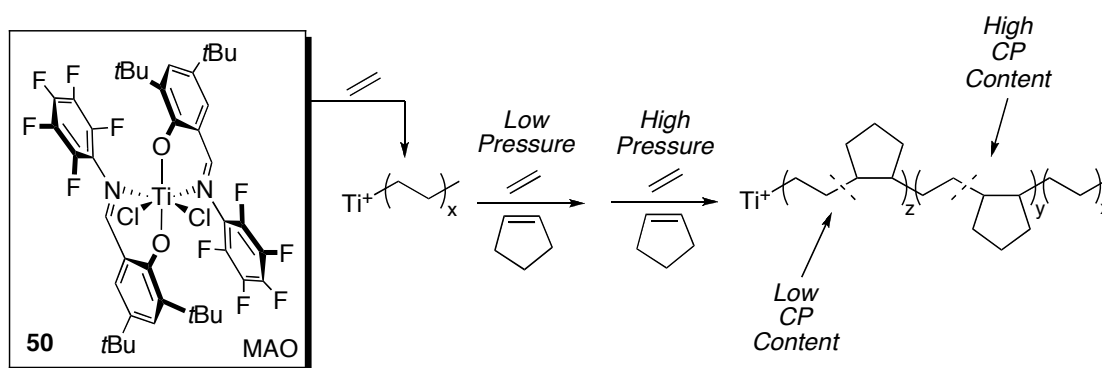


**Figure 1.26.** Bis(phenoxyimine)titanium complexes with varying substitution patterns.

Finally, the role of *N*-aryl fluorination on ethylene polymerization behavior has also been explored. Each of the catalysts **60a-c**/MAO (Figure 1.26) has been shown to be well-behaved for ethylene polymerization at 50 °C and **60a**/MAO and **60b**/MAO produced polymer with narrow molecular weight distributions at reaction times between 1-5 minutes ( $M_w/M_n \sim 1.05$ ,  $M_n = 13,000 - 64,000$  g/mol).<sup>148,168</sup> Fujita and co-workers reported that  $ZnEt_2$  could be used as a chain-transfer agent in the living ethylene polymerization employing **61a**/MAO (Figure 1.26) leading to zinc end-functionalized chains and a titanium species that reinitiates living ethylene polymerization upon the addition of monomer.<sup>169</sup> Despite being living for ethylene polymerization, **61b** was no longer living in the presence of  $ZnEt_2$ .

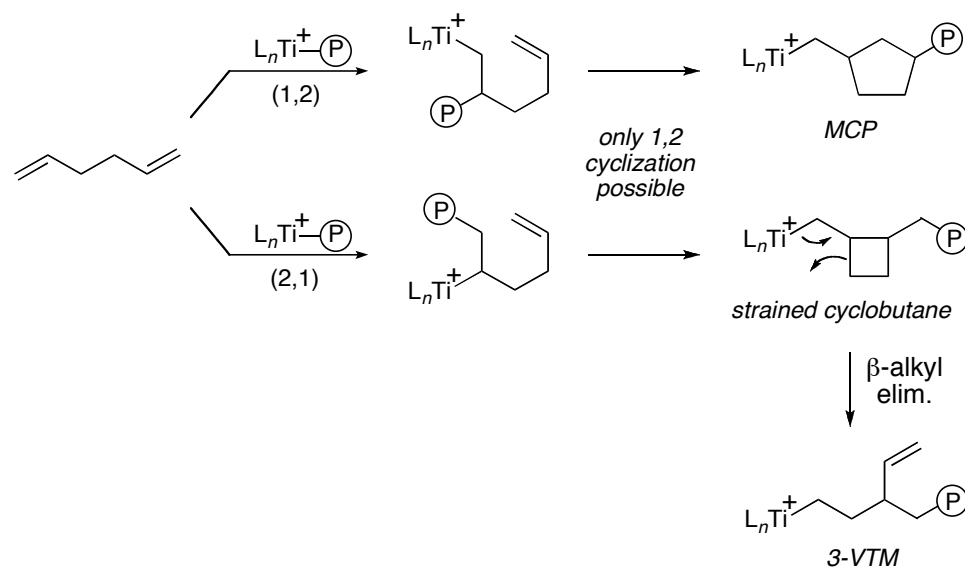


**Scheme 1.7.** Synthesis of ethylene/cyclopentene block copolymers using **50**/MAO.

Bis(phenoxyimine) titanium complexes have also been employed in the living copolymerization of ethylene and cyclic olefins. Utilizing **50**/MAO and varying ethylene pressure, a series of poly(E-co-CP)s with different cyclopentene contents were prepared (Figure 1.22, Scheme 1.7).<sup>170</sup> When ethylene pressure was low (< 1 psi), an almost perfectly alternating copolymer was formed ( $M_n = 21,000$  g/mol,  $M_w/M_n = 1.34$ ,  $T_g = 10.1$  °C). However, the use of higher ethylene pressures (3 psi) resulted in the formation of a random copolymer containing 36 mol% cyclopentene ( $M_n = 133,000$  g/mol,  $M_w/M_n = 1.24$ ,  $T_g = -4.5$  °C). Microstructural analysis using  $^{13}C$

NMR spectroscopy revealed that in both cases, all cyclopentene units were isolated and enchained in a 1,2 fashion. Tri- and multiblock copolymers were synthesized in which the constituent blocks differed in their cyclopentene content.

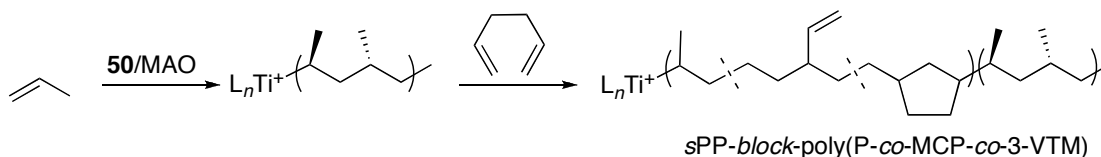
Copolymers from ethylene and norbornene have also been made using **50**/MAO.<sup>171</sup> With this catalyst, a high molecular weight, low PDI poly(E-co-NB) sample was prepared ( $M_n = 238,000$  g/mol,  $M_w/M_n = 1.05$ ) containing 62 mol% ethylene and a  $T_g$  of 86.5 °C. In addition, **50**/MAO was also used to synthesize a high molecular weight poly(E-co-P)-*block*-poly(E-co-NB) sample ( $M_n = 576,000$  g/mol,  $M_w/M_n = 1.13$ ).



**Scheme 1.8.** Polymerization of 1,5-hexadiene using **50**.

In addition to cyclic olefins, Coates and co-workers found that bis(phenoxyimine) titanium complex **50** (Figure 1.22) was also capable of living 1,5-hexadiene polymerization and 1,5-hexadiene/propylene copolymerization.<sup>172</sup> Homopolymerization of 1,5-hexadiene with **50**/MAO at 0 °C produced a high molecular weight polymer with a narrow PDI ( $M_n = 268,000$  g/mol,  $M_w/M_n = 1.27$ ).

The polymer showed the presence of two distinct units – the expected MCP units as well as 3-vinyl tetramethylene (3-VTM) units. As shown in Scheme 1.8, the MCP units are proposed to arise from 1,2-insertion of 1,5-hexadiene followed by a 1,2-cyclization. However, an initial 2,1-insertion of 1,5-hexadiene followed by a 1,2-cyclization forms a strained cyclobutane species. After a  $\beta$ -alkyl elimination, the 3-VTM unit is generated. Additionally, propylene/1,5-hexadiene copolymers with high molecular weights were also produced ( $M_n = 119,000 - 145,000$  g/mol,  $M_w/M_n = 1.09 - 1.16$ ).



**Scheme 1.9.** Synthesis of propylene/1,5-hexadiene block copolymers.

Using **50**/MAO, Coates and Hustad reported the living copolymerization of propylene and 1,5-hexadiene to produce random copolymers comprised of units of propylene, MCP, and 3-VTM.<sup>172</sup> Through sequential monomer addition, a *sPP-block-poly(P-co-MCP-co-3-VTM)* diblock copolymer was synthesized with **50**/MAO (Scheme 1.9). The molecular weight distribution of the block copolymer was low ( $M_w/M_n = 1.11$ ,  $M_n = 93,300$  g/mol) and contained 4.3 mol% MCP units and 2.7 mol% 3-VTM units. A poly(*E-co-P*)-*block-poly(MCP-co-3-VTM)* was also synthesized ( $M_n = 524,700$  g/mol,  $M_w/M_n = 1.13$ ). Lastly, **50**/MAO has been used to produce a high molecular weight poly(*MCP-co-3-VTM*)-*block-poly(E-co-NB)* sample with  $M_n = 451,000$  g/mol and  $M_w/M_n = 1.41$ .<sup>171</sup>

### 1.3.11 Bis(phenoxyketimine)titanium Catalysts

While bis(phenoxyimine) titanium complexes furnish sPP, it had been proposed that placing a substituent at the imine carbon of the ligand could prevent the isomerization responsible for the production of sPP and lead to the formation of *i*PP.<sup>173</sup> Ketimine complexes **62a-c** (Figure 1.27) were synthesized and found to be sparingly active for propylene polymerization, despite the ability to polymerize ethylene in a living fashion upon activation.<sup>163,173</sup> Complexes bearing smaller *ortho* substituents on the phenolate ring were reasoned to enable higher propylene activities by providing a sterically less-encumbered active site. With this in mind, complexes **63a-d** (Figure 1.27) were synthesized and screened for propylene polymerization.<sup>173</sup> Upon activation with MAO at 0 °C, each complex produced PP with a narrow molecular weight distribution ( $M_w/M_n = 1.12 - 1.17$ ,  $M_n = 2,700 - 35,400$  g/mol) and **63c**/MAO was shown to exhibit a linear increase in  $M_n$  as a function of yield. The resulting polymers displayed a variety of tacticities with **63c**/MAO furnishing PP with the highest tacticity ( $[mmmm] = 0.53$ ,  $T_m = 69.5$  °C). As a comparison, the analogous aldimine of **63c** (**63e**) in which  $R^3 = H$ , furnishes atactic PP with  $M_n = 123,100$  g/mol

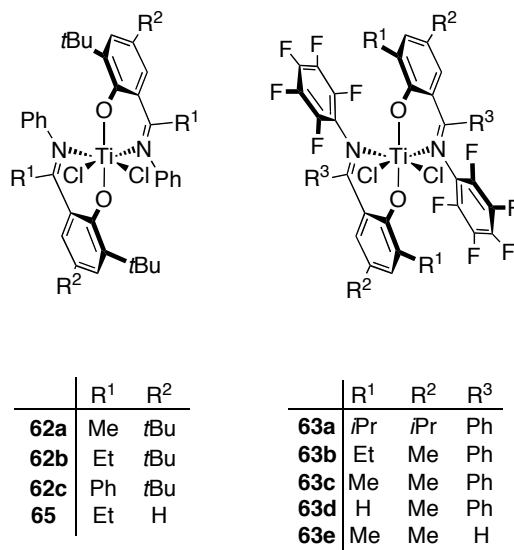


**Figure 1.27.** Bis(phenoxyketimine)titanium complexes.

and  $M_w/M_n = 1.13$ . Further exemplifying the living nature of **63c**/MAO for partially isospecific propylene polymerization, an *i*PP-*block*-poly(E-*co*-P) sample was produced with this catalyst. After polymerization of propylene to form an *i*PP block of  $M_n = 28,100$  g/mol ( $M_w/M_n = 1.10$ ), ethylene was added to the reaction yielding a diblock copolymer with  $M_n = 62,000$  g/mol and  $M_w/M_n = 1.10$ .

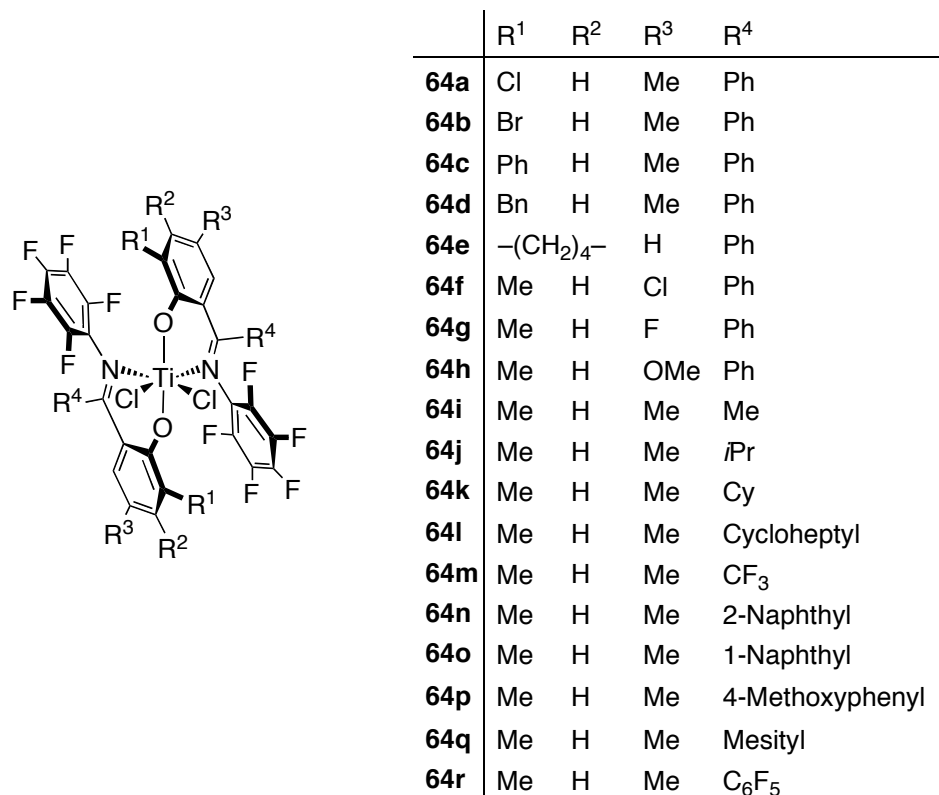


**Figure 1.28.** Bis(phenoxyketimine)titanium complexes with varying substituents.

To obtain higher isoselectivity, Coates and co-workers systematically varied *ortho*-, *meta*-, and *para*-substituents on the phenoxy moiety in addition to the ketimine substituent in complexes **64a-r** (Figure 1.28).<sup>28</sup> All the complexes produced PP with a narrow molecular weight distribution ( $M_w/M_n = 1.07 - 1.33$ ,  $M_n = 3,000 - 364,000$  g/mol) upon activation with MAO except those bearing ancillary methoxy groups in the ligand framework (**64h** and **64p**). The tacticities of the resulting

polymers differed with **64k**/MAO producing PP with the highest tacticity ( $[mmmm] = 0.73$ ,  $T_m = 116.8$  °C) in addition to exhibiting a linear increase in  $M_n$  as a function of polymer yield. Exploiting the living nature of the **64k**/MAO, block copolymers containing *i*PP blocks were prepared via sequential monomer addition.<sup>28</sup> Specifically, an *i*PP-*block*-poly(E-*co*-P)-*block*-*i*PP, *i*PP-*block*-poly(E-*co*-P)-*block*-*i*PP-*block*-poly(E-*co*-P)-*block*-*i*PP, and *i*PP-*block*-poly(E-*co*-P)-*block*-*i*PP-*block*-poly(E-*co*-P)-*block*-*i*PP-*block*-poly(E-*co*-P)-*block*-*i*PP copolymer were prepared. The polymers had narrow molecular weight distributions ( $M_w/M_n = 1.13 - 1.30$ ) and high molecular weights ( $M_n = 102,000 - 235,000$  g/mol). Testing of the tensile properties of the block copolymers showed good elastomeric behavior with the triblock copolymer displaying an elongation to break of 1000%.

In addition to propylene, Coates and co-workers reported that **62a-c** (Figure 1.27) when activated with MAO at 0 and 20 °C all produced PE that exhibited a narrow molecular weight distribution ( $M_w/M_n \leq 1.08$ ) and had number average molecular weights ( $M_n = 15,000 - 47,000$  g/mol) that coincided with  $M_n^{\text{theo}}$ .<sup>163</sup> A linear increase in  $M_n$  with polymer yield for the polymerization catalyzed by **62c**/MAO at 0 °C and for **62b**/MAO at 50 °C was demonstrated. A related complex (**65**, Figure 1.27), when activated with MAO at 50 °C, produced PE with  $M_w/M_n = 1.08$  ( $M_n = 9,000$  g/mol).<sup>165</sup>

### 1.3.12 Bis(pyrrolide-imine)titanium Catalysts

In 2000, Fujita and co-workers reported the behavior of bis(pyrrolide-imine)titanium complexes for ethylene polymerization, however living behavior was not observed.<sup>174</sup> As a result, Fujita and co-workers turned their attention to the copolymerization of ethylene and norbornene.<sup>175-177</sup> At 25 °C, **66a-d**/MAO (Figure 1.29) furnished poly(E-*alt*-NB) with narrow molecular weight distributions and high

molecular weights ( $M_w/M_n = 1.10 - 1.24$ ,  $M_n = 127,000 - 600,000$  g/mol). A linear increase of  $M_n$  with time over the course of 20 minutes was observed. The copolymers were found to contain 95.4% perfectly alternating units. The polymer chain-end structures were consistent with chain initiation by insertion of norbornene into the Ti-Me bond, and a last inserted norbornene unit after termination by protonolysis. This suggests norbornene plays a stabilizing role for the active species against termination processes.

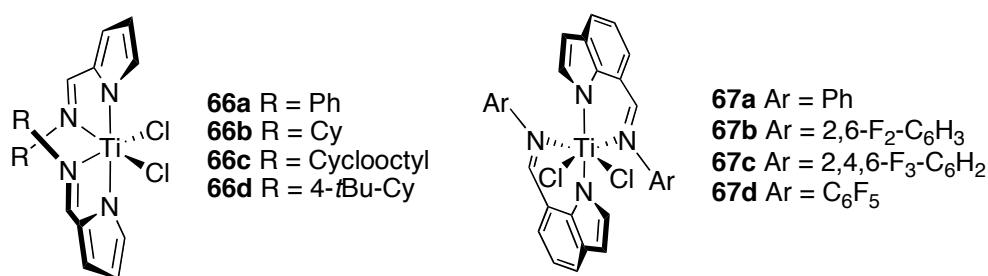
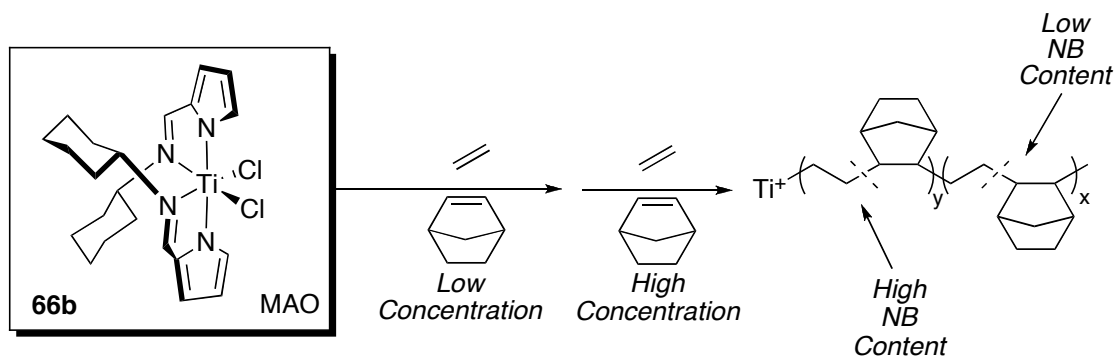


**Figure 1.29.** Bis(pyrrolide-imine)titanium and bis(indolide-imine)titanium complexes.



**Scheme 1.10.** Synthesis of ethylene/norbornene block copolymers.

Utilizing **66b**/MAO (Figure 1.29), Fujita and co-workers were able to prepare block copolymers containing poly(*E-co*-NB) and PE segments as well as block copolymers containing poly(*E-co*-NB) segments with varying degrees of norbornene incorporation.<sup>177</sup> Block copolymers of the type poly(*E-co*-NB)<sub>x</sub>-*block*-poly(*E-co*-NB)<sub>y</sub>,

with 7.6 mol% norbornene incorporation in the first block and 27.4 mol% norbornene overall were prepared by initiating the polymerization with ethylene containing the desired amount of norbornene. After the first block had been formed, supplemental norbornene was added while maintaining the ethylene feed (Scheme 1.10). Additionally, PE-*block*-poly(E-*co*-NB) was prepared through sequential monomer addition. The diblock copolymer exhibited a narrow polydispersity ( $M_w/M_n = 1.56$ ) and  $M_n = 414,000$  g/mol with a norbornene content of 31.5 mol %.

### 1.3.13 Bis(indolide-imine)titanium Catalysts

Expanding on imine ligated catalysts, Fujita and co-workers synthesized bis(indolide-imine)titanium complexes and evaluated their potential as ethylene polymerization catalysts.<sup>178-182</sup> When activated with MAO at room temperature, compounds **67a-c** (Figure 1.29) furnished PE with narrow molecular weight distributions ( $M_w/M_n = 1.11 - 1.23$ ) with  $M_n = 11,000 - \text{ca. } 90,000$  g/mol. At 25 °C, a linear increase of  $M_n$  with increasing polymer yield was observed for **67a-c**/MAO. Exhaustive fluorination of the *N*-aryl moiety (**67d**) resulted in living behavior at -10 °C ( $M_w/M_n = 1.12 - 1.15$ ), while polymerization at 25 °C led to a broadened molecular weight distribution ( $M_w/M_n = 1.93$ ).<sup>179,180</sup> Using **67c**/MAO, Fujita and co-workers were able to prepare PE-*block*-poly(E-*co*-P) copolymers containing 8.0 mol% propylene via sequential monomer addition with  $M_w/M_n = 1.17$  and  $M_n = 31,400$  g/mol.<sup>180,181</sup> TEM visualization of the block copolymer revealed microphase separation of the poly(E-*co*-P) and PE domains, which were evenly dispersed throughout the sample.

### 1.3.14 Bis(enaminoketonato)titanium Catalysts

The synthesis and ethylene polymerization activity of bis(enaminoketonato)titanium complexes was reported by Li and co-workers in 2004.<sup>183</sup> Upon activation with MMAO at 25 °C, **68a,b** (Figure 1.30) furnish linear PEs with narrow molecular weight distributions ( $M_w/M_n = 1.25 - 1.45$ ) and  $M_n = 51,000$  g/mol – 129,000 g/mol. At 25 °C, a linear increase in  $M_n$  with reaction time is observed with **68a**/MMAO. Mecking and co-workers reported *ortho*-fluorination on the *N*-aryl moiety (**69a**, Figure 1.30) furnished living and thermally robust ethylene polymerization catalysts upon MAO activation.<sup>184</sup> A linear increase in  $M_n$  over time was observed at 25, 50, and up to 75 °C. Non-living behavior observed for **69b**/MAO supports the fact that the living behavior of **69a**/MAO is not steric in nature illustrating another example in which *ortho*-fluorination appears beneficial for living polymerization. Employing **69a**/MAO, a PE-*block*-aPP was synthesized through sequential monomer addition.<sup>184</sup> Polymerization of ethylene in a living fashion followed by removal of excess monomer *in vacuo* and subsequent propylene polymerization furnished the diblock copolymer with  $M_n = 190,000$  g/mol and  $M_w/M_n = 1.12$ .

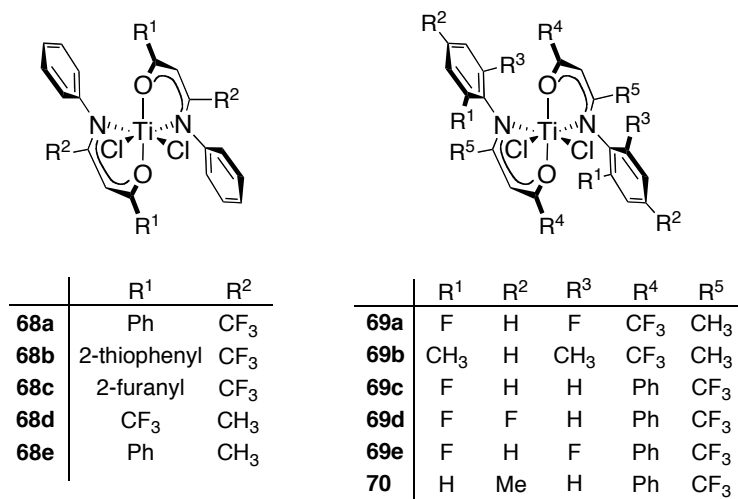


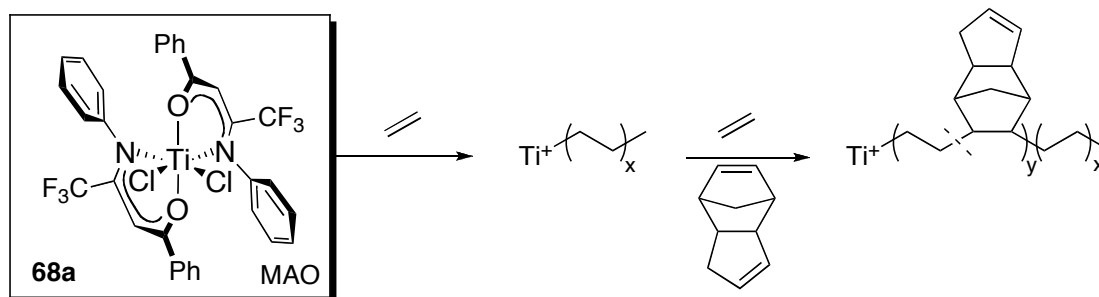
**Figure 1.30.** Bis(enaminoketonato)titanium catalysts for living olefin polymerization.

In addition to ethylene homopolymerization, the copolymerization of ethylene and norbornene by **68a-d**/MMAO was also shown to possess some characteristics of a living polymerization.<sup>183</sup> The polymers obtained from polymerizations conducted at 25 °C displayed narrow molecular weight distributions ( $M_w/M_n = 1.07 - 1.54$ ) with  $M_n = \text{ca. } 150,000 - 580,000 \text{ g/mol}$ . The norbornene content ranged from 35.3 – 55.4 mol%. At 25 °C, a linear increase in  $M_n$  with reaction time was demonstrated for **68a**/MMAO over the course of 20 minutes. Utilizing the living nature of the **68**/MAO, a PE-*block*-poly(E-*co*-NB) block copolymer was prepared through sequential monomer addition. The diblock copolymer had a narrow polydispersity ( $M_w/M_n = 1.38$ ,  $M_n = 143,000 \text{ g/mol}$ ) and a norbornene content of 11.1 mol%. The copolymerization of ethylene and cyclopentene (CP) by **68a**/MMAO and **68d**/MMAO was also shown to possess some characteristics of living behavior.<sup>185</sup> At temperatures from -10 – 30 °C, poly(E-*co*-CP)s with narrow molecular weight distributions ( $M_w/M_n = 1.23 - 1.82$ ) were produced. Additionally, a PE-*block*-poly(E-*co*-CP) was prepared in a manner similar to the PE-*block*-poly(E-*co*-NB).

Li and co-workers discussed the effects of further ligand modifications on the copolymerization behavior of bis(enaminoketonato)titanium catalysts.<sup>186</sup> At 25 °C, **70**/MMAO (Figure 1.30) produced poly(E-*co*-NB) with narrow polydispersities ( $M_w/M_n = 1.18 - 1.31$ ,  $M_n = \text{ca. } 200,000 - 570,000 \text{ g/mol}$ ) and norbornene content ranging from 44.6 – 47.8 mol%. The polymerization displayed a linear increase of  $M_n$  with time from  $t = 5 - 20$  minutes.

In addition to norbornene and cyclopentene, Li and co-workers found **68a** and **69a,c,d** were active for the polymerization of ethylene and dicyclopentadiene upon activation with MAO at 25 °C.<sup>187</sup> Depending on the monomer feed, the resultant polymers contained up to 47.7 mol% dicyclopentadiene with a nearly alternating structure. Over the course of twenty minutes, **68a**/MAO (Scheme 1.11) produced a

copolymer with increasing molecular weights ( $M_n = 47,000$  g/mol) while maintaining narrow polydispersities ( $M_w/M_n = 1.06 - 1.14$ ). Analysis of the  $^{13}\text{C}$  NMR spectra revealed a copolymer containing only unreacted cyclopentene units suggesting the copolymerization proceeds through enchainment of the norbornene portion of the dicyclopentadiene exclusively. Utilizing sequential monomer addition, a PE-*block*-poly(ethylene-*alt*-dicyclopentadiene) was produced. Characterization using atomic force microscopy (AFM) and transmission electron micrograph (TEM) revealed a microphase-separated material. Additionally, Li and co-workers were able to produce functionalized diblock copolymers through reaction of the remaining alkene.

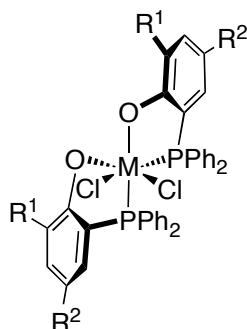


**Scheme 1.11.** Synthesis of ethylene/dicyclopentadiene block copolymers using **68a**.

### 1.3.15 Bis(phosphanylphenoxide)titanium Catalysts

In 2006, Gibson and co-workers reported the synthesis of group 4 metal complexes (**71a-f**, Figure 1.31) featuring two bidentate ligands equipped with phenoxide and phosphine donors.<sup>188</sup> At 25 °C, **71a-f**/MAO were found to be active for both the polymerization ethylene and propylene although polydispersities were broadened ( $M_w/M_n > 1.49$ ). In subsequent report, Li and co-workers synthesized **71g,h** and found **71g**/MAO exhibited a nearly linear increase  $M_n$  over the first ten minutes of the ethylene polymerization.<sup>189</sup> Furthermore, the resultant polymers had relatively

narrow molecular weight distributions ( $M_w/M_n = 1.31 - 1.33$ ), indicative of at least quasi-living behavior.



	M	R <sup>1</sup>	R <sup>2</sup>	R <sup>3</sup>
<b>71a</b>	Ti	H	H	Ph
<b>71b</b>	Ti	Ph	H	Ph
<b>71c</b>	Ti	<i>t</i> Bu	H	Ph
<b>71d</b>	Zr	<i>t</i> Bu	H	Ph
<b>71e</b>	Zr	<i>t</i> Bu	H	<i>i</i> Pr
<b>71f</b>	Hf	<i>t</i> Bu	H	Ph
<b>71g</b>	Ti	<i>t</i> Bu	<i>t</i> Bu	Ph
<b>71h</b>	Ti	SiMe <sub>3</sub>	H	Ph

**Figure 1.31.** Bis(phosphanylphenoxide)titanium precatalysts for living olefin polymerization.

To enhance the living nature of the system, Li and co-workers explored the copolymerization of norbornene and ethylene. Previous reports by Fujita have suggested that norbornene can be effective for the suppression of chain termination or chain transfer events common to olefin polymerizations.<sup>197,199</sup> Indeed, Li and co-workers found that the copolymerization of ethylene and norbornene by **71g**/MAO resulted in polymers with narrow molecular weight distributions ( $M_w/M_n < 1.2$ ) for norbornene incorporation of more than 10 mol%.<sup>189</sup> Additionally, the molecular weight was found to increase linearly with polymer yield. Further exemplifying the living nature of the catalyst, a poly(*E-co-NB*)<sub>x</sub>-*block*-poly(*E-co-NB*)<sub>y</sub> was produced. After formation of the first block containing 25 mol% norbornene, supplemental norbornene was added to the system resulting in a second block containing 44 mol%

norbornene. The resultant block copolymer exhibited high molecular weights ( $M_n = 32,000$  g/mol) and narrow molecular weight distributions ( $M_w/M_n = 1.17$ ).

### 1.3.16 Catalysts Supported by $sp^2$ and $sp^3$ Carbon Donors

One of the more recent classes of catalysts to emerge are the  $C_1$ -symmetric pyridylamidohafnium complexes (**72**, Figure 1.32) developed by Dow and Symyx that furnish high molecular weight and highly isoselective poly( $\alpha$ -olefin)s at high reaction temperatures upon activation.<sup>190-192</sup> Coates and co-workers have shown that the catalyst derived from a  $C_s$ -symmetric pyridylamidohafnium complex (**73**, Figure 1.32) furnished isotactic poly(1-hexene) in a living fashion when activated with  $B(C_6F_5)_3$ .<sup>193</sup> The poly(1-hexene)s exhibited narrow polydispersities ( $M_w/M_n \leq 1.20$ ,  $M_n$  up to 152,000 g/mol) and the  $M_n$  was shown to increase linearly with monomer conversion. At 50 °C, the molecular weight distribution of the polymer produced by **73**/ $B(C_6F_5)_3$  remains narrow suggesting that living behavior is maintained at elevated temperatures.

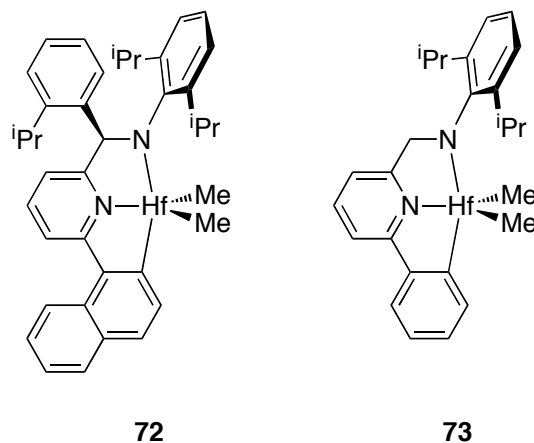


**Figure 1.32.** Pyridylamidohafnium complexes.

In addition to living 1-hexene polymerization, Coates and co-workers have shown that **73**/ $B(C_6F_5)_3$  furnished isotactic PP ( $[mmmm] = 0.56$ ) with a narrow

molecular weight distribution ( $M_n = 68,600$  g/mol,  $M_w/M_n = 1.05$ ) at 20 °C.<sup>193</sup> The mechanism of stereocontrol proceeded by an enantiomorphic site control mechanism, which is quite unusual for a  $C_s$ -symmetric catalyst. Detailed mechanistic studies with **72** (Figure 1.32) by Froese *et al.*<sup>191,194</sup> have shown the 1,2-insertion of an olefin into the Hf-C<sub>Aryl</sub> bond generates an sp<sup>3</sup>-hybridized carbon donor atom that supports the active metal center; it is likely that the isoselectivity observed with **73**/B(C<sub>6</sub>F<sub>5</sub>)<sub>3</sub> results from a similar activation mechanism. With this in mind, Coates and co-workers prepared a new pyridylamidohafnium complex (*rac*-**74**, Figure 1.33) supported by an sp<sup>3</sup>-carbon donor that was generated *via* insertion of a ligand-appended alkene into the neutral pyridylamidohafnium trimethyl precursor generating a mixture of diastereomers (61:39 ratio).<sup>195</sup> Upon activation with B(C<sub>6</sub>F<sub>5</sub>)<sub>3</sub>, *rac*-**74** furnished isotactic PP ( $[mmmm] = 0.80$ ) with a narrow molecular weight distribution ( $M_w/M_n \leq 1.05$ ,  $M_n$  up to 124,400 g/mol) and TOF of 2800 h<sup>-1</sup>. The  $M_n$  was shown to increase linearly with polymer yield over the course of 45 min.

Coates and co-workers were able to further exploit the area of olefin polymerization catalysts supported by sp<sup>3</sup>-carbon donors through the synthesis and subsequent metallation of vinyl-appended phenoxyamine ligands.<sup>196</sup> The resultant complexes of zirconium and hafnium (*rac*-**75a** and *rac*-**75b**, Figure 1.33) bearing six-membered metallacycles were obtained as diastereo-isomeric mixtures resulting from migratory insertion of a benzyl group to the ligand appended vinyl group on the neutral phenoxyamine metal tribenzyl precursor. Upon activation, *rac*-**75a,b** formed highly active polymerization catalysts (TOF > 930 h<sup>-1</sup>) that isoselectively polymerized both 1-hexene and propylene. At 0 °C, *rac*-**75b**/B(C<sub>6</sub>F<sub>5</sub>)<sub>3</sub> produced isotactic poly(1-hexene) in a living fashion. Molecular weights ( $M_n = 70,000 - 240,000$  g/mol) increased linearly as a function of conversion while polydispersities remained narrow

( $M_w/M_n = 1.10 - 1.15$ ). Living 1-hexene polymerization behavior was not observed for the zirconium analogue (*rac-75a*).

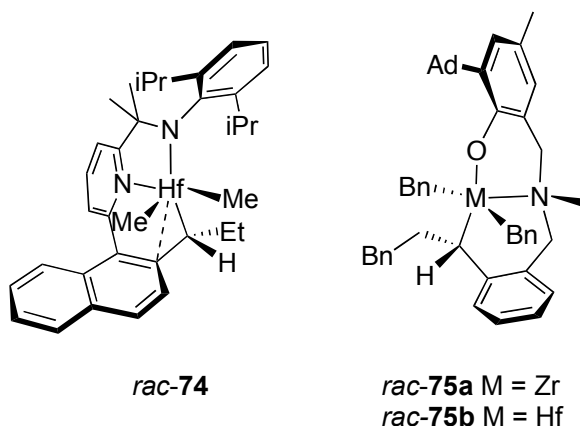


**Figure 1.33.** Hafnium and zirconium pre-catalysts for living olefin polymerization.

Despite its living nature for 1-hexene polymerization, living propylene polymerization behavior was not observed for the hafnium analogue (*rac-75b*), however, living isoselective polymerization of propylene was observed for the zirconium analogue (*rac-75a*). At 0 °C, *rac-75a*/B(C<sub>6</sub>F<sub>5</sub>)<sub>3</sub> produced polypropylene with narrow polydispersities ( $M_w/M_n = 1.17 - 1.19$ ) while molecular weights ( $M_n = 60,000 - 220,000$  g/mol) were observed to increase linearly with propylene yield. Utilizing the living nature of *rac-75a*, a diblock copolymer was synthesized by sequential monomer addition. The resultant *i*PP-*block*-poly(ethylene-*co*-propylene) had an  $M_n = 122,000$  g/mol and a narrow molecular weight distribution ( $M_w/M_n = 1.20$ ).

### 1.3.17 Aminopyridinatozirconium Catalysts

In 2007, Kempe and co-workers described a zirconium catalyst supported by bis(aminopyridinato) ligands (**76**, Figure 1.34) that was living for ethylene polymerization at elevated temperature.<sup>197</sup> Upon activation with [R<sub>2</sub>NMeH][B(C<sub>6</sub>F<sub>5</sub>)<sub>4</sub>]

(R = C<sub>16</sub>H<sub>33</sub> – C<sub>18</sub>H<sub>37</sub>) in the presence of tetra-(2-phenyl-1-propyl)aluminumoxane at 50 °C, **76** furnished linear PE of high molecular weight ( $M_n = 1,745,000 - 2,301,000$  g/mol) and narrow molecular weight distributions ( $M_w/M_n = 1.26 - 1.30$ ). No evidence for  $\beta$ -H elimination or chain transfer was evident and continued chain growth was observed even after polymer precipitation.

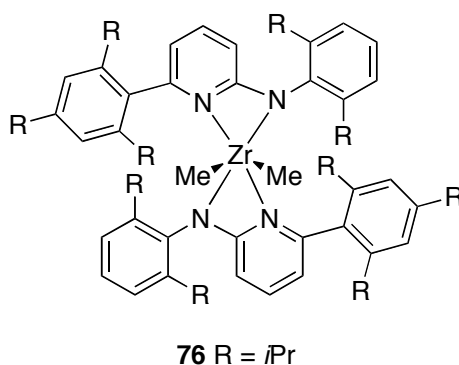


**Figure 1.34.** Aminopyridinatozirconium catalysts.

### 1.3.18 Tris(pyrazolyl)borate Catalysts

In 2008, Jordan and co-workers described tris(pyrazolyl)borate complexes (**77**, **78** Figure 1.35) that displayed characteristics of living ethylene polymerization at low temperatures.<sup>198,199</sup> In the presence of 40 equivalents of ethylene at -78 °C, **77**/[Ph<sub>3</sub>C][B(C<sub>6</sub>F<sub>5</sub>)<sub>4</sub>] furnished linear PE with  $M_n = 2,000$  g/mol that was in good agreement with  $M_n^{\text{theo}}$ . No olefinic resonances were observed. Additionally, quenching with Br<sub>2</sub> furnished double-end-capped PE featuring a benzyl group on one polymer chain end and bromine substituent on the opposite polymer chain end. Similar results were obtained with **78**/[Ph<sub>3</sub>C][B(C<sub>6</sub>F<sub>5</sub>)<sub>4</sub>] in the presence of 38 equivalents of ethylene at -78 °C, however, observed molecular weights ( $M_n = 2,800 - 3,800$  g/mol) were approximately three times higher than  $M_n^{\text{theo}}$ . The authors attribute this apparent disparity to incomplete activation of the hafnium complex. Double-end-capped

polyethylene bearing benzyl and bromine substituents was also synthesized upon bromine quench of **78**/[Ph<sub>3</sub>C][B(C<sub>6</sub>F<sub>5</sub>)<sub>4</sub>].

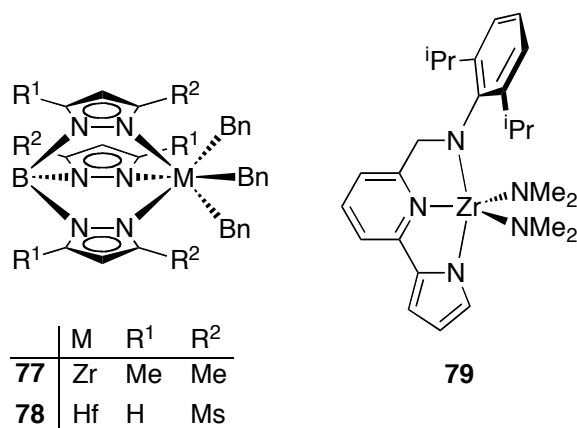


**Figure 1.35.** Tris(pyrazolyl)borate and bis(dimethylamidopyridine)zirconium olefin polymerization catalysts.

### 1.3.19 Bis(dimethylamidopyridine)zirconium Catalysts

In 2009, Pellecchia and co-workers reported a new class of olefin polymerization catalysts bearing dianionic tridentate amidomethylpyridine ligands which exhibited some characteristics of living polymerization.<sup>200</sup> Upon activation with Al<sup>*i*</sup>Bu<sub>2</sub>H/MAO, **79** (Figure 1.35) produced isotactic poly(1-hexene) ([*mmmm*] = 0.99) with narrow molecular weight distributions ( $M_w/M_n = 1.2$ ). Furthermore, **79**/Al<sup>*i*</sup>Bu<sub>2</sub>H/MAO produced polypropylene lacking olefinic end groups with  $M_w = 38,000$  g/mol and  $M_w/M_n = 1.4$ . Activation of **79** with Al<sup>*i*</sup>Bu<sub>2</sub>H and [HNMe<sub>2</sub>Ph][B(C<sub>6</sub>F<sub>5</sub>)<sub>3</sub>] in the presence of ethylene resulted in linear PE with a narrow molecular weight distribution ( $M_w/M_n = 1.2$ ).

## 1.4 Non-Group 4 Early Metal Polymerization Catalysts

While complexes of Group 4 transition metals dominate the field of living olefin polymerization, there are rare examples of group 3 complexes displaying

characteristics of living behavior. In 2005, Ward *et al.* reported the synthesis and 1-hexene polymerization behavior of a unique  $C_3$ -symmetric scandium complex bearing a tripodal trisoxazoline ligand.<sup>201</sup> When treated with two equivalents of  $[\text{Ph}_3\text{C}][\text{B}(\text{C}_6\text{F}_5)_4]$  at  $-30\text{ }^\circ\text{C}$  in the presence of 1-hexene, **80** (Figure 1.36) produced isotactic poly(1-hexene) ( $[mmmm] = 0.90$ ) lacking olefinic end groups with  $M_n = 750,000\text{ g/mol}$  and  $M_w/M_n = 1.18$ .

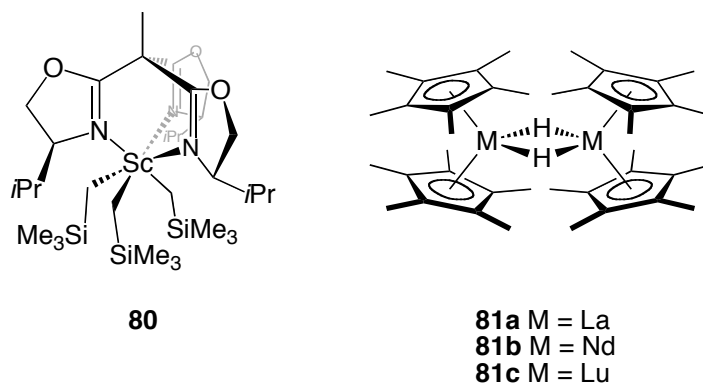


**Figure 1.36.** Non-group 4 early metal olefin polymerization catalysts.

In addition to 1-hexene, living ethylene polymerization has been reported for non-group 4 early metal catalysts. In 1985, Marks and co-workers showed that organolanthanide complexes were promising for living ethylene polymerization.<sup>202</sup> The dimeric bis( $\text{Cp}^*$ ) hydride complexes (**81a-c**, Figure 1.36) furnished high molecular weight PEs ( $M_n = 96,000 - 648,000\text{ g/mol}$ ) and molecular weight distributions were for the most part lower than 2.0 (e.g. **81c** exhibited  $M_w/M_n = 1.37 - 1.68$ ). The living nature of **81a-c** is further supported by observations that catalytic activity is maintained for up to two weeks,  $M_n$  increases with time, and the number of polymer chains per metal center is consistently less than one.

In 2005, Nomura and co-workers reported that arylimido(aryloxo)vanadium dichloride complex **82** (Figure 1.37) activated with  $\text{Et}_2\text{AlCl}$  exhibited characteristics

of living ethylene polymerization.<sup>203</sup> At 0 °C, the PE produced had a narrow molecular weight distribution ( $M_w/M_n = 1.42$ ) and high molecular weight ( $M_n = 2,570,000$  g/mol). Additionally, the  $M_n$  was shown to increase in a linear fashion with increasing TON. In addition to living ethylene polymerization, the ability of **82**/Et<sub>2</sub>AlCl was reported to catalyze the quasi-living copolymerization of ethylene and norbornene.<sup>203</sup> At 0 °C, poly(E-*co*-NB) with 5.1 – 39.9 mol% norbornene content was obtained from **82**/Et<sub>2</sub>AlCl. The polymers exhibited narrow molecular weight distributions ( $M_w/M_n = 1.29 – 1.73$ ) and high molecular weights ( $M_n = 327,000 – 2,570,000$  g/mol).

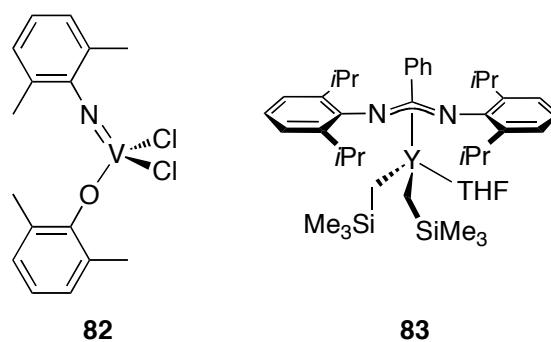


**Figure 1.37.** Vanadium and yttrium polymerization catalysts.

Upon investigating the ethylene polymerization behavior of dialkyl(benzamidinate)yttrium complexes, Hessen and co-workers reported that at least some characteristics of living behavior were observed.<sup>204</sup> When treated with [PhNMe<sub>2</sub>H][B(C<sub>6</sub>F<sub>5</sub>)<sub>4</sub>], **83** (Figure 1.37) furnished PE that displayed narrow molecular weight distributions ( $M_w/M_n = 1.1 – 1.2$ ) and high molecular weights ( $M_w = 430,000 – 1,269,000$  g/mol) with about 1.1 polymer chains per metal center being produced.

While studying a series of Group 5 catalysts, Nakamura and co-workers reported on the synthesis and ethylene polymerization behavior of cyclopentadienyl( $\eta^4$ -diene)tantalum complexes.<sup>205</sup> Upon activation with MAO at

temperatures of -20 °C or below, compounds **84a**, **85a** and **86** (Figure 1.38) furnish PEs with narrow molecular weight distributions ( $M_w/M_n \leq 1.4$ ,  $M_n = 8,600 - 42,900$  g/mol). Below -20 °C, ethylene polymerization by **85a**/MAO displayed a linear increase of  $M_n$  with increasing reaction time. The activity for ethylene polymerization was shown to depend on the substitution pattern of the  $\eta^4$ -diene ligand with the highest activity being obtained in the case where 2,3-dimethyl-1,3-butadiene is used (**85b**); the lowest when isoprene is employed (**85c**).<sup>206</sup> When activated with MAO, the analogous niobium complexes (**87a-d**, Figure 1.38) were also shown to behave as living ethylene polymerization catalysts up to 20 °C ( $M_w/M_n = 1.05 - 1.30$ ,  $M_n = 5,100 - 105,400$  g/mol).<sup>207</sup> The dependence of activity on the  $\eta^4$ -diene ligand employed mirrored that observed for the analogous tantalum compound

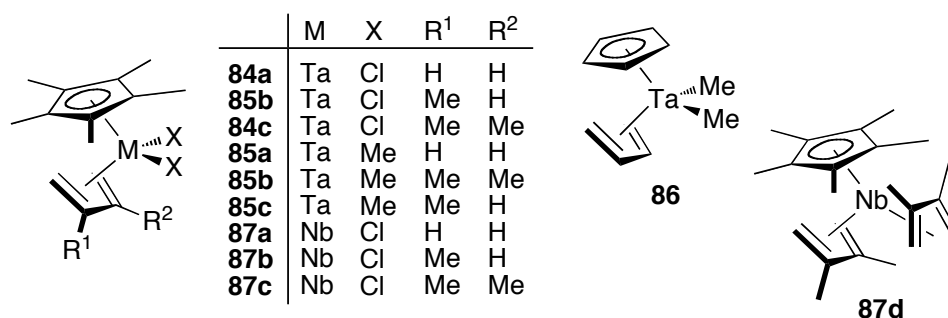


**Figure 1.38.** Group 5 olefin polymerization catalysts.

Finally, Theopold and co-workers investigated chromium complexes bearing 2,4-pentane-*N,N'*-bis(aryl)ketiminato ((Ar)<sub>2</sub>nacnac) ligands for ethylene polymerization.<sup>208</sup> At room temperature in the presence of ethylene, **88** (Figure 1.39) formed linear PE with narrow molecular weight distributions ( $M_w/M_n = 1.17 - 1.4$ ). The  $M_n$  was shown to increase linearly with polymer yield. These results represented the first report of living ethylene polymerization with a chromium-based catalyst.

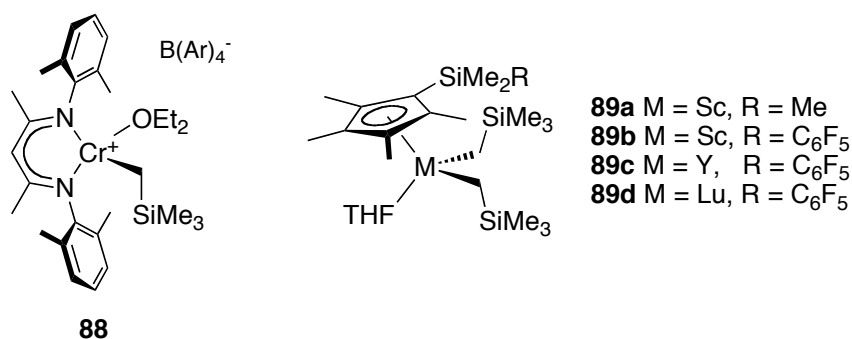


**Figure 1.39.** Non-group 4 olefin polymerization catalysts.

### 1.5 Rare-Earth Metal Catalysts

In addition to early metal catalysts, several living rare-earth metal catalysts have been reported. In 2008, Tritto and co-workers described the copolymerization of ethylene with norbornene catalyzed by rare-earth metal half sandwich complexes **89a-d** (Figure 1.39).<sup>209</sup> Upon activation, **89a,b**/[Ph<sub>3</sub>C][B(C<sub>6</sub>F<sub>5</sub>)<sub>4</sub>] showed excellent activities for the copolymerization of ethylene and norbornene. Specifically, **89b**/[Ph<sub>3</sub>C][B(C<sub>6</sub>F<sub>5</sub>)<sub>4</sub>] furnished poly(E-*co*-NB) with 29 – 42 mol% norbornene. Over 3 minutes, a linear increase in molecular weight ( $M_n = 100,000 - 250,000$  g/mol) was observed while a narrow molecular weight distribution ( $M_w/M_n = 1.22 - 1.35$ ) was maintained. At room temperature with [Ph<sub>3</sub>C][B(C<sub>6</sub>F<sub>5</sub>)<sub>4</sub>], the yttrium analog (**89c**) displayed poor activity for ethylene norbornene copolymerization and the lutetium analog (**89d**) was inactive for the polymerization.

Utilizing [Cp<sub>2</sub>\*SmMe(THF)] and [Cp<sub>2</sub>\*SmH]<sub>2</sub> (**90** and **91**, Figure 1.40), Yasuda and co-workers described the synthesis of block copolymers containing polyethylene (insertion mechanism) with several polar monomers (non-insertion mechanism) such as MMA, methyl acrylate (MA), ethyl acrylate (EA), d-valerolactone (VL), and ε-caprolactone (CL) via sequential addition.<sup>210</sup> Ethylene was first polymerized ( $M_w/M_n = 1.39 - 2.01$ ,  $M_n = 6,600 - 27,000$  g/mol) followed by addition of the respective polar monomer to form a diblock copolymer, however, reversal of monomer addition led to

no block copolymer formation. Thus a PE-*block*-PMMA, PE-*block*-PMA, PE-*block*-PEA, PE-*block*-PVL, and PE-*block*-PCL were synthesized and showed good material properties such as deep coloration with dyes. In a later report, the structurally related **92** (Figure 1.40) was also shown to be a viable block copolymerization catalyst for ethylene, MMA, and CL.<sup>211</sup> Furthermore, Yasuda and co-workers reported on the synthesis of diblock copolymers poly(1-pentene)/poly(1-hexene) and PMMA/PCL using the structurally similar bridged Cp-bearing yttrium and samarium catalysts **93** and **94** (Figure 1.40) via sequential monomer addition.<sup>212</sup>

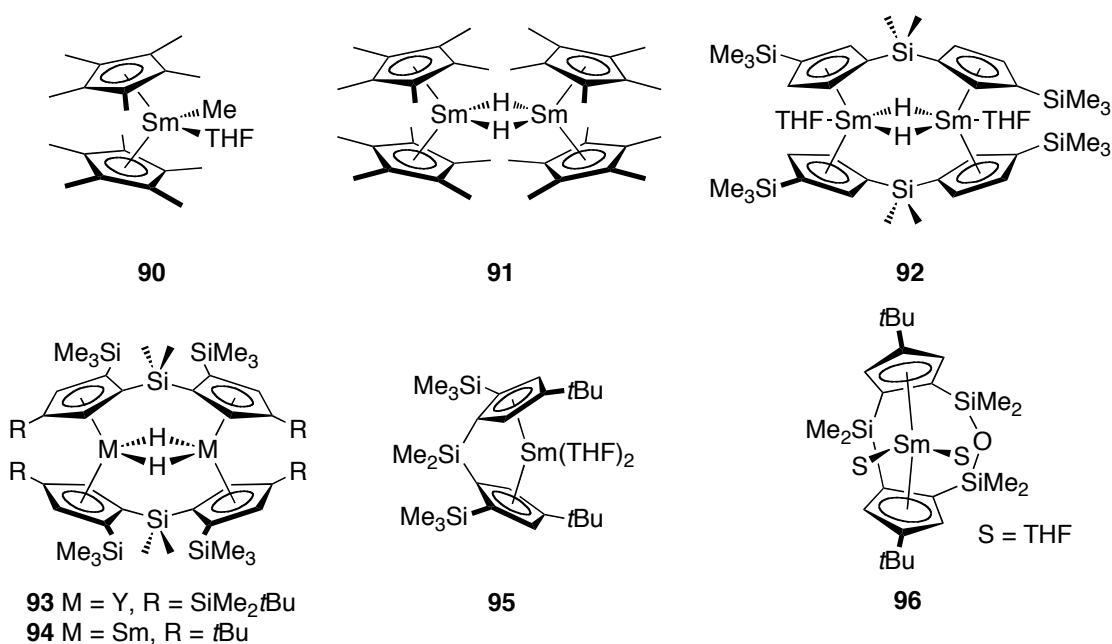
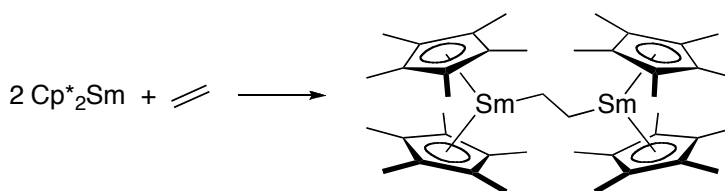


**Figure 1.40.** Rare-earth metal olefin polymerization catalysts.

It had been previously shown that Cp<sub>2</sub>\*Sm is active for ethylene homopolymerization involving coordination of ethylene by two Sm<sup>II</sup> centers followed by electron transfer to form a telechelic initiator (Scheme 1.12).<sup>213</sup> Yasuda and co-workers cleverly applied this observation to the synthesis of triblock copolymers of

ethylene and polar monomers.<sup>214</sup> Thus, triblock copolymers of PMMA-*block*-PE-*block*-PMMA, PCL-*block*-PE-*block*-PCL, and PDTC-*block*-PE-*block*-PDTC (PDTC = poly(2,2-dimethyltrimethylene carbonate)) were prepared through sequential monomer addition with **95** and **96** (Figure 1.40).



**Scheme 1.12.** Formation of a telechelic initiator for ethylene polymerization.

## 1.6 Late Metal Olefin Polymerization Catalysts

### 1.6.1 Nickel and Palladium $\alpha$ -Diimine Catalysts

In the mid 1990s, Brookhart and co-workers reported the synthesis and olefin polymerization activity of  $\alpha$ -diimine complexes of nickel and palladium.<sup>215</sup> These systems were unique among late metal catalysts in their ability to produce high molar mass materials, rather than oligomers, from both ethylene and higher  $\alpha$ -olefins. Furthermore, the metal centers were shown to migrate along polymer chains (“chain walking”),<sup>216</sup> allowing access to polyolefins with a wide variety of microstructures simply by varying ligand substitution patterns, temperature, or pressure. Shortly after the initial reports, conditions were disclosed which allowed the nickel catalysts **97** and **98** (Figure 1.41) to polymerize 1-hexene and 1-octadecene in a living fashion.<sup>217</sup> Upon activation with MAO or MMAO at -10 °C and low monomer concentrations, **97** and **98** resulted in living systems furnishing polymers of  $M_n = 19,000$  to 91,000 g/mol and narrow molecular weight distributions ( $M_w/M_n$  as low as 1.09). The systems were also shown to exhibit a linear increase in  $M_n$  with time. Branching density was less than that calculated for perfect sequential 1,2-insertions as a result of  $\omega$ ,1-enchainment, or

“chain straightening”.<sup>218</sup> Poly(1-hexene) with as few as 118 branches/1000 carbons (vs. 167 expected for perfect 1,2-insertions) and poly(1-octadecene) with as few as 39 branches/1000 carbons (vs. 56 expected) were produced -10 °C. Branching density was controlled by reaction conditions and catalyst structure, with **98** producing more linear polymers than **97**. Studying several palladium and nickel complexes, Merna *et al.*<sup>219,220</sup> reported living 1-hexene polymerization behavior with **97**/MAO and **99**/MAO. These values are considerably more narrow than those reported by Brookhart for similar reactions at 23 °C, although the reason for the improvement is not clear.

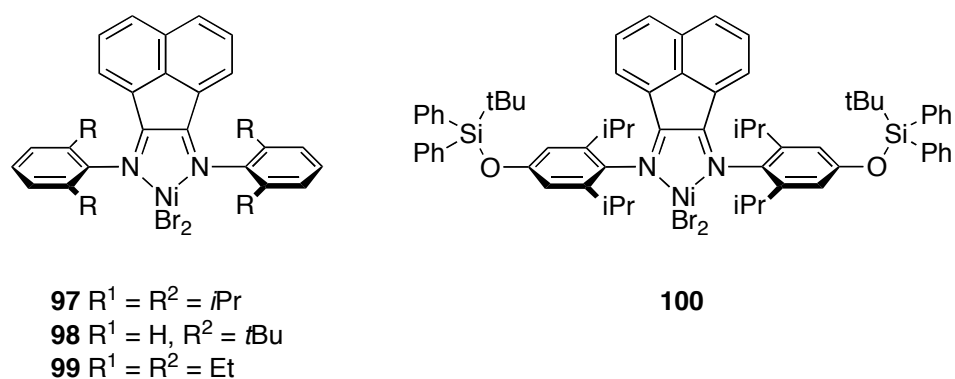


**Figure 1.41.** Nickel  $\alpha$ -diimine precatalysts for olefin polymerization.

A siloxy-substituted analogue of **97** (**100**, Figure 1.41) was synthesized by Marques, Gomes and co-workers<sup>221</sup> who studied its application for the living polymerization of 1-hexene at -11 °C and up to 16 °C. At the higher temperature, the polydispersity increases somewhat ( $M_w/M_n = 1.12 - 1.21$ ), and the increase in molecular weight is only linear for the first 40 minutes. In addition, the polymer has a different microstructure, with branching greatly decreased at 16 °C relative to -10 °C (83 vs. 132 branches/1000 carbons, respectively).

Utilizing a structural variant of **97** featuring a cyclophane diimine ligand (**101**, Figure 1.42), Camacho and Guan reported the first living polymerization at elevated temperatures with nickel.<sup>222</sup> When activated with MMAO, **101** furnished poly(1-hexene)s with narrow molecular weight distributions ( $M_w/M_n = 1.13 - 1.22$ ) up to 75 °C and branching densities (52-58 branches/1000 carbons) approximately one-half of those reported for **97**. The authors attribute the improved behavior to the cyclophane framework which very effectively blocks the axial sites of the nickel center preventing chain transfer.

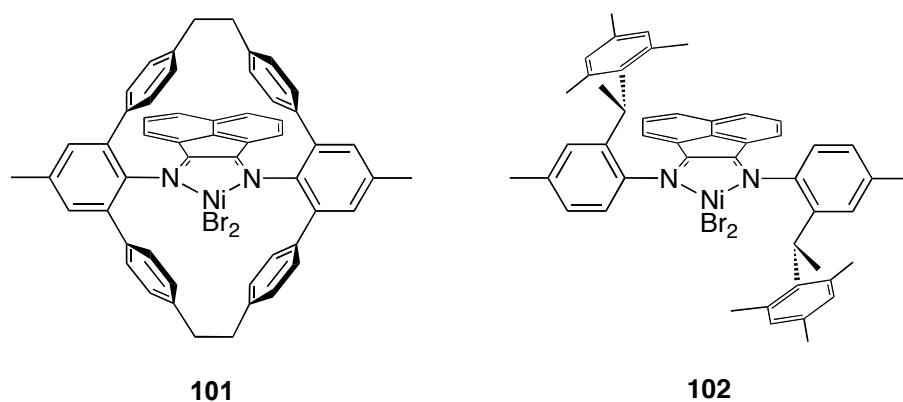
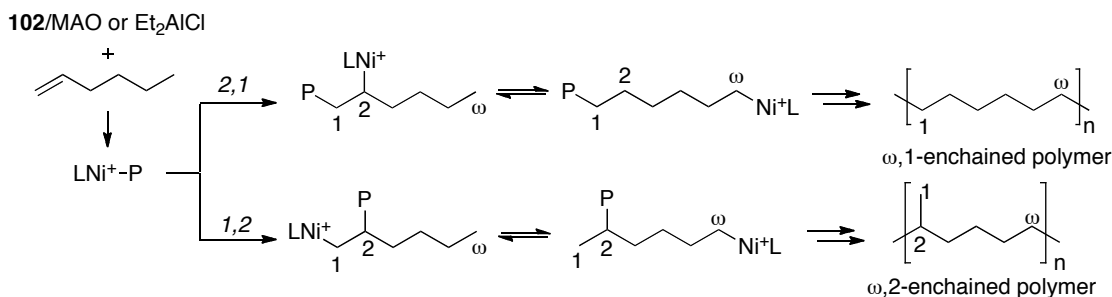


**Figure 1.42.** Nickel α-diimine olefin polymerization catalysts.

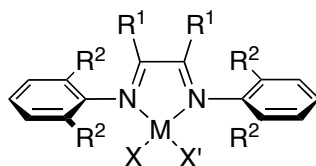
Coates and co-workers employed the chiral, C<sub>2</sub>-symmetric nickel diimine complex **102** (Figure 1.42) to control polymer microstructure for living polymerization of α-olefins.<sup>223</sup> A hallmark of the original nickel diimine catalysts is the ability to undergo successive β-hydride eliminations/reinsertions, commonly referred to as “chain walking”.<sup>21</sup> This may lead to “chain straightening” with α-olefins, generating regioirregular polymers with less branching than expected. Careful tailoring of reaction conditions (low temperatures and high monomer concentration) with catalyst **102** generates high selectivity for ω,2-enchainment, generating predominantly methyl branches at regular intervals between methylene units (illustrated for 1-hexene in

Scheme 1.13). The technique is applicable to a range of  $\alpha$ -olefins, but selectivity for  $\omega,2$ -enchainment was shown to decrease with increasing chain length (96 mol%  $\omega,2$ -enchainment for 1-butene vs. 70% for 1-octene).



**Scheme 1.13.**  $\omega,1$  and  $\omega,2$ -enchainment of 1-hexene.

Suzuki *et al.* have explored  $\alpha$ -diimine complexes of both nickel and palladium (**103a-e**, Figure 1.43) for the polymerization of 1-hexene at very high pressures (up to 750 MPa).<sup>224</sup> While nickel catalysts displayed non-living behavior, the palladium catalysts **103d,e** (Figure 1.43) were living for 1-hexene polymerization and polydispersities decreased at higher pressures ( $M_w/M_n = 1.27 - 1.29$  at 0.1 MPa vs. 1.11 – 1.17 at 500 MPa with **103e**).



	M	R <sup>1</sup> , R <sup>1</sup>	R <sup>2</sup>	X	X'
<b>103a</b>	Ni	Me, Me	<i>i</i> Pr	Br	Br
<b>103b</b>	Ni	Me, Me	Me	Br	Br
<b>103c</b>	Ni	1,8-naphthyl	<i>i</i> Pr	Br	Br
<b>103d</b>	Pd	Me, Me	<i>i</i> Pr	Cl	Cl
<b>103e</b>	Pd	Me, Me	<i>i</i> Pr	Cl	Me

**Figure 1.43.** Nickel and palladium olefin polymerization precatalysts.

Using diimine complexes of palladium, Gottfried and Brookhart have demonstrated conditions which allow for living polymerizations of 1-hexene and 1-octadecene at 0 °C where quenching with Et<sub>3</sub>SiH is required to prevent chain coupling.<sup>225</sup> Relative to **104b**, catalyst **104a** (Figure 1.44) exhibited improved living behavior for 1-hexene polymerization. This was attributed to the ability of the nitrile donor to compete with 1-hexene for the open coordination site in **104b**. Over the course of 3 hours, both **104a** and **104b** showed a linear increase in  $M_n$  with time and furnished poly(1-hexene)s with narrow molecular weight distributions ( $M_w/M_n = 1.10 - 1.15$ ) and branching densities of 75-85 branches/1000 carbons. Catalyst **104b** was likewise applied to the living polymerization of 1-octadecene. The  $M_n$  was observed to increase linearly over the first 3 h at 0 °C, however, the molecular weight distribution increased as well ( $M_w/M_n = 1.34$  after 3 h). This was attributed to precipitation of the polymer at this temperature, which also limits the accessible molecular weights to ~40,000 g/mol. Sen and co-workers reported on a structurally similar diimine palladium complex to **104a** bearing a five-membered ester chelate arising from 1,2-insertion of methyl methacrylate into the cationic palladium precursor (**104c**, Figure 1.27).<sup>226</sup> Over the course of 22 hours, catalyst **104c** displayed “quasi-living” behavior for 1-hexene polymerization showing an increase in  $M_n$  with time.

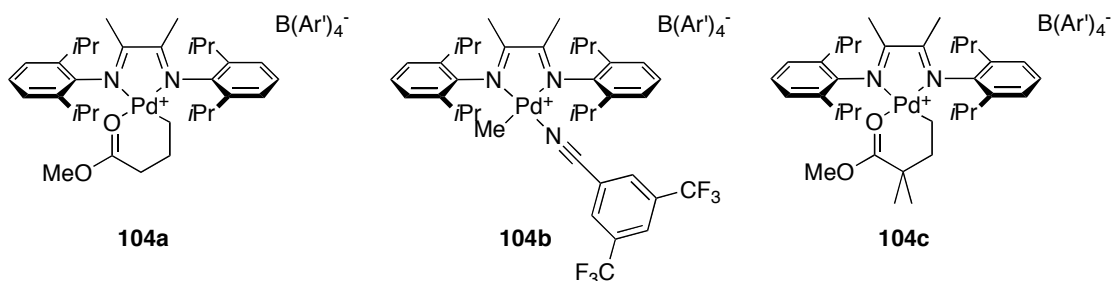
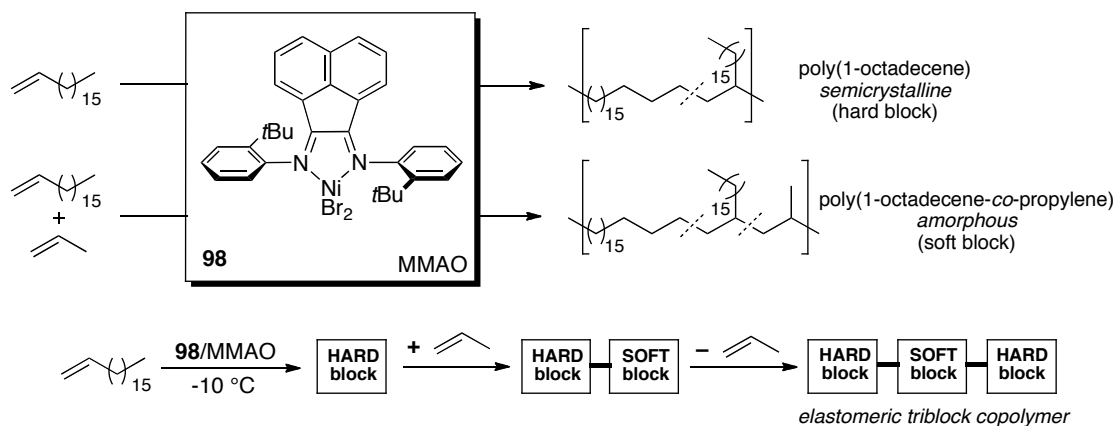


**Figure 1.44.** Palladium pre-catalysts for olefin polymerization.

It was also discovered that addition of carbon monoxide (CO) in the presence of 1-hexene and **104c** afforded an alternating copolymer. Taking advantage of this, a poly(1-hexene)-*block*-poly(1-hexene-*alt*-CO) diblock copolymer was made through sequential monomer addition. Similarly, a PE-*block*-poly(ethylene-*alt*-CO) diblock copolymer was also synthesized through sequential monomer addition.

In addition to 1-hexenes,  $\alpha$ -diimine complexes of nickel were the first late transition metal catalysts reported for the living polymerization of propylene.<sup>215</sup> Upon activation with MMAO at  $-10\text{ }^{\circ}\text{C}$ , catalyst **97** (Figure 1.41) afforded PP with a narrow molecular weight distribution ( $M_w/M_n = 1.13$ ;  $M_n = 160,000\text{ g/mol}$ ) and  $M_n$  was shown to increase linearly with conversion. The material obtained had 159 branches/1000 carbons, far less than the theoretical value of 333 for sequential 1,2-insertions, which was attributed to chain straightening. As branching decreased,  $T_g$  values decreased as well (as low as  $-55\text{ }^{\circ}\text{C}$ ), illustrating the dramatic effects of enchainment mechanism on physical properties.



**Scheme 1.14.** Synthesis of 1-octene/propylene triblock copolymers using **98**/MAO.

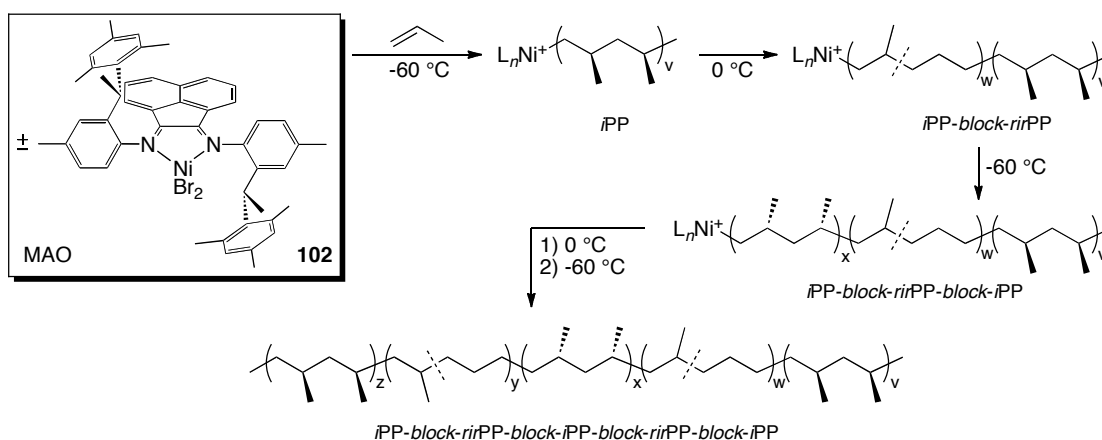
Brookhart and co-workers demonstrated the living nature of nickel catalysts **97** and **98** (Figure 1.41) with the synthesis of well-defined di- and triblock copolymers of

$\alpha$ -olefins.<sup>217</sup> At -15 °C, activation of **97** with MAO followed by sequential addition of monomers afforded PP-*block*-poly(1-hexene) with monomodal, narrow molecular weight distributions ( $M_w/M_n = 1.11 - 1.13$ ), which exhibited less branching than predicted, due to partial chain-straightening. Triblocks were prepared by activation of **97** or **98** with MMAO at -10 °C followed by reaction with 1-octadecene to afford a semicrystalline, chain-straightened block as observed in homopolymerizations with that monomer. Sequential addition of propylene resulted in poly(1-octadecene)-*co*-PP, which was followed by formation of a third poly(1-octadecene) block as propylene was removed (Scheme 1.14). The resultant materials exhibited elastomeric properties as expected based on the “hard-soft-hard” triblock structure of the polymers.

Living polymerization of propylene was also achieved by Marques and Gomes with **100** (Figure 1.41).<sup>221</sup> At -11 °C, **100**/MAO produced PP with narrow molecular weight distribution ( $M_w/M_n = 1.17 - 1.19$ ) and a nearly linear increase in molecular weight over 2 hours. Minimal chain-straightening was observed (316 branches/1000 carbons) and the polymer was moderately syndioenriched ( $[rr] = 0.54$ ). Exploiting the living nature of **100**, di- and triblock copolymers were synthesized.<sup>221</sup> At -15 °C, **100**/MAO polymerized propylene and generated a syndio-rich polypropylene block. Following removal of excess monomer under vacuum, addition of 1-hexene at the same temperature generated a diblock copolymer with  $M_w/M_n = 1.18$  and  $M_n = 46,400$  g/mol. Triblocks were produced with this catalyst in a similar fashion. Polymerization of 1-hexene first, followed by introduction of propylene (with 1-hexene still present), followed by venting and then allowing the residual 1-hexene to react allowed for formation of a shorter ( $M_n = 31,100$  g/mol) ABA triblock copolymer, with the middle block composed of poly(propylene-*ran*-(1-hexene)).

The cyclophane Ni catalyst **101** (Figure 1.42) was employed by Guan and co-workers in a dramatic demonstration of propylene chain-straightening.<sup>222</sup> At

temperatures up to 50 °C, **101**/MAO showed good activity for propylene polymerization, with narrow molecular weight distributions ( $M_w/M_n = 1.06 - 1.16$ ). In addition,  $M_n$  was shown to increase linearly with time at 50 °C. The PPs contain 104 – 113 branches/1000 carbons, indicative of extensive chain-straightening. This implies that the cyclophane ligand geometry favors a 2,1-insertion mechanism.



**Scheme 1.15.** Synthesis of propylene-based block copolymers using **102**/MAO.

Utilizing the chiral,  $C_2$ -symmetric nickel complex **102** (Figure 1.42), Coates and co-workers polymerized propylene in a living fashion at temperatures up to 22 °C in the presence of MAO, with a narrow distribution of molecular weights ( $M_w/M_n \leq 1.11$ ).<sup>227</sup> Both the regio- and stereocontrol of enchainment are temperature dependent, allowing access to a wide variety of polymer microstructures from a single monomer. At low temperatures ( $-78\text{ }^\circ\text{C}$ ), no chain straightening is observed furnishing highly isotactic PP, but the percentage of 3,1-enchainment increases up to 56.2% at 22 °C producing an amorphous and regioirregular PP. Uniquely, this catalyst has ability to maintain living behavior at a variety of temperatures, but with variable tacticity and levels of chain-straightening. Utilizing this temperature dependence, **102**/MAO was used to synthesize regiblock PPs having good elastomeric properties.<sup>27</sup> Both a

triblock and pentablock copolymer were synthesized by simply varying the reaction temperature during the course of the polymerization (Scheme 1.15). For example, an *i*PP-*block-rir*PP-*block-i*PP ( $M_n = 109,000$  g/mol,  $M_w/M_n = 1.14$ ) and *i*PP-*block-rir*PP-*block-i*PP-*block-rir*PP-*block-i*PP ( $M_n = 159,000$  g/mol,  $M_w/M_n = 1.39$ ) pentablock copolymer were prepared by toggling the reaction temperature between -60 and 0 °C. Transmission Electron Microscopy (TEM) revealed no microphase separation. However, the pentablock copolymer exhibited an exceptional strain to break of 2400% and good elastomeric recovery out to strains of 1000%.

In an attempt to obtain higher regio- and isoselectivity at low reaction temperatures, Coates and co-workers introduced new chiral,  $C_2$ -symmetric nickel diimine complexes featuring cumyl-derived ligands.<sup>29</sup> Each of the complexes (**105a-f**, Figure 1.45) exhibited higher regioselectivity than **102** at -60 °C in the presence of MAO. Of the complexes studied at -78 °C, **105f** furnished isotactic PP with the highest melting temperature ( $T_m = 149$  °C). In addition, a linear increase in  $M_n$  with polymer yield is observed at 0 °C. Regioblock polypropylenes were produced with **105f**/MAO that exhibited improved elastomeric performance at elevated temperatures (e.g., 65 °C) over block copolymers synthesized with **102**/MAO.<sup>29</sup>

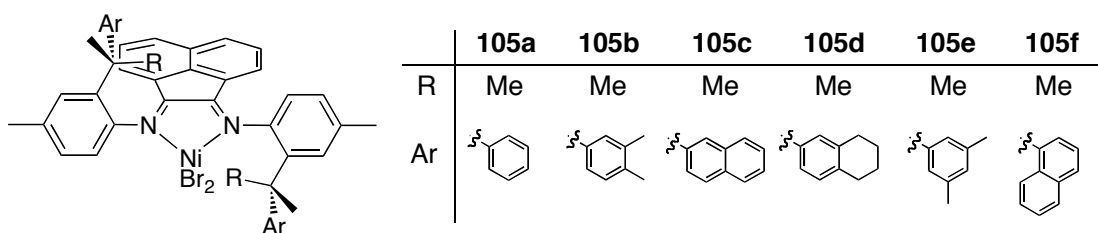


**Figure 1.45** Nickel  $\alpha$ -diimine catalysts derived from cumyl-based ligands.

Using Pd complexes containing diimine ligands (**104b**, Figure 1.44) at 0 °C, Gottfried and Brookhart observed a relatively linear increase in polypropylene  $M_n$  with

time up to approximately 40,000 g/mol.<sup>225</sup> However, living systems were not obtained when the palladium ester chelate catalyst **104a** was employed due to slow initiation relative to propagation. This initiation problem could be circumvented utilizing **104b** because the weakly bound nitrile group is more easily displaced by propylene. Consistent with previous results, PPs generated by this catalyst are chain-straightened, containing approximately 253 branches per 1000 carbons.

In addition to propylene and higher  $\alpha$ -olefins, ethylene polymerization behavior has been investigated using late metal catalysts. First-generation nickel  $\alpha$ -diimine catalysts such as **97** (Figure 1.41) do not polymerize ethylene in a living fashion due to relatively facile chain transfer. Rieger and co-workers have investigated modifications of this framework to prevent chain transfer by enhancing the steric bulk about the metal center.<sup>228</sup> When **106** (Figure 1.46) was activated with MAO at ambient temperature, molecular weight distributions were decreased markedly ( $M_w/M_n$  as low as 1.3) for short reaction times and ultra-high molecular weight ( $> 4,500,000$  g/mol), highly linear PE was produced.

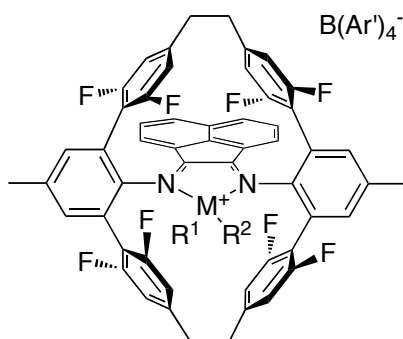


**106** Ar = 4-*t*BuPh

**Figure 1.46.** Nickel  $\alpha$ -diimine precatalysts for olefin polymerization.

Further investigating ethylene polymerization behavior with this class of catalysts, Guan and co-workers extended the study of hindered diimine catalysts with cyclophane complex **101** (Figure 1.42).<sup>229</sup> Upon activation with MMAO, **101** is highly active for production of branched PEs (66-97 branches/1000 carbons) with relatively narrow polydispersities ( $M_w/M_n$  as low as 1.23 at 50 °C). Most significantly, these

catalysts exhibit impressive thermal stability, with good activities even up to 90 °C. However, the polydispersity increases, and the activities decrease somewhat at higher temperatures. Interestingly, a related alkyl cyclophane Ni complex demonstrated almost no activity for ethylene polymerization.<sup>230</sup>



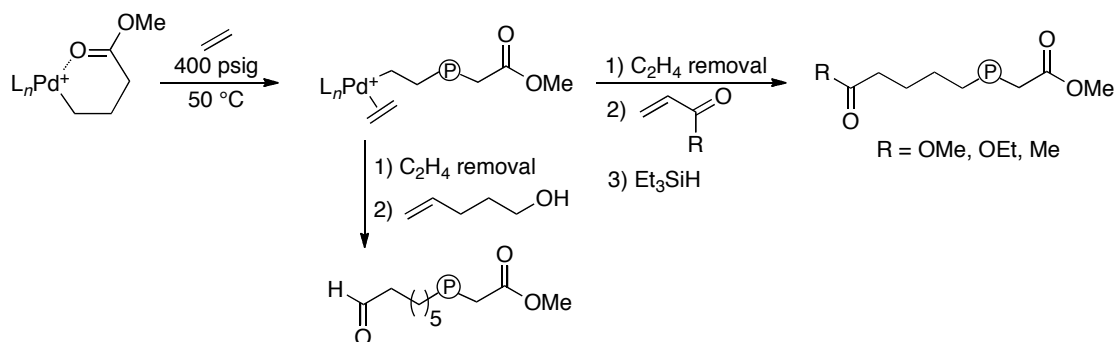
**107** M = Ni, R<sup>1</sup> = R<sup>2</sup> = -OC(CH<sub>3</sub>)CHC(CH<sub>3</sub>)O-

**108** M = Pd, R<sup>1</sup> = Me, R<sup>2</sup> = NCAr

**Figure 1.47.** Nickel complexes bearing fluorinated cyclophane ligands.

In a subsequent report, Guan and co-workers found a significant effect on polymer properties and reactivity upon fluorination of the cyclophane ligand (**107**, Figure 1.47).<sup>231</sup> The fluorinated nickel complex (**107**) showed improved thermal stability relative to its non-fluorination counterpart (**101**). After 70 minutes at 105 °C, **107**/TIBA produced high molecular weight PE ( $M_n = 190,000$  g/mol) with a unimodal molecular weight distribution ( $M_w/M_n = 2.7$ ). The palladium complex bearing the fluorinated cyclophane (**108**, Figure 1.47) was observed to produce higher molecular weight polymer than variations of the catalyst containing non-fluorinated ligands. Upon activation with TIBA at 35 °C, **108** yielded PE with a narrow polydispersity ( $M_w/M_n = 1.3$ ) and high molecular weight ( $M_n = 264,000$  g/mol). Both the nickel (**107**) and palladium (**108**) complexes exhibited a significant decrease in chain branching compared to their non-fluorinated counterparts. The authors postulate that the fluorine

atom stabilizes the electrophilic metal center through electron donation. This type of stabilization is well known in early-metal polymerization systems, but this report represents the first example of positive fluorine interactions in late-metal olefin polymerization.



**Scheme 1.16.** Synthesis of telechelic polyethylene.

To achieve living polymerization of ethylene with palladium catalysts **104a** and **104b** (Figure 1.44), Brookhart and co-workers demonstrated that specific reaction conditions, particularly quenching reactions with  $Et_3SiH$  to prevent chain coupling, were crucial.<sup>232</sup> At 5 °C, highly branched (~100 branches / 1000 carbons), amorphous PEs with very narrow molecular weight distributions ( $M_w/M_n < 1.1$ ) were produced, and  $M_n$  was shown to increase linearly over at least 6 hours. At 27 °C,  $M_n$  of 237,000 g/mol could be obtained in 2 hours with broadened molecular weight distributions ( $M_w/M_n = 1.19$ ). To ensure rapid initiation of **104a**, high pressures of ethylene (400 psig) were required to displace the chelated carbonyl group, which is retained in the highly branched PE product. Compound **104b** exhibited similar activity at high pressures, while also yielding polymers with relatively narrow polydispersities ( $M_w/M_n = 1.15$  at 5 °C) at 1 atm ethylene. A telechelic polymer could be produced with **104a** by addition of alkyl acrylates before the silane quench.<sup>225</sup> Acrylates undergo

one insertion into the growing chain, forming stable chelates, but do not insert further, allowing for clean end-functionalization to generate polymers with two distinct ester end groups. Additionally, aldehyde end groups could be generated by quenching with 4-penten-1-ol. The vinyl group inserts, followed by Pd migration down the chain, and finally  $\beta$ -hydride elimination to generate the difunctional polymers shown in Scheme 1.16.

Given that palladium diimine catalysts produce highly branched, amorphous materials with ethylene, and produce semicrystalline polymers from long chain  $\alpha$ -olefins via a “chain straightening” mechanism, copolymers containing these two segments are an attractive goal. Gottfried and Brookhart investigated this block copolymer synthesis in detail.<sup>225</sup> Using **104b** (Figure 1.44), block copolymers of ethylene and 1-octadecene were prepared by opposite orders of addition to furnish PE-*block*-poly(1-octadecene) and poly(1-octadecene)-*block*-PE. In all cases, materials with narrow molecular weight distributions were obtained ( $M_w/M_n = 1.06 - 1.22$ ). Depending on the order of monomer addition, the copolymer microstructures differed. When ethylene was introduced first, the number of ethyl and propyl branches decreases substantially relative to the case where 1-octadecene is added first.

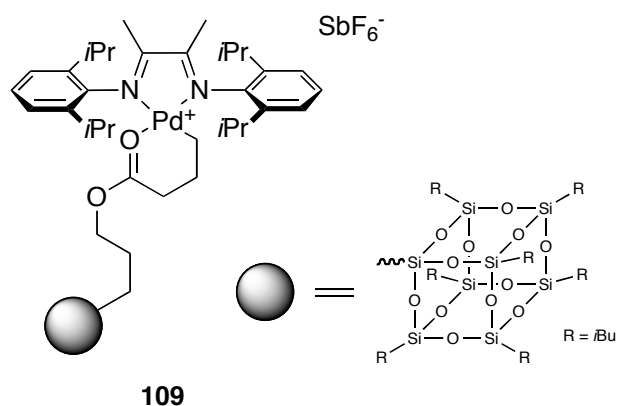


**Figure 1.48.** POSS supported palladium complex.

Extending the study of **104a**, Ye and co-workers modified the palladium ester chelate by immobilization on a polyhedral oligomeric silsesquioxane (POSS) support (**109**, Figure 1.48) which furnished POSS end-functionalized PEs.<sup>233</sup> The  $M_n$  was shown to increase linearly with time. In a subsequent report, Ye and co-workers immobilized the palladium ester chelate on silica nanoparticles as a versatile surface-initiated living ethylene polymerization technique for grafting from silica nanoparticles.<sup>234</sup> After cleavage of the PE brushes from the silica nanoparticles, the polymers were found to possess narrow PDIs ( $M_w/M_n \sim 1.18$ ).

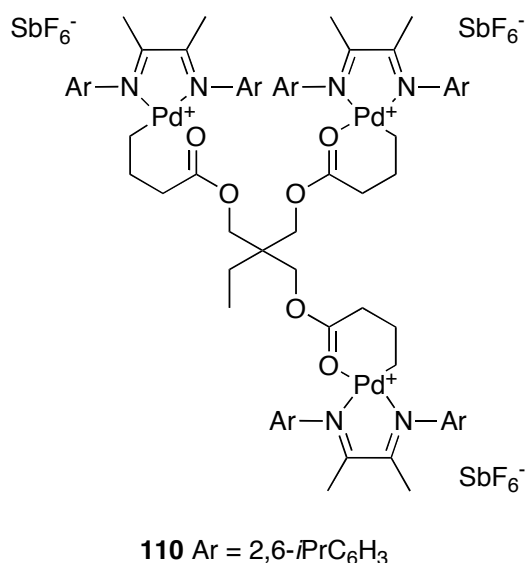
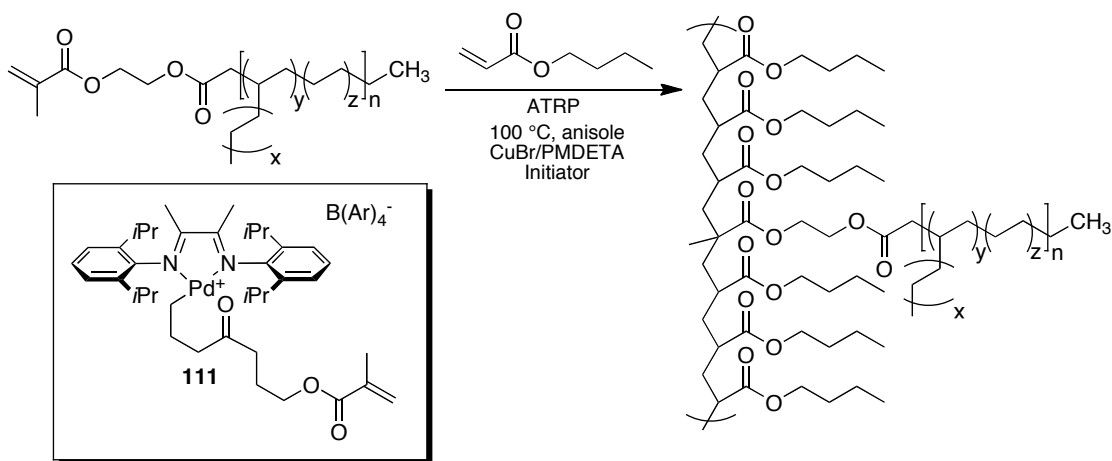


**Figure 1.49.** Trinuclear palladium olefin polymerization catalyst.

Utilizing a triacrylate, Subramanian and co-workers synthesized a trinuclear palladium  $\alpha$ -diimine catalyst (**110**, Figure 1.49) for the production of star PE.<sup>235</sup> At 5 °C in the presence of ethylene, **110** produced three-arm star polymers with narrow molecular weight distributions ( $M_w/M_n = 1.05 - 1.12$ ) and molecular weights ( $M_n = 32,000 - 135,000$ ) that increased over the course of five hours. Cleavage of the star polymer revealed arm molecular weights ( $M_n = 11,000 - 44,000$  g/mol) that were

approximately three times smaller than the corresponding star polymer. Analysis of the intrinsic viscosity of the polymer was consistent with star polymers exhibiting more compact chain conformation.

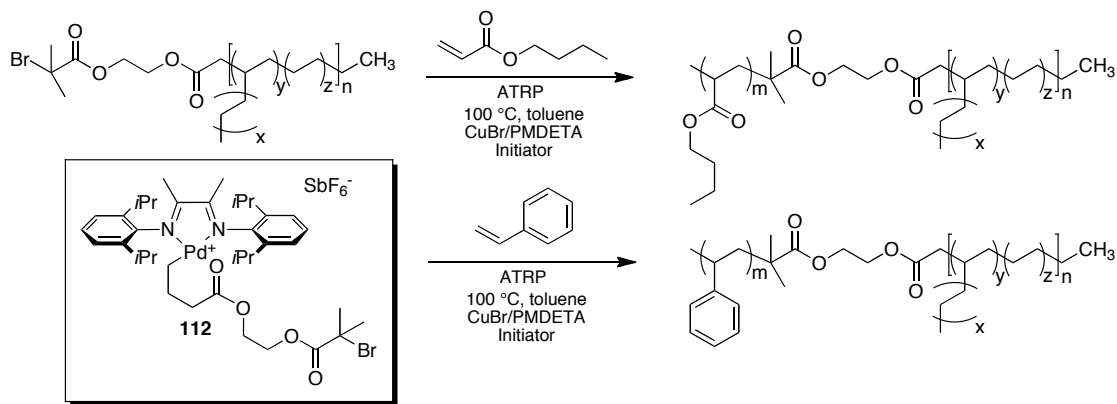
To synthesize graft copolymers, Brookhart and Matyjaszewski combined living insertion polymerization with living ATRP (Atom Transfer Radical Polymerization) techniques. Palladium diimine chelate complexes have been previously used for living polymerization of ethylene, affording end-functionalized, branched polyethylenes.<sup>236</sup> Catalyst **111** (Scheme 1.17) builds on this strategy by appending an acrylate ester forming a PE macromonomer that was incorporated into a living ATRP polymerization of *n*-butyl acrylate to generate poly(*n*-butyl acrylate)-*graft*-PE. Graft copolymers of moderate molecular weight ( $M_n$  = up to 115,000 g/mol) were obtained with approximately 4-5 grafts per chain and relatively narrow molecular weight distribution ( $M_w/M_n$  as low as 1.4).



**Scheme 1.17.** Graft copolymer synthesis using living insertion and ATRP.

Combining living insertion polymerization with living ATRP techniques, Ye and co-workers generated block copolymers with a functionalized palladium diimine catalyst.<sup>237</sup> Catalyst **112** (Scheme 1.18) appended with bromo-functionality

forms a PE macroinitiator that was incorporated into a living ATRP polymerization of *n*-butyl acrylate or styrene to generate poly(*n*-butyl acrylate)-*block*-PE and PS-*block*-PE diblock copolymers (Scheme 1.18).

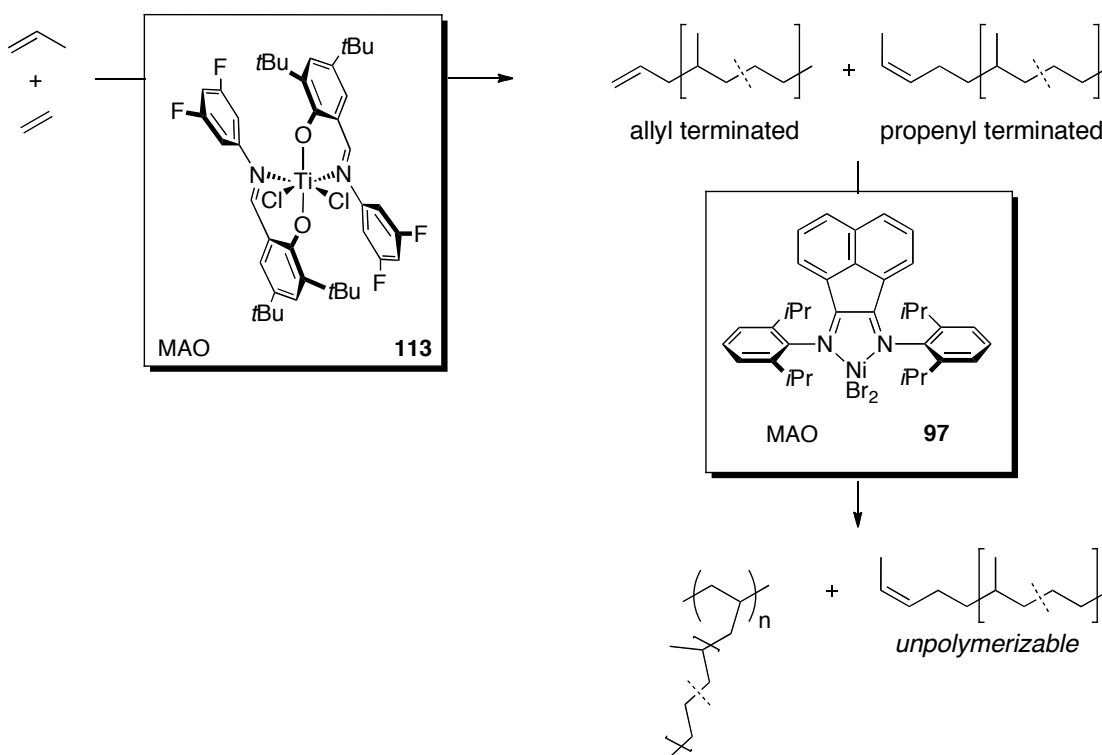


**Scheme 1.18.** Synthesis of PE-*block*-poly(*n*-butylacrylate) and polystyrene diblock copolymers.

To generate a series of poly(*E-co*-P) comb polymers, Coates and co-workers have polymerized poly(*E-co*-P) macromonomers.<sup>238</sup> Using a non-living titanium bis(phenoxyimine) catalyst (**113**, Scheme 19) poly(*E-co*-P) macromonomers featuring one unsaturated chain end were synthesized. The monomers contained a mixture of allyl (polymerizable) and propenyl (unpolymerizable) end groups. The macromonomers were then homopolymerized using a living nickel diimine catalyst, **97**/MAO (Figure 1.26, Scheme 1.19), to generate poly(*E-co*-P) comb polymers featuring approximately 7 to 14 arms/molecule after fractionation from the unpolymerizable residual macromonomer; these values correspond well to the theoretical values based on reaction stoichiometry. The molecular weight distributions remained relatively low ( $M_w/M_n = 1.51 - 1.90$ ,  $M_n = 74,000 - 209,000$  g/mol).

Beyond unfunctionalized olefins, **97** is also capable of polymerizing olefin monomers that incorporate polar functional groups. Copolymers of polar monomers

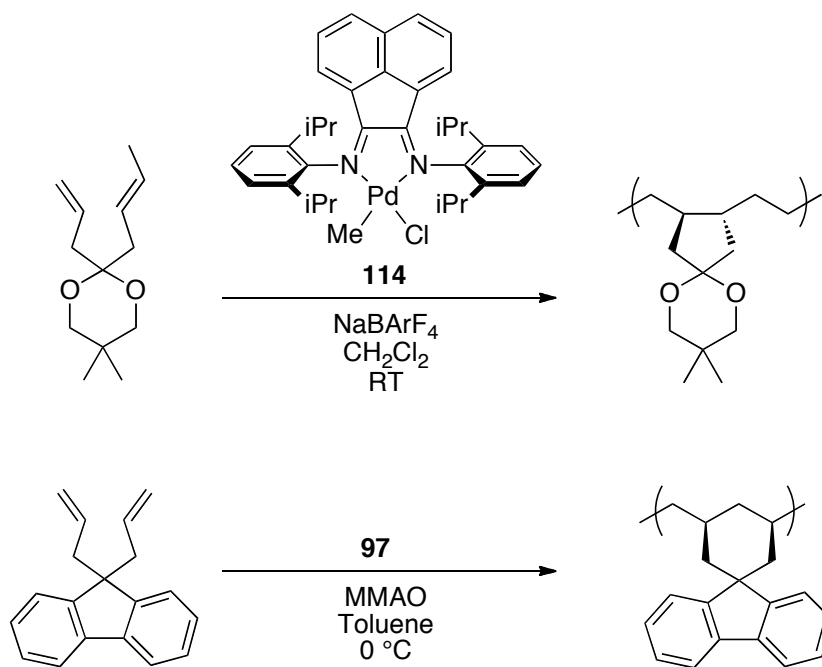
with olefins are attractive due to enhanced physical properties such as biocompatibility and ease of processing.<sup>36</sup> Coates and co-workers synthesized polyolefin elastomers by addition of small amounts of ureidopyrimidinone (UP) functionalized hexene to polymerizations of 1-hexene.<sup>239</sup> Nickel catalyst **97**/Et<sub>2</sub>AlCl (Figure 1.41) was used, exploiting the dual ability of Et<sub>2</sub>AlCl to activate the nickel center and to protect the Lewis basic nitrogen functional groups. Polymers incorporating ~2% UP-functionalized monomer were obtained with narrow molecular weight distributions ( $M_w/M_n = 1.2 - 1.4$ ). The resultant polymers exhibited reversible, non-covalent crosslinking through hydrogen bonding interactions, and thus have elastomeric properties at room temperature.



**Scheme 1.19.** Synthesis of poly(E-co-P) combs.

In addition to simple linear  $\alpha$ -olefins, Osakada and co-workers reported the polymerization of a number of 1,6-dienes catalyzed by palladium complexes to afford

polymers with *trans*-1,2-disubstituted five-membered rings.<sup>240</sup> In a subsequent report, **114**/NaBArF<sub>4</sub> was shown to polymerize 5-allyl-5-crotyl-2,2-dimethyl-1,3-dioxane in a living fashion (Scheme 1.20).<sup>241</sup> A linear increase in  $M_n$  with monomer conversion was demonstrated with molecular weight distributions remaining relatively narrow ( $M_w/M_n = 1.20 - 1.24$ ). Later, Osakada and co-workers reported that **97**/MMAO was capable of polymerizing 9,9-diallylfuorene (Scheme 1.20) yielding a polymer with  $M_n = 6,100$  g/mol and  $M_w/M_n = 1.36$  after three hours.<sup>242</sup> The resultant polymer contained predominately six-membered rings with *cis* geometry as evidenced by <sup>13</sup>C NMR spectroscopy.



**Scheme 1.20.** Polymerization of dienes using **114**/NaBArF<sub>4</sub> and **97**/MMAO.

The copolymerization of ethylene and diethyl diallylmalonate was investigated by Liu and co-workers in 2009 using **115** (Figure 1.50).<sup>243</sup> Due to extensive chain-walking, ethylene homopolymerization produces polymer with a hyperbranched

structure. Incorporation of the diethyl diallylmalonate reduces the amount of branching in the polymer produced because the catalyst is unable to chain-walk through the resultant five-membered ring. At 35 °C, **115** produced PE containing 97 branches per 1000 carbons with  $M_w = 78,000$  g/mol and a narrow molecular weight distribution ( $M_w/M_n = 1.44$ ). Upon incorporation of diethyl diallylmalonate (0.40 M), molecular weight ( $M_w = 25,000$  g/mol) and polydispersity ( $M_w/M_n = 1.202$ ) decreased along with branch density, which was reduced to 81 per 1000 carbons. Therefore, polymer topology can be tuned from hyperbranched to linear as a function of diethyl diallylmalonate incorporation.

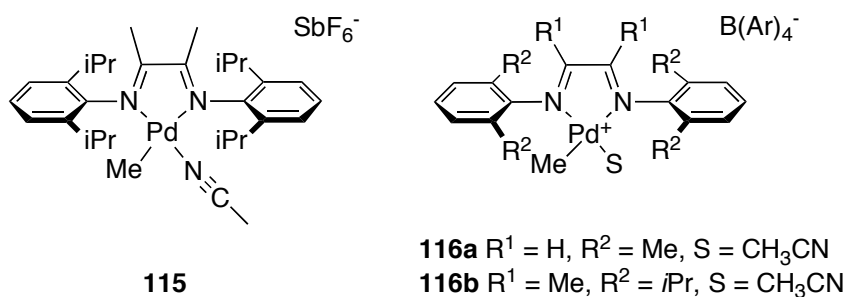


**Figure 1.50.** Palladium catalysts for olefin polymerization.

Finally, Kaminsky and Kiesewetter applied a combinatorial screening approach to identify catalysts for the copolymerization of norbornene with ethylene.<sup>244</sup> Catalysts **116a** and **116b** (Figure 1.50) were identified and furnished poly(E-co-NB) with 9-62 mol% norbornene incorporation and relatively narrow molecular weight distributions ( $M_w/M_n$  as low as 1.4) indicating “quasi-living” behavior.

### 1.6.2 Nickel $\alpha$ -Keto- $\beta$ -Diimine Catalysts

Bazan and co-workers recently described the synthesis and olefin polymerization behavior of a nickel  $\alpha$ -keto- $\beta$ -diimine complex.<sup>245,246</sup> At 0 °C,

activation of **117** (Figure 1.51) with MAO in the presence of 1-hexene furnished atactic poly(1-hexene) possessing  $M_n = 157,000$  g/mol and  $M_w/M_n = 1.2$ . Over the course of 120 minutes, molecular weights of the polymers obtained from the polymerization were observed to increase while polydispersities remained narrow. Microstructural analysis of the polymer by  $^{13}\text{C}$  NMR spectroscopy revealed mainly butyl (81.9%) and methyl (12.0%) branches; signatures arising from 2,1-insertions were not detected.

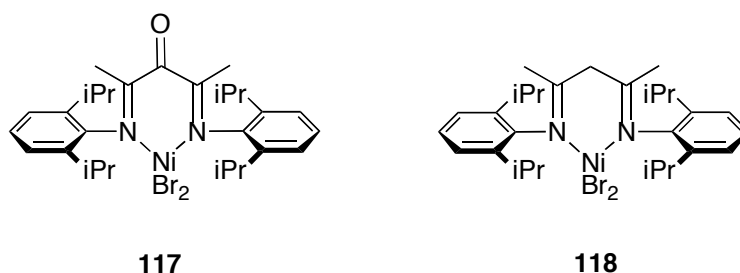


**Figure 1.51.** Nickel- $\alpha$ -keto- $\beta$ -diimine olefin polymerization catalysts.

In addition to polymerizing 1-hexene in a living fashion, Bazan and co-workers reported that **117**/MAO (Figure 1.51) was living for propylene polymerization.<sup>245,246</sup> At 0 °C, **117**/MAO furnished high molecular weight PP ( $M_n = 138,000$  g/mol) with narrow polydispersity ( $M_w/M_n = 1.1$ ). Over the course of 120 minutes, molecular weights of the polymers obtained from the polymerization increased while molecular weight distributions remained narrow. Analysis of the resultant polymers showed no evidence of 2,1-insertions. The material is best described as an ethylene-propylene copolymer, however, observed propylene sequences are moderately isotactic ( $[m] = 0.77$ ).

Bazan and co-workers have also shown that **117**/MAO (Figure 1.51) is living for ethylene polymerization.<sup>245,246</sup> At 10 °C, **117**/MAO produces branched PE (19 branches/1000 carbons) with  $M_n = 260,000$  g/mol and  $M_w/M_n = 1.1$ . Due to the small

amount of branching, the PE exhibits a  $T_m = 122$  °C. At 32 °C, high molecular weight ( $M_n = 1,112,000$  g/mol) branched PE (47 branches/1000 carbons) is obtained with a slightly broadened polydispersity ( $M_w/M_n = 1.3$ ). The carbonyl functionality leads to an increase in activity of approximately two orders of magnitude for ethylene polymerization over the analogous  $\beta$ -diimine catalyst (**118**, Figure 1.51) with no carbonyl functionality. The increase in reactivity was attributed to the attachment of a Lewis acid (from the aluminum cocatalyst) to the exocyclic oxygen site on the propagating cationic species.

### 1.6.3 Other Nickel Catalysts

Brookhart and co-workers have also investigated a series of anilinetropone based nickel catalysts **119a-c** (Figure 1.52).<sup>247</sup> Upon activation by  $\text{Ni}(\text{COD})_2$ , high activities and long lifetimes were observed for the polymerization of ethylene, particularly in the aryl-substituted cases, **119b** and **119c**. Over time, the  $M_n$  was shown to increase in nearly linear fashion with polydispersities remaining relatively narrow (as low as 1.2) at room temperature. However, increasing both the reaction temperature and time lead to a subsequent increase in polydispersity.

In 2009, Chen and co-workers reported the synthesis of  $\alpha$ -aminoaldimine nickel complexes (**120a-e**, Figure 1.52) for ethylene polymerization.<sup>248</sup> After 3 hours at 25 °C, **120d**/MAO produced polyethylene with high molecular weight ( $M_n = 164,000$  g/mol) and narrow molecular weight distribution ( $M_w/M_n = 1.31$ ). Increasing reaction time to 24 hours resulted in an increased molecular weight ( $M_n = 393,000$  g/mol) while maintaining a narrow polydispersity ( $M_w/M_n = 1.23$ ).

Finally, Bazan and co-workers have investigated nickel diimine variants **121a-g** (Figure 1.52).<sup>249,250</sup> At 20 °C, **121a**/ $\text{Ni}(\text{COD})_2$  produced PE with low branching (12 – 19 methyl branches/1000 carbons) and  $M_n$  was observed to increase linearly with

time up to 30 minutes. Additionally, the molecular weight distributions remained narrow for all the catalysts studied ( $M_w/M_n = 1.1 - 1.4$ ). Investigation into the role of the ligand revealed that as the steric bulk increased an increase in polymerization activity was observed.

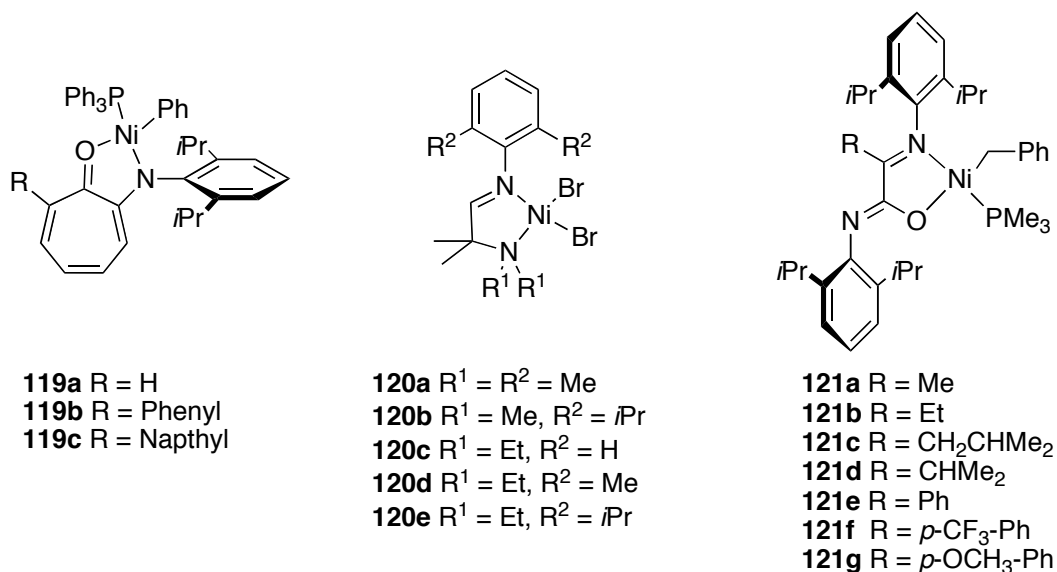
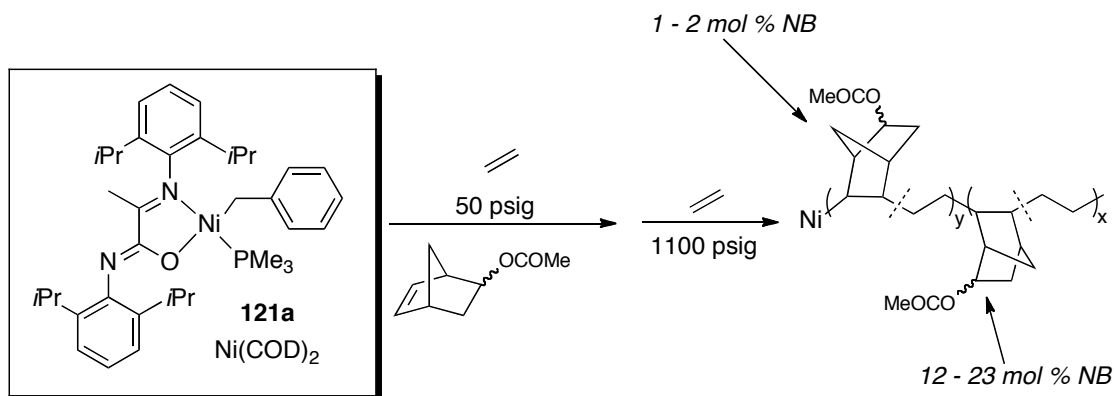


**Figure 1.52.** Nickel precatalysts for olefin polymerization

Utilizing **121**, Bazan and co-workers achieved the first quasi-living copolymerization of ethylene with a polar monomer, 5-norbornen-2-yl acetate.<sup>249,250</sup> Upon activation with Ni(COD)<sub>2</sub>, **121a-g** (Figure 1.52) incorporated 1-17 mol% 5-norbornen-2-yl acetate into a polyethylene backbone. Molecular weight distributions were relatively narrow ( $M_w/M_n = 1.2 - 1.6$ ), and the  $M_n$  exhibited a nearly linear increase with conversion. To synthesize block copolymers with different ratios of ethylene, Bazan and co-workers adopted a strategy based on a pressure-jump technique.<sup>251</sup> Polymerization of 5-norbornen-2-yl acetate and 50 psi ethylene generates an amorphous copolymer with approximately 25% polar monomer incorporation. After a given reaction time (8 – 45 minutes), the ethylene pressure was increased to

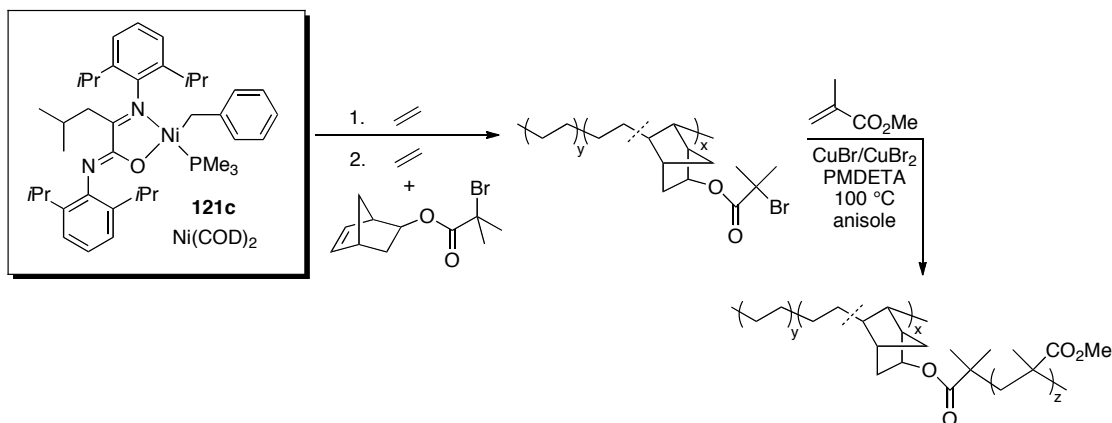
1100 psi leading to formation of an essentially PE block (Scheme 1.21) with relatively narrow polydispersities ( $M_w/M_n = 1.3 - 1.6$ ). Analysis of GPC and DSC data is consistent with diblock formation. TEM analysis demonstrated that the materials are microphase separated, consistent with blocks of distinct compositions. Tapered copolymers (TCP) have also been prepared with this system that allows depletion of 5-norbornen-2-yl acetate under a constant ethylene pressure.<sup>252</sup> It was observed that as 5-norbornen-2-yl acetate concentration depletes semicrystalline properties are obtained after specific reaction times, consistent with the fact that ethylene-rich segments are formed indicating pseudo-diblock copolymer formation. This strategy was used to make pseudo-tetrablock copolymers by addition of a second batch of 5-norbornen-2-yl acetate after a prescribed time<sup>253</sup> Tensile testing revealed a strain to break of about 1000% at 65 °C with 80% elastic recovery.



**Scheme 1.21.** Synthesis of ethylene/5-norbornen-2-yl acetate block copolymers.

In a later report, Bazan and co-workers combined living insertion polymerization with living ATRP techniques to synthesize graft copolymers.<sup>254</sup> Polymerization of ethylene followed by copolymerization with 5-norbornen-2-yl-2'-bromo-2'-methyl propanoate using **121c** (Figure 1.52) activated with Ni(COD)<sub>2</sub>

furnished a PE macroinitiator. Subsequent polymerization with MMA by living ATRP methods furnished PE-*graft*-PMMA copolymers (Scheme 1.22).



**Scheme 1.22.** Synthesis of PE-*graft*-PMMA copolymers using **121c** and ATRP.

#### 1.6.4 Other Palladium Catalysts

The field of palladium-mediated living olefin polymerization was advanced in 1995 by Novak with the design of  $\sigma,\pi$ -bicyclic Pd catalyst **122** (Figure 1.53), which is both highly air- and moisture-stable, due to chelation by the appended olefin, but exhibits good activity for living polymerization.<sup>255</sup> This unique, robust living behavior was demonstrated by the synthesis of well-defined block copolymers of norbornene and diethyl 7-oxabicyclo[2.2.1]hepta-2,5-diene-2,3-dicarboxylate. A subsequent retro-Diels-Alder reaction on this polymer afforded a discrete PNB-*block*-poly(acetylene) copolymer.

While investigating another palladium complex, Risse reported on the polymerization of norbornene (NB) in a controlled fashion with catalyst **123** (Figure 1.53) obtaining saturated polymers.<sup>256</sup> Renewed chain growth was observed with sequential addition of monomer, but only for low conversion. At 0 °C, narrow molecular weight distributions were obtained for short reaction times ( $t_{\text{rxn}} = 20$  minutes; 54% conversion;  $M_n = 21,400$  g/mol;  $M_w/M_n = 1.07$ ), but broadened as

conversion increased ( $M_w/M_n = 1.34$  at 100% conversion). Risse also showed that **123** polymerized a wide variety of ester-functionalized norbornenes, in some cases with narrow molecular weight distributions, and with linear increase in  $M_n$  over time.<sup>257</sup> Sequential addition of a norbornene monomer with different substitution pattern afforded diblock copolymers of moderate molecular weight.

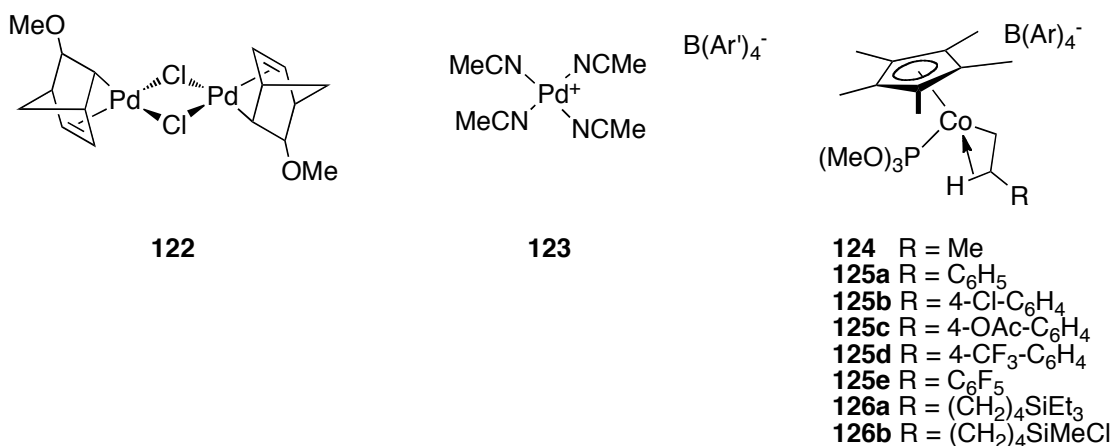


**Figure 1.53.** Palladium and cobalt pre-catalysts for olefin polymerization.

### 1.6.5 Monocyclopentadienyl Cobalt Catalysts

In 1991, Brookhart and co-workers identified Cp\* cobalt complex **124** (Figure 1.53) as a competent catalyst for polymerization of ethylene in a controlled fashion to low molecular weights ( $M_n = 13,600$  g/mol;  $M_w/M_n = 1.17$ ).<sup>258</sup> Soon thereafter, aryl or silyl groups were introduced in the catalyst framework that prevent chain migration and allow for the production of a variety of end-functionalized PEs under living conditions.<sup>259</sup> Reaction of **125a-e** (Figure 1.53) with ethylene led to the formation of aryl-substituted PEs with quite narrow molecular weight distributions ( $M_n$  up to 21,200 g/mol;  $M_w/M_n = 1.11 - 1.16$ ). Triethylsilane-capped PEs were furnished with catalyst **126** ( $M_n = 16,100$  g/mol;  $M_w/M_n = 1.15$ ).

## 1.7 Outlook And Summary

The last decade has seen significant new advances achieved in the field of living olefin polymerization. Many efficient and selective catalysts are now available for the living polymerization of ethylene in addition to living and stereoselective polymerization of  $\alpha$ -olefins. Resulting in the creation of unlimited new polymer architectures, such as block copolymers and end-functionalized macromolecules. The ability to synthesize such polymers will allow the detailed study of the effect of polymer microstructure on the mechanical and physical properties of this new class of materials.

As we wrote in our previous reviews,<sup>2-4</sup> the main challenge facing this new field is that these expensive metal complexes only form one polymer chain during the polymerization reaction, resulting in economically non-viable materials for commodity applications. Significant research in developing catalytic systems that can produce multiple chains per metal center must be conducted. One strategy to accomplish this goal is to add excess amounts of an inexpensive metal complex that will rapidly transmetallate the active living catalyst, producing many chains per metal center.<sup>93-95,260-264</sup> This strategy can then be used to create multiple block copolymers per metal center by varying polymerization conditions.<sup>82,265</sup> A second strategy is to add an external agent at specific intervals during the living polymerization to terminate a chain and begin a new one.<sup>169</sup> Third, metal complexes that transmetallate at rates slower than monomer enchainment but faster than chain formation have the potential to produce block copolymers when two different polymerization catalysts are used.<sup>24,25,266-268</sup> Finally, non-living catalysts that can be induced to introduce blocks on a time-scale faster than that of chain formation can be used to make block copolymers.<sup>23</sup>

Future research will continue to uncover new living systems capable of making unique polyolefin structures, and these advances will greatly expand the range of polyolefin materials. New strategies for developing catalyst systems capable of furnishing multiple chains per metal center will allow commodity polyolefin production from living catalysts. Undoubtedly, the future for specialty materials is a bright one in light of continued new developments in the field of living olefin polymerization.

## REFERENCES

- (1) Resconi, L.; Cavallo, L.; Fait, A.; Piemontesi, F. *Chem. Rev.* **2000**, 100, 1253-1345.
- (2) Coates, G. W.; Hustad, P. D.; Reinartz, S. *Angew. Chem. Int. Ed.* **2002**, 41, 2236-2257.
- (3) Domski, G. J.; Rose, J. M.; Coates, G. W.; Bolig, A. D.; Brookhart, M. *Prog. Polym. Sci.* **2007**, 32, 30-92.
- (4) Edson, J. B.; Domski, G. J.; Rose, J. M.; Bolig, A. D.; Brookhart, M.; Coates, G. W., *Controlled and Living Polymerizations: From Mechanisms to Applications*. Wiley-VCH: Weinheim, Germany, 2009; p 169-237.
- (5) Szwarc, M. *J. Polym. Sci. Part A: Polym. Chem.* **1998**, 36, IX-XV.
- (6) Webster, O. W. *Science* **1991**, 251, 887-893.
- (7) Vasile, C., *Handbook of Polyolefins*. Second ed.; Marcel Dekker Inc.: New York, 2000.
- (8) Ziegler, K.; Holzkamp, E.; Breil, H.; Martin, H. *Angew. Chem.* **1955**, 67, 426.
- (9) Natta, G.; Pino, P.; Corradini, P.; Danusso, F.; Mantica, E.; Mazzanti, G.; Moraglio, G. *J. Am. Chem. Soc.* **1955**, 77, 1708-1710.
- (10) Coates, G. W. *Chem. Rev.* **2000**, 100, 1223-1252.
- (11) Hsieh, H. L.; Quirk, R. P., *Anionic Polymerization: Principles and Practical Applications*. Marcel Dekker Inc.: New York, 1996.
- (12) Matyjaszewski, K., *Cationic Polymerizations: Mechanisms, Synthesis, and Applications*. Marcel Dekker Inc.: New York, 1996.
- (13) Aoshima, S.; Kanaoka, S. *Chem. Rev.* **2009**, 109, 5245-5287.
- (14) Hawker, C. J.; Bosman, A. W.; Harth, E. *Chem. Rev.* **2001**, 101, 3661-3688.
- (15) Kamigaito, M.; Ando, T.; Sawamoto, M. *Chem. Rev.* **2001**, 101, 3689-3746.
- (16) Matyjaszewski, K.; Xia, J. H. *Chem. Rev.* **2001**, 101, 2921-2990.
- (17) Braunecker, W. A.; Matyjaszewski, K. *Prog. Polym. Sci.* **2007**, 32, 93-146.
- (18) Ouchi, M.; Terashima, T.; Sawamoto, M. *Chem. Rev.* **2009**, 109, 4963-5050.

- (19) Bates, F. S. *Science* **1991**, 251, 898-905.
- (20) Ruzette, A. V.; Leibler, L. *Nat. Mater.* **2005**, 4, 19-31.
- (21) Ittel, S. D.; Johnson, L. K.; Brookhart, M. *Chem. Rev.* **2000**, 100, 1169-1203.
- (22) Mallin, D. T.; Rausch, M. D.; Lin, Y. G.; Dong, S. Z.; Chien, J. C. W. *J. Am. Chem. Soc.* **1990**, 112, 2030-2031.
- (23) Coates, G. W.; Waymouth, R. M. *Science* **1995**, 267, 217-219.
- (24) Chien, J. C. W.; Iwamoto, Y.; Rausch, M. D.; Wedler, W.; Winter, H. H. *Macromolecules* **1997**, 30, 3447-3458.
- (25) Lieber, S.; Brintzinger, H. H. *Macromolecules* **2000**, 33, 9192-9199.
- (26) Harney, M. B.; Zhang, Y. H.; Sita, L. R. *Angew. Chem. Int. Ed.* **2006**, 45, 2400-2404.
- (27) Hotta, A.; Cochran, E.; Ruokolainen, J.; Khanna, V.; Fredrickson, G. H.; Kramer, E. J.; Shin, Y.-W.; Shimizu, F.; Cherian, A. E.; Rose, J. M.; Coates, G. W. *Proc. Natl. Acad. Sci. U. S. A.* **2006**, 42, 15327-15332.
- (28) Edson, J. B.; Wang, Z. G.; Kramer, E. J.; Coates, G. W. *J. Am. Chem. Soc.* **2008**, 130, 4968-4977.
- (29) Rose, J. M.; Deplace, F.; Lynd, N. A.; Wang, Z.; Hotta, A.; Lobkovsky, E. B.; Kramer, E. J.; Coates, G. W. *Macromolecules* **2008**, 41, 9548-9555.
- (30) Karian, H. G., *Handbook of Polypropylene and Polypropylene Composites*. Marcel Dekker Inc.: New York, 2003.
- (31) Peacock, A. J., *Handbook of Polyethylene*. Marcel Dekker Inc.: New York, 2000.
- (32) Coates, G. W.; Waymouth, R. M. *J. Am. Chem. Soc.* **1991**, 113, 6270-6271.
- (33) Kumudini, C. J.; Keaton, R. J.; Henningsen, D. A.; Sita, L. R. *J. Am. Chem. Soc.* **2000**, 122, 10490-10491.
- (34) Mathers, R. T.; Coates, G. W. *Chem. Commun.* **2004**, 422-423.
- (35) Tritto, I.; Boggioni, L.; Ferro, D. R. *Coord. Chem. Rev.* **2006**, 250, 212-241.
- (36) Boffa, L. S.; Novak, B. M. *Chem. Rev.* **2000**, 100, 1479-1493.
- (37) Quirk, R. P.; Lee, B. *Polym. Int.* **1992**, 27, 359-367.

- (38) Zambelli, A.; Natta, G.; Pasquon, I.; Signorin, R. *J. Polym. Sci., Part C: Polym. Symp.* **1967**, 2485.
- (39) Doi, Y.; Takada, M.; Keii, T. *Bull. Chem. Soc. Jpn.* **1979**, 52, 1802.
- (40) Doi, Y.; Ueki, S.; Keii, T. *Macromolecules* **1979**, 12, 814-819.
- (41) Doi, Y.; Ueki, S.; Keii, T. *Makromol. Chem., Macromol. Chem. Phys.* **1979**, 180, 1359-1361.
- (42) Ueki, S.; Doi, Y.; Keii, T. *Makromol. Chem., Rapid Commun.* **1981**, 2, 403-406.
- (43) Doi, Y.; Ueki, S.; Keii, T. *Makromol. Chem., Rapid Commun.* **1982**, 3, 225-229.
- (44) Doi, Y.; Suzuki, S.; Soga, K. *Makromol. Chem., Rapid Commun.* **1985**, 6, 639-642.
- (45) Doi, Y.; Suzuki, S.; Soga, K. *Macromolecules* **1986**, 19, 2896-2900.
- (46) Doi, Y.; Suzuki, S.; Hizal, G.; Soga, K. *Trans. Met. Catal. Polym.* **1988**, 182-194.
- (47) Doi, Y.; Tokuhiko, N.; Suzuki, S.; Soga, K. *Makromol. Chem., Rapid Commun.* **1987**, 8, 285-290.
- (48) Doi, Y.; Watanabe, Y.; Ueki, S.; Soga, K. *Makromol. Chem., Rapid Commun.* **1983**, 4, 533-537.
- (49) Doi, Y.; Murata, M.; Soga, K. *Makromol. Chem., Rapid Commun.* **1984**, 5, 811-814.
- (50) Doi, Y.; Keii, T. *Adv. Polym. Sci.* **1986**, 73/74, 201.
- (51) Doi, Y.; Hizal, G.; Soga, K. *Makromol. Chem.* **1987**, 188, 1273-1279.
- (52) Ueki, S.; Furuhashi, H.; Murakami, N.; Murata, M.; Doi, Y. *Science And Technology In Catalysis, 1994* **1995**, 92, 359-362.
- (53) Doi, Y.; Koyama, T.; Soga, K. *Makromol. Chem., Macromol. Chem. Phys.* **1985**, 186, 11-15.
- (54) Doi, Y.; Tokuhiko, N.; Soga, K. *Makromol. Chem., Macromol. Chem. Phys.* **1989**, 190, 643-651.
- (55) Chen, E. Y. X.; Marks, T. J. *Chem. Rev.* **2000**, 100, 1391-1434.

- (56) Fukui, Y.; Murata, M.; Soga, K. *Macromol. Rapid Commun.* **1999**, 20, 637-640.
- (57) Kotzabasakis, V.; Kostakis, K.; Pitsikalis, M.; Hadjichristidis, N.; Lohse, D. J.; Mavromoustakos, T.; Potamitis, C. *J. Polym. Sci. Part A: Polym. Chem.* **2009**, 47, 4314-4325.
- (58) Nomura, K.; Fudo, A. *J. Mol. Catal. A: Chem.* **2004**, 209, 9-17.
- (59) Sassmannshausen, J.; Bochmann, M. E.; Rosch, J.; Lilge, D. *J. Organomet. Chem.* **1997**, 548, 23-28.
- (60) Fukui, Y.; Murata, M. *Macromol. Chem. Phys.* **2001**, 202, 1430-1434.
- (61) Fukui, Y.; Murata, M. *Appl. Catal., A* **2002**, 237, 1-10.
- (62) Fukui, Y.; Murata, M. *Macromol. Chem. Phys.* **2001**, 202, 1473-1477.
- (63) Turner, H. W.; Hlatky, G. G. *Block Copolymers from Ionic Catalysts*. 1991.
- (64) Starzewski, A. O.; Steinhauser, N.; Xin, B. S. *Macromolecules* **2008**, 41, 4095-4101.
- (65) di Lena, F.; Chen, P. *Helvetica Chimica Acta* **2009**, 92, 890-896.
- (66) Jansen, J. C.; Mendichi, R.; Locatelli, P.; Tritto, I. *Macromol. Rapid Commun.* **2001**, 22, 1394-1398.
- (67) Jansen, J. C.; Mendichi, R.; Sacchi, M. C.; Tritto, I. *Macromol. Chem. Phys.* **2003**, 204, 522-530.
- (68) Hagihara, H.; Shiono, T.; Ikeda, T. *Macromolecules* **1998**, 31, 3184-3188.
- (69) Nishii, K.; Shiono, T.; Ikeda, T. *Kobunshi Ronbunshu* **2002**, 59, 371-376.
- (70) Hasan, T.; Ioku, A.; Nishii, K.; Shiono, T.; Ikeda, T. *Macromolecules* **2001**, 34, 3142-3145.
- (71) Nishii, K.; Matsumae, T.; Dare, E. O.; Shiono, T.; Ikeda, T. *Macromol. Chem. Phys.* **2004**, 205, 363-369.
- (72) Nishii, K.; Shiono, T.; Ikeda, T. *Macromol. Rapid Commun.* **2004**, 25, 1029-1032.
- (73) Cai, Z. G.; Nakayama, Y.; Shiono, T. *Macromolecules* **2008**, 41, 6596-6598.
- (74) Cai, Z. G.; Ikeda, T.; Akita, M.; Shiono, T. *Macromolecules* **2005**, 38, 8135-8139.

- (75) Shiono, T.; Harada, R.; Cai, Z. G.; Nakayama, Y. *Top. Catal.* **2009**, *52*, 675-680.
- (76) Nishii, K.; Ikeda, T.; Akita, M.; Shiono, T. *J. Mol. Catal. A: Chem.* **2005**, *231*, 241-246.
- (77) Dare, E. O.; Ogunniyi, D. S.; Olatunji, G. A.; Chattopadhyay, P. *Bull. Chem. Soc. Ethiopia* **2004**, *18*, 131-141.
- (78) Hasan, T.; Shiono, T.; Ikeda, T. *Macromol. Symp.* **2004**, *213*, 123-129.
- (79) Hasan, T.; Ikeda, T.; Shiono, T. *Macromolecules* **2004**, *37*, 8503-8509.
- (80) Hasan, T.; Ikeda, T.; Shiono, T. *Macromolecules* **2005**, *38*, 1071-1074.
- (81) Shiono, T.; Sugimoto, M.; Hasan, T.; Cai, Z.; Ikeda, T. *Macromolecules* **2008**, *41*, 8292-8294.
- (82) Cai, Z.; Nakayama, Y.; Shiono, T. *Macromol. Rapid Commun.* **2008**, *29*, 525-529.
- (83) Cai, Z. G.; Nakayama, Y.; Shiono, T. *Macromolecules* **2006**, *39*, 2031-2033.
- (84) Jayaratne, K. C.; Sita, L. R. *J. Am. Chem. Soc.* **2000**, *122*, 958-959.
- (85) Zhang, Y. H.; Sita, L. R. *Chem. Commun.* **2003**, 2358-2359.
- (86) Kissounko, D. A.; Zhang, Y. H.; Harney, M. B.; Sita, L. R. *Adv. Synth. Cat.* **2005**, *347*, 426-432.
- (87) Zhang, Y. H.; Keaton, R. J.; Sita, L. R. *J. Am. Chem. Soc.* **2003**, *125*, 9062-9069.
- (88) Keaton, R. J.; Jayaratne, K. C.; Henningsen, D. A.; Koterwas, L. A.; Sita, L. R. *J. Am. Chem. Soc.* **2001**, *123*, 6197-6198.
- (89) Zhang, Y. H.; Reeder, E. K.; Keaton, R. J.; Sita, L. R. *Organometallics* **2004**, *23*, 3512-3520.
- (90) Yasumoto, T.; Yamagata, T.; Mashima, K. *Organometallics* **2005**, *24*, 3375-3377.
- (91) Harney, M. B.; Zhang, Y. H.; Sita, L. R. *Angew. Chem. Int. Ed.* **2006**, *45*, 6140-6144.
- (92) Zhang, W.; Sita, L. R. *Adv. Synth. Cat.* **2008**, *350*, 439-447.
- (93) Zhang, W.; Sita, L. R. *J. Am. Chem. Soc.* **2008**, *130*, 442-443.

- (94) Kempe, R. *Chem. Eur. J.* **2007**, 13, 2764-2773.
- (95) Zhang, W.; Wei, J.; Sita, L. R. *Macromolecules* **2008**, 41, 7829-7833.
- (96) Jayaratne, K. C.; Keaton, R. J.; Henningsen, D. A.; Sita, L. R. *J. Am. Chem. Soc.* **2000**, 122, 10490-10491.
- (97) Britovsek, G. J. P.; Gibson, V. C.; Wass, D. F. *Angew. Chem. Int. Ed.* **1999**, 38, 428-447.
- (98) Gibson, V. C.; Spitzmesser, S. K. *Chem. Rev.* **2003**, 103, 283-315.
- (99) Scollard, J. D.; McConville, D. H. *J. Am. Chem. Soc.* **1996**, 118, 10008-10009.
- (100) Jeon, Y. M.; Park, S. J.; Heo, J.; Kim, K. *Organometallics* **1998**, 17, 3161-3163.
- (101) Hagimoto, H.; Shiono, T.; Ikeda, T. *Macromol. Rapid Commun.* **2002**, 23, 73-76.
- (102) Hagimoto, H.; Shiono, T.; Ikeda, T. *Macromolecules* **2002**, 35, 5744-5745.
- (103) Hagimoto, H.; Shiono, T.; Ikeda, T. *Science and Technology in Catalysis, 2002* **2003**, 145, 129-132.
- (104) Shiono, T. *Catalysis Surveys from Asia* **2003**, 7, 47-62.
- (105) Hagimoto, H.; Shiono, T.; Ikeda, T. *Macromol. Chem. Phys.* **2004**, 205, 19-26.
- (106) Baumann, R.; Davis, W. M.; Schrock, R. R. *J. Am. Chem. Soc.* **1997**, 119, 3830-3831.
- (107) Schrock, R. R.; Baumann, R.; Reid, S. M.; Goodman, J. T.; Stumpf, R.; Davis, W. M. *Organometallics* **1999**, 18, 3649-3670.
- (108) Mehrkhodavandi, P.; Bonitatebus, P. J.; Schrock, R. R. *J. Am. Chem. Soc.* **2000**, 122, 7841-7842.
- (109) Mehrkhodavandi, P.; Schrock, R. R. *J. Am. Chem. Soc.* **2001**, 123, 10746-10747.
- (110) Mehrkhodavandi, P.; Schrock, R. R.; Pryor, L. L. *Organometallics* **2003**, 22, 4569-4583.
- (111) Schrock, R. R.; Adamchuk, J.; Ruhland, K.; Lopez, L. P. H. *Organometallics* **2003**, 22, 5079-5091.

- (112) Liang, L. C.; Schrock, R. R.; Davis, W. M.; McConville, D. H. *J. Am. Chem. Soc.* **1999**, 121, 5797-5798.
- (113) Schrock, R. R.; Bonitatebus, P. J.; Schrodi, Y. *Organometallics* **2001**, 20, 1056-1058.
- (114) Schrock, R. R.; Adamchuk, J.; Ruhland, K.; Lopez, L. P. H. *Organometallics* **2005**, 24, 857-866.
- (115) Tshuva, E. Y.; Goldberg, I.; Kol, M.; Goldschmidt, Z. *Inorg. Chem. Commun.* **2000**, 3, 611-614.
- (116) Gendler, S.; Groysman, S.; Goldschmidt, Z.; Shuster, M.; Kol, M. *J. Polym. Sci. Part A: Polym. Chem.* **2006**, 44, 1136-1146.
- (117) Tshuva, E. Y.; Goldberg, I.; Kol, M. *J. Am. Chem. Soc.* **2000**, 122, 10706-10707.
- (118) Segal, S.; Goldberg, I.; Kol, M. *Organometallics* **2005**, 24, 200-202.
- (119) Tshuva, E. Y.; Goldberg, I.; Kol, M.; Goldschmidt, Z. *Chem. Commun.* **2001**, 2120-2121.
- (120) Groysman, S.; Goldberg, I.; Kol, M.; Genizi, E.; Goldschmidt, Z. *Inorg. Chim. Acta* **2003**, 345, 137-144.
- (121) Groysman, S.; Tshuva, E. Y.; Goldberg, I.; Kol, M.; Goldschmidt, Z.; Shuster, M. *Organometallics* **2004**, 23, 5291-5299.
- (122) Tshuva, E. Y.; Groysman, S.; Goldberg, I.; Kol, M.; Goldschmidt, Z. *Organometallics* **2002**, 21, 662-670.
- (123) Groysman, S.; Goldberg, I.; Kol, M.; Genizi, E.; Goldschmidt, Z. *Organometallics* **2003**, 22, 3013-3015.
- (124) Busico, V.; Cipullo, R.; Ronca, S.; Budzelaar, P. H. M. *Macromol. Rapid Commun.* **2001**, 22, 1405-1410.
- (125) Busico, V.; Cipullo, R.; Friederichs, N.; Ronca, S.; Togrou, M. *Macromolecules* **2003**, 36, 3806-3808.
- (126) Busico, V.; Cipullo, R.; Friederichs, N.; Ronca, S.; Talarico, G.; Togrou, M.; Wang, B. *Macromolecules* **2004**, 37, 8201-8203.
- (127) Cipullo, R.; Busico, V.; Fraldi, N.; Pellicchia, R.; Talarico, G. *Macromolecules* **2009**, 42, 3869-3872.
- (128) Manivannan, R.; Sundararajan, G. *Macromolecules* **2002**, 35, 7883-7890.

- (129) Sudhakar, P.; Sundararajan, G. *Macromol. Rapid Commun.* **2005**, 26, 1854-1859.
- (130) Sudhakar, P. *J. Polym. Sci. Part A: Polym. Chem.* **2007**, 45, 5470-5479.
- (131) Beckerle, K.; Manivannan, R.; Spaniol, T. P.; Okuda, J. *Organometallics* **2006**, 25, 3019-3026.
- (132) Zhang, H.; Nomura, K. *J. Am. Chem. Soc.* **2005**, 127, 9364-9365.
- (133) Matsui, S.; Mitani, M.; Saito, J.; Tohi, Y.; Makio, H.; Tanaka, H.; Fujita, T. *Chem. Lett.* **1999**, 1263-1264.
- (134) Matsui, S.; Tohi, Y.; Mitani, M.; Saito, J.; Makio, H.; Tanaka, H.; Nitabaru, M.; Nakano, T.; Fujita, T. *Chem. Lett.* **1999**, 1065-1066.
- (135) Matsui, S.; Mitani, M.; Saito, J.; Matsukawa, N.; Tanaka, H.; Nakano, T.; Fujita, T. *Chem. Lett.* **2000**, 554-555.
- (136) Tian, J.; Coates, G. W. *Angew. Chem. Int. Ed.* **2000**, 39, 3626-3629.
- (137) Saito, J.; Mitani, M.; Onda, M.; Mohri, J. I.; Ishi, J. I.; Yoshida, Y.; Nakano, T.; Tanaka, H.; Matsugi, T.; Kojoh, S. I.; Kashiwa, N.; Fujita, T. *Macromol. Rapid Commun.* **2001**, 22, 1072-1075.
- (138) Hustad, P. D.; Tian, J.; Coates, G. W. *J. Am. Chem. Soc.* **2002**, 124, 3614-3621.
- (139) Lamberti, M.; Pappalardo, D.; Zambelli, A.; Pellicchia, C. *Macromolecules* **2002**, 35, 658-663.
- (140) Milano, G.; Cavallo, L.; Guerra, G. *J. Am. Chem. Soc.* **2002**, 124, 13368-13369.
- (141) Talarico, G.; Busico, V.; Cavallo, L. *J. Am. Chem. Soc.* **2003**, 125, 7172-7173.
- (142) Corradini, P.; Guerra, G.; Cavallo, L. *Acc. Chem. Res.* **2004**, 37, 231-241.
- (143) Tian, J.; Hustad, P. D.; Coates, G. W. *J. Am. Chem. Soc.* **2001**, 123, 5134-5135.
- (144) Ruokolainen, J.; Mezzenga, R.; Fredrickson, G. H.; Kramer, E. J.; Hustad, P. D.; Coates, G. W. *Macromolecules* **2005**, 38, 851-860.
- (145) Radulescu, A.; Mathers, R. T.; Coates, G. W.; Richter, D.; Fetters, L. J. *Macromolecules* **2004**, 37, 6962-6971.

- (146) Saito, J.; Mitani, M.; Mohri, J.; Ishii, S.; Yoshida, Y.; Matsugi, T.; Kojoh, S.; Kashiwa, N.; Fujita, T. *Chem. Lett.* **2001**, 576-577.
- (147) Kojoh, S.; Matsugi, T.; Saito, J.; Mitani, M.; Fujita, T.; Kashiwa, N. *Chem. Lett.* **2001**, 822-823.
- (148) Mitani, M.; Mohri, J.; Yoshida, Y.; Saito, J.; Ishii, S.; Tsuru, K.; Matsui, S.; Furuyama, R.; Nakano, T.; Tanaka, H.; Kojoh, S.; Matsugi, T.; Kashiwa, N.; Fujita, T. *J. Am. Chem. Soc.* **2002**, 124, 3327-3336.
- (149) Sakuma, A.; Weiser, M. S.; Fujita, T. *Polym. J.* **2007**, 39, 193-207.
- (150) Nakayama, Y.; Saito, J.; Bando, H.; Fujita, T. *Macromol. Chem. Phys.* **2005**, 206, 1847-1852.
- (151) Mason, A. F.; Tian, J.; Hustad, P. D.; Lobkovsky, E. B.; Coates, G. W. *Isr. J. Chem.* **2002**, 42, 301-306.
- (152) Mason, A. F.; Coates, G. W. *J. Am. Chem. Soc.* **2004**, 126, 10798-10799.
- (153) Mason, A. F. Ph.D. Thesis. Cornell University, Ithaca, NY, 2005.
- (154) Saito, J.; Mitani, M.; Onda, M.; Mohri, J.; Ishii, S.; Yoshida, Y.; Furuyama, R.; Nakano, T.; Kashiwa, N.; Fujita, T. *Science and Technology in Catalysis, 2002* **2003**, 145, 515-516.
- (155) Mitani, M.; Furuyama, R.; Mohri, J.; Saito, J.; Ishii, S.; Terao, H.; Kashiwa, N.; Fujita, T. *J. Am. Chem. Soc.* **2002**, 124, 7888-7889.
- (156) Mitani, M.; Furuyama, R.; Mohri, J.; Saito, J.; Ishii, S.; Terao, H.; Nakano, T.; Tanaka, H.; Fujita, T. *J. Am. Chem. Soc.* **2003**, 125, 4293-4305.
- (157) Weiser, M. S.; Mulhaupt, R. *Macromol. Symp.* **2006**, 236, 111-116.
- (158) Weiser, M. S.; Wesolek, M.; Mulhaupt, R. *J. Organomet. Chem.* **2006**, 691, 2945-2952.
- (159) Cherian, A. E.; Lobkovsky, E. B.; Coates, G. W. *Macromolecules* **2005**, 38, 6259-6268.
- (160) Saito, J.; Mitani, M.; Mohri, J.; Yoshida, Y.; Matsui, S.; Ishii, S.; Kojoh, S.; Kashiwa, N.; Fujita, T. *Angew. Chem. Int. Ed.* **2001**, 40, 2918-2920.
- (161) Makio, H.; Fujita, T. *Macromol. Rapid Commun.* **2007**, 28, 698-703.
- (162) Weiser, M. S.; Thomann, Y.; Heinz, L. C.; Pasch, H.; Mulhaupt, R. *Polymer* **2006**, 47, 4505-4512.

- (163) Reinartz, S.; Mason, A. F.; Lobkovsky, E. B.; Coates, G. W. *Organometallics* **2003**, 22, 2542-2544.
- (164) Ivanchev, S. S.; Badaev, V. K.; Ivancheva, N. I.; Khaikin, S. Y. *Dokl. Phys. Chem.* **2004**, 394, 46-49.
- (165) Furuyama, R.; Saito, J.; Ishii, S.; Makio, H.; Mitani, M.; Tanaka, H.; Fujita, T. *J. Organomet. Chem.* **2005**, 690, 4398-4413.
- (166) Ivanchev, S. S.; Trunov, V. A.; Rybakov, V. B.; Al'bov, D. V.; Rogozin, D. G. *Dokl. Phys. Chem.* **2005**, 404, 165-168.
- (167) Furuyama, R.; Mitani, M.; Mohri, J.; Mori, R.; Tanaka, H.; Fujita, T. *Macromolecules* **2005**, 38, 1546-1552.
- (168) Makio, H.; Kashiwa, N.; Fujita, T. *Adv. Synth. Cat.* **2002**, 344, 477-493.
- (169) Mitani, M.; Mohri, J.; Furuyama, R.; Ishii, S.; Fujita, T. *Chem. Lett.* **2003**, 32, 238-239.
- (170) Fujita, M.; Coates, G. W. *Macromolecules* **2002**, 35, 9640-9647.
- (171) Yoon, J.; Mathers, R. T.; Coates, G. W.; Thomas, E. L. *Macromolecules* **2006**, 39, 1913-1919.
- (172) Hustad, P. D.; Coates, G. W. *J. Am. Chem. Soc.* **2002**, 124, 11578-11579.
- (173) Mason, A. F.; Coates, G. W. *J. Am. Chem. Soc.* **2004**, 126, 16326-16327.
- (174) Yoshida, Y.; Matsui, S.; Takagi, Y.; Mitani, M.; Nitabaru, M.; Nakano, T.; Tanaka, H.; Fujita, T. *Chem. Lett.* **2000**, 1270-1271.
- (175) Yoshida, Y.; Saito, J.; Mitani, M.; Takagi, Y.; Matsui, S.; Ishii, S.; Nakano, T.; Kashiwa, N.; Fujita, T. *Chem. Commun.* **2002**, 1298-1299.
- (176) Yoshida, Y.; Matsui, S.; Takagi, Y.; Mitani, M.; Saito, J.; Ishii, S. I.; Nakano, T.; Tanaka, H.; Kashiwa, N.; Fujita, T. *Science and Technology in Catalysis, 2002* **2003**, 145, 521-522.
- (177) Yoshida, Y.; Mohri, J.; Ishii, S.; Mitani, M.; Saito, J.; Matsui, S.; Makio, H.; Nakano, T.; Tanaka, H.; Onda, M.; Yamamoto, Y.; Mizuno, A.; Fujita, T. *J. Am. Chem. Soc.* **2004**, 126, 12023-12032.
- (178) Matsugi, T.; Matsui, S.; Kojoh, S.; Takagi, Y.; Inoue, Y.; Fujita, T.; Kashiwa, N. *Chem. Lett.* **2001**, 566-567.
- (179) Matsugi, T.; Kojoh, S.; Fujita, T.; Kashiwa, N. *Kobunshi Ronbunshu* **2002**, 59, 410-414.

- (180) Matsugi, T.; Matsui, S.; Kojoh, S.; Takagi, Y.; Inoue, Y.; Nakano, T.; Fujita, T.; Kashiwa, N. *Macromolecules* **2002**, *35*, 4880-4887.
- (181) Matsugi, T.; Matsui, S.; Kojoh, S.; Takagi, Y.; Inoue, Y.; Nakano, T.; Fujita, T.; Kashiwa, N. *Science and Technology in Catalysis, 2002* **2003**, *145*, 523-524.
- (182) Yoshida, Y.; Matsui, S.; Fujita, T. *J. Organomet. Chem.* **2005**, *690*, 4382-4397.
- (183) Li, X. F.; Dai, K.; Ye, W. P.; Pan, L.; Li, Y. S. *Organometallics* **2004**, *23*, 1223-1230.
- (184) Yu, S. M.; Mecking, S. *J. Am. Chem. Soc.* **2008**, *130*, 13204-13205.
- (185) Tang, L. M.; Duan, Y. Q.; Pan, L.; Li, Y. S. *J. Polym. Sci. Part A: Polym. Chem.* **2005**, *43*, 1681-1689.
- (186) Tang, L. M.; Hu, T.; Bo, Y. J.; Li, Y. S.; Hu, N. H. *J. Organomet. Chem.* **2005**, *690*, 3125-3133.
- (187) Pan, L.; Hong, M.; Liu, J. Y.; Ye, W. P.; Li, Y. S. *Macromolecules* **2009**, *42*, 4391-4393.
- (188) Long, R. J.; Gibson, V. C.; White, A. J. P.; Williams, D. J. *Inorg. Chem.* **2006**, *45*, 511-513.
- (189) He, L. P.; Liu, J. Y.; Li, Y. G.; Liu, S. R.; Li, Y. S. *Macromolecules* **2009**, *42*, 8566-8570.
- (190) Boussie, T. R.; Diamond, G. M.; Goh, C.; Hall, K. A.; LaPointe, A. M.; Leclerc, M. K.; Murphy, V.; Shoemaker, J. A. W.; Turner, H.; Rosen, R. K.; Stevens, J. C.; Alfano, F.; Busico, V.; Cipullo, R.; Talarico, G. *Angew. Chem. Int. Ed.* **2006**, *45*, 3278-3283.
- (191) Froese, R. D. J.; Hustad, P. D.; Kuhlman, R. L.; Wenzel, T. T. *J. Am. Chem. Soc.* **2007**, *129*, 7831-7840.
- (192) Zuccaccia, C.; Macchioni, A.; Busico, V.; Cipullo, R.; Talarico, G.; Alfano, F.; Boone, H. W.; Frazier, K. A.; Hustad, P. D.; Stevens, J. C.; Vosejpk, P. C.; Abboud, K. A. *J. Am. Chem. Soc.* **2008**, *130*, 10354-10368.
- (193) Domski, G. J.; Lobkovsky, E. B.; Coates, G. W. *Macromolecules* **2007**, *40*, 3510-3513.

- (194) Zuccaccia, C.; Busico, V.; Cipullo, R.; Talarico, G.; Froese, R. D. J.; Vosejпка, P. C.; Hustad, P. D.; Macchioni, A. *Organometallics* **2009**, *28*, 5445-5458.
- (195) Domski, G. J.; Edson, J. B.; Keresztes, I.; Lobkovsky, E. B.; Coates, G. W. *Chem. Commun.* **2008**, *46*, 6137-6139.
- (196) Edson, J. B.; Keresztes, I.; Lobkovsky, E. B.; Coates, G. W. *ChemCatChem* **2009**, *1*, 122-130.
- (197) Kretschmer, W. P.; Hessen, B.; Noor, A.; Scott, N. M.; Kempe, R. J. *Organomet. Chem.* **2007**, *692*, 4569-4579.
- (198) Lee, H.; Nienkemper, K.; Jordan, R. F. *Organometallics* **2008**, *27*, 5075-5081.
- (199) Nienkemper, K.; Lee, H.; Jordan, R. F.; Ariaifard, A.; Dang, L.; Lin, Z. Y. *Organometallics* **2008**, *27*, 5867-5875.
- (200) Annunziata, L.; Pappalardo, D.; Tedesco, C.; Pellecchia, C. *Macromolecules* **2009**, *42*, 5572-5578.
- (201) Ward, B. D.; Bellemin-Laponnaz, S.; Gade, L. H. *Angew. Chem. Int. Ed.* **2005**, *44*, 1668-1671.
- (202) Jeske, G.; Lauke, H.; Mauermann, H.; Swepston, P. N.; Schumann, H.; Marks, T. J. *J. Am. Chem. Soc.* **1985**, *107*, 8091-8103.
- (203) Wang, W.; Nomura, K. *Macromolecules* **2005**, *38*, 5905-5913.
- (204) Bambirra, S.; van Leusen, D.; Meetsma, A.; Hessen, B.; Teuben, J. H. *Chem. Commun.* **2003**, 522-523.
- (205) Mashima, K.; Fujikawa, S.; Urata, H.; Tanaka, E.; Nakamura, A. *J. Am. Chem. Soc.* **1993**, *115*, 10990-10991.
- (206) Mashima, K.; Fujikawa, S.; Tanaka, Y.; Urata, H.; Oshiki, T.; Tanaka, E.; Nakamura, A. *Organometallics* **1995**, *14*, 2633-2640.
- (207) Mashima, K.; Fujikawa, S.; Urata, H.; Tanaka, E.; Nakamura, A. *J. Chem. Soc.-Chem. Commun.* **1994**, 1623-1624.
- (208) MacAdams, L. A.; Buffone, G. P.; Incarvito, C. D.; Rheingold, A. L.; Theopold, K. H. *J. Am. Chem. Soc.* **2005**, *127*, 1082-1083.
- (209) Ravasio, A.; Zampa, C.; Boggioni, L.; Tritto, I.; Hitzbleck, J.; Okuda, J. *Macromolecules* **2008**, *41*, 9565-9569.

- (210) Yasuda, H.; Furo, M.; Yamamoto, H.; Nakamura, A.; Miyake, S.; Kibino, N. *Macromolecules* **1992**, *25*, 5115-5116.
- (211) Desurmont, G.; Li, Y.; Yasuda, H.; Maruo, T.; Kanehisa, N.; Kai, Y. *Organometallics* **2000**, *19*, 1811-1813.
- (212) Desurmont, G.; Tokimitsu, T.; Yasuda, H. *Macromolecules* **2000**, *33*, 7679-7681.
- (213) Evans, W. J.; Decoster, D. M.; Greaves, J. *Macromolecules* **1995**, *28*, 7929-7936.
- (214) Desurmont, G.; Tanaka, M.; Li, Y.; Yasuda, H.; Tokimitsu, T.; Tone, S.; Yanagase, A. *J. Polym. Sci. Part A: Polym. Chem.* **2000**, *38*, 4095-4109.
- (215) Johnson, L. K.; Killian, C. K.; Brookhart, M. *J. Am. Chem. Soc.* **1995**, *117*, 6414-6415.
- (216) Guan, Z.; Cotts, P. M.; McCord, E. F.; McLain, S. J. *Science* **1999**, *283*, 2059-2062.
- (217) Killian, C. M.; Tempel, D. J.; Johnson, L. K.; Brookhart, M. *J. Am. Chem. Soc.* **1996**, *118*, 11664-11665.
- (218) Mohring, V. M.; Fink, G. *Angew. Chem. Int. Ed.* **1985**, *24*, 1001-1003.
- (219) Merna, J.; Cihlar, J.; Kucera, M.; Deffieux, A.; Cramail, H. *Eur. Polym. J.* **2005**, *41*, 303-312.
- (220) Merna, J.; Host'alek, Z.; Peleska, J.; Roda, J. *Polymer* **2009**, *50*, 5016-5023.
- (221) Yuan, J. C.; Silva, L. C.; Gomes, P. T.; Valerga, B.; Campos, J. M.; Ribeiro, M. R.; Chien, J. C. W.; Marques, M. M. *Polymer* **2005**, *46*, 2122-2132.
- (222) Camacho, D. H.; Guan, Z. B. *Macromolecules* **2005**, *38*, 2544-2546.
- (223) Rose, J. M.; Cherian, A. E.; Coates, G. W. *J. Am. Chem. Soc.* **2006**, *128*, 4186-4187.
- (224) Suzuki, N.; Yu, J.; Masubuchi, Y.; Horiuchi, A.; Wakatsuki, Y. *J. Polym. Sci. Part A: Polym. Chem.* **2003**, *41*, 293-302.
- (225) Gottfried, A. C.; Brookhart, M. *Macromolecules* **2003**, *36*, 3085-3100.
- (226) Borkar, S.; Yennawar, H.; Sen, A. *Organometallics* **2007**, *26*, 4711-4714.
- (227) Cherian, A. E.; Rose, J. M.; Lobkovsky, E. B.; Coates, G. W. *J. Am. Chem. Soc.* **2005**, *127*, 13770-13771.

- (228) Schmid, M.; Eberhardt, R.; Klinga, M.; Leskela, M.; Rieger, B. *Organometallics* **2001**, 20, 2321-2330.
- (229) Camacho, D. H.; Salo, E. V.; Ziller, J. W.; Guan, Z. B. *Angew. Chem. Int. Ed.* **2004**, 43, 1821-1825.
- (230) Camacho, D. H.; Salo, E. V.; Guan, Z. B.; Ziller, J. W. *Organometallics* **2005**, 24, 4933-4939.
- (231) Popeney, C. S.; Rheingold, A. L.; Guan, Z. B. *Organometallics* **2009**, 28, 4452-4463.
- (232) Gottfried, A. C.; Brookhart, M. *Macromolecules* **2001**, 34, 1140-1142.
- (233) Zhang, Y. W.; Ye, Z. B. *Chem. Commun.* **2008**, 1178-1180.
- (234) Zhang, Y. W.; Ye, Z. B. *Macromolecules* **2008**, 41, 6331-6338.
- (235) Zhang, K. J.; Ye, Z. B.; Subramanian, R. *Macromolecules* **2009**, 42, 2313-2316.
- (236) Hong, S. C.; Jia, S.; Teodorescu, M.; Kowalewski, T.; Matyjaszewski, K.; Gottfried, A. C.; Brookhart, M. *J. Polym. Sci. Part A: Polym. Chem.* **2002**, 40, 2736-2749.
- (237) Zhang, K.; Ye, Z.; Subramanian, R. *Macromolecules* **2008**, 41, 640-649.
- (238) Rose, J. M.; Mourey, T. H.; Slater, L. A.; Keresztes, I.; Fetters, L. J.; Coates, G. W. *Macromolecules* **2008**, 41, 559-567.
- (239) Rieth, L. R.; Eaton, R. F.; Coates, G. W. *Angew. Chem. Int. Ed.* **2001**, 40, 2153-2156.
- (240) Park, S.; Takeuchi, D.; Osakada, K. *J. Am. Chem. Soc.* **2006**, 128, 3510-3511.
- (241) Okada, T.; Park, S.; Takeuchi, D.; Osakada, K. *Angew. Chem. Int. Ed.* **2007**, 46, 6141-6143.
- (242) Takeuchi, D.; Fukuda, Y.; Park, S.; Osakada, K. *Macromolecules* **2009**, 42, 5909-5912.
- (243) Xiang, P.; Ye, Z. B.; Morgan, S.; Xia, X. W.; Liu, W. *Macromolecules* **2009**, 42, 4946-4949.
- (244) Kiesewetter, J.; Kaminsky, W. *Chem. Eur. J.* **2003**, 9, 1750-1758.
- (245) Azoulay, J. D.; Rojas, R. S.; Serrano, A. V.; Ohtaki, H.; Galland, G. B.; Wu, G.; Bazan, G. C. *Angew. Chem. Int. Ed.* **2008**, 48, 1089-1092.

- (246) Azoulay, J. D.; Schneider, Y.; Galland, G. B.; Bazan, G. C. *Chem. Comm.* **2009**, 6177-9.
- (247) Hicks, F. A.; Jenkins, J. C.; Brookhart, M. *Organometallics* **2003**, 22, 3533-3545.
- (248) Yang, F.-Z.; Chen, Y.-C.; Lin, Y.-F.; Yu, K.-H.; Liu, Y.-H.; Wang, Y.; Liu, S.-T.; Chen, J.-T. *Dalton Trans* **2009**, 1243-50.
- (249) Diamanti, S. J.; Ghosh, P.; Shimizu, F.; Bazan, G. C. *Macromolecules* **2003**, 36, 9731-9735.
- (250) Azoulay, J. D.; Itigaki, K.; Wu, G.; Bazan, G. C. *Organometallics* **2008**, 27, 2273-2280.
- (251) Diamanti, S. J.; Khanna, V.; Hotta, A.; Yamakawa, D.; Shimizu, F.; Kramer, E. J.; Fredrickson, G. H.; Bazan, G. C. *J. Am. Chem. Soc.* **2004**, 126, 10528-10529.
- (252) Diamanti, S. J.; Khanna, V.; Hotta, A.; Coffin, R. C.; Yamakawa, D.; Kramer, E. J.; Fredrickson, G. H.; Bazan, G. C. *Macromolecules* **2006**, 39, 3270-3274.
- (253) Coffin, R. C.; Diamanti, S. J.; Hotta, A.; Khanna, V.; Kramer, E. J.; Fredrickson, G. H.; Bazan, G. C. *Chem. Commun.* **2007**, 3550-3552.
- (254) Schneider, Y.; Azoulay, J. D.; Coffin, R. C.; Bazan, G. C. *J. Am. Chem. Soc.* **2008**, 130, 10464-10465.
- (255) Safir, A. L.; Novak, B. M. *Macromolecules* **1995**, 28, 5396-5398.
- (256) Mehler, C.; Risse, W. *Macromolecules* **1992**, 25, 4226-4228.
- (257) Breunig, S.; Risse, W. *Makromol. Chem.* **1992**, 193, 2915-2927.
- (258) Brookhart, M.; Volpe Jr., A. F.; DeSimone, J. M. *Polym. Prepr. (Am. Chem. Soc., Div. Polym. Chem.)* **1991**, 32, 461-462.
- (259) Brookhart, M.; DeSimone, J. M.; Grant, B. E.; Tanner, M. J. *Macromolecules* **1995**, 28, 5378-5380.
- (260) Kaneyoshi, H.; Inoue, Y.; Matyjaszewski, K. *Macromolecules* **2005**, 38, 5425-5435.
- (261) van Meurs, M.; Britovsek, G. J. P.; Gibson, V. C.; Cohen, S. A. *J. Am. Chem. Soc.* **2005**, 127, 9913-9923.
- (262) Alfano, F.; Boone, H. W.; Busico, V.; Cipullo, R.; Stevens, J. C. *Macromolecules* **2007**, 40, 7736-7738.

- (263) Hustad, P. D.; Kuhlman, R. L.; Carnahan, E. M.; Wenzel, T. T.; Arriola, D. J. *Macromolecules* **2008**, 41, 4081-4089.
- (264) Sita, L. R. *Angew. Chem. Int. Ed.* **2009**, 48, 2464-2472.
- (265) Hustad, P. D.; Kuhlman, R. L.; Arriola, D. J.; Carnahan, E. M.; Wenzel, T. T. *Macromolecules* **2007**, 40, 7061-7064.
- (266) Chien, J. C. W.; Iwamoto, Y.; Rausch, M. D. *J. Polym. Sci. Part A: Polym. Chem.* **1999**, 37, 2439-2445.
- (267) Jayaratne, K. C.; Sita, L. R. *J. Am. Chem. Soc.* **2001**, 123, 10754-10755.
- (268) Arriola, D. J.; Carnahan, E. M.; Hustad, P. D.; Kuhlman, R. L.; Wenzel, T. T. *Science* **2006**, 312, 714-719.

## **Chapter 2**

### Synthesis and Functionalization of Allyl-Terminated Syndiotactic Polypropylene

## 2.1 Introduction

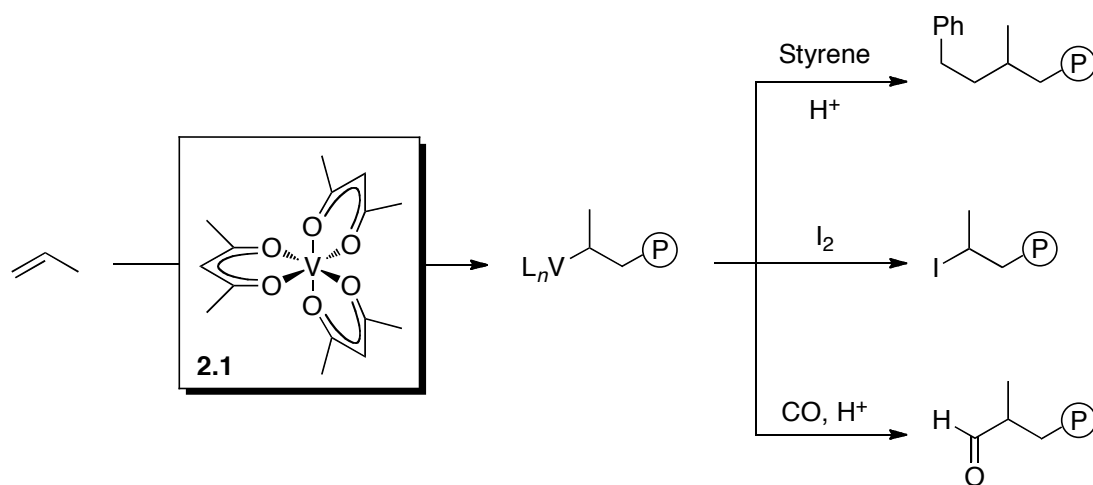
Polyolefins are one of the most important classes of commercial polymers on the market today with worldwide production exceeding 100 million tons per year.<sup>1</sup> The materials obtained from olefin polymerizations are useful in applications from garbage bags to automobile parts due in part to their robust chemical and physical properties combined with low cost.<sup>2</sup> Because of their non-polar nature polyolefin materials often display poor adhesion properties and low compatibility with polar additives which often inhibits printability and dyeability.<sup>3,4</sup> Fortunately, incorporation of even small amounts of polar functional groups into a polyolefin chain can dramatically improve these previously lackluster properties.<sup>5</sup>



**Figure 2.1.** Chemical structures of a propylene/polar olefin random copolymer and an end-functionalized polypropylene.

In general, there are two ways to envision the functionalization of polyolefins (Figure 2.1); polar functional groups may be randomly incorporated into the polyolefin main-chain or exclusively onto the chain-end.<sup>6</sup> Currently, commercial processes require radical polymerization methods to incorporate polar comonomers, which limits the type of materials produced.<sup>7</sup> However, transition-metal catalyzed coordination-insertion polymerization has recently been targeted as a synthetic method to afford new functionalized polyolefin materials.<sup>6-11</sup> Copolymerization of polar monomers and olefins by transition metal catalysts generally results in a small amount of functional group incorporation. Although early metals complexes are capable of catalyzing copolymerization with polar comonomers,<sup>12-15</sup> late metal catalysts are more

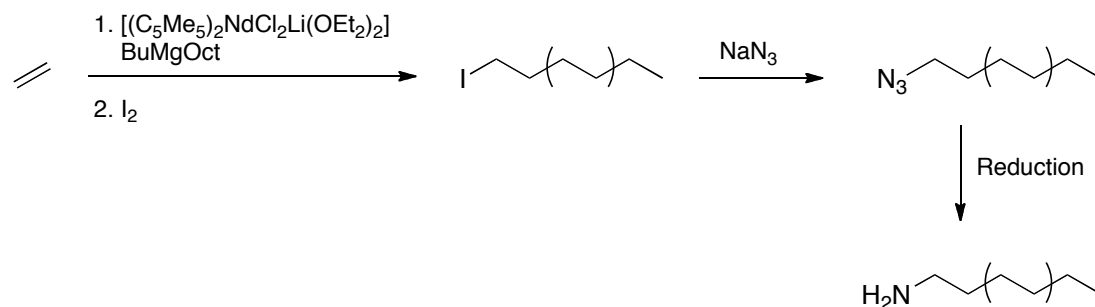
functional group tolerant due to their low oxophilicity.<sup>9,16-20</sup> For a more detailed discussion on the copolymerization of olefins with polar monomers and the properties of the resultant polymers refer to chapter five. This chapter will focus on the synthesis of the other major class of functionalized polyolefins, polymers bearing functional groups at the terminus, which are useful in the production of discrete materials with complex architectures<sup>21</sup> such as block copolymers<sup>22-26</sup>, star polymers<sup>27-34</sup> and comb polymers.<sup>22,32,35</sup>



**Scheme 2.1.** Synthesis of end-functionalized polypropylene through living polymerization with vanadium catalyst **2.1** followed by quenching with electrophiles.

End-functionalized polyolefins may be produced using a variety of different methods including thermal degradation<sup>36,37</sup> and chain transfer polymerization<sup>38-44</sup> as well as living<sup>45-52</sup> and non-living<sup>53-65</sup> transition metal catalysis. Living polymerization systems, which are void of chain termination events, are particularly useful in the production of uniform polymers containing functional groups on every chain end. In the 1980s, Doi and co-workers reported the end-functionalization of polypropylene utilizing vanadium-based catalysts such as **2.1** (Scheme 2.1).<sup>45-49,51</sup> The living chain end was capable of reacting with a variety of different electrophiles including styrene,

iodine and carbon monoxide to give polypropylene terminated with a number of functional groups. Currently, living polymerization systems are employed in the synthesis of end-functionalized polyolefins, but are limited in their ability to produce only one chain per metal center.<sup>50,52</sup> Therefore, it is important to identify and utilize systems that are capable of producing multiple chains per metal center.

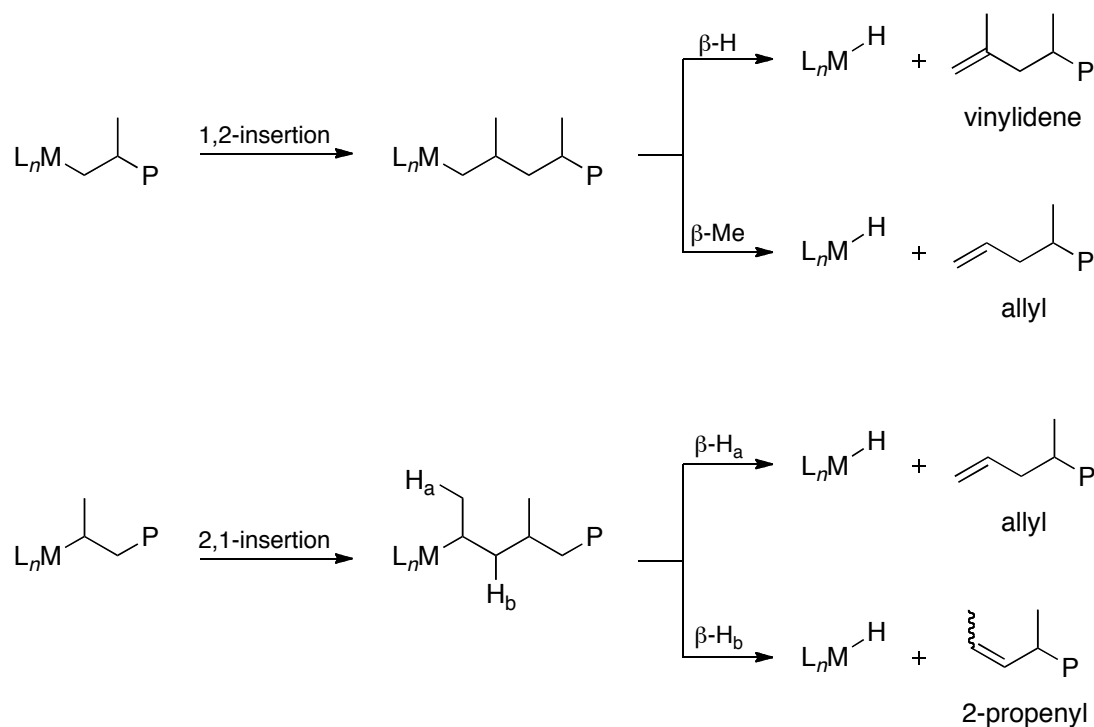


**Scheme 2.2.** Catalytic production of end-functionalized polyethylene using neodymium and *n*-butyloctylmagnesium.

Functionalized polyolefins can be produced in a catalytic fashion using transition metal catalysts capable of undergoing chain transfer in the presence of zinc,<sup>38,40</sup> borane,<sup>39,42</sup> aluminum<sup>41,43</sup> or magnesium reagents.<sup>44</sup> In a recent example, Briquel and co-workers utilized a neodymium complex (Scheme 2.2) that catalyzes the polymerization of ethylene and undergoes chain transfer in the presence of *n*-butyloctylmagnesium resulting in multiple polyethylene chains per neodymium.<sup>44</sup> The PE-Mg-PE was sufficiently nucleophilic and resulted in end-functionalized polyethylene upon reaction with iodine. Substitution of the iodine-terminated polyethylene with sodium azide afforded a polymer capable of copper catalyzed cycloaddition reactions in the presence of alkynes. The azide-terminated polymer was also reduced to the corresponding amine-terminated polyethylene using lithium aluminum hydride. The amine-terminated macromolecule was combined with methyl

methacrylate to produce a diblock copolymer, polyethylene-*b*-polymethylmethacrylate. By utilizing transition-metal polymerization capable of chain-transfer, end-functionalized polyolefins were produced in a catalytic fashion.

Other transition metal olefin polymerization catalysts produce multiple chains per metal center without the addition of a chain transfer agent.<sup>66</sup>  $\beta$ -Hydrogen or  $\beta$ -methyl transfers occur through several different pathways (Scheme 2.3) resulting in a number of different alkene-terminated polyolefins. A 1,2-propylene insertion into the growing polymer chain followed by  $\beta$ -hydrogen transfer gives vinylidene-terminated polypropylene. Alternatively,  $\beta$ -methyl transfer following a 1,2-insertion of propylene results in allyl-terminated polypropylene. A handful of metallocene catalysts have been observed to produce allyl end-groups following 1,2-propylene insertion, however, selectivities are at best 90% with vinylidenes making up the remaining



**Scheme 2.3.** Chain release processes following 1,2- or 2,1-propylene insertions.

chain-ends.<sup>63,67-69</sup> In systems that are capable of inserting propylene in a 2,1 fashion,  $\beta$ -hydrogen transfer could result in two different alkene-terminated polymers. Transfer of a  $\beta$ -hydrogen from the terminal  $\text{CH}_3$  ( $\beta\text{-H}_a$ ) results in allyl-terminated polypropylene, whereas  $\beta$ -hydrogen transfer from the internal  $\text{CH}_2$  ( $\beta\text{-H}_b$ ) gives a 2-propenyl end-group. Complexes of both titanium<sup>70</sup> and iron<sup>71-74</sup> have been shown to undergo 2,1 propylene insertions and subsequent  $\beta$ -hydrogen transfer resulting in polypropylene with allyl groups at the terminus.<sup>71-74</sup> In fact, when 2,1-insertion dominates propylene polymerization, terminal allyl groups are almost exclusively observed.<sup>70</sup> These alkene-terminated polypropylenes are useful synthetic intermediates and many researchers have utilized these materials in the production of polymers with alternative functional groups such as alcohols and amines.<sup>53-65</sup> Furthermore, end-functionalized polymers are attractive building blocks for the synthesis of more complex architectures such as block copolymers<sup>22-26</sup> and star polymers<sup>27-34</sup> due to decreased steric congestion at the chain-end.

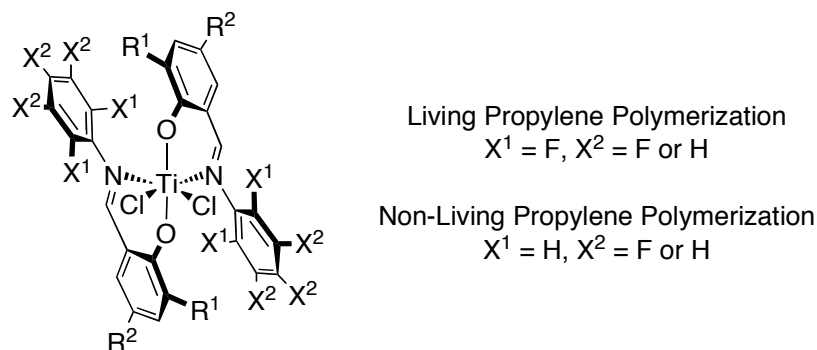
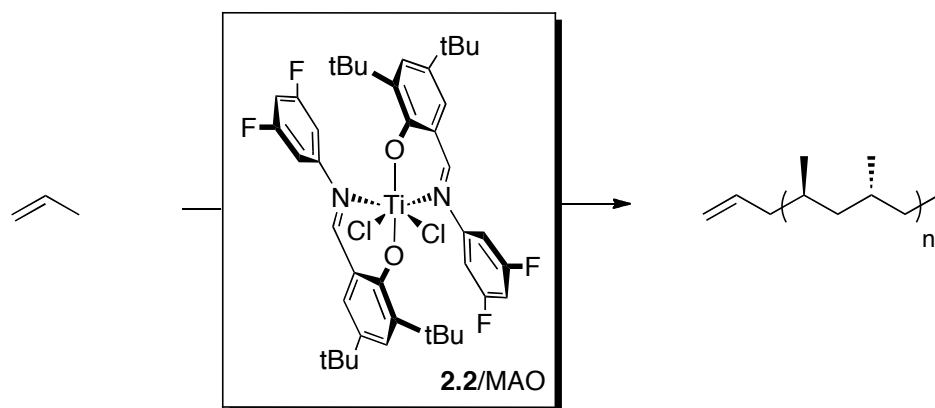


**Figure 2.2.** Living and non-living bis(phenoxy-imine) titanium catalysts.

In addition to allyl-termination, a polymer with stereoregularity was desired for the purposes of this study. Semicrystalline polymers including isotactic and syndiotactic polypropylene typically display high melting temperatures ( $T_m = 165$  and

148 °C, respectively) making the materials useful in commercial applications unlike their amorphous, stereoirregular counter part, atactic polypropylene ( $T_m = \text{none}$ ), which has limited commercial uses.<sup>5</sup> The bis(phenoxyimine)titanium catalysts (Figure 2.2) have been widely exploited in the field of olefin polymerization for their ability to produce highly syndiotactic polypropylene.<sup>70,75-89</sup> Studies have shown the fluorination pattern of the N-aryl ring has a significant effect on the nature of the polymerization.<sup>70,84,90</sup> With at least one fluorine present in the *ortho* position of the N-aryl ring, the bis(phenoxyimine)titanium complexes catalyze the living polymerization of propylene resulting in polypropylene with completely saturated groups. When all fluorines are removed from the *ortho* position of the N-aryl ring, the subsequent propylene polymerization is no longer living.<sup>70</sup> The <sup>1</sup>H NMR spectrum of the polypropylene produced from the non-living bis(phenoxyimine)titanium catalysts reveals only allyl-termination with no vinylidene or internal alkenes observed. For this study, a bis(phenoxyimine)titanium complexes (**2.2**, Scheme 2.4) bearing *t*-butyl groups on the *ortho* and *para* positions of the phenolate ring as well as fluorines on the 3- and 5-positions of the N-aryl ring was utilized. Upon activation with



**Scheme 2.4.** Synthesis of allyl-terminated syndiotactic polypropylene from a non-living bis(phenoxyimine)titanium complex.

methylaluminoxane (MAO), complex **2.2** produces polypropylene with modest molecular weight ( $M_n$  ( $^1\text{H NMR}$ ) = 5,800 g/mol) and syndiotacticity ( $[rrrr] = 0.76$ ). The polypropylene obtained from **2.2**/MAO was soluble in many organic solvents making it an ideal polymer for a variety of end-functionalization reactions.

In this chapter we explore the polymerization and subsequent end-functionalization of allyl-terminated syndiotactic polypropylene obtained from propylene polymerization with **2.2**/MAO. A number of polymers with varying functional groups have been produced utilizing a range of different organic transformations. Many of these end-functionalized polymers are useful for the production of polymers with more complex architectures such as block copolymers, star polymers and comb polymers. The synthesis of branched polymers from end-functionalized syndiotactic polypropylene will be discussed in the following chapters.

## **2.2 Results and Discussion**

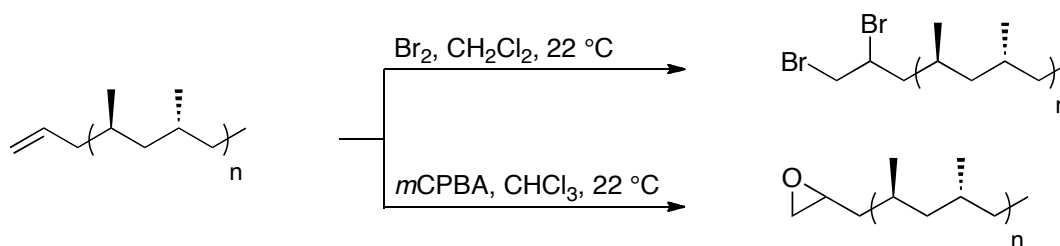
### **2.2.1 Propylene Polymerization with 2.2/MAO**

Activation of the bis(phenoxyimine) titanium complex **2.2** with MAO in the presence of propylene resulted in low molecular weight polypropylene ( $M_n$  ( $^1\text{H NMR}$ ) = 5,800 g/mol) terminated with allyl groups.<sup>70</sup> Analysis of the  $^{13}\text{C}$  NMR spectrum revealed polypropylene with moderate syndiotacticity ( $[rrrr] = 0.76$ ). Examination of the  $^1\text{H}$  NMR spectrum revealed resonances at  $\delta$  5.8 and 5.01 ppm, which have been assigned to the allyl functional group (Figure 2.3). The bis(phenoxyimine) titanium complexes have been shown to insert propylene in a 2,1 fashion (Scheme 2.3) and therefore chain transfer reactions could result in a 2-propenyl end-group in addition to the allyl-terminated polymer. Further analysis of the  $^1\text{H}$  NMR spectrum shows no resonance at  $\delta$  5.5, which would be indicative of a 2-propenyl end-group. Thus,

complex **2.2** cleanly produces syndiotactic polypropylene with only terminal allyl moieties.

### 2.2.2 Synthesis of Dibromo-Terminated Syndiotactic Polypropylene

Using the alkene moiety as a synthetic handle, a number of different functional groups were installed on the end of the polymer chain. Adding bromine to a slurry of allyl-terminated syndiotactic polypropylene (Scheme 2.5) in methylene chloride results in dibromo-terminated polypropylene. Analysis of the polymeric material by  $^1\text{H}$  NMR spectroscopy (Figure 2.3) revealed three new multiplets ( $\delta$  4.27, 3.89 and 3.69 ppm) and their chemical shifts were consistent with reported literature values for dibromoalkanes.<sup>91</sup> Additionally, the signals corresponding to the allyl end-group were not observed. The reaction proceeded to high conversion (94%) as evidenced by the end-group molecular weight analysis ( $M_n$  ( $^1\text{H}$  NMR) = 6,200 g/mol). The dibromo-terminated polymer was exposed to different bases (DBU and KOH) in several solvents (toluene, THF and DMF) in an effort to obtain alkyne-terminated polypropylene, which was a desired building block for the synthesis of more complex polymer architectures utilizing click chemistry. Even though signals corresponding to the dibromo end-group were not observed in the  $^1\text{H}$  NMR spectrum, resonances for the alkyne were also not observed and subsequent cycloaddition reactions in the



**Scheme 2.5.** Synthesis of *s*PP-CH<sub>2</sub>CHBrCH<sub>2</sub>Br and *s*PP-CH<sub>2</sub>CH(O)CH<sub>2</sub> from *s*PP-CH<sub>2</sub>CH=CH<sub>2</sub>.

presence of azides and copper iodide were unsuccessful. Despite the inability to produce alkyne-terminated polymer under the conditions screened, the dibromo polymer itself could serve as a useful dielectrophile in nucleophilic substitution reactions.<sup>92-94</sup>

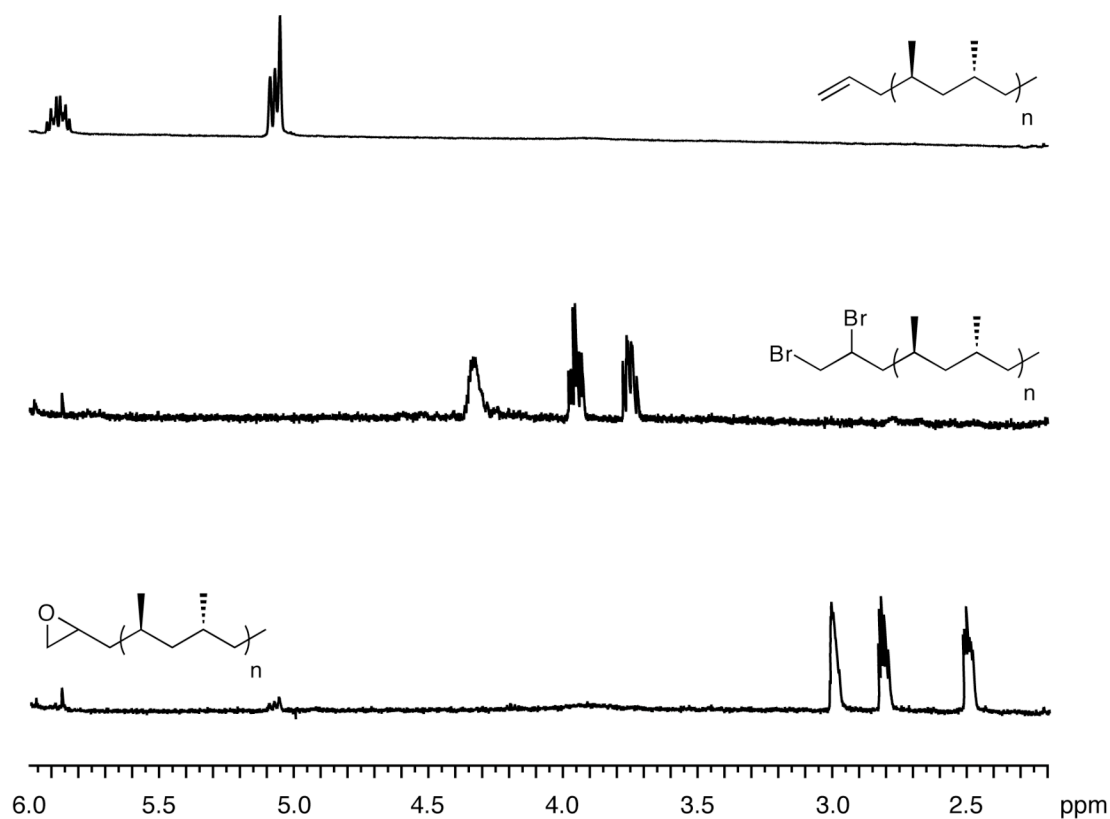
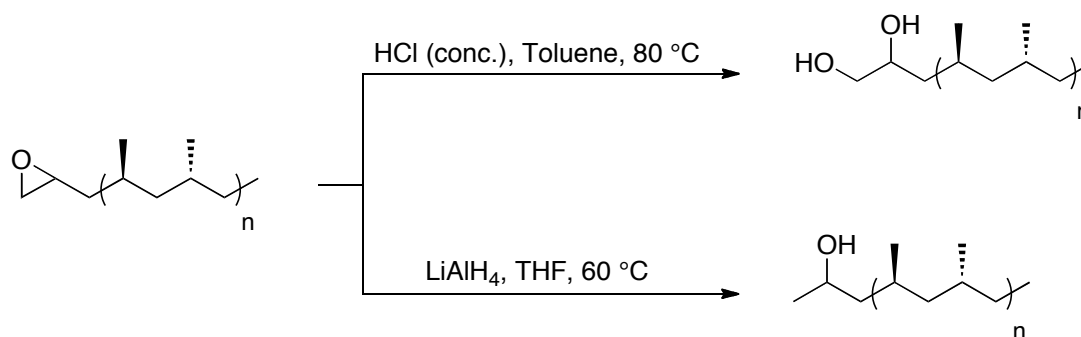


**Figure 2.3.**  $^1\text{H}$  NMR spectra of  $s\text{PP-CH}_2\text{CH}=\text{CH}_2$ ,  $s\text{PP-CH}_2\text{CHBrCH}_2\text{Br}$  and  $s\text{PP-CH}_2\text{CH}(\text{O})\text{CH}_2$  (500 MHz, 1,1,2,2-tetrachloroethane- $d_2$ , 75 °C).

### 2.2.3 Synthesis and Ring Opening of Epoxide-Terminated Polypropylene

In addition to bromination, the allyl-terminated polypropylene can be readily converted to the epoxide-terminated polymer (Scheme 2.5) with chloroform and *meta*-chloroperoxybenzoic acid (*m*CPBA) at room temperature. The epoxidation proceeds with high conversion (95%) as evidenced end-group analysis ( $M_n$  ( $^1\text{H}$  NMR) = 6,100

g/mol). Examination of the  $^1\text{H}$  NMR spectrum (Figure 2.3) confirmed the presence of three new resonances ( $\delta$  2.93, 2.74 and 2.42 ppm) and the complete disappearance of the alkene residues ( $\delta$  5.8 and 5.01 ppm). Epoxide-terminated syndiotactic polypropylene is a useful type of end-functionalized polymer due to their potential use in a number of different polymerization<sup>95,96</sup> and organic transformations.<sup>97</sup>



**Scheme 2.6.** Ring opening of  $s\text{PP-CH}_2\text{CH(O)CH}_2$  under acidic and basic conditions.

Epoxides are known to readily undergo ring opening by nucleophiles in the presence of acids or bases resulting in the either primary or secondary alcohols. Dissolving the polymer in toluene and adding HCl resulted in complete consumption of the epoxide-terminated polypropylene (Scheme 2.6). Ring opening was confirmed by  $^1\text{H}$  NMR spectroscopy (Figure 2.4) with the disappearance of the epoxide resonances and the appearance of new resonances ( $\delta$  3.90, 3.63 and 3.48 ppm), which were suggestive of the dihydroxyl-terminated polymer. However, molecular weight determination by end-group analysis of the  $^1\text{H}$  NMR spectrum showed poor conversion (25%) of the epoxide to the dihydroxyl. In contrast to the acidic conditions, exposing the epoxide to basic ring-opening conditions proved to be highly successful. Heating a mixture of the polymer, THF and lithium aluminum hydride to 60 °C produced the secondary alcohol with high conversion (99%) as evidenced by

molecular weight determination ( $M_n$  ( $^1\text{H NMR}$ ) = 5,400 g/mol) through end-group analysis. Then  $^1\text{H NMR}$  spectrum revealed a signal ( $\delta$  3.88) consistent with the formation of the secondary alcohol. The alcohol proved to be reactive upon exposure to a number of different acid chlorides as well as *para*-toluenesulfonyl chloride, however, the steric bulk of the secondary alcohol ultimately limited its use in the production of more complex polymer architectures such as star polymers. Therefore, the efficient synthesis of syndiotactic polypropylene terminated with primary hydroxyl groups was targeted.

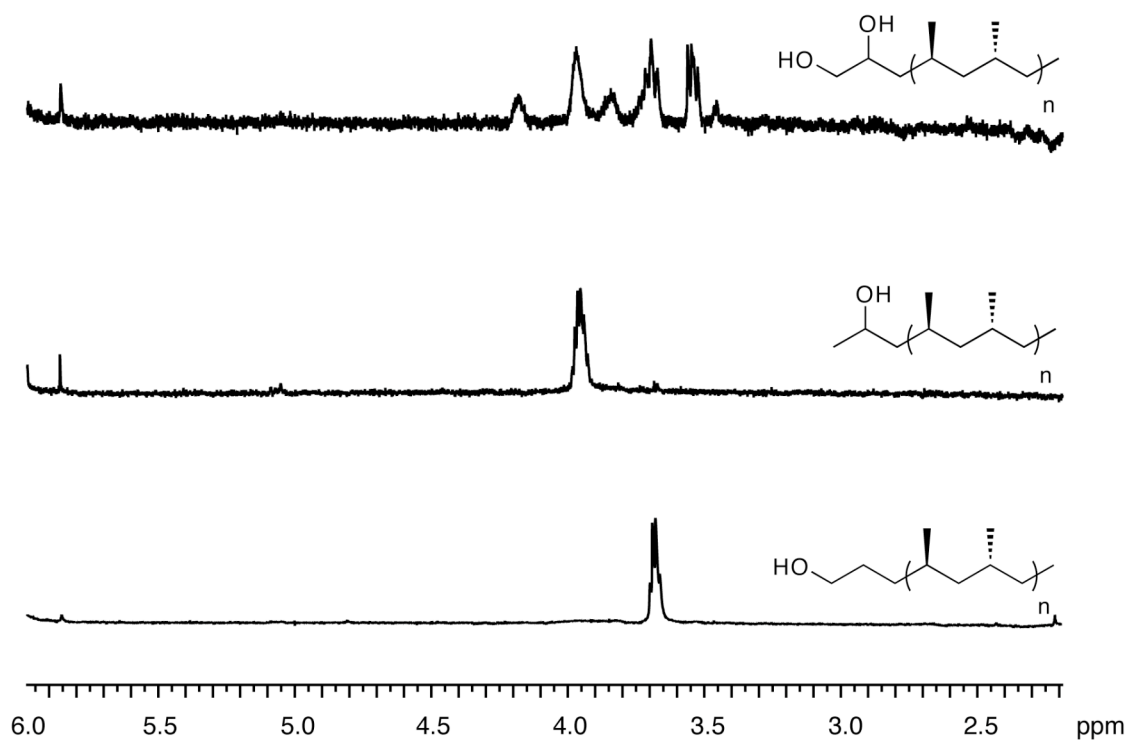
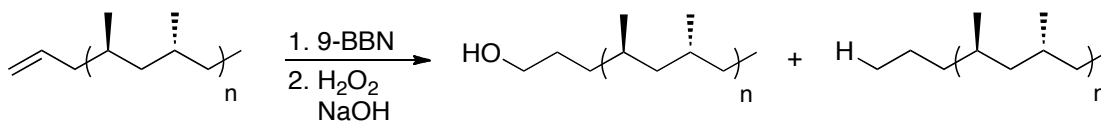


**Figure 2.4.**  $^1\text{H NMR}$  spectra of  $s\text{PP-CH}_2\text{CH(OH)CH}_2\text{OH}$ ,  $s\text{PP-CH}_2\text{CH(OH)CH}_3$ ,  $s\text{PP-(CH}_2)_3\text{OH}$  (500 MHz, 1,1,2,2-tetrachloroethane- $d_2$ , 75°C).

#### 2.2.4 Synthesis of Hydroxyl-Terminated Syndiotactic Polypropylene

The allyl-terminated polypropylene can be converted to a primary hydroxyl-terminated polypropylene using hydroboration-oxidation (Scheme 2.7). In 2005,

Hagiwara and coworkers were able to convert vinylidene-terminated polypropylene formed through controlled thermal degradation to the primary alcohol using a borane-THF complex and subsequent hydrogen peroxide oxidation.<sup>37</sup> Conversion of the vinylidene to a hydroxyl end-group was achieved in greater than 90% yields for most of the polymers utilized in their study. Using a similar procedure, the allyl-terminated syndiotactic polypropylene was converted to the primary hydroxyl using 9-BBN at 65 °C followed by the addition of sodium hydroxide and hydrogen peroxide. Analysis of the <sup>1</sup>H NMR spectrum (Figure 2.6) showed complete disappearance of the alkene resonances and the appearance of a new resonance at  $\delta$  3.61, which is consistent with literature reports for hydroxyl-terminated polymers.<sup>37</sup> The percent end-functionalization of the polymer was dependent on the solvent, time and temperature at which the oxidation was performed. When the oxidation was carried out at room temperature in toluene, the reaction proceeded to approximately 76% conversion with the remaining 24% corresponding to alkane-terminated polymer (Table 2.1). The molecular weight of the hydroxyl-terminated polypropylene was equivalent to that of the allyl-terminated polypropylene by GPC ( $M_n$  (GPC) = 4,600 g/mol), which supports the formation of alcohol-terminated and alkane-terminated polypropylene. Upon increasing the temperature of the oxidation step to 45 °C in toluene, no observable change in conversion (76%) was observed after one hour, however, increasing the reaction time to four hours showed a significant decrease in conversion (58%). Similar effects were observed for oxidations carried out at 65 °C for 24 hours in toluene



**Scheme 2.7.** Hydroboration/oxidation of sPP-CH<sub>2</sub>CH=CH<sub>2</sub>.

**Table 2.1.** Optimization of the *s*PP-CH<sub>2</sub>CH=CH<sub>2</sub> oxidation following hydroboration with 9-BBN.

Entry	Solvent	$T_{\text{oxidation}}$ (°C)	$t_{\text{oxidation}}$ (hr)	$M_n$ (g/mol) <sup>a</sup>	Functionalization (%) <sup>a</sup>
1	Toluene	25	4	7,500	77
2	Toluene	25	24	7,600	76
3	Toluene	45	1	7,600	76
4	Toluene	45	4	10,000	58
5	Toluene	65	24	10,000	58
6	THF	25	4	7,500	77
7	THF	45	0.25	30,000	19
8	THF	45	0.5	8,900	65
9	THF	45	1	6,400	91
10	THF	45	4	6,600	88
11	THF	65	24	13,000	45

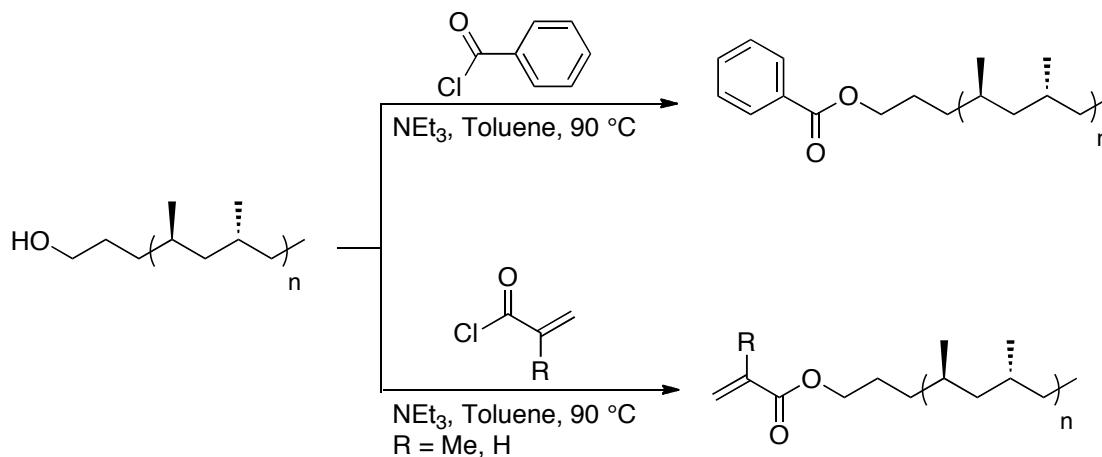
<sup>a</sup> Determined using <sup>1</sup>H NMR spectroscopy in 1,1,2,2-tetrachloroethane-*d*<sub>2</sub> at 75 °C.

(58%). Switching the solvent from toluene to THF and carrying the oxidation out at room temperature had no effect on the amount of hydroxyl-terminated polymer obtained (76%). Upon increasing the oxidation temperature to 45 °C, a noticeable change in the amount of hydroxyl-terminated polymer was observed. When short oxidation times (15 and 30 min) were utilized, incomplete conversion to product was observed (19 and 65%, respectively). However, after just one hour, a significant amount of hydroxyl-terminated polypropylene was obtained (91%). Increasing the reaction time further resulted in a slight decrease in the amount of end-functionalized product obtained (88%). Finally, increasing the temperature of the oxidation step to 65 °C in THF for 24 hours, showed a marked decrease in the amount of alcohol-terminated polymer that was obtained (45%). Based on all of these results, THF appears to be the optimal solvent for the hydroboration/oxidation of ally-terminated syndiotactic polypropylene. The temperature and length of the oxidation step greatly affected the amount of functionalized polymer that was obtained. Long reaction times (>4 hrs) and high oxidation temperatures (>45 °C) lead to decreased functionalization. Carrying this oxidation out at 45 °C for 1 hour gave hydroxyl terminated polymer in high conversion (91%).

### **2.2.5 Reaction of Hydroxyl-Terminated Polypropylene with Acid Chlorides**

Installing the primary hydroxyl group on the end of the polypropylene chain resulted in a polymer that was useful in a number of organic transformations. In particular, reaction of the terminal alcohol with several different acid chlorides was facile. Initial hydroxyl reactivity was investigated through reaction of the alcohol-terminated polymer with benzoyl chloride in the presence of toluene and triethyl amine (Scheme 2.8). The resultant polypropylene displayed three aromatic resonances ( $\delta$  8.04, 7.57 and 7.45 ppm) as well as a resonance characteristic of the methylene

adjacent to the ester ( $\delta$  4.31) in the  $^1\text{H}$  NMR spectrum (Figure 2.5). Further analysis of the  $^1\text{H}$  NMR spectra revealed a molecular weight ( $M_n$  ( $^1\text{H}$  NMR) = 11,000 g/mol) consistent with 69% conversion of the hydroxyl-terminated polypropylene produced from hydroboration/oxidation in toluene at room temperature to the ester.



**Scheme 2.8.** Reaction of *s*PP-(CH<sub>2</sub>)<sub>3</sub>OH with acid chlorides.

The reactivity of the hydroxyl-terminated polymer with acid chlorides was further explored in an effort to produce end-functionalized polypropylene molecules that would be useful in radical polymerization processes. Combining the alcohol-terminated polymer with toluene, triethyl amine and methacryloyl chloride at room temperature resulted in the methylacrylate-terminated polypropylene, however, molecular weights ( $M_n$  ( $^1\text{H}$  NMR) = 34,000 g/mol) obtained suggested a low degree of end-functionalization (17%) as well as a secondary product, which could not be identified. Upon substituting acryloyl chloride for methacryloyl chloride, functionalization was significantly improved. Analysis of the resultant  $^1\text{H}$  NMR spectrum for the polypropylene produced showed three alkene resonances ( $\delta$  6.38,

6.15 and 5.80 ppm) as well as an ester resonance ( $\delta$  4.20), which were all indicative of formation of the acrylate ester (Figure 2.5). Overall functionalization (61%,  $M_n$  ( $^1\text{H}$  NMR) = 9,500 g/mol) obtained through end-group analysis using  $^1\text{H}$  NMR spectroscopy was significantly higher and overall the reaction was cleaner than the corresponding methacrylate ester. These acrylate-terminated polymers represent a particularly intriguing class of polymers due to their usefulness in radical polymerization.<sup>98,99</sup>

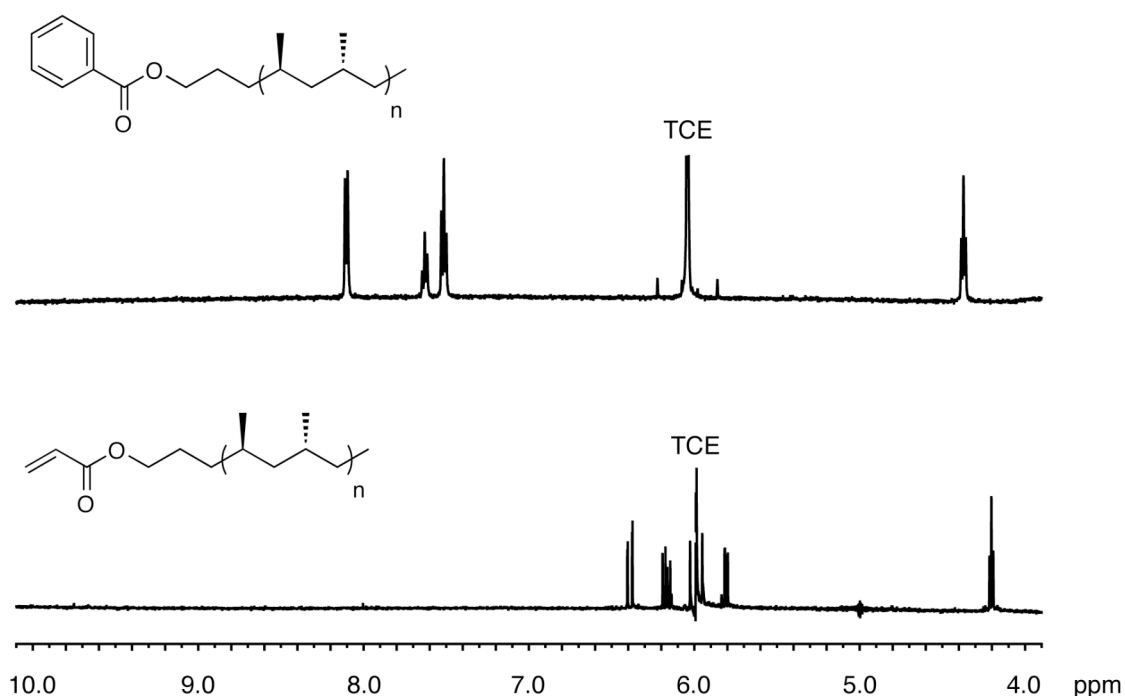
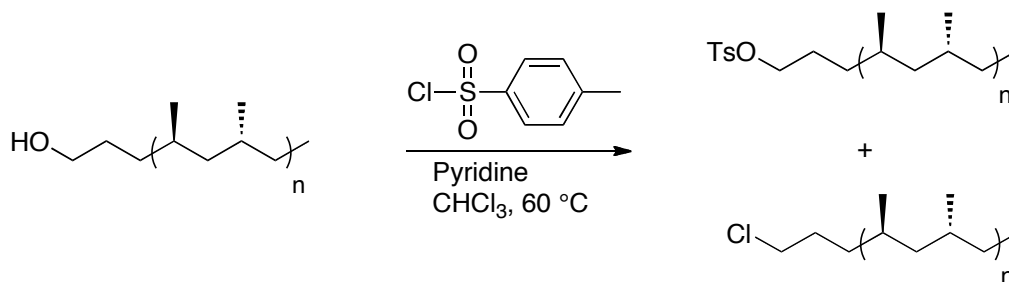


**Figure 2.5.**  $^1\text{H}$  NMR spectra of  $s\text{PP}-(\text{CH}_2)_3\text{OCOC}_6\text{H}_5$  and  $s\text{PP}-(\text{CH}_2)_3\text{OCOCH}=\text{CH}_2$  (500 MHz, 1,1,2,2-tetrachloroethane- $d_2$  (TCE), 75 °C).

### 2.2.6 Synthesis of Tosyl-Terminated Syndiotactic Polypropylene

Conversion of the hydroxyl-terminated polymer to the tosyl-terminated polypropylene was also achieved by dissolving the polymer in chloroform and adding

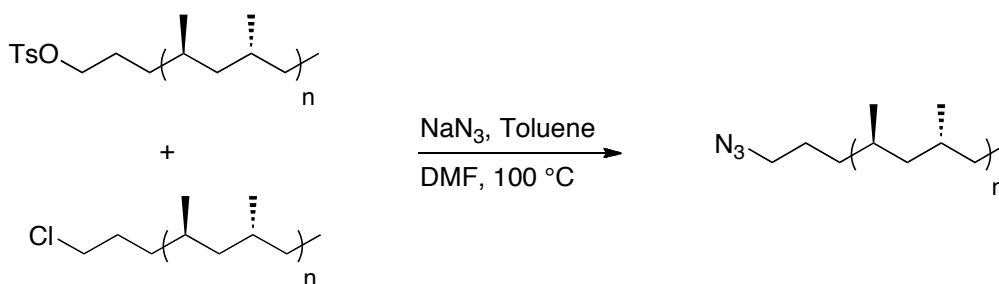
pyridine and tosyl chloride to the mixture (Scheme 2.9). After stirring for one day at 60 °C, the resultant polymer was analyzed by <sup>1</sup>H NMR spectroscopy, which revealed a mixture of two products. One of the products was the expected tosylated polymer, which was confirmed by the presence of two aromatic resonances (δ 7.78 and 7.35 ppm), a methyl resonance (δ 2.46) and a signal for the protons adjacent to the tosyl group (δ 4.03). The other product exhibited a single resonance (δ 3.46) and was determined to be the chloro-terminated polypropylene. Displacement of the tosylate by the chloride has been shown to occur at elevated reaction temperatures for extended periods of time.<sup>100</sup> Using end-group analysis of the <sup>1</sup>H NMR spectrum (Figure 2.7), high conversion of the hydroxyl group to either a chloride or a tosylate was observed (84%). By GPC, the polymer mixture had a molecular weight ( $M_n = 5,000$  g/mol) consistent with the starting polymer ( $M_n = 4,600$  g/mol). Despite the mixture of end groups the polymer was still used in the next step of the synthesis as both the tosyl and the chloro groups were expected to leave the end of the polymer chain in the presence of a nucleophile.



**Scheme 2.9.** Reaction of hydroxyl-terminated polypropylene with tosyl chloride to produce tosyl- and chloro-terminated polypropylene.

### 2.2.7 Synthesis of Azide-Terminated Syndiotactic Polypropylene

It has previously been shown that tosyl-terminated<sup>41</sup> or halide-terminated<sup>101</sup> polymers may be converted to the azide-terminated polymer, therefore, we predicted our polymer mixture could be converted to a single product. The polypropylene mixture was combined with sodium azide, toluene and DMF at 100 °C (Scheme 2.10). After three days, the mixture was determined to have undergone conversion to the azide-terminated polymer. Analysis of the <sup>1</sup>H NMR spectrum (Figure 2.6) revealed a single new resonance ( $\delta$  3.26), which was consistent with azide formation, as well as no signals corresponding to the tosyl- or chloro-terminated polypropylene.<sup>101</sup> A slight increase in the polymer molecular weight was determined by GPC ( $M_n$  (GPC) = 7,700 g/mol) and end group analysis ( $M_n$  (<sup>1</sup>H NMR) = 13,500 g/mol). This molecular weight increase was attributed to fractionation of more soluble, lower molecular weight polymers during the workup process resulting in moderate conversion (69%) to azide-terminated polymer. An IR spectrum (Figure 2.8) of the polypropylene was obtained and a large peak was observed (2100 cm<sup>-1</sup>), which was consistent with the presence of azide moieties.<sup>101</sup> Furthermore, IR spectrum of the tosyl-terminated (Figure 2.7) and amine terminated (discussed below) were also obtained. Both polymers showed no noticeable peaks in the azide region, which confirms both addition and removal of the functionality is possible.



**Scheme 2.10.** Synthesis of azide-terminated polypropylene from tosyl- and chloro-terminated polypropylene.

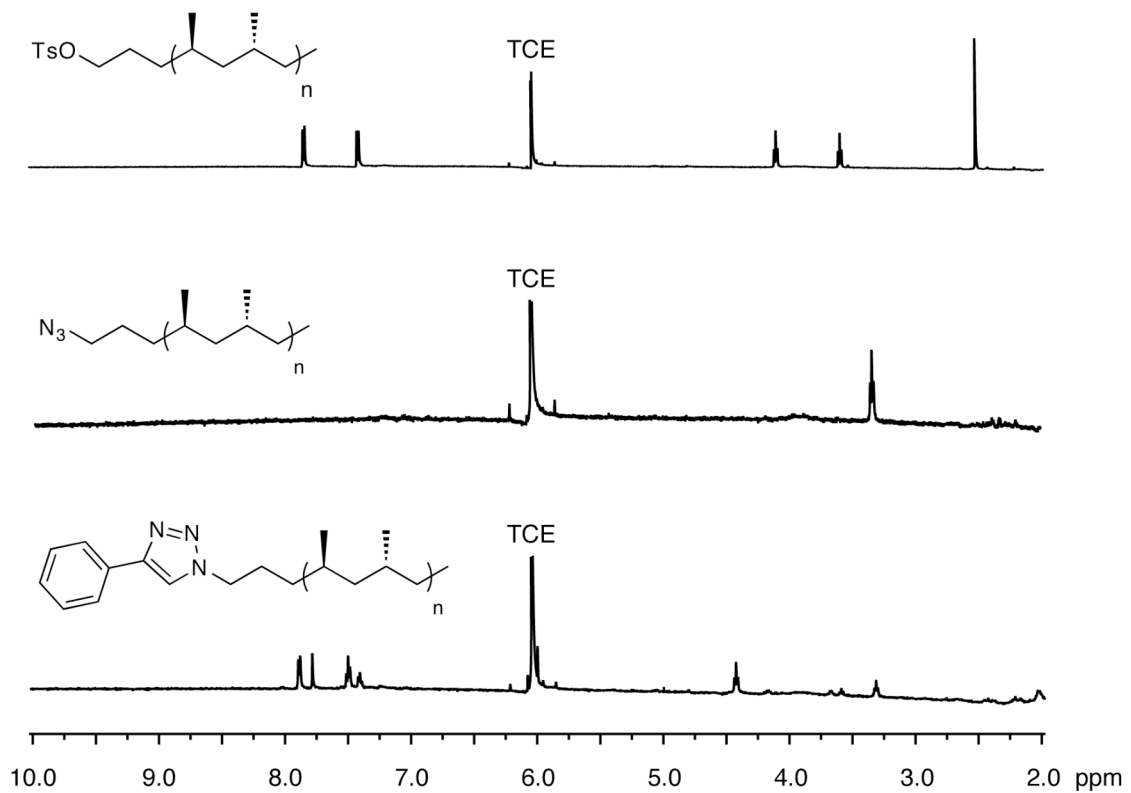


**Figure 2.6.**  $^1\text{H}$  NMR spectra of  $s\text{PP}-(\text{CH}_2)_3\text{OTs}$ ,  $s\text{PP}(\text{CH}_2)_3\text{N}_3$  and  $s\text{PP}-(\text{CH}_2)_3\text{C}_2\text{HN}_3\text{C}_6\text{H}_5$  (500 MHz, 1,1,2,2-tetrachloroethane- $d_2$  (TCE), 75 °C).

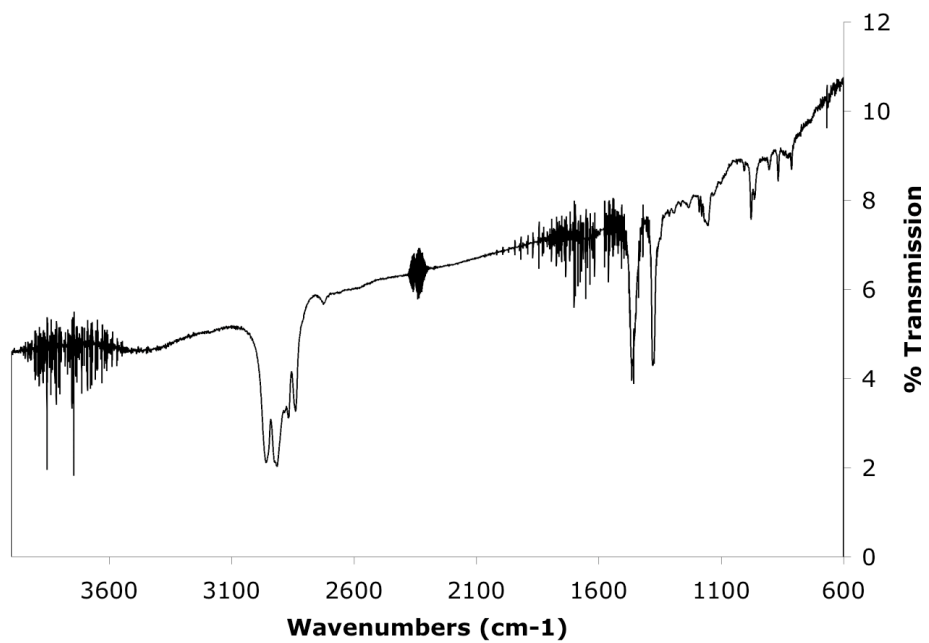


**Figure 2.7.** IR spectrum of tosyl-terminated polypropylene.

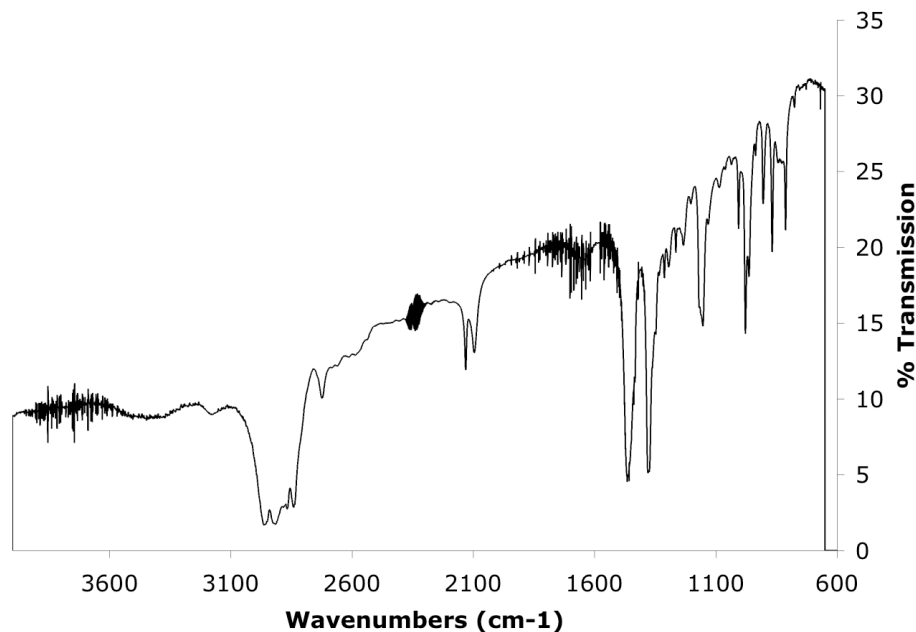
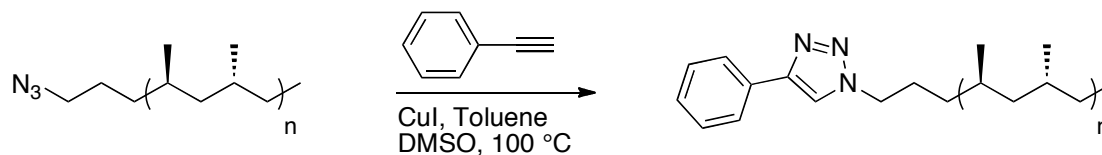


**Figure 2.8.** IR spectrum of azide-terminated polypropylene.

### 2.2.8 Click Chemistry and Azide-Terminated Syndiotactic Polypropylene

Recently, click chemistry utilizing azides and alkynes usually in the presence of copper has been widely used to form triazoles.<sup>22,102-106</sup> These are typically high yielding, selective reactions and are therefore ideal for polymer end-functionalization. Exposure of the azide-terminated syndiotactic polypropylene to phenyl acetylene in the presence of copper iodide, toluene and DMSO resulted in syndiotactic polypropylene end-functionalized with a triazole moiety (Scheme 2.11). The <sup>1</sup>H NMR spectrum (Figure 2.6) showed four new aromatic resonances ( $\delta$  7.83, 7.73, 7.44 and 7.35 ppm) as well as one new resonance, which can be attributed to the methylene adjacent to the triazole ( $\delta$  4.37). The 1,4-disubstituted triazole was the only regioisomer present, which is the expected product from a copper catalyzed cycloaddition reaction.<sup>106</sup> The azide-terminated polypropylene was completely consumed, however only a modest amount of end-functionalization (23%) was

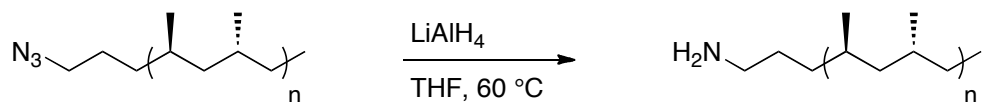
observed utilizing end-group analysis ( $M_n = 33,000$  g/mol). Despite the low conversion, the ability to click acetylenes onto the end of syndiotactic polypropylene chains opens the door to new functional groups and reactivities.<sup>22,103-106</sup>



**Scheme 2.11.** Click reaction of sPP-(CH<sub>2</sub>)<sub>3</sub>N<sub>3</sub> with phenyl acetylene.

### 2.2.9 Synthesis of Amine-Terminated Syndiotactic Polypropylene

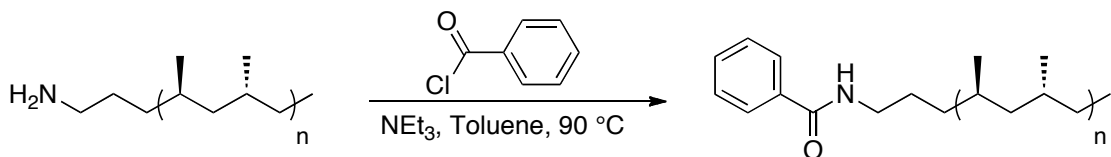
It has been previously shown that azide-terminated polyethylene can be converted to amine-terminated polyethylene through reduction of the azide functionality.<sup>44</sup> The azide-terminated syndiotactic polypropylene was also easily converted to the corresponding amine using lithium aluminum hydride in THF at  $60\text{ }^\circ C$  (Scheme 2.12). Analysis of the  $^1H$  NMR spectrum showed complete disappearance of the resonance at  $\delta$  3.26 and the appearance of a single new resonance at  $\delta$  2.65, which is indicative of amine formation.<sup>44</sup> Conversion of the azide to the amine-terminated polymer proceeded with high efficiency (87%) according to molecular weight analysis ( $M_n = 15,000$  g/mol) using  $^1H$  NMR spectroscopy (Figure 2.9). A slight increase in the molecular weight of the polymer ( $M_n = 8,300$  g/mol) was observed by GPC, which would explain the increase in molecular weight observed using  $^1H$  NMR spectroscopy. The IR spectrum (Figure 2.10) of the amine-terminated polypropylene showed no peak at  $2100\text{ cm}^{-1}$ , which confirmed the complete removal of the azide functionality. The amine functional group is a useful synthetic handle due to its facile reactivity with a number of organic compounds including alkyl halide and acid chlorides.



**Scheme 2.12.** Reduction of  $sPP-(CH_2)_3N_3$  to  $sPP-(CH_2)_3NH_2$  using  $LiAlH_4$ .

### 2.2.10 Reaction of Amine-Terminated Polypropylene with Acid Chlorides

In fact, the amine-terminated syndiotactic polypropylene was found to readily react with acid chlorides. In the presence of benzoyl chloride, triethyl amine and toluene at 100 °C, amide-terminated polypropylene was easily obtained from the amine (Scheme 2.13). Analysis of the  $^1H$  NMR spectrum (Figure 2.9) showed complete disappearance of the resonance at  $\delta$  2.65 and the appearance of three new aromatic resonances ( $\delta$  7.42, 7.28 and 7.19 ppm) and a new resonance at  $\delta$  3.98, which can be attributed to the methylene adjacent to the amide. The reaction proceeded to moderately high conversion (83%) as evidenced by end-group analysis ( $M_n = 18,000$  g/mol). Molecular weight determination using GPC suggests a slight decrease in molecular weight ( $M_n = 6,400$  g/mol) compared with the amine-terminated polymer ( $M_n = 8,300$  g/mol). It is possible that hydrogen bonding between amine-terminated polymers results in artificially high molecular weight being obtained by GPC. This effect has been observed in polyaniline systems capable of hydrogen bonding.<sup>107</sup> Due to the relative ease of this reaction, a host of different amide substituted polypropylenes could easily be synthesized possibly resulting in polypropylene materials with new structures and reactivity.



**Scheme 2.13.** Reaction of  $sPP-(CH_2)_3NH_2$  with benzoyl chloride.

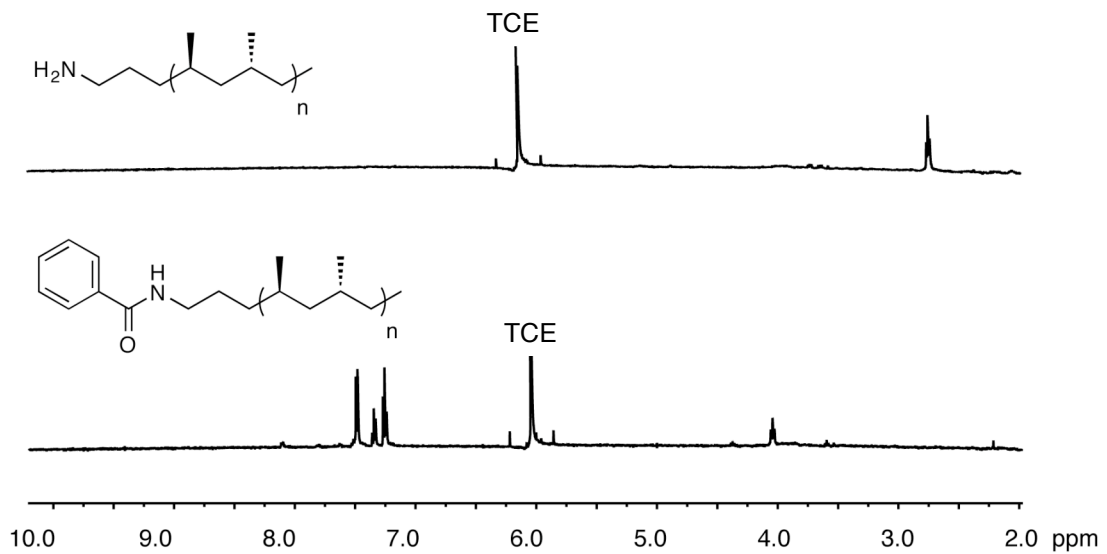


**Figure 2.9.**  $^1\text{H}$  NMR spectra of  $s\text{PP}-(\text{CH}_2)_3\text{NH}_2$  and  $s\text{PP}-(\text{CH}_2)_3\text{NHCOC}_6\text{H}_5$  (500 MHz, 1,1,2,2-tetrachloroethane- $d_2$  (TCE), 75 °C).

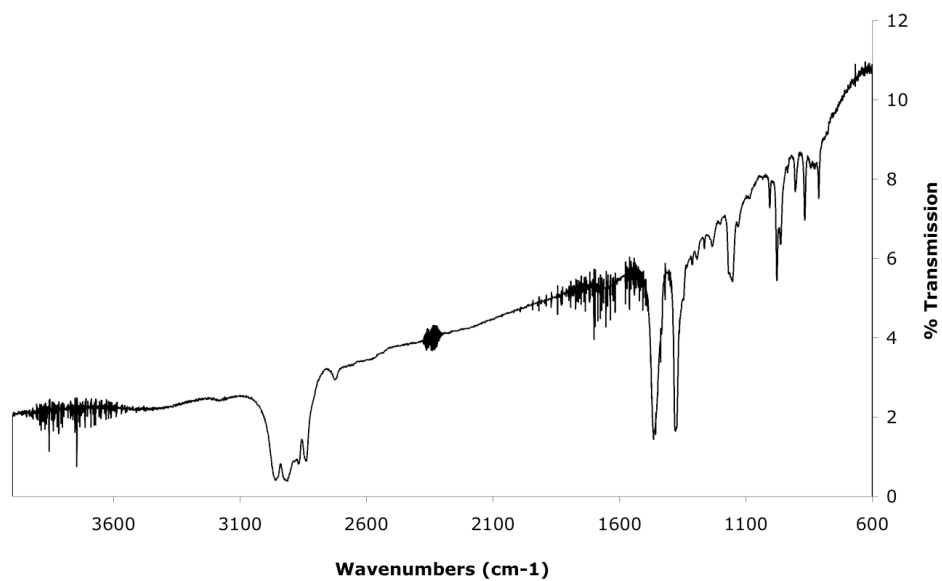


**Figure 2.10.** IR spectrum of amine-terminated syndiotactic polypropylene.

## 2.3 Conclusion

From allyl-terminated syndiotactic polypropylene, we obtained a variety of different end-functionalized polymers including, but not limited to epoxides, alcohols, esters, azides and amines. Most of the reactions explored here proceeded with selectivity towards a single product. Therefore, the end-functionalized polymers were isolated with uniform functional groups at each terminus. Imparting functionality to polypropylene has been shown to improve properties such as adhesion, hygroscopicity and miscibility in polymer blends.<sup>3-5</sup> Furthermore, these end-functionalized polymers may be useful in the production of a number of branch polymers<sup>21</sup> such as block copolymers,<sup>22-26</sup> star polymers<sup>27-34</sup> and comb polymers,<sup>22,32,35</sup> which will be discussed at length in the following chapters.

## 2.4 Experimental

**General Procedures.** All manipulations of air- and/or water-sensitive compounds were carried out under dry nitrogen using Braun UniLab drybox or standard Schlenk techniques. <sup>1</sup>H and <sup>13</sup>C{<sup>1</sup>H} NMR spectra of polymers were recorded using a Varian UnityInova (500 MHz) spectrometer equipped with a <sup>1</sup>H/BB switchable with Z-pulse field gradient probe operating and referenced versus residual non-deuterated solvent shifts. The polymer samples were dissolved in 1,1,2,2-tetrachloroethane-*d*<sub>2</sub> in a 5 mm O.D. tube, and spectra were collected at 75 °C. End-group analysis for molecular weight determination was achieved by relative integration of the end-group vs alkyl peaks in the <sup>1</sup>H NMR spectra. Additionally, molecular weights ( $M_n$  and  $M_w$ ) and polydispersities ( $M_w/M_n$ ) were determined by high temperature gel permeation chromatography (GPC). Analyses were performed with a Waters Alliance GPCV 2000 GPC equipped with a Waters DRI detector and viscometer. The column set (four Waters HT 6E and one Waters HT 2) was eluted with 1,2,4-trichlorobenzene

containing 0.01 wt % di-*tert*-butyl-hydroxytoluene (BHT) at 1.0 mL/min at 140 °C. Data were calibrated using monomodal polyethylene standards (from Polymer Standards Service).

**Materials.** Toluene was purified over columns of alumina and copper (Q5). THF was purified over an alumina column and degassed by three freeze-pump-thaw cycles before use. Propylene (Airgas, research purity) was purified over columns (40 cm inner diameter x 120 cm long) of BASF catalyst R3-12, BASF catalyst R3-11, and 4Å molecular sieves. PMAO-IP (13 wt % Al in toluene, Akzo Nobel) was dried in vacuo to remove residual trimethyl aluminum and used as a solid white powder. Complex **2.2** was prepared according to a previously reported procedure.<sup>70</sup> Pyridine and triethylamine were stirred over CaH<sub>2</sub> for several days and vacuum distilled. Bromine, methylene chloride, *meta*-chloroperoxybenzoic acid, chloroform, methacryloyl chloride, acryloyl chloride, benzoyl chloride, *para*-toluenesulfonyl chloride, LiAlH<sub>4</sub>, sodium azide, copper iodide, phenyl acetylene, DMF (anhydrous, 99.8%), DMSO (anhydrous, 99.9%) and 1,1,2,2-tetrachloroethane-*d*<sub>2</sub> were purchased from commercial sources and used as received.

**sPP-CH<sub>2</sub>CH=CH<sub>2</sub>.** In a glovebox, a 12 oz Laboratory Crest reaction vessel (Andrews Glass) was charged with dried PMAO (1.15 g, 20 mmol) and toluene (300 mL). The vessel was purged with propylene gas three times and equilibrated at 0 °C and 30 psig propylene. After 15 minutes, a solution of the **2.2** (100 μmol, [Al]/[Ti] = 200) in toluene (10 mL) was injected into the reactor. After 9 h, the reaction mixture was quenched with methanol (10 mL) and the polymer was precipitated into a copious amount of acidic methanol (5% HCl(aq)) and stirred overnight. The polymer was isolated and rinsed with methanol. To purify the sample, the polymer was dissolved in hot toluene and filtered through a glass frit layered with silica, alumina, and Celite. The toluene was removed and the polymer was dried in vacuo to constant weight

(9.11 g).  $M_n(\text{GPC}) = 4,500 \text{ g/mol}$ ,  $M_w/M_n = 1.90$ ,  $M_n(^1\text{H NMR}) = 5,800 \text{ g/mol}$ .  $^1\text{H NMR}$  (500 MHz,  $\text{C}_2\text{D}_2\text{Cl}_4$ , 75 °C):  $\delta$  5.81 (dd, 1H),  $\delta$  5.01 (m, 2H),  $\delta$  0.68-1.72 (m, 800H).

**sPP-CH<sub>2</sub>CHBrCH<sub>2</sub>Br.** A 20 mL scintillation vial was charged with sPP-CH<sub>2</sub>CH=CH<sub>2</sub> (0.10 g, 0.017 mmol) and CH<sub>2</sub>Cl<sub>2</sub> (8 mL). The vial was heated to 45 °C to dissolve as much of the polymer as possible. The mixture was cooled to room temperature and bromine (0.09 mL, 1.67 mmol) was syringed into the vial. After stirring at room temperature for 30 minutes, the mixture was poured into saturated sodium thiosulfate and stirred for an additional 30 minutes. The polymer was collected, dissolved in hot toluene and filtered through a glass frit layered with silica, alumina, and Celite. The toluene was removed and the polymer was dried in vacuo to constant weight (0.06 g, 60% yield).  $M_n(\text{GPC}) = 5,500 \text{ g/mol}$ ,  $M_w/M_n = 1.80$ ,  $M_n(^1\text{H NMR}) = 6,200 \text{ g/mol}$ .  $^1\text{H NMR}$  (500 MHz,  $\text{C}_2\text{D}_2\text{Cl}_4$ , 75 °C):  $\delta$  4.27 (m, 1H),  $\delta$  3.89 (m, 1H),  $\delta$  3.69 (m, 1H),  $\delta$  0.68-1.72 (m, 880H).

**sPP-CH<sub>2</sub>CH(O)CH<sub>2</sub>.** An oven-dried Schlenk tube was cooled under vacuum and charged with sPP-CH<sub>2</sub>CH=CH<sub>2</sub> (0.25 g, 0.042 mmol). Dry toluene (10 mL) was cannulated into the tube and the mixture was heated to 45 °C to dissolve the polymer. The solution was cooled to room temperature and *meta*-chloroperoxybenzoic acid (0.22 g, 1.25 mmol) was added to the flask. After stirring for 7 days at room temperature, the mixture was poured into copious methanol. The polymer was collected, dissolved in hot toluene and filtered through a glass frit layered with silica, alumina, and Celite. The toluene was removed and the polymer was dried in vacuo to constant weight (0.23 g, 92% yield).  $M_n(\text{GPC}) = 5,000 \text{ g/mol}$ ,  $M_w/M_n = 1.86$ ,  $M_n(^1\text{H NMR}) = 6,100 \text{ g/mol}$ .  $^1\text{H NMR}$  (500 MHz,  $\text{C}_2\text{D}_2\text{Cl}_4$ , 75 °C):  $\delta$  2.93 (m, 1H),  $\delta$  2.74 (m, 1H),  $\delta$  2.42 (m, 1H),  $\delta$  0.68-1.72 (m, 880H).

**sPP-CH<sub>2</sub>CH(OH)CH<sub>3</sub>.** An oven-dried Schlenk tube was cooled under vacuum and charged with sPP-CH<sub>2</sub>CH(O)CH<sub>2</sub> (0.10 g, 0.017 mmol) and LiAlH<sub>4</sub> (0.007 g, 0.17 mmol). Dry THF (10 mL) was cannulated into the tube and the mixture was heated to 60 °C. After 12 hours, the mixture was cooled to 0 °C and quenched with copious methanol. The polymer was collected, dissolved in hot toluene and filtered through a glass frit layered with silica, alumina, and Celite. The toluene was removed and the polymer was dried in vacuo to constant weight (0.08 g, 80% yield).  $M_n(\text{GPC}) = 5,000$  g/mol,  $M_w/M_n = 1.86$ ,  $M_n(^1\text{H NMR}) = 5,400$  g/mol.  $^1\text{H NMR}$  (500 MHz, C<sub>2</sub>D<sub>2</sub>Cl<sub>4</sub>, 75 °C):  $\delta$  3.88 (m, 1H),  $\delta$  0.68-1.72 (m, 780H).

**sPP-(CH<sub>2</sub>)<sub>3</sub>OH.** An oven-dried 1 L round bottom flask was cooled under vacuum and charged with sPP-CH<sub>2</sub>CH=CH<sub>2</sub> (20.0 g, 3.33 mmol). Toluene or THF (500 mL) was cannulated into the flask and the mixture was heated to 45 °C. After 15 minutes, the 9-BBN (23.3 mL, 11.66 mmol) was added drop wise to the flask and the solution was heated to 65 °C. The mixture was cooled to the prescribed oxidation temperature after 3 hours. A sodium hydroxide solution (1.5 M in H<sub>2</sub>O, 49.95 mmol) was added followed immediately by a hydrogen peroxide solution (1.22 M in THF, 36.63 mmol). After a given amount of time, the mixture was poured into copious methanol. The polymer was collected, dissolved in hot toluene and filtered through a glass frit layered with silica, alumina, and Celite. The toluene was removed and the polymer was dried in vacuo to constant weight (19.0 g, 95% yield).  $M_n(\text{GPC}) = 4,600$  g/mol,  $M_w/M_n = 1.90$ ,  $M_n(^1\text{H NMR}) = 6,400 - 30,000$  g/mol (depending on oxidation temperature).  $^1\text{H NMR}$  (500 MHz, C<sub>2</sub>D<sub>2</sub>Cl<sub>4</sub>, 75 °C):  $\delta$  3.61 (q, 2H),  $\delta$  0.68-1.72 (m, 900 - 3400H).

**sPP-(CH<sub>2</sub>)<sub>3</sub>OCOC<sub>6</sub>H<sub>5</sub>.** An oven-dried Schlenk tube was cooled under vacuum and charged with sPP-(CH<sub>2</sub>)<sub>3</sub>OH (0.50 g, 0.083 mmol). Tetrachloroethane (1 mL) and triethylamine (0.01 mL, 0.083 mmol) were syringed into the flask followed by the

benzoyl chloride (0.01 mL, 0.083 mmol). The reaction mixture was heated to 120 °C. After 2 days, the solution was cooled to room temperature and the polymer was precipitated with methanol (100 mL). The polymer was collected, dissolved in hot toluene and filtered through a glass frit layered with silica, alumina, and Celite. The toluene was removed and the polymer was dried in vacuo to constant weight (0.30 g, 60% yield).  $M_n(\text{GPC}) = 6,000 \text{ g/mol}$ ,  $M_w/M_n = 1.60$ ,  $M_n(^1\text{H NMR}) = 11,000 \text{ g/mol}$ .  $^1\text{H NMR}$  (500 MHz,  $\text{C}_2\text{D}_2\text{Cl}_4$ , 75 °C):  $\delta$  8.04 (d, 2H),  $\delta$  7.57 (t, 1H),  $\delta$  7.45 (t, 2H),  $\delta$  4.31 (t, 2H),  $\delta$  0.68-1.72 (m, 1500H).

**sPP-(CH<sub>2</sub>)<sub>3</sub>OCOC(CH<sub>2</sub>)CH<sub>3</sub>.** An oven-dried Schlenk tube was cooled under vacuum and charged with sPP-(CH<sub>2</sub>)<sub>3</sub>OH (0.50 g, 0.083 mmol). Dry toluene (50 mL) was cannulated into the flask and heated until the polymer was in solution. The mixture was cooled to room temperature. Triethylamine (0.11 mL, 0.83 mmol) was syringed into the flask followed by methacryloyl chloride (0.08 mL, 0.83 mmol). The mixture continued to stir at room temperature for 24 hours. The polymer was precipitated with copious methanol, collected, dissolved in hot toluene and filtered through a glass frit layered with silica, alumina, and Celite. The toluene was removed and the polymer was dried in vacuo to constant weight (0.49 g, 98% yield).  $M_n(^1\text{H NMR}) = 34,000 \text{ g/mol}$ .  $^1\text{H NMR}$  (500 MHz,  $\text{C}_2\text{D}_2\text{Cl}_4$ , 75 °C):  $\delta$  6.10 (s, 1H),  $\delta$  5.55 (s, 1H),  $\delta$  4.20 (t, 2H),  $\delta$  4.14 (m, 5H),  $\delta$  0.68-1.72 (m, 4900H).

**sPP-(CH<sub>2</sub>)<sub>3</sub>OCOCHCH<sub>2</sub>.** An oven-dried Schlenk adapted round bottom flask was cooled under vacuum and charged with sPP-(CH<sub>2</sub>)<sub>3</sub>OH (2.0 g, 0.33 mmol). Dry toluene (250 mL) was cannulated into the flask and the mixture was heated to 45 °C to dissolve the polymer. The solution was cooled to room temperature and triethylamine (0.23 mL, 1.67 mmol) was syringed into the flask followed immediately by acryloyl chloride (0.13 mL, 1.67 mmol). After stirring for 12 hours, the mixture was poured into copious methanol. The polymer was collected, dissolved in hot toluene and

filtered through a glass frit layered with silica, alumina, and Celite. The toluene was removed and the polymer was dried in vacuo to constant weight (1.96 g, 98% yield).  $M_n(\text{GPC}) = 5,500 \text{ g/mol}$ ,  $M_w/M_n = 2.60$ ,  $M_n(^1\text{H NMR}) = 9,500 \text{ g/mol}$ .  $^1\text{H NMR}$  (500 MHz,  $\text{C}_2\text{D}_2\text{Cl}_4$ , 75 °C):  $\delta$  6.38 (dd, 1H),  $\delta$  6.15 (dd, 1H),  $\delta$  5.80 (dd, 1H),  $\delta$  4.20 (t, 2H),  $\delta$  0.68-1.72 (m, 11350H).

**sPP-(CH<sub>2</sub>)<sub>3</sub>OSO<sub>3</sub>C<sub>6</sub>H<sub>4</sub>CH<sub>3</sub>.** An oven-dried 1 L round bottom flask was cooled under vacuum and charged with sPP-(CH<sub>2</sub>)<sub>3</sub>OH (30.0 g, 5.0 mmol), *para*-toluenesulfonyl chloride (28.6 g, 150 mmol), and chloroform (500 mL). Pyridine (12.1 mL, 150 mmol) was added by syringe and the mixture was heated to 60 °C. After 2 days, the mixture was cooled to room temperature and the polymer was precipitated in methanol (1 L). The polymer was collected, dissolved in hot toluene and filtered through a glass frit layered with silica, alumina, and Celite. The toluene was removed and the polymer was dried in vacuo to constant weight (20.3 g, 68% yield).  $M_n(\text{GPC}) = 5,000 \text{ g/mol}$ ,  $M_w/M_n = 1.84$ ,  $M_n(^1\text{H NMR}) = 9,000 \text{ g/mol}$ .  $^1\text{H NMR}$  (500 MHz,  $\text{C}_2\text{D}_2\text{Cl}_4$ , 75 °C):  $\delta$  7.80 (d, 2H),  $\delta$  7.37 (d, 2H),  $\delta$  4.04 (t, 2H),  $\delta$  3.54 (t, 2H),  $\delta$  2.46 (s, 3H),  $\delta$  0.68-1.72 (m, 1300H).

**sPP-(CH<sub>2</sub>)<sub>3</sub>N<sub>3</sub>.** An oven-dried 1L round bottom flask was cooled under vacuum and charged with sPP-(CH<sub>2</sub>)<sub>3</sub>OSO<sub>3</sub>C<sub>6</sub>H<sub>4</sub>CH<sub>3</sub> (19.5 g, 3.25 mmol) and sodium azide (2.11 g, 32.5 mmol). Toluene (100 mL) and DMF (100 mL) were cannulated into the flask and the mixture was heated to 100 °C. After 3 days, the mixture was cooled to room temperature and the polymer was precipitated in water (1 L). The polymer was collected, dissolved in hot toluene and filtered through a glass frit layered with silica, alumina, and Celite. The toluene was removed and the polymer was dried in vacuo to constant weight (14.2 g, 73% yield).  $M_n(\text{GPC}) = 7,700 \text{ g/mol}$ ,  $M_w/M_n = 1.48$ ,  $M_n(^1\text{H NMR}) = 13,000 \text{ g/mol}$ .  $^1\text{H NMR}$  (500 MHz,  $\text{C}_2\text{D}_2\text{Cl}_4$ , 75 °C):  $\delta$  3.26 (d, 2H),  $\delta$  0.68-1.72 (m, 2000H).

**sPP-(CH<sub>2</sub>)<sub>3</sub>CHN<sub>3</sub>C<sub>6</sub>H<sub>5</sub>.** An oven-dried Schlenk tube was cooled under vacuum and charged with sPP-(CH<sub>2</sub>)<sub>3</sub>N<sub>3</sub> (0.30 g, 0.05 mmol), phenyl acetylene (0.051 g, 0.50 mmol), and copper iodide (0.01 g, 0.05 mmol). Toluene (3 mL) and DMSO (3 mL) were syringed into the flask. The mixture was heated to 80 °C. After 18 hours, the solution was cooled to room temperature and the polymer was precipitated with methanol (100 mL). The polymer was collected, dissolved in hot toluene and filtered through a glass frit layered with silica, alumina, and Celite. The toluene was removed and the polymer was dried in vacuo to constant weight (0.22 g, 73% yield).  $M_n(\text{GPC}) = 6,700 \text{ g/mol}$ ,  $M_w/M_n = 1.70$ ,  $M_n(^1\text{H NMR}) = 33,000 \text{ g/mol}$ .  $^1\text{H NMR}$  (500 MHz, C<sub>2</sub>D<sub>2</sub>Cl<sub>4</sub>, 75 °C):  $\delta$  7.83 (d, 2H),  $\delta$  7.73 (s, 1H),  $\delta$  7.44 (t, 2H),  $\delta$  7.35 (t, 1H),  $\delta$  4.37 (t, 2H),  $\delta$  0.68-1.72 (m, 4800H).

**sPP-(CH<sub>2</sub>)<sub>3</sub>NH<sub>2</sub>.** An oven-dried 300 mL Schlenk adapted round bottom flask was cooled under vacuum and charged with sPP-(CH<sub>2</sub>)<sub>3</sub>N<sub>3</sub> (4.0 g, 0.67 mmol) and LiAlH<sub>4</sub> (0.13 g, 3.33 mmol). THF (150 mL) was cannulated into the flask and the mixture was heated to 60 °C. After 4 hours, the solution was cooled to 0 °C and methanol was added slowly to the flask. The polymer was collected, dissolved in hot toluene and filtered through a glass frit layered with silica, alumina, and Celite. The toluene was removed and the polymer was dried in vacuo to constant weight (3.7 g, 92% yield).  $M_n(\text{GPC}) = 8,300 \text{ g/mol}$ ,  $M_w/M_n = 1.50$ ,  $M_n(^1\text{H NMR}) = 15,000 \text{ g/mol}$ .  $^1\text{H NMR}$  (500 MHz, C<sub>2</sub>D<sub>2</sub>Cl<sub>4</sub>, 75 °C):  $\delta$  2.65 (d, 2H),  $\delta$  0.68-1.72 (m, 2000H).

**sPP-(CH<sub>2</sub>)<sub>3</sub>NHCOC<sub>6</sub>H<sub>5</sub>.** An oven-dried Schlenk tube was cooled under vacuum and charged with sPP-(CH<sub>2</sub>)<sub>3</sub>NH<sub>2</sub> (0.15 g, 0.025 mmol). Toluene (1 mL) and triethylamine (0.035 mL, 0.25 mmol) were syringed into the flask followed by the benzoyl chloride (0.03 mL, 0.25 mmol). The reaction mixture was then heated to 100 °C. After 12 hours, the solution was cooled to room temperature and the polymer was precipitated with methanol (100 mL). The polymer was collected, dissolved in hot toluene and

filtered through a glass frit layered with silica, alumina, and Celite. The toluene was removed and the polymer was dried in vacuo to constant weight (0.12 g, 80% yield).  $M_n(\text{GPC}) = 6,400 \text{ g/mol}$ ,  $M_w/M_n = 1.72$ ,  $M_n(^1\text{H NMR}) = 18,000 \text{ g/mol}$ .  $^1\text{H NMR}$  (500 MHz,  $\text{C}_2\text{D}_2\text{Cl}_4$ , 75 °C):  $\delta$  7.42 (d, 2H),  $\delta$  7.28 (t, 1H),  $\delta$  7.19 (t, 2H),  $\delta$  3.98 (t, 2H),  $\delta$  0.68-1.72 (m, 2600H).

## REFERENCES

- (1) Lopez, R. G.; D'Agosto, F.; Boisson, C. *Prog. Polym. Sci.* **2007**, *32*, 419-454.
- (2) Chung, T. C. *Prog. Polym. Sci.* **2002**, *27*, 39-85.
- (3) Avella, M.; Laurienzon, P.; Malinconico, M.; Martuscelli, E.; Volpe, M. G., Functionalized Polyolefins: Synthesis and Application in Blends and Composites. In *Handbook of Polyolefins*, 2nd ed.; Vasile, C., Ed. Marcel Dekker, Inc.: New York, **2000**; pp 723-771.
- (4) Zhou, X.; Dai, G.; Guo, W.; Lin, Q. *J. Appl. Poly. Sci.* **2000**, *76*, 1359-1365.
- (5) Vasile, C., General Survey of the Properties of Polyolefins. In *Handbook of Polyolefins*, 2nd ed.; Vasile, C., Ed. Marcel Dekker Inc.: New York, **2000**; pp 401-412.
- (6) Boffa, L. S.; Novak, B. M. *Chem. Rev.* **2000**, *100*, 1479-1493.
- (7) Nakamura, A.; Ito, S.; Nozaki, K. *Chem. Rev.* **2009**, *109*, 5215-5244.
- (8) Chen, E. Y.-X. *Chem. Rev.* **2009**, *109*, 5157-5214.
- (9) Guan, Z.; Popeney, C. S. *Top. Organomet. Chem.* **2008**, *26*, 179-220.
- (10) Goodall, B. L. *Top. Organomet. Chem.* **2009**, *26*, 159-178.
- (11) Sen, A.; Borkar, S. *J. Organomet. Chem.* **2007**, *692*, 3291-3299.
- (12) Yang, X.-H.; Liu, C.-R.; Wang, C.; Sun, X.-L.; Guo, Y.-H.; Wang, X.-K.; Wang, Z.; Xie, Z.; Tang, Y. *Angew. Chem. Int. Ed.* **2009**, *48*, 8099-8102.
- (13) Stojcevic, G.; Baird, M. C. *Dalton Trans.* **2009**, 8864-8877.
- (14) Sahre, K.; Schulze, U.; Eichhorn, K.-J.; Voit, B. *Macromol. Mater. Eng.* **2009**, *294*, 250-255.
- (15) Yasuda, H.; Desurmont, G. *Polym. Int.* **2004**, *53*, 1017-1024.

- (16) Popeney, C. S.; Camacho, D. H.; Guan, Z. *J. Am. Chem. Soc.* **2007**, *129*, 10062-10063.
- (17) Chen, G.; Ma, X. S.; Guan, Z. *J. Am. Chem. Soc.* **2003**, *125*, 6697-6704.
- (18) Deubel, D. V.; Ziegler, T. *Organometallics* **2002**, *21*, 4432-4441.
- (19) Ittel, S. D.; Johnson, L. K.; Brookhart, M. *Chem. Rev.* **2000**, *100*, 1169-1203.
- (20) Johnson, L. K.; Mecking, S.; Brookhart, M. *J. Am. Chem. Soc.* **1996**, *118*, 267-268.
- (21) Verso, F. L.; Likos, C. N. *Polymer* **2008**, *49*, 1425-1434.
- (22) Iha, R. K.; Wooley, K. L.; Nystrom, A. M.; Burke, D. J.; Kade, M. J.; Hawker, C. J. *Chem. Rev.* **2009**, *109*, 5620-5686.
- (23) Petzetakis, N.; Pitsikalis, M.; Hadjichristidis, N. *J. Poly. Sci., Part A: Poly. Chem.* **2010**, *48*, 1092-1103.
- (24) Inglis, A. J.; Paulohrl, T.; Barner-Kowollik, C. *Macromolecules* **2010**, *43*, 33-36.
- (25) Bellas, V.; Rehahn, M. *Macromol. Chem. Phys.* **2009**, *210*, 320-330.
- (26) Li, M.; De, P.; Gondi, S. R.; Sumerlin, B. S. *J. Poly. Sci., Part A: Poly. Chem.* **2008**, *46*, 5093-5100.
- (27) Dag, A.; Durmaz, H.; Sirkecioglu, O.; Hizal, G.; Tunca, U. *J. Poly. Sci., Part A: Poly. Chem.* **2009**, *47*, 2344-2351.
- (28) Ohno, S.; Gao, H.; Cusick, B.; Kowalewski, T.; Matyjaszewski, K. *Macromol. Chem. Phys.* **2009**, *210*, 421-430.
- (29) Dag, A.; Durmaz, H.; Tunca, U.; Hizal, G. *J. Poly. Sci., Part A: Poly. Chem.* **2009**, *47*, 178-187.
- (30) Gao, H.; Matyjaszewski, K. *J. Am. Chem. Soc.* **2007**, *129*, 11828-11834.
- (31) Urbani, C. N.; Bell, C. A.; Lonsdale, D. E.; Whittaker, M. R.; Monteiro, M. J. *Macromolecules* **2007**, *40*, 7056-7059.

- (32) Hirao, A.; Hayashi, M.; Loykulnant, S.; Sugiyama, K.; Ryu, S. W.; Haraguchi, N.; Matsuo, A.; Higashihara, T. *Prog. Polym. Sci.* **2005**, *30*, 111-1182.
- (33) Hirao, A.; Tokuda, Y. *Macromolecules* **2003**, *36*, 6081-6086.
- (34) Lammens, M.; Fournier, D.; Fijten, M. W. M.; Hoogenboom, R.; Prez, F. D. *Macromol. Rapid Commun.* **2009**, *30*, 2049-2055.
- (35) Muehlebach, A.; Rime, F. *J. Poly. Sci., Part A: Poly. Chem.* **2003**, *41*, 3425-3439.
- (36) Mowery, D. M.; Assink, R. A.; Derzon, D. K.; Klamo, S. B.; Clough, R. L.; Bernstein, R. *Macromolecules* **2005**, *38*, 5035-5046.
- (37) Hagiwara, T.; Saitoh, H.; Tobe, A.; Sasaki, D.; Yano, S.; Sawaguchi, T. *Macromolecules* **2005**, *38*, 10373-10378.
- (38) Shiono, T.; Hiroki, K.; Soga, K. *Macromolecules* **1994**, *27*, 2635-2637.
- (39) Chung, T. C.; Xu, G.; Lu, Y.; Hu, Y. *Macromolecules* **2001**, *34*, 8040-8050.
- (40) Kaneyoshi, H.; Inoue, Y.; Matyjaszewski, K. *Macromolecules* **2005**, *38*, 5425-5435.
- (41) Hagihara, H.; Ishihara, T.; Ban, H. T.; Shiono, T. *J. Poly. Sci.: Part A: Poly. Chem.* **2008**, *46*, 1738-1747.
- (42) Lin, W.; Dong, J.; Chung, T. C. M. *Macromolecules* **2008**, *41*, 8452-8457.
- (43) Yi, Q.; Fan, G.; Wen, X.; Dong, J.-Y.; Han, C. C. *Macromol. React. Eng.* **2009**, *3*, 91-100.
- (44) Briquel, R.; Mazzolini, J.; Le Bris, T.; Boyron, O.; Boisson, F.; Delolme, F.; D'Agosto, F.; Boisson, C.; Spitz, R. *Angew. Chem. Int. Ed.* **2008**, *47*, 9311-9313.
- (45) Doi, Y.; Hizal, G.; Soga, K. *Makromol. Chem.* **1987**, *188*, 1273-1279.
- (46) Doi, Y.; Keii, T. *Adv. Polym. Sci* **1986**, *73/74*, 201.
- (47) Doi, Y.; Murata, M.; Soga, K. *Makromol. Chem., Rapid Commun.* **1984**, *5*, 811-814.

- (48) Doi, Y.; Tokuhira, N.; Suzuki, S.; Soga, K. *Makromol. Chem., Rapid Commun.* **1987**, *8*, 285-290.
- (49) Doi, Y.; Watanabe, Y.; Ueki, S.; Soga, K. *Makromol. Chem., Rapid Commun.* **1983**, *4*, 533-537.
- (50) Gottfried, A. C.; Brookhart, M. *Macromolecules* **2003**, *36*, 3085-3100.
- (51) Ueki, S.; Furuhashi, H.; Murakami, N.; Murata, M.; Doi, Y. *Science and Technology in Catalysis* **1995**, *92*, 359-362.
- (52) Makio, H.; Fujita, T. *Macromol. Rapid Commun.* **2007**, *28*, 698-703.
- (53) Kuo, J.-C.; Lin, W.-F.; Yu, C.-H.; Tsai, J.-C.; Wang, T.-C.; Chung, T.-M.; Ho, R.-M. *Macromolecules* **2008**, *41*, 7967-7977.
- (54) Lin, W.-F.; Tsai, J.-C. *J. Poly. Sci.: Part A: Poly. Chem.* **2008**, *46*, 2167-2176.
- (55) Lin, W.-F.; Hsiao, T.-J.; Tsai, J.-C.; Chung, T.-M.; Ho, R.-M. *J. Poly. Sci.: Part A: Poly. Chem.* **2008**, *46*, 4843-4856.
- (56) Reddy, K. R.; Kumar, B.; Rana, S.; Tevtia, A. K.; Singh, R. P. *J. Appl. Poly. Sci.* **2007**, *104*, 1596-1602.
- (57) Lehmus, P.; Kokko, E.; Leino, R.; Luttikhedde, H. J. G.; Rieger, B.; Seppala, J. V. *Macromolecules* **2000**, *33*, 8534-8540.
- (58) Kojoh, S.; Tsutsui, T.; Kioka, M.; Kashiwa, N. *Polym. Journal* **1999**, *31*, 332-335.
- (59) Koo, K.; Marks, T. J. *J. Am. Chem. Soc.* **1999**, *121*, 8791-8802.
- (60) Kaneyoshi, H.; Matyjaszewski, K. *J. Appl. Poly. Sci.* **2007**, *105*, 3-13.
- (61) Shiono, T.; Kurosawa, H.; Ishida, O.; Soga, K. *Macromolecules* **1993**, *26*, 2085-2089.
- (62) Shiono, T.; Soga, K. *Macromolecules* **1992**, *25*, 3356-3361.
- (63) Weng, W.; Markel, E. J.; Dekmezian, A. H. *Macromol. Rapid Commun.* **2000**, *21*, 1103-1107.

- (64) Kaneko, H.; Matsugi, T.; Kawahara, N.; Matsuo, S.; Kojoh, S.; Kashiwa, N. *Kinetics and Catalysis* **2006**, *47*, 227-233.
- (65) Kawahara, N.; Kojoh, S.; Matsuo, S.; Kaneko, H.; Matsugi, T.; Toda, Y.; Mizuno, A.; Kashiwa, N. *Polymer* **2004**, *45*, 2883-2888.
- (66) Resconi, L.; Cavallo, L.; Fait, A.; Piemontesi, F. *Chem. Rev.* **2000**, *100*, 1253-1345.
- (67) Resconi, L.; Camurati, I.; Sudmeijer, O. *Top. Catal.* **1999**, *7*, 145-163.
- (68) Lahelin, M.; Kokko, E.; Lehmus, P.; Pitkanen, P.; Lofgren, B.; Seppala, J. *Macromol. Chem. Phys.* **2003**, *204*, 1323-1337.
- (69) Resconi, L.; Jones, R. L.; Rheingold, A. L.; Yap, G. P. A. *Organometallics* **1996**, *15*, 998-1005.
- (70) Cherian, A. E.; Lobkovsky, E. B.; Coates, G. W. *Macromolecules* **2005**, *38*, 6259-6268.
- (71) Ye, Z.; Zhu, S. *J. Poly. Sci., Part A: Poly. Chem.* **2003**, *41*, 1152-1159.
- (72) Britovsek, G. J. P.; Gibson, V. C.; Kimberley, B. S.; Maddox, P. J.; McTavish, S. J.; Solan, G. A.; White, A. J. P.; Williams, D. J. *Chem. Commun.* **1998**, 849-850.
- (73) Pellicchia, C.; Mazzeo, M.; Pappalardo, D. *Macromol. Rapid Commun.* **1998**, *19*, 651-655.
- (74) Small, B. L.; Brookhart, M. *Macromolecules* **1999**, *32*, 2120-2130.
- (75) Hustad, P. D.; Tian, J.; Coates, G. W. *J. Am. Chem. Soc.* **2002**, *124*, 3614-3621.
- (76) Makio, H.; Kashiwa, N.; Fujita, T. *Adv. Synth. Catal.* **2002**, *344*, 477-493.
- (77) Mitani, M.; Saito, J.; Ishii, S.; Nakayama, Y.; Makio, H.; Matsukawa, N.; Matsui, S.; Mohri, J.; Furuyama, R.; Terao, H.; Bando, H.; Tanaka, H.; Fujita, T. *Chem. Rec.* **2004**, *4*, 137-158.
- (78) Tian, J.; Coates, G. W. *Angew. Chem. Int. Ed.* **2000**, *39*, 3626-3629.
- (79) Milano, G.; Fiorello, G.; Guerra, G.; Cavallo, L. *Macromol. Chem. Phys.* **2002**, *203*, 1564-1572.

- (80) Lamberti, M.; Gliubizzi, R.; Mazzeo, M.; Tedesco, C.; Pellicchia, C. *Macromolecules* **2004**, *37*, 276-282.
- (81) Talarico, G.; Busico, V.; Cavallo, L. *J. Am. Chem. Soc.* **2003**, *123*, 7172-7173.
- (82) Saito, J.; Mitani, M.; Onda, M.; Mohri, J. I.; Ishi, J. I.; Yoshida, Y.; Nakano, T.; Tanaka, H.; Matsugi, T.; Kojoh, S. I.; Kashiwa, N.; Fujita, T. *Macromol. Rapid Commun.* **2001**, *22*, 1072-1075.
- (83) Tian, J.; Hustad, P. D.; Coates, G. W. *J. Am. Chem. Soc.* **2001**, *123*, 5134-5135.
- (84) Mason, A. F.; Tian, J.; Hustad, P. D.; Lobkovsky, E. B.; Coates, G. W. *Isr. J. Chem* **2002**, *42*, 301-306.
- (85) Mitani, M.; Mohri, J.; Yoshida, Y.; Saito, J.; Ishii, S.; Tsuru, K.; Matsui, S.; Furuyama, R.; Nakano, T.; Tanaka, H.; Kojoh, S.; Matsugi, T.; Kashiwa, N.; Fujita, T. *J. Am. Chem. Soc.* **2002**, *124*, 3327-3336.
- (86) Mitani, M.; Furuyama, R.; Mohri, J.; Saito, J.; Ishii, S.; Terao, H.; Nakano, T.; Tanaka, H.; Fujita, T. *J. Am. Chem. Soc.* **2003**, *125*, 4293-4305.
- (87) Talarico, G.; Busico, V.; Cavallo, L. *Organometallics* **2004**, *23*, 5989-5993.
- (88) Mitani, M.; Nakano, T.; Fujita, T. *Chem. Eur. J.* **2003**, *9*, 2396-2403.
- (89) Lamberti, M.; Pappalardo, D.; Zambelli, A.; Pellicchia, C. *Macromolecules* **2002**, *35*, 658-663.
- (90) Mason, A. F.; Coates, G. W. *J. Am. Chem. Soc.* **2004**, *126*, 10798-10799.
- (91) Barton, T. J.; Tillman, N. *J. Am. Chem. Soc.* **1987**, *109*, 6711-6716.
- (92) Takaya, J.; Udagawa, S.; Kusama, H.; Iwasawa, N. *Angew. Chem. Int. Ed.* **2008**, *47*, 4906-4909.
- (93) Ahmed, E. K. *Heteroatom Chem.* **2003**, *14*, 201-207.
- (94) Bungard, C. J.; Morris, J. C. *J. Org. Chem.* **2002**, *67*, 2361-2364.
- (95) Wu, L.-C.; Yu, A.-F.; Zhange, M.; Liu, B.-H.; Chen, L.-B. *J. Appl. Poly. Sci.* **2004**, *92*, 1302-1309.

- (96) Ajiro, H.; Peretti, K.; Lobkovsky, E. B.; Coates, G. W. *Dalton Trans.* **2009**, 8828-8830.
- (97) Bertolini, T. *J. Chem. Ed.* **2002**, *79*, 828.
- (98) Patten, T. E.; Matyjaszewski, K. *Adv. Mater.* **1998**, *10*, 901-915.
- (99) Barbey, R.; Lavanant, L.; Paripovic, D.; Schuwer, N.; Sugnaux, C.; Tugulu, S.; Klok, H.-A. *Chem. Rev.* **2009**, *109*, 5437-5527.
- (100) Kabalka, G. W.; Yao, M.-L. *Synthesis* **2003**, *18*, 2890-2893.
- (101) Kamalraj, V. R.; Kannan, S. P. *J. Mol. Struct.* **2008**, *892*, 210-215.
- (102) Golas, P. L.; Matyjaszewski, K. *Chem. Soc. Rev.* **2010**, *39*, 1338-1354.
- (103) Barner-Kowollik, C.; Inglis, A. J. *Macromol. Chem. Phys.* **2009**, *210*, 987-992.
- (104) Nandivada, H.; Jiang, X.; Lahann, J. *Adv. Mater.* **2007**, *19*, 2197-2208.
- (105) Fournier, D.; Hoogenboom, R.; Schubert, U. S. *Chem. Soc. Rev.* **2007**, *36*, 1369-1380.
- (106) Moses, J. E.; Moorhouse, A. D. *Chem. Soc. Rev.* **2007**, *36*, 1249-1262.
- (107) Zheng, W.; Angelopoulos, M.; Epstein, A. J.; MacDiarmid, A. G. *Macromolecules* **1997**, *30*, 2952-2955.

## **Chapter 3**

Synthesis of Star, Miktoarm Star, and H-Polymers from  
Allyl-Terminated Syndiotactic Polypropylene

### 3.1 Introduction

The ability to control bulk polymer properties through manipulation of molecular weight, stereochemistry and polymer structure remains an overarching goal in the field of polymer chemistry. For single site olefin polymerization catalysts,<sup>1,2</sup> control over polymer stereochemistry ultimately results in polymers with dramatically different properties. For example, atactic polypropylene is an amorphous polymer ( $T_m = \text{none}$ ) with no stereoregularity observed for the pendant methyl groups, whereas syndiotactic and isotactic polypropylene are semicrystalline polymers ( $T_m = 148\text{ }^\circ\text{C}$  and  $165\text{ }^\circ\text{C}$ , respectively) with high degrees of stereoregularity present in both polymers.<sup>3</sup> In addition to stereochemical control, the regulation of molecular weight has been achieved using living polymerization methods, which are void of chain termination events. Cationic,<sup>4,5</sup> anionic,<sup>6</sup> radical<sup>7-9</sup> and coordination-insertion<sup>10,11</sup> polymerization systems have been extensively studied for their ability to produce polymers with controlled molecular weights. Beyond simple linear polymers, many of these controlled polymerization systems have been employed in the synthesis of well-defined branched polymers including star, miktoarm star and H-polymers (Figure 3.1).<sup>6,12-15</sup>

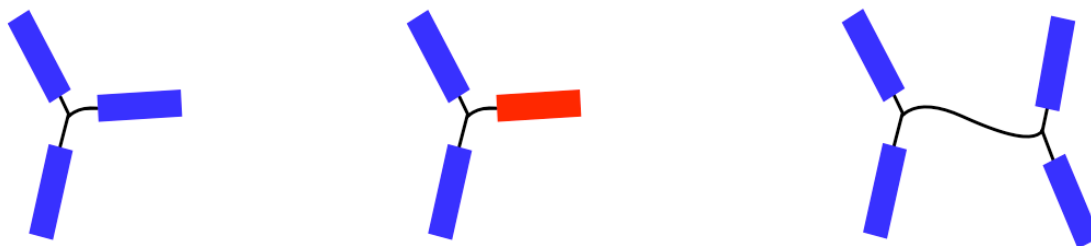


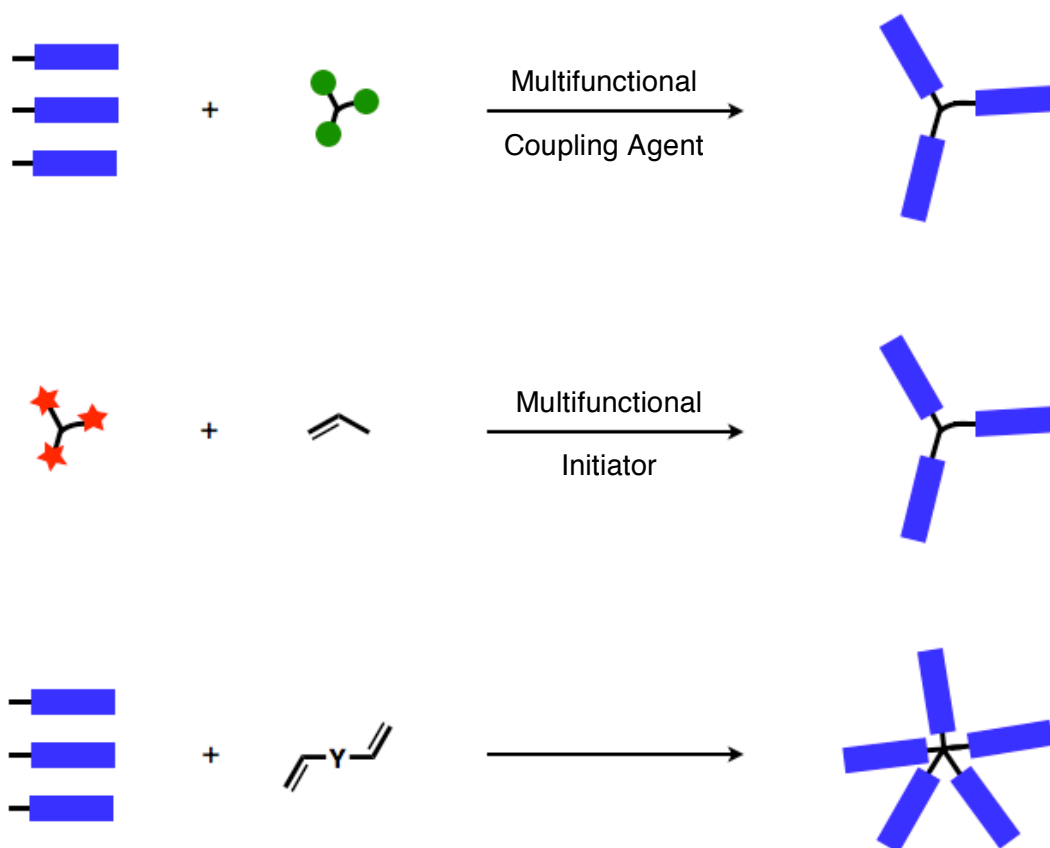
**Figure 3.1.** Representative structures of star (left), miktoarm star (middle) and H-polymers (right).

Interestingly, the presence of even a small amount of long-chain branching in a polymer has been shown to significantly affect the observed physical properties.<sup>16,17</sup> This is particularly evident when one compares low-density polyethylene (LDPE, Figure 3.2), a branched polymer, to its linear counterpart, high-density polyethylene (HDPE). While many physical properties of HDPE (e.g. tensile strength, toughness, hardness, etc.)<sup>16,17</sup> are superior to those of LDPE; it has been shown that LDPE is far easier to process than HDPE due to the presence of long-chain branches. The high melt strength of LDPE compared with HDPE makes LDPE an ideal polymer for applications such as blow molding, thermoforming and foaming.<sup>18,19</sup> These processing applications are also typically unsuccessful with conventional linear polypropylene, which also has poor melt strength.<sup>20-25</sup> However, the incorporation of long chain branches in polypropylene has been shown to increase the melt strength of the polymer up to ten times that of its linear analog.<sup>25</sup> It is quite apparent that the presence of long-chain branches in polyethylene and polypropylene improves processability, but the effects of this long-chain branching can be difficult to quantify in randomly branched systems such as LDPE. Therefore, the synthesis of well-defined branched polymer systems has been targeted by many different research groups in an effort to relate branching to observed polymer properties.<sup>26-38</sup>



**Figure 3.2.** Schematic representation of HDPE (left) and LDPE (right).

The simplest branched polymer is the star polymer, which consists of linear polymer chains emanating from a single core. Star polymers are typically synthesized through one of three different methods (Scheme 3.1): (1) coupling of functionalized polymer arms to a multifunctional core, (2) core out polymerization utilizing a multifunctional initiator or (3) through the addition of a dialkene at the end of the polymerization.<sup>6</sup> The first two synthesis methods result in well-defined star polymers with a known number of branches, whereas the final method results in star-like polymers with an average number of branches. In addition to basic star polymers, these synthesis methods have also been utilized in the production of more complex

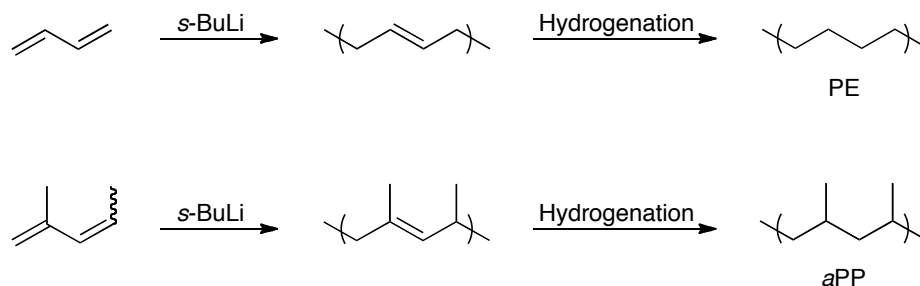


**Scheme 3.1.** General star polymer synthesis methods.

branched polymers, namely miktoarm stars and h-polymers. Miktoarm stars are simply star polymers containing chemical asymmetry, which includes star polymers with different molecular weight arms, end groups or arm compositions.<sup>39</sup> Slightly more complex in nature, H-polymers contain four linear polymers emanating from two cores (2 polymers per core) that are typically linked together by a polymer chain which may or may not be the same chemical composition as the arms.<sup>6,12</sup>

In 1948, Schaeffgen and Flory described the synthesis of the first star polymers through reaction of  $\epsilon$ -caprolactam with either cyclohexanone tetrapropionic or dicyclohexanone octacarboxylic acid to obtain the four or eight arm star, respectively.<sup>40</sup> Since that seminal discovery, anionic polymerization methods have lead the field in the production of well-defined branched polymers.<sup>6</sup> In particular, quenching living anionic polymerizations with multifunctional electrophiles such as chlorosilanes has resulted in the successful production of polystyrene,<sup>41-43</sup> polybutadiene<sup>44-46</sup> and polymethylmethacrylate<sup>47,48</sup> star polymers, to name a few. Anionic polymerization methods have also been utilized in the production of polyethylene model compounds with well-defined branching. For example, the anionic polymerization of butadiene (Scheme 3.2) resulting in 1,4-butadiene enchainments followed by hydrogenation results in linear polyethylene.<sup>45,46</sup> Quenching the butadiene polymerization with trichloromethylsilane and hydrogenating results in a three-arm polyethylene star suitable for the systematic study of long-chain branching in polyethylene. Similarly, the anionic polymerization of 2-methyl-1,3-pentadiene (Scheme 3.2) and subsequent hydrogenation of the polymer results in polypropylene.<sup>49</sup> Overall, the polymer hydrogenation is unselective and atactic polypropylene is obtained from the anionic polymerization. Quenching the anionic polymerization of 2-methyl-1,3-pentadiene with polystyrene functionalized chlorosilanes has been achieved and the resultant miktoarm star studied in detail.<sup>50,51</sup> Despite all of the advances in the

field, anionic polymerization techniques have not resulted in star polymers equipped with isotactic or syndiotactic polypropylene arms due to the unselective nature of the hydrogenation.



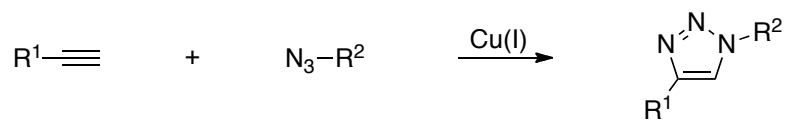
**Scheme 3.2.** Synthesis of polyethylene and atactic polypropylene using anionic polymerization/hydrogenation of butadiene and 2-methyl-1,3-pentadiene.

Stereoregular polypropylene can be obtained through the use of heterogeneous and homogenous single-site olefin polymerization catalysts, which offer remarkable control over polymer stereochemistry and molecular weight.<sup>1</sup> Unlike anionic polymerization, well-defined branched polyolefins can be challenging to produce using traditional metal mediated polymerizations. In 2008, Coates and coworkers reported the homo polymerization of allyl-terminated poly(ethylene-*co*-propylene) using a living nickel  $\alpha$ -diimine catalyst, which resulted in star-like polymers containing up to 16 branches per sample. Although not nominally stars, these polymers were shown to possess star-like conformations in dilute solutions.<sup>52</sup> In another example employing end-functionalized polymers, Kaneko and co-workers utilized methacryloyl terminated poly(ethylene-*co*-propylene) in free radical copolymerization with methyl methacrylate.<sup>53,54</sup> With this method, graft and star copolymers were produced containing poly(methyl methacrylate) backbones and poly(ethylene-*co*-propylene) branches. The first example of a well-defined star

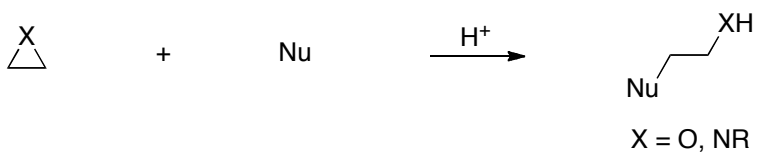
polyolefin produced using coordination-insertion polymerization came from Zhang and coworkers in 2009.<sup>55</sup> Utilizing a trinuclear  $\alpha$ -diimine Pd catalyst capable of living ethylene polymerization, a series of three-arm star polymers containing mostly linear polyethylene with some short chain branches was produced. There remain a limited number well-defined branched polyolefins produced from transition metal catalysts reported in the literature today. To the best of our knowledge, star polymers containing isotactic or syndiotactic polypropylene arms have not been reported to date.

Therefore, our efforts focused on the synthesis of star polymers containing syndiotactic polypropylene arms utilizing end-functionalized polymers and multifunctional coupling agents. For a detailed discussion on the synthesis of end-functionalized polyolefins, refer to chapter two. To synthesize well-defined branched materials, multifunctional compounds capable of efficient reaction with end-functionalized polymers were employed. In 2001, the term “click chemistry” was coined by Sharpless and coworkers<sup>56</sup> and describes reactions that are high yielding, modular, wide in scope and stereospecific.<sup>57-60</sup> In addition, simple reaction conditions that result in facile product isolation from inoffensive byproducts are required, making these reactions ideally suited for the production of branched polyolefins. Most click reactions fall into one of four reaction classes (Scheme 3.3): (1) cycloadditions of unsaturated species including 1,3-dipolar cycloadditions and Diels-Alder reactions (2) nucleophilic substitution, in particular ring-opening reactions of strained heterocyclic electrophiles such as aziridines and epoxides (3) non-aldol carbonyl chemistry for the formation of ureas, thioureas, aromatic heterocycles, hyrazones and amides (4) addition to carbon-carbon multiple bonds including epoxidation, dihydroxylation and aziridination. These high yielding reactions have been exploited in a variety of different areas including drug discovery,<sup>61</sup> biomedical applications<sup>62</sup> and polymeric

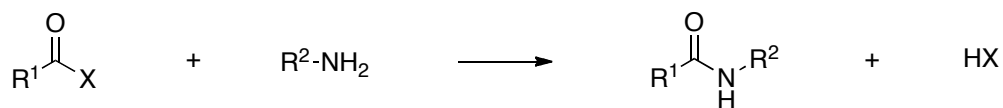
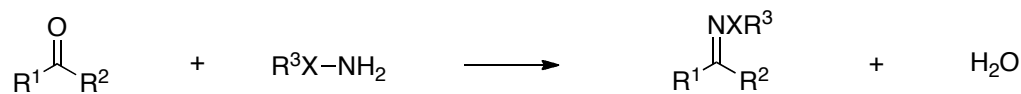
### 1. Cycloadditions



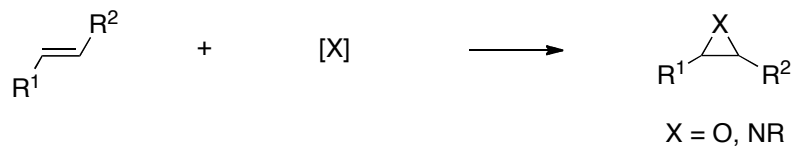
### 2. Nucleophilic Ring Opening



### 3. Carbonyl Chemistry



### 4. Carbon Multiple Bond Additions



**Scheme 3.3.** “Click” reactions in organic chemistry.

materials.<sup>63-74</sup> In particular, polymer chemists have utilized “click chemistry” to produce block, star, comb and graft polymers, many of which would be difficult to produce using traditional polymerization methods.<sup>63-74</sup>

Herein we report the synthesis of several branched polyolefin materials. Utilizing trifunctional-coupling agents along with end-functionalized syndiotactic polypropylene, three-arm star polymers containing different cores were produced. Di- and trifunctional coupling agents with orthogonal functionalities were also synthesized and employed in the production of diblock, triblock, miktoarm star and H-polymers. To the best of our knowledge, well-defined branched polymers of isotactic or syndiotactic polypropylene have not been reported to date. This represents the first report of star, miktoarm star and H-polymers bearing semicrystalline polypropylene.

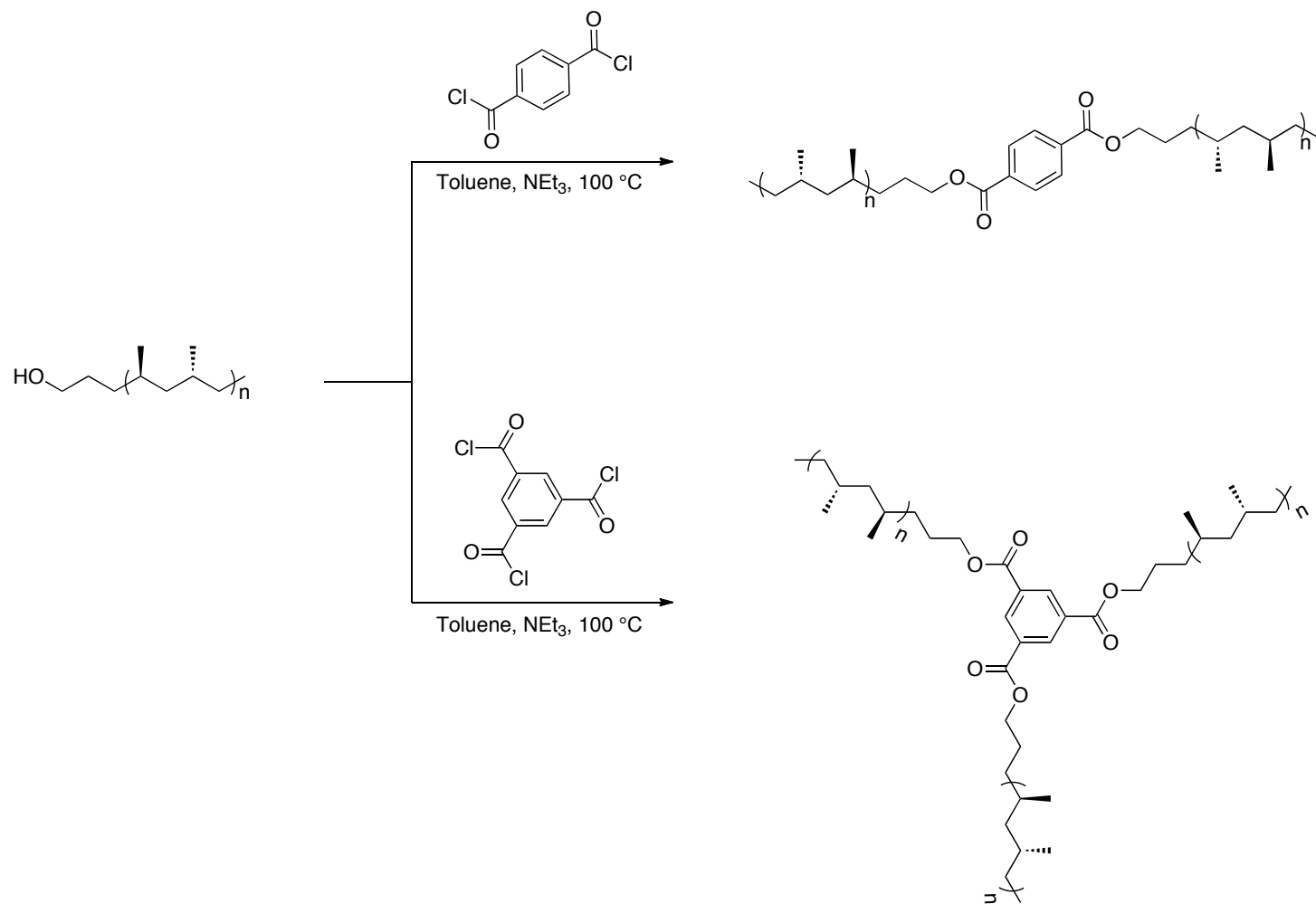
## **3.2 Results and Discussion**

### **3.2.1 Synthesis of Star Polymers Containing Ester Functional Groups**

Employing the end-functionalized polypropylene discussed in chapter two, several star polymers were produced. Initial investigations focused on using hydroxyl-terminated syndiotactic polypropylene (see section 2.2.4) in conjunction with acid chlorides to generate ester-functionalized polypropylene. In addition to a three-arm star polymer, model compounds were also produced. The reactivity of the hydroxyl-terminated polymer was initially tested with benzoyl chloride (Scheme 2.8), an acid chloride containing a single reactive functional group. Combining the polymer with benzoyl chloride, triethylamine and toluene at 100 °C resulted in conversion of the hydroxyl- to ester-terminated polypropylene. Examination of the <sup>1</sup>H NMR spectrum (Figure 3.3) revealed three resonances in the aromatic region ( $\delta$  8.04, 7.57 and 7.45 ppm) and a signal attributed to the protons adjacent to the ester ( $\delta$  4.31) as well as complete disappearance any starting material resonances. Under the same reaction

conditions described above (Scheme 3.4), two equivalents of the hydroxyl-terminated polymer were combined with a single equivalent of terephthaloyl chloride and a two-arm, linear polymer was obtained. By GPC (Figure 3.4), an increase in the molecular weight and a decrease in molecular weight distribution was observed for the two-arm polymer ( $M_n = 8,100$  g/mol,  $M_w/M_n = 1.59$ , Table 3.1) compared with the hydroxyl-terminated polymer ( $M_n = 4,600$  g/mol,  $M_w/M_n = 1.90$ ). According to polymer theory laid out by Schulz and Flory, star polymer molecular weight distribution will decrease as the number of arms linked together increases.<sup>40,75,76</sup> By relating the molecular weight distribution of the individual polymer arm ( $(M_w/M_n)_{\text{arm}}$ ) to the total number of arms ( $f$ ) a theoretical molecular weight distribution for the star polymer [ $(M_w/M_n)^{\text{Theo}}$ ] can be obtained (Equation 3.1). For the two-arm polymer, theory predicts a narrower molecular weight distribution ( $(M_w/M_n)^{\text{Theo}} = 1.45$ ) based on the molecular weight distribution of the starting hydroxyl-terminated polypropylene ( $(M_w/M_n)_{\text{arm}} = 1.90$ ). The presence of unfunctionalized polymer chains in the starting material explains the slight increase in molecular weight distribution compared to the theoretical value. Additionally, analysis of the  $^1\text{H}$  NMR spectrum revealed an aromatic signal ( $\delta$  8.10) along with a single resonance ( $\delta$  4.34) attributed to the protons adjacent to the ester. Finally, the three-arm star polymer was produced by combining the hydroxyl-terminated polypropylene with 1,3,5-benzenetricarbonyl trichloride, triethylamine and toluene at 100 °C. End-group analysis of the resultant polymer revealed a single aromatic resonance ( $\delta$  8.83) as well as a signal ( $\delta$  4.34) attributed to the protons adjacent to the ester. By GPC (Figure 3.4, Table 3.1), the molecular weight ( $M_n = 13,000$  g/mol) increased compared with the hydroxyl-terminated polymer, which is

**Equation 3.1.** 
$$(M_w/M_n)^{\text{Theo}} = 1 + [(M_w/M_n)_{\text{arm}} - 1]/f$$



**Scheme 3.4.** Synthesis of  $(\text{sPP}(\text{CH}_2)_3\text{OCO})_2\text{C}_6\text{H}_4$  (two-arms) and  $(\text{sPP}(\text{CH}_2)_3\text{OCO})_3\text{C}_6\text{H}_3$  (three-arms).

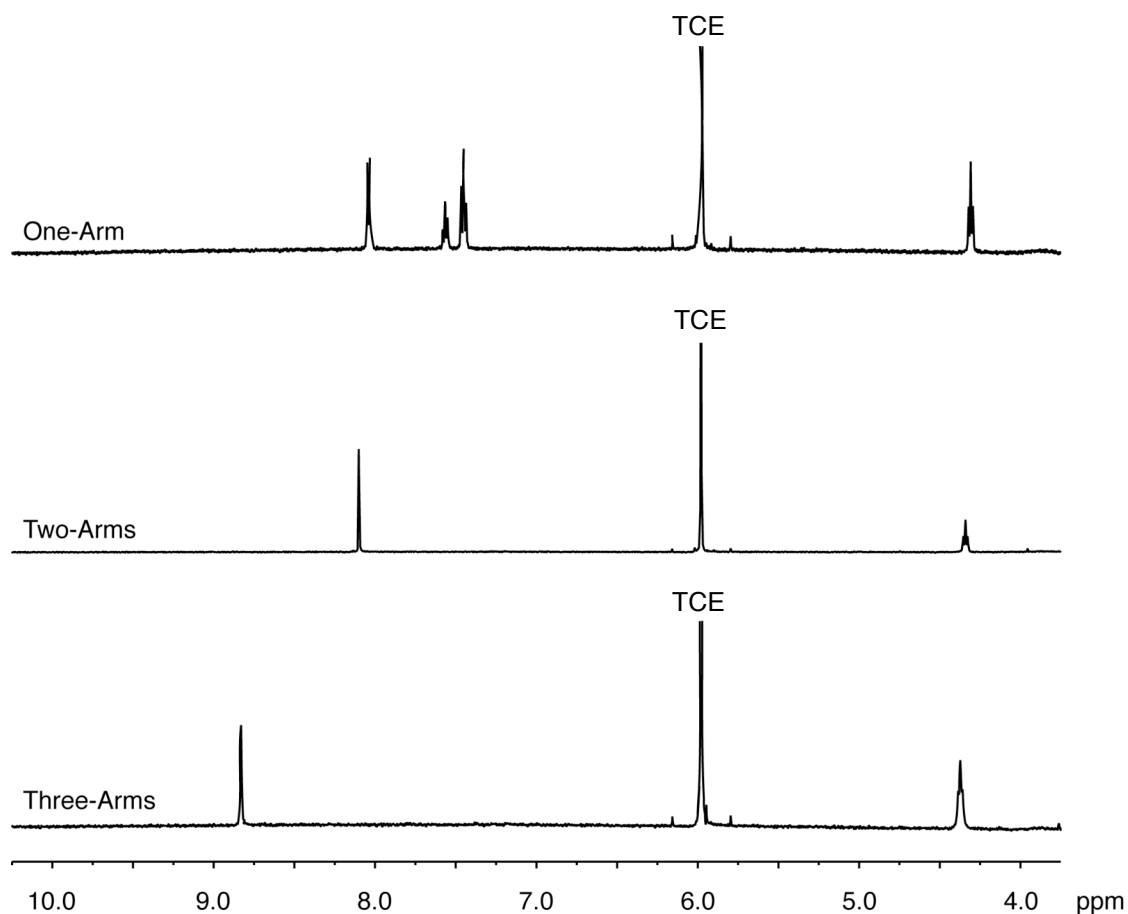


**Figure 3.3.**  $sPP(CH_2)_3OCOC_6H_5$  (one-arm),  $(sPP(CH_2)_3OCO)_2C_6H_4$  (two-arms) and  $(sPP(CH_2)_3OCO)_3C_6H_3$  (three-arms)  $^1H$  NMR spectra (500 MHz, 1,1,2,2-tetrachloroethane- $d_2$  (TCE), 75 °C).

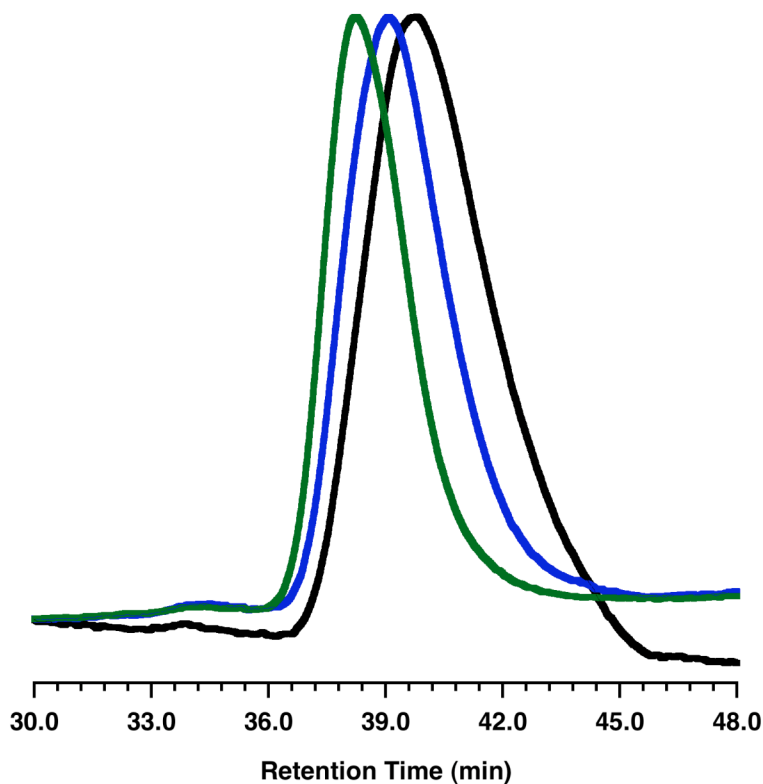
consistent with coupling three chains to a single core. Furthermore, the observed molecular weight distribution ( $M_w/M_n = 1.43$ ) compares well with the theoretical molecular weight distribution ( $(M_w/M_n)^{Theo} = 1.30$ ).

The thermal properties of the ester-functionalized polypropylenes (Table 3.1) were investigated in collaboration with Dr. Rufina Alamo and her graduate student, Syed Asif Abdullah, at Florida State University. Comparison of the crystallization temperatures for the linear and branched polymers reveals that the three-arm star

**Table 3.1.** Syndiotactic polypropylene with ester functionality characterization.

	Polymer	$f^a$	$M_n$ (g/mol) <sup>b</sup>	$M_w/M_n^b$	$M_w/M_n^{\text{Theo}}$	$T_c$ (°C) <sup>d</sup>	$T_m$ (°C) <sup>d</sup>	$\Delta H_m$ (J/g) <sup>d</sup>
1	sPP-OH	1	4,600	1.90	1.90 <sup>c</sup>	66	110	46
2	sPP-OCOC <sub>6</sub> H <sub>5</sub>	1	6,000	1.60	1.90 <sup>c</sup>	72	116	10
3	(sPP-OCO) <sub>2</sub> C <sub>6</sub> H <sub>4</sub>	2	8,100	1.59	1.45 <sup>c</sup>	58	109	44
4	(sPP-OCO) <sub>3</sub> C <sub>6</sub> H <sub>3</sub>	3	13,000	1.43	1.30 <sup>c</sup>	73	110	43

<sup>a</sup> total number of arms. <sup>b</sup> Molecular weight ( $M_n$ ) and molecular weight distribution ( $M_w/M_n$ ) were determined by gel permeation chromatography at 140 °C in 1,2,4-trichlorobenzene relative to polyethylene standards. <sup>c</sup> Theoretical molecular weight distribution ( $M_w/M_n^{\text{Theo}}$ ) was determined using the equation:  $1 + [(M_w/M_n)_{\text{arm}} - 1]/f$  where  $(M_w/M_n)_{\text{arm}}$  is the molecular weight distribution of sPP-OH (1.90). <sup>d</sup> Determined using differential scanning calorimetry (second heat).

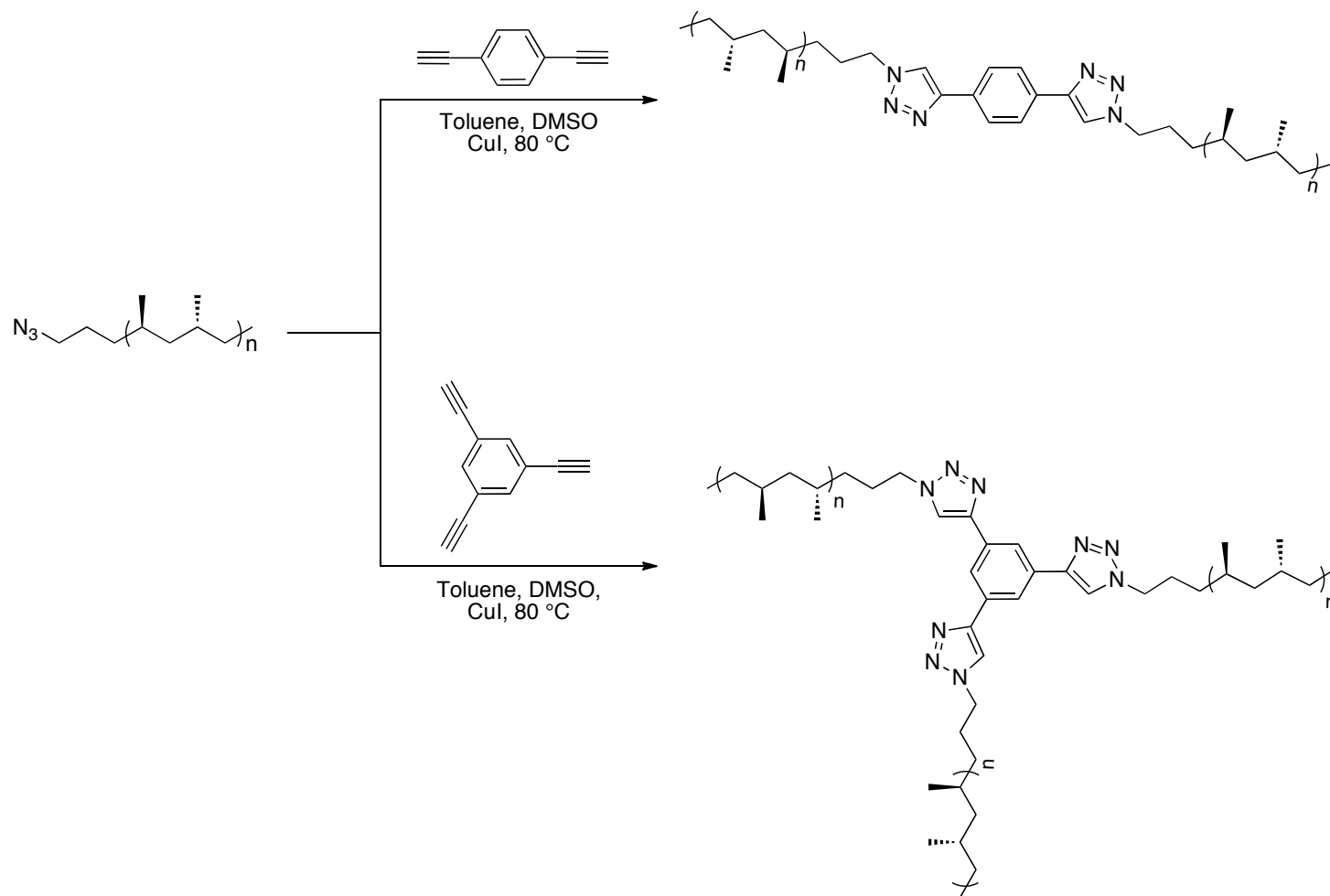
**Figure 3.4.** GPC chromatogram of sPP(CH<sub>2</sub>)<sub>3</sub>OH (black), (sPP(CH<sub>2</sub>)<sub>3</sub>OCO)<sub>2</sub>C<sub>6</sub>H<sub>4</sub> (blue) and (sPP(CH<sub>2</sub>)<sub>3</sub>OCO)<sub>3</sub>C<sub>6</sub>H<sub>3</sub> (green).

polymer ( $T_c = 73\text{ }^\circ\text{C}$ ) crystallized much faster than the hydroxyl-terminated polymer ( $T_c = 66\text{ }^\circ\text{C}$ ). Faster nucleation of the star polymer is a result of increased restrictions to crystal evolution due to the long-chain branched nature of the polymer. Interestingly, the two-arm linear polymer ( $T_c = 58\text{ }^\circ\text{C}$ ) actually displays a lower crystallization temperature than the hydroxyl-terminated polymer. It is possible that the presence of the benzene ring is enough of a perturbation in the chain to effect nucleation and growth. It is postulated that the effect of this perturbation is not large enough to override long-chain branching in the three-arm star polymer and thus increased crystallization is still observed. Branching was not found to have a dramatic effect on melting temperature with the three-arm polymer ( $T_m = 110\text{ }^\circ\text{C}$ ) exhibiting a nearly identical melting temperature to the hydroxyl-terminated polymer ( $T_m = 110\text{ }^\circ\text{C}$ ). Based on  $^1\text{H}$  NMR and GPC evidence as well as observed changes in crystallization behavior, a new three-arm star polymer along with one-arm and two-arm model compounds bearing syndiotactic polypropylene arms have been synthesized through reaction of an end-functionalized polymer with mono-, di- or tri-acid chlorides.

### 3.2.2 Synthesis of Star Polymers with Triazole Functional Groups

Utilizing a copper (I) catalyzed cycloaddition reaction of azide-terminated syndiotactic polypropylene (see section 2.2.7) and a trialkyne, a star polymer bearing triazole functionalities was produced. Several alkynes were investigated for their reactivity with the azide-terminated polypropylene. Initial reactivity was explored using phenylacetylene, a mono-alkyne (Scheme 2.11), along with azide-terminated syndiotactic polypropylene and copper iodide at  $80\text{ }^\circ\text{C}$ . The reaction did not proceed to completion in toluene or DMSO, however, a mixture of the two solvents resulted in complete conversion to azide-terminated polymer. Toluene was deemed necessary to

keep the syndiotactic polymer in solution and DMSO was required for the cycloaddition reaction to proceed. The solvent ratio proved to be very important with 3:1 toluene:DMSO giving complete conversion to product. End group analysis (Figure 3.5) of the resultant polymer revealed four aromatic resonances ( $\delta$  7.83, 7.73, 7.44 and 7.35 ppm) as well as a signal for the protons adjacent to the triazole new triazole ring ( $\delta$  4.37). Utilizing the conditions described above, two equivalents of the azide-terminated polypropylene were combined with a dialkyne, 1,4-diethynylbenzene (Scheme 3.5), and the two-arm, linear polymer was obtained. Analysis of the  $^1\text{H}$  NMR spectrum of the resultant polymer revealed a new resonance for the protons adjacent to the triazole ring ( $\delta$  4.38) as well as two aromatic resonances ( $\delta$  7.90 and 7.77 ppm). By GPC (Table 3.2), the molecular weight ( $M_n = 13,000$  g/mol) increased compared with the azide-terminated polymer ( $M_n = 7,700$  g/mol,  $M_w/M_n = 1.48$ ) and molecular weight distribution remained constant ( $M_w/M_n = 1.45$ ). Finally, a three-arm star polymer was produced utilizing the above reaction conditions along with three equivalents of azide-terminated polypropylene and a trialkyne, 1,3,5-triethynylbenzene. End-group analysis of the resultant polymer revealed two aromatic resonances ( $\delta$  8.30 and 7.94 ppm) and a single resonance associated with the protons adjacent to the triazole ring ( $\delta$  4.41). By GPC (Figure 3.6, Table 3.2), the molecular weight of the polymer ( $M_n = 13,000$  g/mol,  $M_w/M_n = 1.59$ ) was determined and found to be smaller than expected due to the presence of some unreacted azide-terminated polymer ( $M_n = 7,700$  g/mol,  $M_w/M_n = 1.48$ ) in the product mixture. Filtration of the polymer mixture over silica gel with hot toluene successfully removed residual one or two-arm polymers, however, attempts to separate the three-arm polymer from the azide-terminated polymer were unsuccessful.



**Scheme 3.5.** Synthesis of  $(sPP(CH_2)_3C_2HN_3)_2C_6H_4$  (two-arms) and  $(sPP(CH_2)_3C_2HN_3)_3C_6H_3$  (three-arms) polymers.

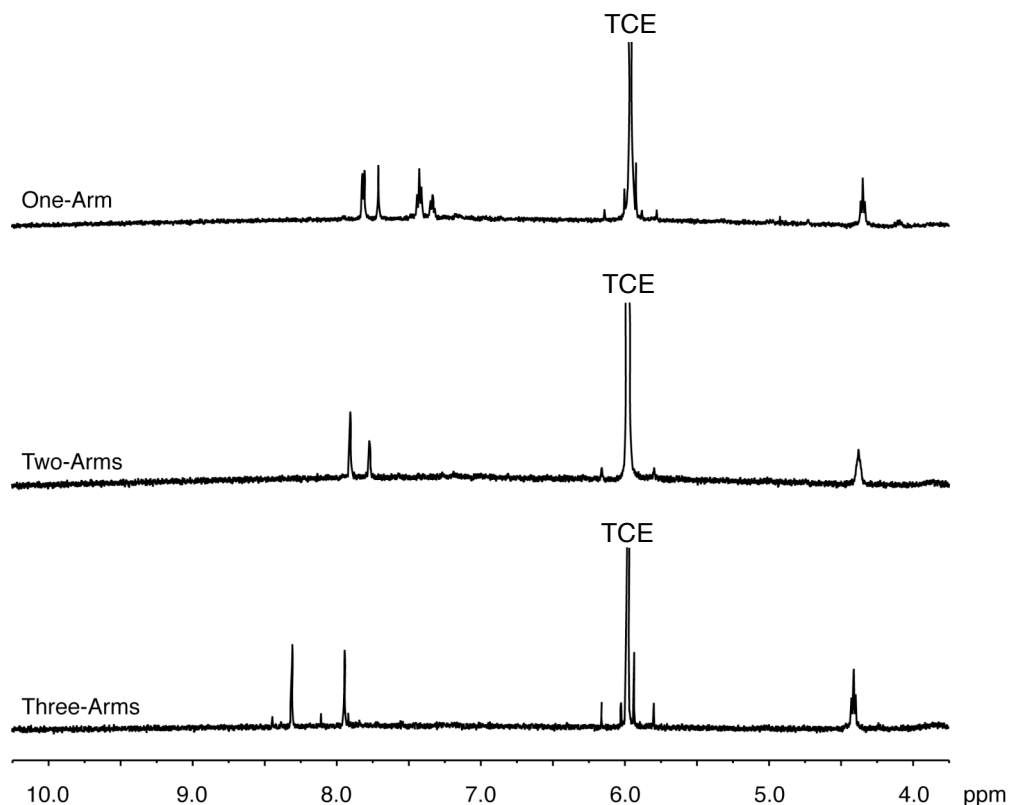


**Figure 3.5.**  $sPP(CH_2)_3C_2HN_3C_6H_5$  (one-arm),  $(sPP(CH_2)_3C_2HN_3)_2C_6H_4$  (two-arms) and  $(sPP(CH_2)_3C_2HN_3)_3C_6H_3$  (three-arms)  $^1H$  NMR spectra (500 MHz, 1,1,2,2-tetrachloroethane- $d_2$  (TCE), 75 °C).

**Table 3.2.** Syndiotactic polypropylene with triazole functionality characterization.

	Polymer	$f^a$	$M_n$ (g/mol) <sup>b</sup>	$M_w/M_n^b$	$M_w/M_n^{Theo}$	$T_c$ (°C) <sup>d</sup>	$T_m$ (°C) <sup>d</sup>	$\Delta H_m$ (J/g) <sup>d</sup>
1	$sPP-N_3$	1	7,700	1.48	1.48 <sup>c</sup>	75	114	23
2	$sPP-C_2HN_3C_6H_5$	1	6,700	1.70	1.48 <sup>c</sup>	72	114	30
3	$(sPP-C_2HN_3)_2C_6H_4$	2	13,000	1.45	1.24 <sup>c</sup>	NM <sup>e</sup>	NM <sup>e</sup>	NM <sup>e</sup>
4	$(sPP-C_2HN_3)_3C_6H_3$	3	13,000	1.59	1.16 <sup>c</sup>	68	114	37

<sup>a</sup> total number of arms. <sup>b</sup> Molecular weight ( $M_n$ ) and molecular weight distribution ( $M_w/M_n$ ) were determined by gel permeation chromatography at 140 °C in 1,2,4-trichlorobenzene relative to polyethylene standards. <sup>c</sup> Theoretical molecular weight distribution ( $M_w/M_n^{Theo}$ ) was determined using the equation:  $1 + [(M_w/M_n)_{arm} - 1]/f$  where  $(M_w/M_n)_{arm}$  is the molecular weight distribution of  $sPP-N_3$  (1.48). <sup>d</sup> Determined using differential scanning calorimetry (second heat). <sup>e</sup> Not measured.

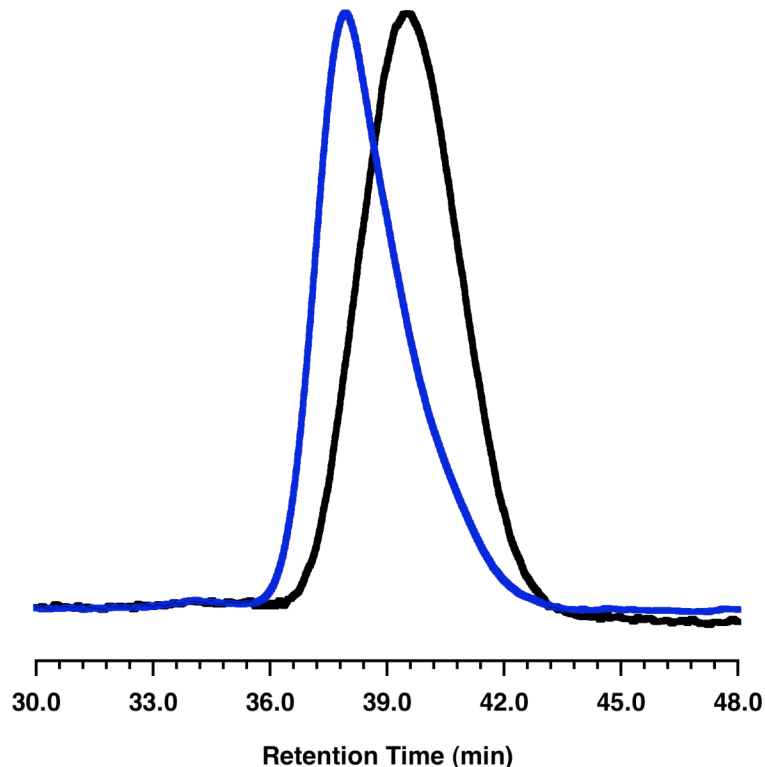


**Figure 3.6.**  $sPP(CH_2)_3C_2HN_3C_6H_5$  (black) and  $(sPP(CH_2)_3C_2HN_3)_3C_6H_3$  (blue) GPC chromatogram.

Investigations into the thermal properties of the triazole-functionalized polymers were also carried out (Table 3.2). Unlike the ester-functionalized polymers, a decrease in crystallization temperature ( $T_c = 68\text{ }^\circ\text{C}$ ) was observed for the three-arm polymer compared with the azide-terminated polypropylene ( $T_c = 75\text{ }^\circ\text{C}$ ). The presence of residual azide-terminated polymer in the three-arm star is likely effecting the crystallization behavior and therefore increased temperatures are not observed for the star polymer. Similar to the ester series, the three-arm star polymer ( $T_m = 114\text{ }^\circ\text{C}$ ) displayed a similar melting temperature to the linear, azide-terminated polypropylene ( $T_m = 114\text{ }^\circ\text{C}$ ). Based on  $^1\text{H}$  NMR and GPC data, a new three-arm star polymer as well

as linear one-arm and two-arm model compounds were produced using a copper (I) catalyzed cycloaddition reaction.

### 3.2.3 Synthesis of Star Polymers with Amide Functional Groups

A final set of polymers was synthesized utilizing amine-terminated syndiotactic polypropylene (see section 2.2.9). To probe the reactivity of the amine-terminated polymer, the synthesis of a model compound was investigated (Scheme 2.13). Combining the amine-terminated polymer with benzoyl chloride, triethylamine and toluene at 100 °C results in the formation of a new amide linkage. End-group analysis (Figure 3.7) of the resultant polypropylene revealed complete disappearance of the amine resonance ( $\delta$  2.65) and the appearance of three aromatic signals ( $\delta$  7.42, 7.28 and 7.19 ppm) as well as a resonance attributed to the protons adjacent to the amide ( $\delta$  3.98). Using the procedure established for the mono-amide, the corresponding di-amide was synthesized from two equivalents of the amine-terminated polypropylene and terephthaloyl chloride (Scheme 3.6). By GPC (Figure 3.8, Table 3.3), molecular weight ( $M_n = 12,000$  g/mol) of the resultant two-arm polymer was observed to increase and the molecular weight distribution ( $M_w/M_n = 1.44$ ) decreased compared to the amine-terminated polymer ( $M_n = 8,300$  g/mol,  $M_w/M_n = 1.50$ ), which is consistent with linking polymer chains together. Analysis of the  $^1\text{H}$  NMR spectrum showed an aromatic signal ( $\delta$  7.81) as well as a single resonance ( $\delta$  3.48) attributed to the protons adjacent to the amide. Having successfully synthesized the linear two-arm polymer, the star polymer was produced through reaction of three equivalents of the amine-terminated polypropylene with 1,3,5-benzenetricarbonyl trichloride in the presence of triethylamine and toluene at 100°C. The resultant polymer displayed an increase in molecular weight ( $M_n = 13,000$  g/mol) by GPC as well as an increase in molecular weight distribution ( $M_w/M_n = 1.73$ ). End-group

analysis of the amide linkages in the star polymer was not possible due to significant broadening of the  $^1\text{H}$  NMR spectrum (Figure 3.7). Triamides, like the three-arm star polymer produced here, are known to form supramolecular structures through intermolecular hydrogen bonding.<sup>77-80</sup> It is likely that the triamide cores in the three-arm star syndiotactic polypropylene are stacking on top of one another forming a supramolecular polymer resulting in broadening of both the GPC and  $^1\text{H}$  NMR spectra. This behavior was not observed for the one-arm or two-arm polymers, which further confirms the formation of the three-arm star polymer.

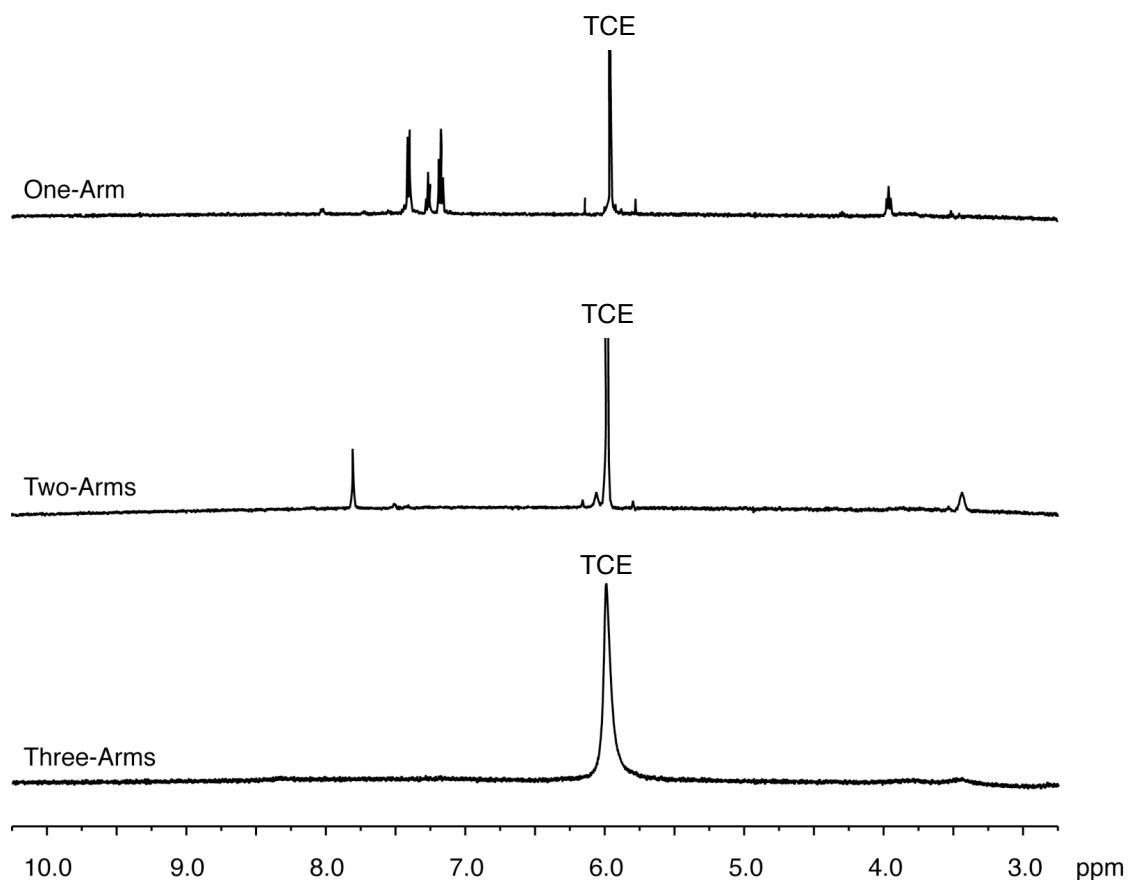


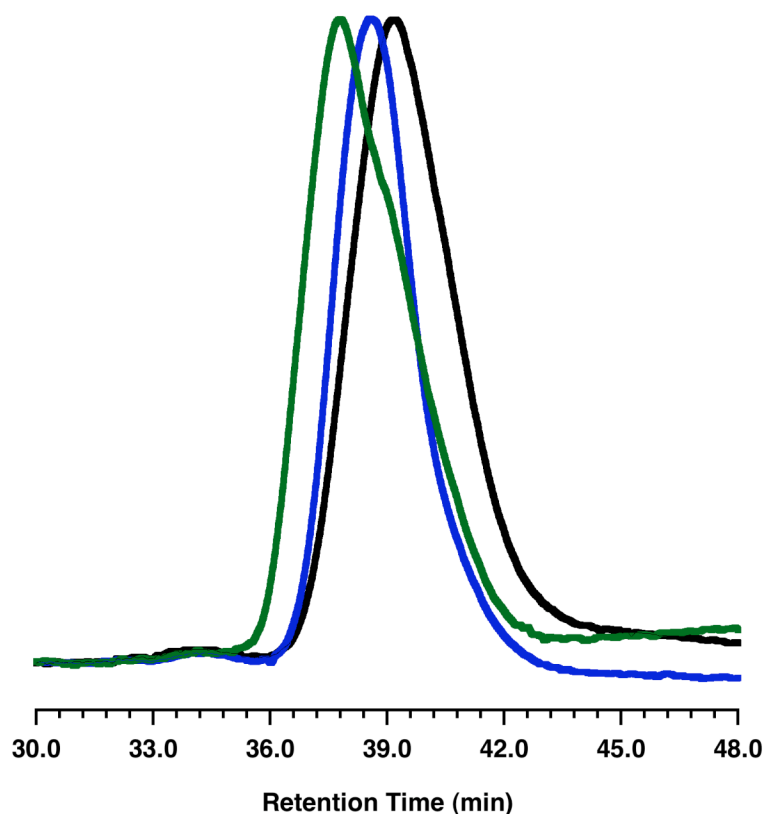
**Figure 3.7.**  $s\text{PP}(\text{CH}_2)_3\text{NHCOC}_6\text{H}_5$  (one-arm),  $(s\text{PP}(\text{CH}_2)_3\text{NHCO})_2\text{C}_6\text{H}_4$  (two-arms) and  $(s\text{PP}(\text{CH}_2)_3\text{NHCO})_3\text{C}_6\text{H}_3$  (three-arms)  $^1\text{H}$  NMR spectra (500 MHz, 1,1,2,2-tetrachloroethane- $d_2$  (TCE), 75 °C).



**Table 3.3.** Syndiotactic polypropylene with amide functionality characterization.

Polymer	$f^a$	$M_n$ (g/mol) <sup>b</sup>	$M_w/M_n^b$	$M_w/M_n^{\text{Theo}}$	$T_c$ (°C) <sup>d</sup>	$T_m$ (°C) <sup>d</sup>	$\Delta H_m$ (J/g) <sup>d</sup>
1 <i>s</i> PP-NH <sub>2</sub>	1	8,300	1.50	1.50 <sup>c</sup>	76	116	37
2 <i>s</i> PP-NHCOC <sub>6</sub> H <sub>5</sub>	1	6,400	1.72	1.50 <sup>c</sup>	67	114	25
3 ( <i>s</i> PP-NHCO) <sub>2</sub> C <sub>6</sub> H <sub>4</sub>	2	12,000	1.44	1.25 <sup>c</sup>	70	114	36
4 ( <i>s</i> PP-NHCO) <sub>3</sub> C <sub>6</sub> H <sub>3</sub>	3	13,000	1.73	1.17 <sup>c</sup>	85	111	26

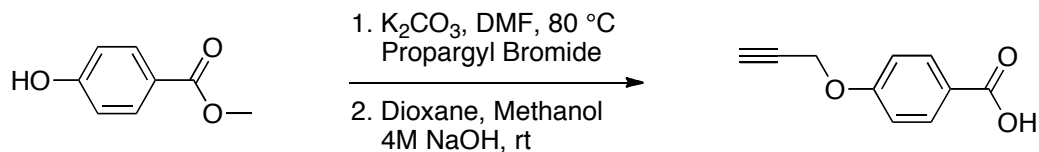
<sup>a</sup> total number of arms. <sup>b</sup> Molecular weight ( $M_n$ ) and molecular weight distribution ( $M_w/M_n$ ) were determined by gel permeation chromatography at 140 °C in 1,2,4-trichlorobenzene relative to polyethylene standards. <sup>c</sup> Theoretical molecular weight distribution ( $M_w/M_n^{\text{Theo}}$ ) was determined using the equation:  $1 + [(M_w/M_n)_{\text{arm}} - 1]/f$  where  $(M_w/M_n)_{\text{arm}}$  is the molecular weight distribution of *s*PP-NH<sub>2</sub> (1.50). <sup>d</sup> Determined using differential scanning calorimetry (second heat).

**Figure 3.8.** *s*PP(CH<sub>2</sub>)<sub>3</sub>NHCOC<sub>6</sub>H<sub>5</sub> (black), (*s*PP(CH<sub>2</sub>)<sub>3</sub>NHCO)<sub>2</sub>C<sub>6</sub>H<sub>4</sub> (blue) and (*s*PP(CH<sub>2</sub>)<sub>3</sub>NHCO)<sub>3</sub>C<sub>6</sub>H<sub>3</sub> (green) GPC chromatogram.

The thermal properties of the amide-functionalized polymers were investigated using differential scanning calorimetry (Table 3.3). Long-chain branching in the three-arm polymer was found to significantly alter crystallization temperature ( $T_c = 85\text{ }^\circ\text{C}$ ) compared with the amine-terminated polymer ( $T_c = 76\text{ }^\circ\text{C}$ ) and the mono-amide, *sPP-NHCOC<sub>6</sub>H<sub>5</sub>* ( $T_c = 67\text{ }^\circ\text{C}$ ). The linear two-arm polymer, (*sPP-NHCO*)<sub>2</sub>C<sub>6</sub>H<sub>4</sub>, also displayed a decreased crystallization temperature ( $T_c = 70\text{ }^\circ\text{C}$ ) compared with the three-arm star polymer. Small differences in melting temperatures were observed for the three-arm polymer ( $T_m = 111\text{ }^\circ\text{C}$ ), two-arm polymer ( $T_m = 114\text{ }^\circ\text{C}$ ) and the amine-terminated polypropylene ( $T_m = 116\text{ }^\circ\text{C}$ ). Based on the <sup>1</sup>H NMR, GPC and thermal data, a three-arm star polymer bearing amide functional groups has been produced. Furthermore, three different click reactions were utilized to produce three new syndiotactic star polymers from different end-functionalized polypropylenes. To the best of our knowledge, this is the first report of star polymers bearing syndiotactic polypropylene arms.

### 3.2.4 Synthesis of *sPP-block-PEG*

In an attempt to produce the more complex miktoarm star and H-polymer we investigated a series of amphiphilic block copolymers. These types of block copolymers have been shown to exhibit unique self-assembly properties due to the presence of hydrophobic and hydrophilic polymers.<sup>81-84</sup> In 1997, Hillmyer and coworkers were able to produce diblock copolymers of polyethylene glycol and poly(ethyl ethylene). The resultant block copolymers formed ordered structures through aggregation of the hydrophobic polymer chain ends resulting in a micellar structure.<sup>85</sup> To the best of our knowledge, amphiphilic block copolymers of syndiotactic polypropylene and polyethylene glycol have not be reported to date.

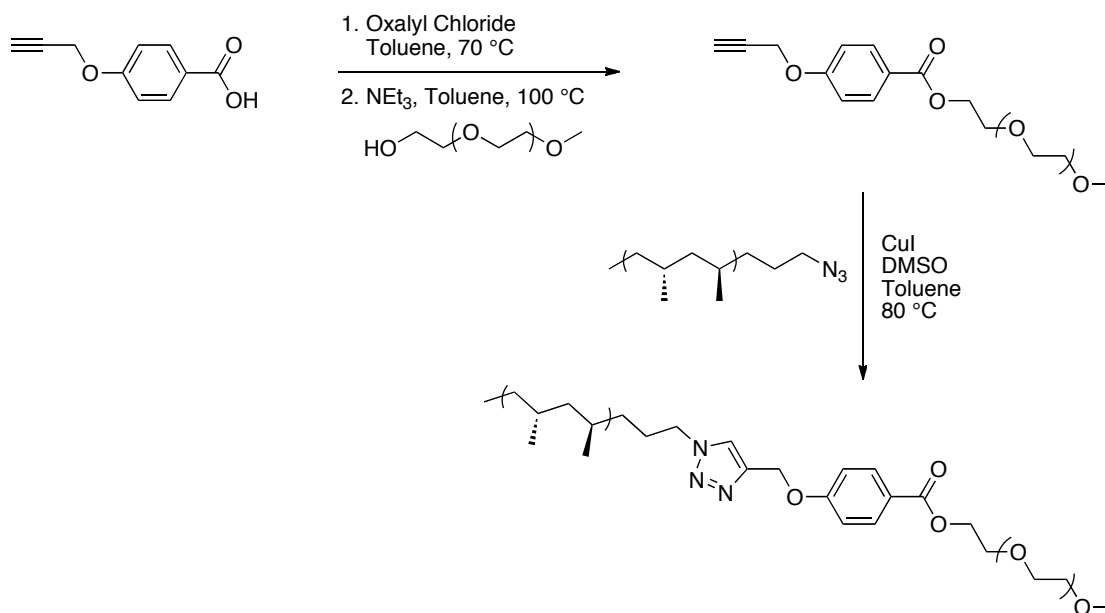


**Scheme 3.7.** Synthesis of a difunctional coupling agent.

Before synthesizing the more structurally complex miktoarm and h-polymers, the synthesis of di- and triblock copolymers was investigated. Production of these block copolymers required the synthesis of a difunctional coupling agent containing orthogonal functional groups, which were capable of reacting with end-functionalized polymers in an efficient manner. Inspired by work in the area of amino acid based dendrimers,<sup>86-88</sup> a difunctional coupling agent containing an alkyne as well as a carboxylic acid, which could easily be converted to the corresponding acid chloride, was synthesized (Scheme 3.7). Combining the commercially available methyl-4-hydroxybenzoate with propargyl bromide and potassium carbonate in DMF at room temperature resulted in the propargyl substitution of the hydroxyl moiety. The methyl ester was then converted to the carboxylic acid through reaction with sodium hydroxide in a mixture of dioxane and methanol. Having a small molecule, which was capable of reaction with hydroxyl- or azide-terminated polypropylene, the production of diblock and triblock copolymers was pursued.

To enhance reactivity with hydroxyl-terminated polymers, the carboxylic acid was converted to an acid chloride through reaction with oxalyl chloride in toluene at 70 °C. Immediately upon removal of the excess oxalyl chloride, the resultant acid chloride was combined with polyethylene glycol methyl ether ( $M_n = 5,000$  g/mol), triethylamine and toluene at 100 °C (Scheme 3.8). End group analysis of the resultant functionalized polyethylene glycol (Figure 3.9) revealed two aromatic signals ( $\delta$  8.00

and 6.98 ppm), a single resonance attributed to the protons adjacent to the ester ( $\delta$  4.43) and two signals for the propargyl group ( $\delta$  4.73 and 2.56 ppm). To produce the diblock copolymer, the functionalized polyethylene glycol was combined with azide-terminated syndiotactic polypropylene ( $M_n = 7,700$  g/mol,  $M_w/M_n = 1.48$ ), copper iodide, and a mixture of DMSO and toluene at 80 °C. By GPC (Figure 3.10, Table 3.4), the molecular weight of the resultant polymer ( $M_n = 10,000$  g/mol) increased and the molecular weight distribution ( $M_w/M_n = 1.37$ ) decreased relative to the starting polymers, which is consistent with linking polymer chains together. End-group analysis of the diblock copolymer revealed two aromatic resonances attributed to the benzene ring ( $\delta$  8.01 and 7.06 ppm), three signals attributed to the triazole ring and the protons adjacent to it ( $\delta$  7.59, 5.26 and 4.43 ppm) as well as a single resonance attributed to the protons adjacent to the ester ( $\delta$  4.34 ppm).



**Scheme 3.8.** Synthesis of PEG bearing one difunctional coupling agent and sPP-*block*-PEG.

The thermal properties of the *sPP-co*-PEG and its polymer precursors were investigated using differential scanning calorimetry. As expected, the diblock copolymer displayed two melting temperatures ( $T_m = 53$  and  $113$  °C). The first endotherm results from the PEG and is much lower than the melting temperature observed for the PEG homopolymer bearing one difunctional coupling agent ( $T_m = 63$  °C). The melting temperature of azide-terminated syndiotactic polypropylene ( $T_m = 114$  °C) is very similar to the second endotherm of the diblock copolymer. Analysis of the crystallization behavior revealed similar results with two crystallization temperatures ( $T_c = 36$  and  $69$  °C) observed. The lower temperature exotherm corresponds to the PEG segment of the diblock and is comparable to the PEG homopolymer ( $T_c = 40$  °C). The crystallization temperature of the azide-terminated syndiotactic polypropylene ( $T_c = 75$  °C) is also similar to the higher temperature exotherm ( $T_c = 69$  °C) of the diblock copolymer. The  $^1\text{H}$  NMR spectrum coupled with the molecular weight and thermal data confirms the formation of *sPP-block*-PEG.

**Table 3.4.** Characterization of di- and triblock copolymers containing *sPP* and PEG.

	Polymer	$M_n$ (g/mol) <sup>a</sup>	$M_w/M_n$ <sup>a</sup>	$T_c$ (°C) <sup>b</sup>	$T_m$ (°C) <sup>b</sup>	$\Delta H_m$ (J/g) <sup>b</sup>
1	Diblock	10,000	1.37	36 69	53 113	8 11
2	Triblock	11,000	1.39	33 74	50 110	18 36

<sup>a</sup> Molecular weight ( $M_n$ ) and molecular weight distribution ( $M_w/M_n$ ) were determined by gel permeation chromatography at  $140$  °C in 1,2,4-trichlorobenzene relative to polyethylene standards. <sup>b</sup> Differential scanning calorimetry (second heat).

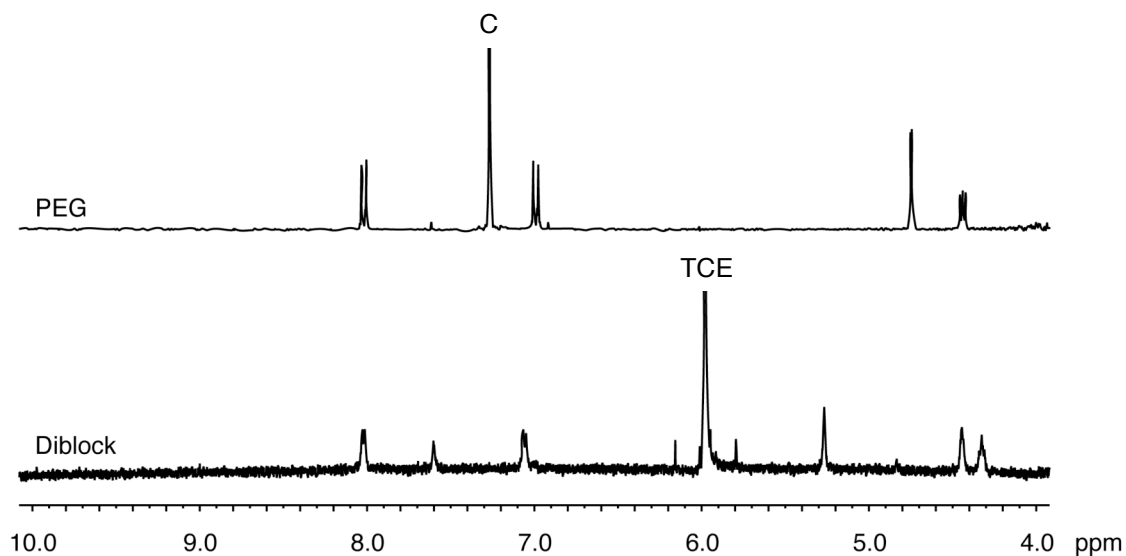


**Figure 3.9.**  $^1\text{H}$  NMR spectra of PEG bearing one difunctional coupling agent (500 MHz, chloroform- $d$  (C), 22 °C) and *sPP-block*-PEG (500 MHz, 1,1,2,2-tetrachloroethane- $d_2$  (TCE), 75 °C).

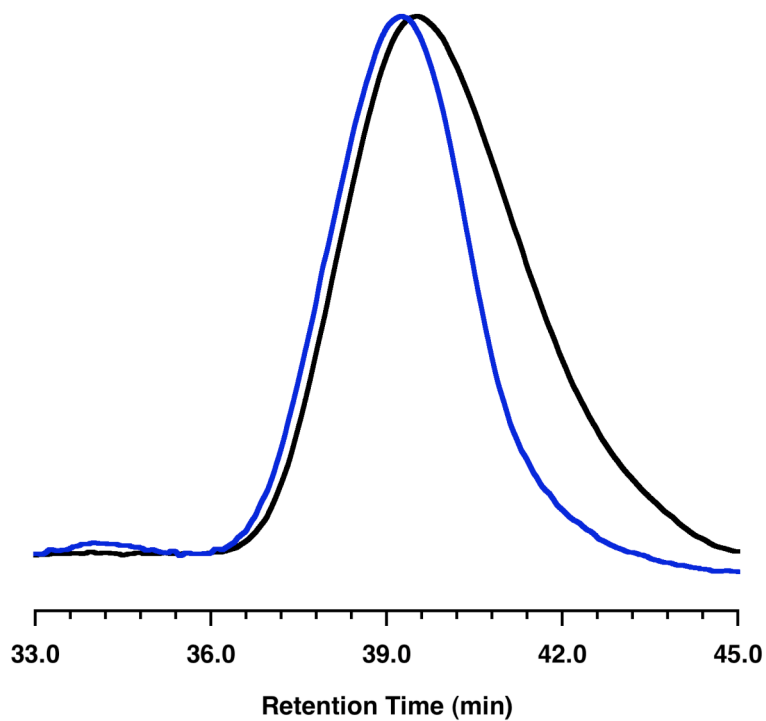
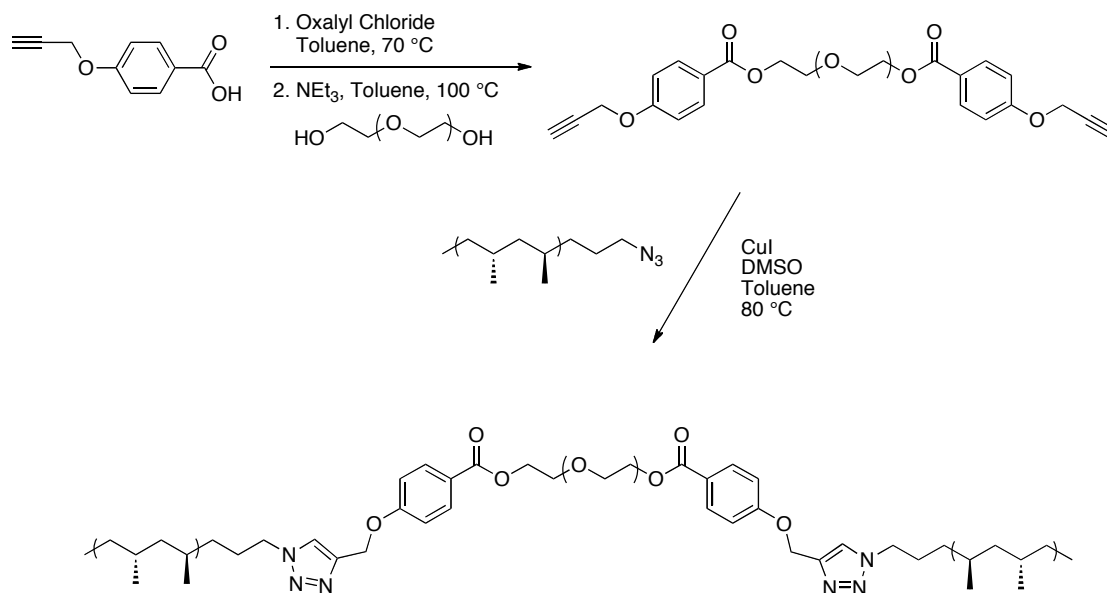


**Figure 3.10.** *sPP*-( $\text{CH}_2$ ) $_3$ - $\text{N}_3$  (black) and *sPP-block*-PEG (blue) GPC chromatogram.

### 3.2.5 Synthesis of sPP-block-PEG-block-sPP

Having successfully produced a diblock copolymer of syndiotactic polypropylene and polyethylene glycol, the production of a triblock copolymer was targeted. After converting the carboxylic acid to the acid chloride utilizing oxalyl chloride, two equivalents the difunctional coupling agent were combined with dihydroxyl-terminated polyethylene glycol ( $M_n = 8,000$  g/mol) in the presence of triethylamine and toluene at 100 °C (Scheme 3.9). End-group analysis of the resultant polymer (Figure 3.11) revealed two aromatic signals ( $\delta$  8.00 and 6.99 ppm), a single resonance associated with the protons adjacent ester ( $\delta$  4.44) and two signals attributed to the propargyl group and the protons adjacent to it ( $\delta$  4.76 and 2.56 ppm). The



**Scheme 3.9.** Synthesis of PEG bearing two difunctional coupling agents and sPP-block-PEG-block-sPP.

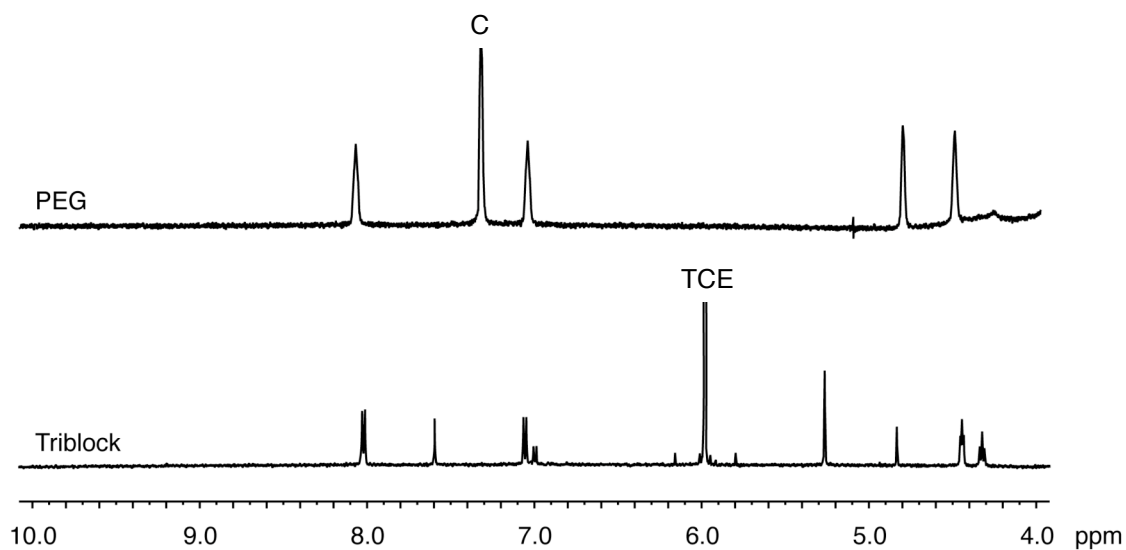


**Figure 3.11.** Synthesis of PEG bearing two difunctional coupling agents (500 MHz, chloroform-*d* (C), 22 °C) and *sPP-block-PEG-block-sPP* (500 MHz, 1,1,2,2-tetrachloroethane-*d*<sub>2</sub> (TCE), 75 °C).

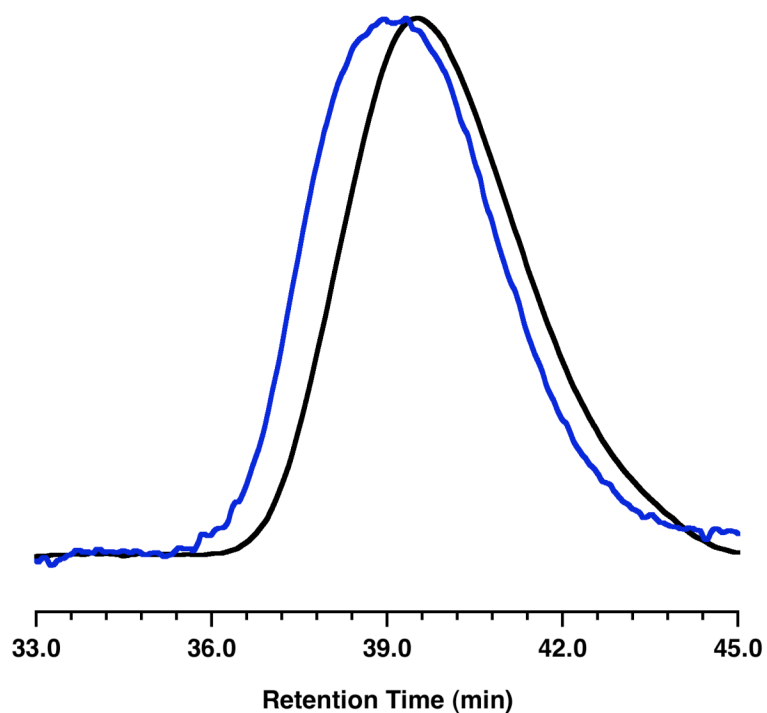


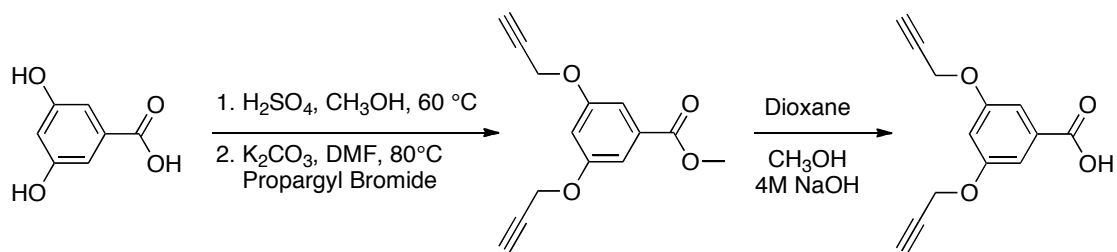
**Figure 3.12.** *sPP-(CH<sub>2</sub>)<sub>3</sub>-N<sub>3</sub>* (black) and *sPP-block-PEG-block-sPP* (blue) GPC chromatogram.

functionalized polyethylene glycol was then combined with two equivalents of the azide-terminated syndiotactic polypropylene ( $M_n = 7,700$  g/mol,  $M_w/M_n = 1.48$ ), copper iodide, DMSO and toluene at 80 °C. By GPC (Figure 3.12, Table 3.3), the resultant polymer displayed an increase in molecular weight ( $M_n = 11,000$  g/mol) and a decrease in molecular weight distribution ( $M_w/M_n = 1.39$ ) relative to the starting polymers, which are both indicative of successful linking of the polymer chains. Furthermore, end-group analysis showed the appearance of three resonances attributed to the triazole ring and protons adjacent to it ( $\delta$  7.60, 5.26 and 4.45 ppm) as well as two aromatic signals for the benzene ring ( $\delta$  8.02 and 7.05 ppm) and a single resonance for the protons adjacent to the ester ( $\delta$  4.32).

Using differential scanning calorimetry, the thermal properties of the *sPP-co-PEG-co-sPP* and its polymer precursors were investigated. Similar to the diblock copolymer, the triblock copolymer displayed two melting temperatures ( $T_m = 50$  and 110 °C). The first endotherm results from the PEG midblock and is again lower than the melting temperature observed for the PEG homopolymer ( $T_m = 55$  °C). Good agreement between the melting temperature of azide-terminated syndiotactic polypropylene ( $T_m = 114$  °C) and the second endotherm of the diblock copolymer was obtained. Analysis of the crystallization behavior revealed similar results with two crystallization temperatures ( $T_c = 33$  and 74 °C) observed. The crystallization temperature of the azide-terminated syndiotactic polypropylene ( $T_c = 75$  °C) is nearly identical to the higher temperature exotherm ( $T_c = 74$  °C) of the triblock copolymer. The lower temperature exotherm, which results from the PEG segment, is comparable to the PEG homopolymer ( $T_c = 38$  °C). Based on the  $^1\text{H}$  NMR spectrum, molecular weight and thermal data, the triblock copolymer, *sPP-block-PEG-block-sPP*, was produced.

### 3.2.6 Synthesis of (sPP)<sub>2</sub>-block-PEG

After successful synthesizing linear block copolymers, the production of simple branched polymers, namely miktoarm star and h-polymers, containing polyethylene glycol and syndiotactic polypropylene was investigated. To synthesize these branched block copolymers, a trifunctional coupling agent bearing orthogonal functional groups was required (Scheme 3.10). The commercially available carboxylic acid, 3,5-dihydroxybenzoic acid, was converted to the methyl ester with methanol and sulfuric acid. Using a mixture of potassium carbonate, DMF and propargyl bromide, the alkyne substituted compound was obtained. Finally, the methyl ester was converted back to the carboxylic acid through reaction with sodium hydroxide in a mixture of dioxane and methanol. With a small molecule bearing one carboxylic acid and two alkynes in hand, the production of a miktoarm star and h-polymer was pursued.

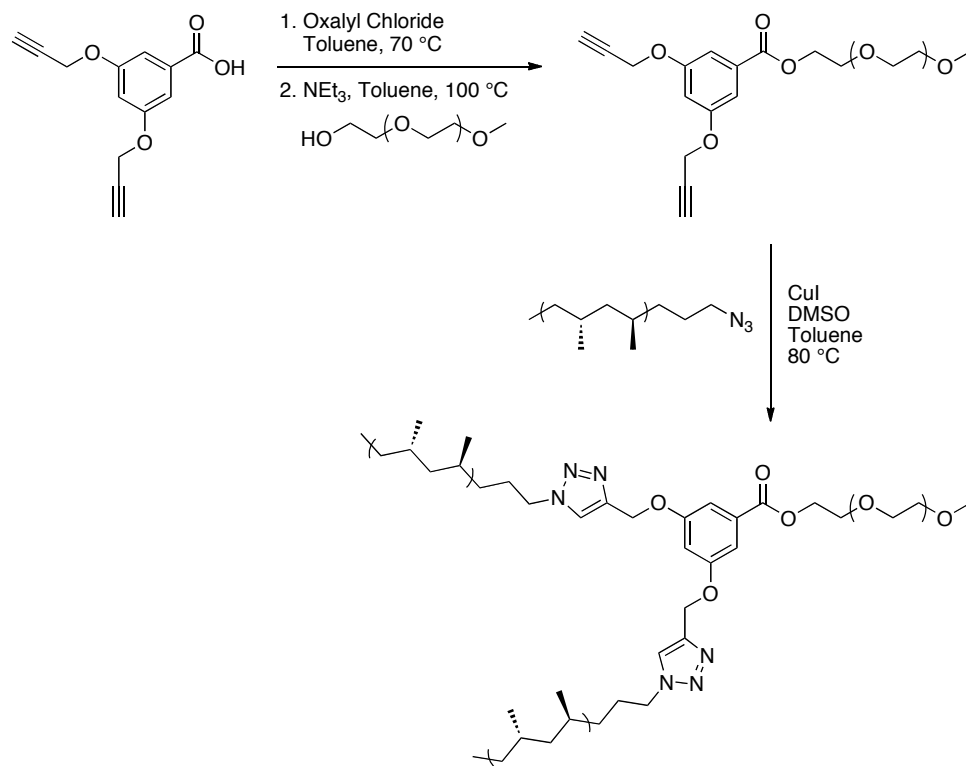


**Scheme 3.10.** Synthesis of a trifunctional coupling agent.

To synthesize the miktoarm star, the trifunctional coupling agent was converted to the acid chloride through reaction with oxalyl chloride in toluene at  $70\text{ }^\circ\text{C}$ . Upon removal of excess oxalyl chloride, the acid chloride was combined with polyethylene glycol methyl ether ( $M_n = 5,000\text{ g/mol}$ ) in the presence of triethylamine and toluene at  $100\text{ }^\circ\text{C}$  (Scheme 3.11). End-group analysis of the resultant polymer

(Figure 3.13) revealed two aromatic signals ( $\delta$  7.29 and 6.80 ppm), a single resonance attributed to the protons adjacent to the ester ( $\delta$  4.44) and two signals for the propargyl group ( $\delta$  4.70 and 2.5 ppm). To produce the miktoarm star, the functionalized polyethylene glycol was combined with two equivalents of the azide-terminated syndiotactic polypropylene ( $M_n = 7,700$  g/mol,  $M_w/M_n = 1.48$ ), copper iodide and a mixture of DMSO and toluene at 80 °C. By GPC (Figure 3.14, Table 3.5), the molecular weight of the resultant polymer ( $M_n = 11,000$  g/mol,  $M_w/M_n = 1.46$ ) increased relative to the molecular weight of the starting polymers, indicating chain coupling. Furthermore, end-group analysis of the miktoarm star revealed two aromatic resonances attributed to the benzene ring ( $\delta$  7.33 and 6.93 ppm), three signals for the triazole ring and the protons adjacent to it ( $\delta$  7.63, 5.23 and 4.44 ppm) as well as a single resonance attributed to the protons adjacent to the ester ( $\delta$  4.32).

The thermal properties of the  $(sPP)_2$ -*co*-PEG and the polymers used in its synthesis were investigated. Similar to the di- and triblock copolymers, the miktoarm star displayed two melting temperatures ( $T_m = 53$  and 109 °C). The PEG segment corresponds to the first endotherm and is lower than the melting temperature observed for the PEG homopolymer ( $T_m = 57$  °C). The second endotherm also displayed a somewhat lower melting temperature than the corresponding azide-terminated syndiotactic polypropylene ( $T_m = 114$  °C). The miktoarm star showed different crystallization behavior than the di- and triblock copolymers with only one crystallization temperature ( $T_c = 52$  °C) observed. The crystallization temperature is midway between the azide-terminated syndiotactic polypropylene ( $T_c = 75$  °C) and the PEG homopolymer ( $T_c = 43$  °C). The  $^1H$  NMR spectrum coupled with the thermal data and observed increases in molecular weight confirms the formation of the miktoarm star,  $(sPP)_2$ -*block*-PEG.



**Scheme 3.11.** Synthesis of PEG bearing one trifunctional coupling agent and  $(sPP)_2$ -*block*-PEG.

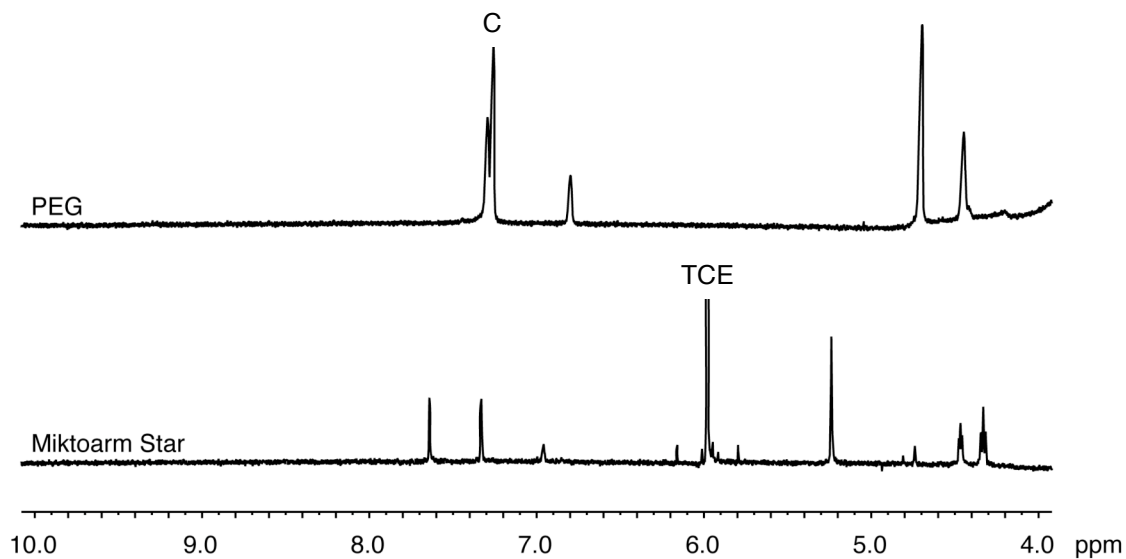


**Figure 3.13.**  $^1H$  NMR spectra of PEG bearing one trifunctional coupling agent (500 MHz, chloroform- $d$  (C), 22 °C) and  $(sPP)_2$ -*block*-PEG (500 MHz, 1,1,2,2-tetrachloroethane- $d_2$  (TCE), 75 °C).

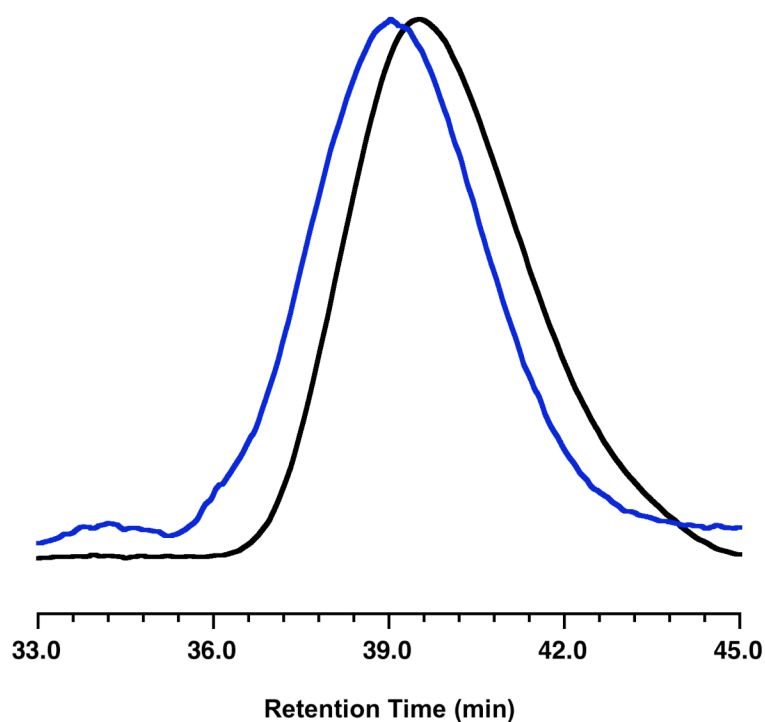


**Figure 3.14.** *sPP*-(CH<sub>2</sub>)<sub>3</sub>-N<sub>3</sub> (black) and (*sPP*)<sub>2</sub>-*block*-PEG (blue) GPC chromatogram.

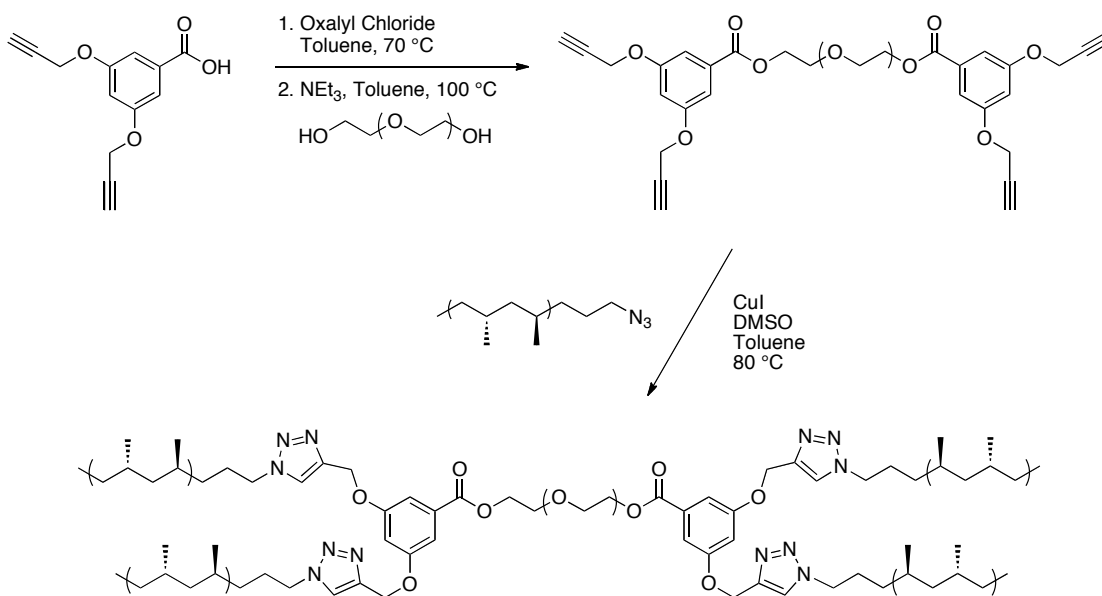
**Table 3.5.** Characterization of mikroarm and h-polymers containing *sPP* and PEG.

	Polymer	$M_n$ (g/mol) <sup>a</sup>	$M_w/M_n$ <sup>a</sup>	$T_c$ (°C) <sup>b</sup>	$T_m$ (°C) <sup>b</sup>	$\Delta H_m$ (J/g) <sup>b</sup>
2	Miktoarm	10,000	1.37	52	53 109	3 18
3	H-polymer	11,000	1.39	84	59 121	3 26

<sup>a</sup> Molecular weight ( $M_n$ ) and molecular weight distribution ( $M_w/M_n$ ) were determined by gel permeation chromatography at 140 °C in 1,2,4-trichlorobenzene relative to polyethylene standards. <sup>b</sup> Differential scanning calorimetry (second heat).

### 3.2.7 Synthesis of (sPP)<sub>2</sub>-block-PEG-block-(sPP)<sub>2</sub>

Having successfully produced a miktoarm star polymer of syndiotactic polypropylene and polyethylene glycol, the synthesis of the H-polymer was targeted. After converting the trifunctional coupling agent to an acid chloride using oxalyl chloride, two equivalents of the resultant acid chloride were combined with the dihydroxyl-terminated polyethylene glycol ( $M_n = 8,000$  g/mol) in the presence of triethylamine and toluene at 100 °C (Scheme 3.12). End-group analysis of the resultant polymer (Figure 3.16) revealed two aromatic signals ( $\delta$  7.30 and 6.80 ppm), a single resonance associated with the protons adjacent ester ( $\delta$  4.44) and two signals attributed to the propargyl and protons adjacent to it ( $\delta$  4.70 and 2.57 ppm). The functionalized polyethylene glycol was then combined with azide-terminated syndiotactic polypropylene, copper iodide, DMSO and toluene at 80 °C. By GPC



**Scheme 3.12.** Synthesis of PEG bearing two trifunctional coupling agents and (sPP)<sub>2</sub>-block-PEG-block-(sPP)<sub>2</sub>.

(Figure 3.15, Table 3.5), the resultant polymer displayed an increase in molecular weight ( $M_n = 10,00$  g/mol,  $M_w/M_n = 1.51$ ) relative to the starting polymers, indicating successful linking of the polymer chains. Additionally, end-group analysis revealed three resonances attributed to the triazole and protons adjacent to it ( $\delta$  7.61, 5.27 and 4.34 ppm) as well as two aromatic signals for the benzene ring ( $\delta$  7.36 and 6.98 ppm) and a single resonance for the protons adjacent to the ester ( $\delta$  4.48).

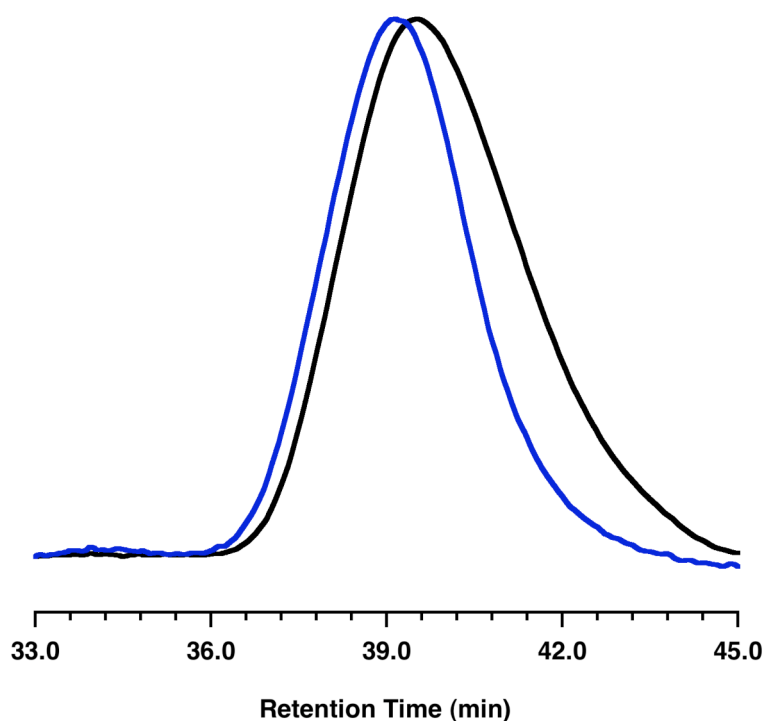


**Figure 3.15.**  $sPP-(CH_2)_3-N_3$  (black) and  $(sPP)_2$ -*block*-PEG-*block*-( $sPP$ )<sub>2</sub> (blue) GPC chromatogram.

The thermal properties of the H-polymer,  $(sPP)_2$ -*co*-PEG-*co*-( $sPP$ )<sub>2</sub>, and its precursors were investigated. Similar to the other amphiphilic block copolymers, the

H-polymer displayed two melting temperatures ( $T_m = 59$  and  $121$  °C). Interestingly, both endotherms were higher than the corresponding PEG ( $T_m = 56$  °C) and azide-terminated syndiotactic polypropylene ( $T_m = 114$  °C) homopolymers used to produce the H-polymer. This increase in melting temperature was not observed with the previous copolymers. The H-polymer also displayed only one crystallization temperature ( $T_c = 84$  °C), which was higher than the crystallization temperature of the azide-terminated syndiotactic polypropylene ( $T_c = 75$  °C) and the PEG homopolymer ( $T_c = 37$  °C). This increase is consistent with the crystallization behavior of the star polymers, which also contained long-chain branches. Based on the  $^1\text{H}$  NMR spectrum as well as molecular weight and thermal data, the H-polymer,  $(sPP)_2$ -*block*-PEG-*block*-( $sPP$ ) $_2$ , was produced.

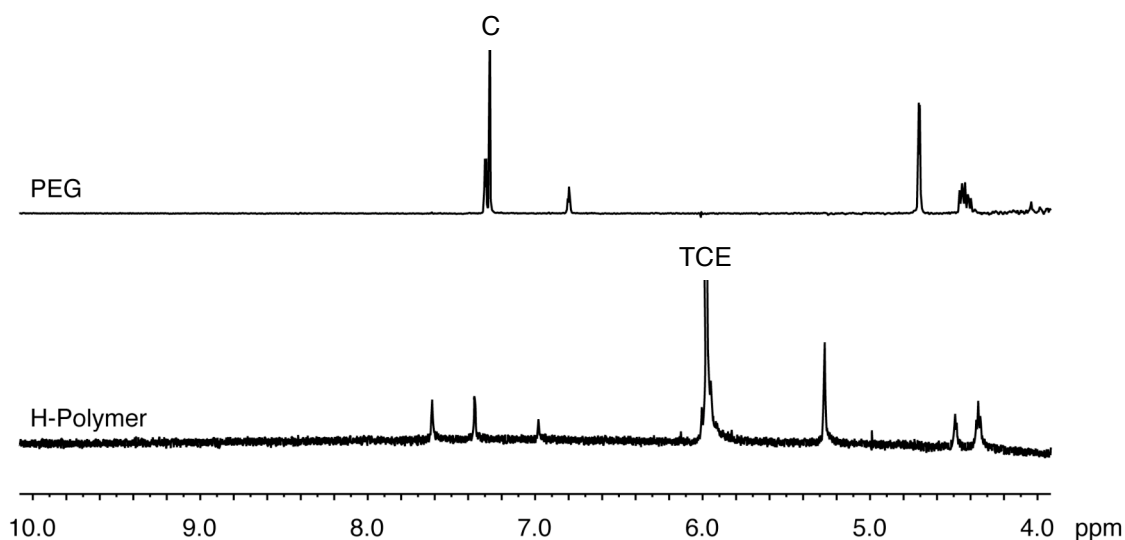


**Figure 3.16.**  $^1\text{H}$  NMR spectra of PEG bearing two trifunctional coupling agents (500 MHz, chloroform- $d_2$  (C), 22 °C) and  $(sPP)_2$ -*block*-PEG-*block*-( $sPP$ ) $_2$  (500 MHz, 1,1,2,2-tetrachloroethane- $d_2$  (TCE), 75 °C).

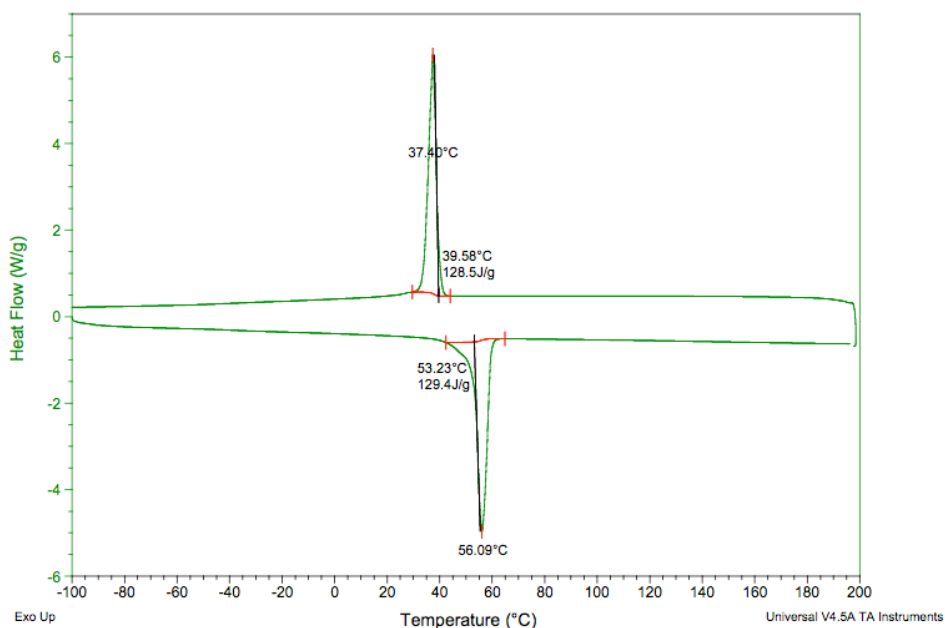


**Figure 3.17.** Differential scanning calorimetry (10 °C/min, second heat) thermogram of PEG bearing two trifunctional coupling agents.

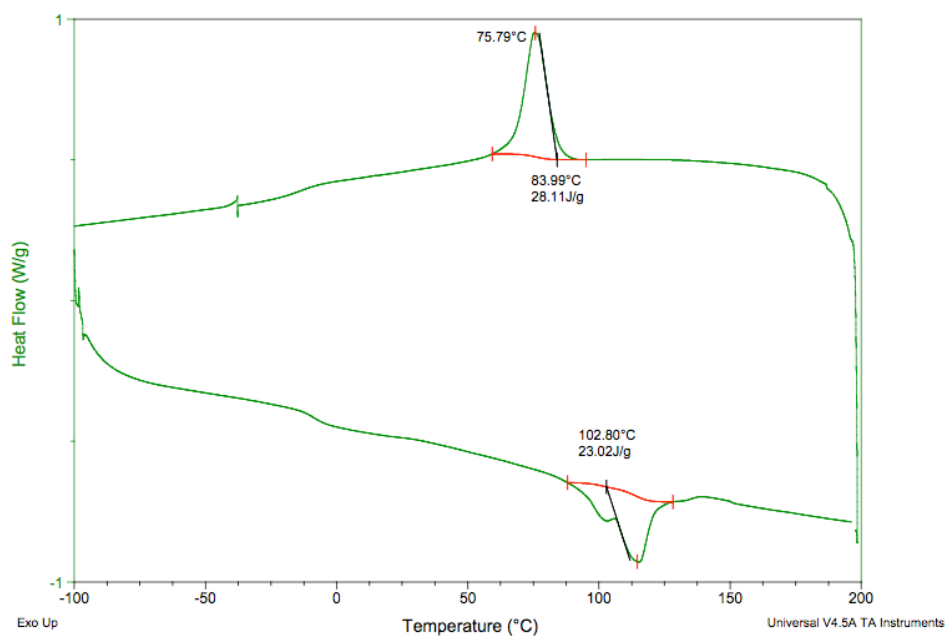


**Figure 3.18.** Differential scanning calorimetry (10 °C/min, second heat) thermogram of azide-terminated syndiotactic polypropylene.

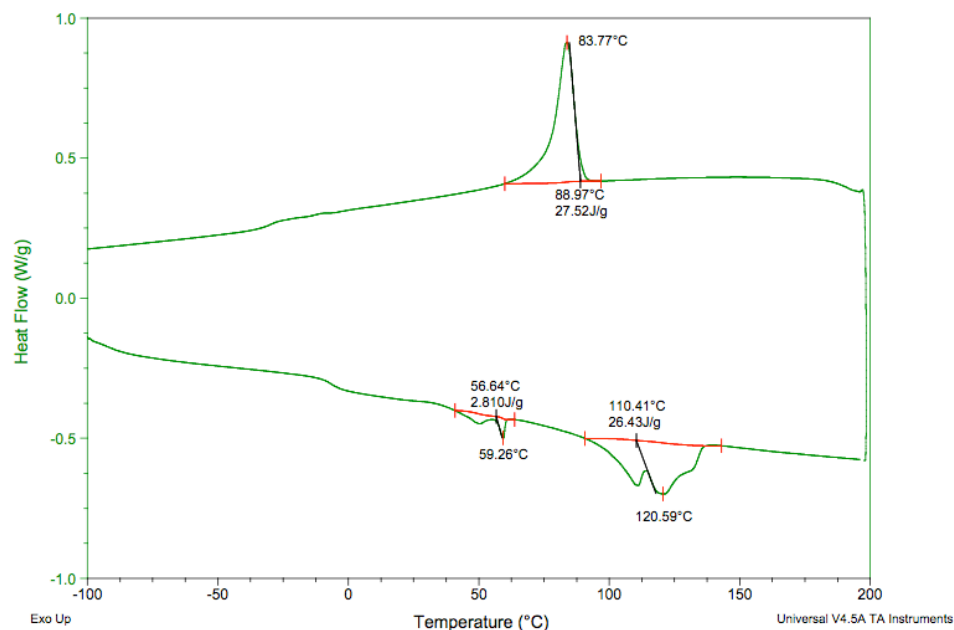


**Figure 3.19.** Differential scanning calorimetry (10 °C/min, second heat) thermogram of  $(sPP)_2$ -block-PEG-block- $(sPP)_2$ .

### 3.3 Conclusion

Traditionally, well-defined and branched polymers of syndiotactic or isotactic polypropylene have been difficult to synthesize with coordination-insertion polymerization. Utilizing end-functionalized syndiotactic polypropylene along with multifunctional coupling agents, several branched polymers were synthesized. To the best of our knowledge, this is the first report of a star, miktoarm star or an H-polymer bearing semicrystalline polypropylene arms.

### 3.4 Experimental

**General Procedures.** All manipulations of air- and/or water-sensitive compounds were carried out under dry nitrogen using Braun UniLab drybox or standard Schlenk techniques.  $^1H$  and  $^{13}C\{^1H\}$  NMR spectra of polymers were recorded using a Varian UnityInova (500 MHz) spectrometer equipped with a  $^1H/BB$  switchable with Z-pulse

field gradient probe operating and referenced versus residual non-deuterated solvent shifts. The polymer samples were dissolved in 1,1,2,2-tetrachloroethane- $d_2$  in a 5 mm O.D. tube, and spectra were collected at 75 °C. End-group analysis for molecular weight determination was achieved by relative integration of the end-group vs alkyl peaks in the  $^1\text{H}$  NMR spectra. Additionally, molecular weights ( $M_n$  and  $M_w$ ) and molecular weight distributions ( $M_w/M_n$ ) were determined by high temperature gel permeation chromatography (GPC). Analyses were performed with a Waters Alliance GPCV 2000 GPC equipped with a Waters DRI detector and viscometer. The column set (four Waters HT 6E and one Waters HT 2) was eluted with 1,2,4-trichlorobenzene containing 0.01 wt % di-*tert*-butyl-hydroxytoluene (BHT) at 1.0 mL/min at 140 °C. Data were calibrated using monomodal polyethylene standards (from Polymer Standards Service). Differential scanning calorimetric analyses were performed in aluminum pans under nitrogen using a TA Instruments Q1000 calorimeter equipped with an automated sampler. Data were collected from the second heating run at a heating rate of 10 °C/min from 0 to 200 °C and were processed with the TA Q series software package.

**Materials.** Toluene and THF were purified over columns of alumina and copper (Q5). For preparation of  $s\text{PP}-(\text{CH}_2)_3\text{OH}$ ,  $s\text{PP}-(\text{CH}_2)_3\text{OC}(\text{O})\text{C}_6\text{H}_5$ ,  $s\text{PP}-(\text{CH}_2)_3\text{N}_3$ ,  $s\text{PP}-(\text{CH}_2)_3(\text{C}_2\text{HN}_3)\text{C}_6\text{H}_5$ ,  $s\text{PP}-(\text{CH}_2)_3\text{NH}_2$  and  $s\text{PP}-(\text{CH}_2)_3\text{NHC}(\text{O})\text{C}_6\text{H}_5$  see chapter two. Triethylamine was stirred over  $\text{CaH}_2$  for several days and vacuum distilled. Terephthaloyl chloride, 1,3,5-benzenetricarbonyl trichloride, 1,4-diethynylbenzene, 1,3,5-triethynylbenzene, copper iodide, DMSO (anhydrous, >99%), methyl hydroxybenzoate, DMF (anhydrous, >98%), propargyl bromide, poly(ethylene glycol methyl ether), oxalyl chloride, poly(ethylene glycol), 3,5-dihydroxy benzoic acid were purchased from commercial sources and used as received.

**(sPP-(CH<sub>2</sub>)<sub>3</sub>OCO)<sub>2</sub>-C<sub>6</sub>H<sub>4</sub>.** An oven-dried Schlenk flask was cooled under vacuum and charged with sPP-(CH<sub>2</sub>)<sub>3</sub>OH (0.50 g, 0.083 mmol) and 4 Å molecular sieves. Toluene (2 mL) was syringed into the flask followed by triethylamine (0.01 mL, 0.083 mmol) and a 0.25 M THF solution of terephthaloyl chloride (0.18 mL, 0.046 mmol). The reaction mixture was heated to 100 °C. After 5 days, the flask was cooled to room temperature and the polymer was precipitated in methanol (100 mL). The polymer was collected, dissolved in hot toluene and filtered through a glass frit layered with silica, alumina, and Celite. The toluene was removed under reduced pressure and the polymer was dried in vacuo to constant weight (0.43 g, 86% yield).  $M_n(\text{GPC}) = 8,100$  g/mol,  $M_w/M_n = 1.59$ ,  $M_n(^1\text{H NMR}) = 18,000$  g/mol.  $^1\text{H NMR}$  (500 MHz, C<sub>2</sub>D<sub>2</sub>Cl<sub>4</sub>, 75 °C):  $\delta$  8.10 (s, 4H), 4.34 (t, 4H), 0.68-1.72 (m, 2500H).

**(sPP-(CH<sub>2</sub>)<sub>3</sub>OCO)<sub>3</sub>-C<sub>6</sub>H<sub>3</sub>.** An oven-dried Schlenk flask was cooled under vacuum and charged with sPP-(CH<sub>2</sub>)<sub>3</sub>OH (2.50 g, 0.42 mmol) and 4 Å molecular sieves. Toluene (10 mL) was syringed into the flask followed by triethylamine (0.042 mL, 0.42 mmol) and a 0.25 M THF solution of 1,3,5-benzenetricarbonyl trichloride (0.56 mL, 0.14 mmol). The reaction mixture was heated to 100 °C. After 8 days, the flask was cooled to room temperature and the polymer was precipitated in methanol (400 mL). The polymer was collected, dissolved in hot toluene and filtered through 8 in. of silica gel. The first 80 mL of toluene were collected, removed under reduced pressure and the polymer was dried in vacuo to constant weight (0.16 g, 6.4% yield).  $M_n(\text{GPC}) = 13,000$  g/mol,  $M_w/M_n = 1.43$ ,  $M_n(^1\text{H NMR}) = 26,000$  g/mol.  $^1\text{H NMR}$  (500 MHz, C<sub>2</sub>D<sub>2</sub>Cl<sub>4</sub>, 75 °C):  $\delta$  8.83 (s, 3H), 4.37 (t, 6H), 0.68-1.72 (m, 3800H).

**(sPP-(CH<sub>2</sub>)<sub>3</sub>C<sub>2</sub>HN<sub>3</sub>)<sub>2</sub>-C<sub>6</sub>H<sub>4</sub>.** An oven-dried Schlenk flask was cooled under vacuum and charged with sPP-(CH<sub>2</sub>)<sub>3</sub>N<sub>3</sub> (0.30 g, 0.05 mmol) and copper iodide (0.01 g, 0.05 mmol). Toluene (3 mL) and DMSO (3 mL) were syringed into the flask followed by a 0.1 M DMSO solution of 1,4-diethynylbenzene (0.25 mL, 0.025 mmol). The reaction

mixture was heated to 80 °C. After 5 days, the solution was cooled to room temperature and the polymer was precipitated in methanol (100 mL). The polymer was collected, dissolved in hot toluene and filtered through silica, alumina, and Celite. The toluene was removed under reduced pressure and the polymer was dried in vacuo to constant weight (0.24 g, 80% yield).  $M_n(\text{GPC}) = 13,000 \text{ g/mol}$ ,  $M_w/M_n = 1.45$ ,  $M_n(^1\text{H NMR}) = 50,000 \text{ g/mol}$ .  $^1\text{H NMR}$  (500 MHz,  $\text{C}_2\text{D}_2\text{Cl}_4$ , 75 °C):  $\delta$  7.83 (d, 2H), 7.73 (s, 1H), 7.44 (t, 2H), 7.35 (t, 1H), 4.37 (t, 2H), 0.68-1.72 (m, 7100H).

**(sPP-(CH<sub>2</sub>)<sub>3</sub>C<sub>2</sub>HN<sub>3</sub>)<sub>3</sub>-C<sub>6</sub>H<sub>3</sub>.** An oven-dried Schlenk flask was cooled under vacuum and charged with sPP-(CH<sub>2</sub>)<sub>3</sub>N<sub>3</sub> (1.0 g, 0.125 mmol) and copper iodide (0.024 g, 0.125 mmol). Toluene (15 mL) and DMSO (5 mL) were syringed into the flask followed by a 0.05 M DMSO solution of 1,3,5-triethynylbenzene (0.84 mL, 0.042 mmol). The reaction mixture was heated to 80 °C. After 8 days, the solution was cooled to room temperature and the polymer was precipitated in methanol (100 mL). The polymer was collected, dissolved in hot toluene and filtered through silica, alumina, and Celite. The toluene was removed under reduced pressure and the polymer was dried in vacuo to constant weight (0.81 g, 81% yield).  $M_n(\text{GPC}) = 13,000 \text{ g/mol}$ ,  $M_w/M_n = 1.59$ ,  $M_n(^1\text{H NMR}) = 59,000 \text{ g/mol}$ .  $^1\text{H NMR}$  (500 MHz,  $\text{C}_2\text{D}_2\text{Cl}_4$ , 75 °C):  $\delta$  8.30 (s, 3H), 7.94 (s, 3H), 4.41 (t, 6H), 0.68-1.72 (m, 8400H).

**(sPP-(CH<sub>2</sub>)<sub>3</sub>NHCO)<sub>2</sub>-C<sub>6</sub>H<sub>4</sub>.** An oven-dried Schlenk tube was cooled under vacuum and charged with sPP-(CH<sub>2</sub>)<sub>3</sub>NH<sub>2</sub> (0.30 g, 0.05 mmol) and 4 Å molecular sieves. Toluene (4 mL) and triethylamine (0.01 mL, 0.07 mmol) were syringed into the flask followed by a 0.1 M THF solution of terephthaloyl chloride (0.25 mL, 0.025 mmol). The reaction mixture was heated to 100 °C. After 7 days, the solution was cooled to room temperature and the polymer was precipitated in methanol (100 mL). The polymer was collected, dissolved in hot toluene and filtered silica, alumina, and Celite. The toluene was removed under reduced pressure and the polymer was dried in vacuo

to constant weight (0.23 g, 77% yield).  $M_n(\text{GPC}) = 12,000 \text{ g/mol}$ ,  $M_w/M_n = 1.44$ ,  $M_n(^1\text{H NMR}) = 48,000 \text{ g/mol}$ .  $^1\text{H NMR}$  (500 MHz,  $\text{C}_2\text{D}_2\text{Cl}_4$ , 75 °C):  $\delta$  7.81 (s, 4H), 3.48 (t, 4H), 0.68-1.72 (m, 6900H).

**(sPP-(CH<sub>2</sub>)<sub>3</sub>NHCO)<sub>3</sub>-C<sub>6</sub>H<sub>3</sub>**. An oven-dried Schlenk tube was cooled under vacuum and charged with sPP-(CH<sub>2</sub>)<sub>3</sub>NH<sub>2</sub> (1.0 g, 0.33 mmol) and 4 Å molecular sieves. Toluene (10 mL) and triethylamine (0.05 mL, 0.33 mmol) were syringed into the flask followed by a 0.25 M THF solution of 1,3,5-benzenetricarbonyl trichloride (0.44 mL, 0.11 mmol). The reaction mixture was heated to 100 °C. After 7 days, the solution was cooled to room temperature and the polymer was precipitated in methanol (100 mL). The polymer was collected, dissolved in hot toluene and filtered through 8 in. of silica gel. The first 100 mL of toluene were collected, the toluene was removed under reduced pressure and the polymer was dried in vacuo to constant weight (0.48 g, 48% yield).  $M_n(\text{GPC}) = 18,000 \text{ g/mol}$ ,  $M_w/M_n = 1.52$ ,  $^1\text{H NMR}$  (500 MHz,  $\text{C}_2\text{D}_2\text{Cl}_4$ , 75 °C):  $\delta$  0.68-1.72 (br).

**methyl 4-(prop-2-yn-1-yloxy)benzoate**. An oven-dried 250 mL Schlenk adapted round bottom flask was cooled under vacuum and charged with methyl hydroxybenzoate (10.0 g, 65.7 mmol) and potassium carbonate (11.8 g, 85.4 mmol). DMF (100 mL) was added via cannula and propargyl bromide (8.4 mL, 75.6 mmol) was syringed into the flask. After stirring for 24 hours at room temperature, the mixture was filtered, washed with saturated  $\text{NaHCO}_3$  (100 mL), washed with saturated  $\text{NaCl}$  (100 mL) and extracted with methylene chloride (3 x 100 mL). The combined organic layers were dried with  $\text{Na}_2\text{SO}_4$ , filtered and dried in vacuo to constant weight (8.44 g, 68% yield).  $^1\text{H NMR}$  (300 MHz,  $\text{CDCl}_3$ ):  $\delta$  8.00 (d, 2H), 6.99 (d, 2H), 4.73 (d, 2H), 3.87 (s, 3H), 2.56 (t, 1H).  $^{13}\text{C}\{^1\text{H}\}$  NMR (600 MHz,  $\text{CDCl}_3$ ):  $\delta$  166.93, 161.34, 131.77, 123.64, 114.67, 78.00, 76.29, 56.02, 52.17.

**4-(prop-2-yn-1-yloxy)benzoic acid.** A 300 mL round bottom flask was charged with the methyl 4-(prop-2-yn-1-yloxy)benzoate (8.2 g, 43.1 mmol), methanol (50 mL), dioxane (150 mL), and 4 M NaOH (16.1 mL, 64.7 mmol). After stirring at room temperature for 12 hours, the mixture was neutralized with 2 M HCl and the solvent was removed in vacuo. The residual solid was taken up in ethyl acetate, washed with saturated NaHCO<sub>3</sub> (100 mL), washed with saturated NaCl (100 mL) and extracted with ethyl acetate (3 x 100 mL). The combined organic layers were dried with Na<sub>2</sub>SO<sub>4</sub>, filtered and dried in vacuo to constant weight (5.32 g, 70% yield). <sup>1</sup>H NMR (300 MHz, DMSO-d<sub>6</sub>): δ 7.90 (d, 2H), 7.06 (d, 2H), 4.88 (d, 2H), 3.63 (t, 1H), 3.45 (br s, 1H) <sup>13</sup>C{<sup>1</sup>H} NMR (300 MHz, DMSO-d<sub>6</sub>): δ 166.93, 160.73, 131.28, 123.68, 114.66, 78.78, 78.71, 55.63.

**PEG-OC(O)C<sub>6</sub>H<sub>4</sub>OCH<sub>2</sub>C=CH.** An oven-dried Schlenk tube was cooled under vacuum and charged with 4-(prop-2-yn-1-yloxy)benzoic acid (0.10 g, 0.57 mmol) and toluene (10 mL). Oxalyl chloride (0.12 mL, 1.42 mmol) was syringed into the flask and the mixture was warmed to 70 °C. After 4 hours, the solvent was removed and the residual solid was dried in vacuo. Poly(ethylene glycol methyl ether) (1.14 g, 0.23 mmol) was added to the flask followed by toluene (10 mL) and triethylamine (0.08 mL, 0.57 mmol). After stirring at 100 °C for 18 hours, the mixture was cooled to room temperature, washed with water (100 mL) and extracted with chloroform (3 x 100 mL). The combined organic layers were dried with Na<sub>2</sub>SO<sub>4</sub>, filtered and dried in vacuo to constant weight (1.18 g, 98% yield). <sup>1</sup>H NMR (600 MHz, CDCl<sub>3</sub>): δ 8.02 (d, 2H), 6.99 (d, 2H), 4.75 (d, 2H), 4.44 (t, 2H), 3.63 (s, 688H), 3.40 (s, 3H), 2.57 (t, 1H). <sup>13</sup>C{<sup>1</sup>H} NMR (600 MHz, CDCl<sub>3</sub>): δ 169.02, 131.86, 114.62, 88.78, 78.47 76.36, 70.72, 69.46, 64.11, 61.85, 55.99.

**PEG-*block*-sPP.** An oven-dried Schlenk tube was cooled under vacuum and charged with sPP-(CH<sub>2</sub>)<sub>3</sub>N<sub>3</sub> (0.20 g, 0.033 mmol), PEG-OC(O)C<sub>6</sub>H<sub>4</sub>OCH<sub>2</sub>CCH (0.15 g (0.030

mmol) and copper iodide (1.0 mg, 0.006 mmol). Toluene (3 mL) and DMSO (1 mL) were syringed into the tube and the mixture was heated to 80 °C. After 36 hours, the mixture was cooled to room temperature and the solution was poured into copious cold diethyl ether. The polymer was filtered and dried in vacuo to constant weight (0.20 g, 61% yield).  $M_n(\text{GPC}) = 10,000 \text{ g/mol}$ ,  $M_w/M_n = 1.37$ ,  $M_n(^1\text{H NMR}) = 26,000 \text{ g/mol}$ .  $^1\text{H NMR}$  (500 MHz,  $\text{C}_2\text{D}_2\text{Cl}_4$ , 75 °C):  $\delta$  8.01 (d, 2H), 7.60 (s, 1H), 7.05 (d, 2H), 5.26 (s, 2H), 4.44 (t, 2H), 4.32 (t, 2H), 3.63 (t, 886H), 0.68-1.72 (m, 2400H).

**CH=CCH<sub>2</sub>OC<sub>6</sub>H<sub>4</sub>(O)CO-PEG-OC(O)C<sub>6</sub>H<sub>4</sub>OCH<sub>2</sub>CC=H.** An oven-dried Schlenk tube was cooled under vacuum and charged with monopropargyl carboxylic acid (0.10 g, 0.57 mmol) and toluene (10 mL). Oxalyl chloride (0.12 mL, 1.42 mmol) was syringed into the flask and the mixture was warmed to 70 °C. After 4 hours, the solvent was removed and the residual solid was dried in vacuo. Poly(ethylene glycol) (0.91 g, 0.11 mmol) was added to the flask followed by toluene (10 mL) and triethyl amine (0.08 mL, 0.57 mmol). After stirring at 100 °C for 18 hours, the mixture was cooled to room temperature, washed with water (100 mL) and extracted with chloroform (3 x 100 mL). The combined organic layers were dried with  $\text{Na}_2\text{SO}_4$ , filtered and dried in vacuo to constant weight (0.92 g, 97% yield).  $^1\text{H NMR}$  (300 MHz,  $\text{CDCl}_3$ ):  $\delta$  8.01 (d, 4H), 6.98 (d, 4H), 4.75 (s, 4H), 4.43 (t, 4H), 3.63 (s, 621H), 2.57 (s, 1H).  $^{13}\text{C}\{^1\text{H}\}$  NMR (100 MHz,  $\text{CDCl}_3$ ):  $\delta$  166.16, 131.86, 114.62, 107.73, 89.46, 76.36, 70.72, 69.46, 64.11, 55.99.

**sPP-block-PEG-block-sPP.** An oven-dried Schlenk tube was cooled under vacuum and charged with sPP-(CH<sub>2</sub>)<sub>3</sub>N<sub>3</sub> (0.17 g, 0.0275 mmol), CHCCH<sub>2</sub>OC<sub>6</sub>H<sub>4</sub>(O)CO-PEG-OC(O)C<sub>6</sub>H<sub>4</sub>OCH<sub>2</sub>CCH (0.10 g, 0.0125 mmol) and copper iodide (1.0 mg, 0.006 mmol). Toluene (3 mL) and DMSO (1 mL) were syringed into the tube and the mixture was heated to 80 °C. After 36 hours, the mixture was cooled to room temperature and the solution was poured into copious cold diethyl ether. The polymer

was filtered and dried in vacuo to constant weight (0.20 g, 80% yield).  $M_n(\text{GPC}) =$  g/mol,  $M_w/M_n =$ ,  $M_n(^1\text{H NMR}) = 36,000$  g/mol.  $^1\text{H NMR}$  (500 MHz,  $\text{C}_2\text{D}_2\text{Cl}_4$ , 75 °C):  $\delta$  8.01 (d, 4H),  $\delta$  7.60 (s, 2H),  $\delta$  7.05 (d, 4H),  $\delta$  5.26 (s, 4H),  $\delta$  4.44 (t, 4H),  $\delta$  4.33 (t, 4H),  $\delta$  3.63 (s, 1600)  $\delta$  0.68-1.72 (m, 2600H).

**Methyl 3,5-dihydroxybenzoate.** Methanol (300 mL), 3,5-dihydroxy benzoic acid (10.0 g, 64.9 mmol) and sulfuric acid (0.6 mL) were combined in a 500 mL round bottom flask and heated to reflux. After 18 hours, the solution was cooled to room temperature and neutralized with 2 M HCl. The methanol was removed in vacuo and the residual solid was taken up in ethyl acetate, washed with saturated NaCl, dried with  $\text{Na}_2\text{SO}_4$ , filtered and dried in vacuo to constant weight (10.4 g, 95% yield).  $^{13}\text{C}\{^1\text{H}\}$  NMR (600 MHz,  $\text{DMSO}-d_6$ ) : 166.27, 158.56, 131.29, 107.28, 107.17, 107.07, 52.04.

**methyl 3,5-bis(prop-2-yn-1-yloxy)benzoate.** An oven-dried 250 mL Schlenk adapted round bottom flask was cooled under vacuum and charged with the diester (7.50 g, 44.6 mmol) and potassium carbonate (8.00 g, 58.0 mmol). DMF (75 mL) was added via cannula and propargyl bromide (5.71 mL, 51.3 mmol) was syringed into the flask. After stirring for 24 hours at room temperature, the mixture was filtered, washed with saturated  $\text{NaHCO}_3$  (100 mL), washed with saturated NaCl (100 mL) and extracted with methylene chloride (3 x 100 mL). The combined organic layers were dried with  $\text{Na}_2\text{SO}_4$ , filtered and dried in vacuo to constant weight (8.04 g, 74% yield).  $^1\text{H NMR}$  (300 MHz,  $\text{CDCl}_3$ ):  $\delta$  7.27 (s, 2H), 6.79 (s, 1H), 4.70 (s, 4H), 3.89 (s, 3H), 2.54 (s, 1H).  $^{13}\text{C}\{^1\text{H}\}$  NMR (600 MHz,  $\text{CDCl}_3$ ): 166.69, 158.70, 132.34, 109.06, 107.71, 78.14, 76.19, 56.32, 52.60.

**3,5-bis(prop-2-yn-1-yloxy)benzoic acid.** A 250 mL round bottom flask was charged with the methyl 3,5-bis(prop-2-yn-1-yloxy)benzoate (5.0 g, 20.5 mmol), methanol (50 mL), dioxane (150 mL) and 4 M NaOH (7.7 mL, 30.7 mmol). After stirring at room

temperature for 12 hours, the mixture was neutralized with 2 M HCl and the solvent was removed in vacuo. The residual solid was taken up in ethyl acetate, washed with saturated NaHCO<sub>3</sub> (100 mL), washed with saturate NaCl (100 mL) and extracted with ethyl acetate (3 x 100 mL). The combined organic layers were dried with Na<sub>2</sub>SO<sub>4</sub>, filtered and dried in vacuo to constant weight (3.2 g, 69% yield). <sup>1</sup>H NMR (300 MHz, DMSO-d<sub>6</sub>): δ 7.17 (s, 2H), 6.79 (s, 1H), 4.83 (s, 4H), 3.60 (s, 2H). <sup>13</sup>C{<sup>1</sup>H} NMR (600 MHz, DMSO-d<sub>6</sub>): 166.99, 158.11, 134.17, 108.30, 106.47, 78.98, 78.60, 55.74.

**PEG-OC(O)C<sub>6</sub>H<sub>3</sub>(OCH<sub>2</sub>C=CH)<sub>2</sub>.** An oven-dried Schlenk tube was cooled under vacuum and charged with 3,5-bis(prop-2-yn-1-yloxy)benzoic acid (0.10 g, 0.44 mmol) and toluene (10 mL). Oxalyl chloride (0.10 mL, 1.11 mmol) was syringed into the flask and the mixture was warmed to 70 °C. After 4 hours, the solvent was removed and the residual solid was dried in vacuo. Poly(ethylene glycol methyl ether) (0.88 g, 0.18 mmol) was added to the flask followed by toluene (10 mL) and triethylamine (0.06 mL, 0.44 mmol). After stirring at 100 °C for 18 hours, the mixture was cooled to room temperature, washed with water (100 mL) and extracted with chloroform (3 x 100 mL). The combined organic layers were dried with Na<sub>2</sub>SO<sub>4</sub>, filtered and dried in vacuo to constant weight (0.88 g, 97% yield). <sup>1</sup>H NMR (300 MHz, CDCl<sub>3</sub>): δ 7.31 (d, 2H), 6.80 (t, 1H), 4.71 (d, 4H), 4.45 (t, 2H), 3.63 (s, 559H), 3.38 (s, 3H), 2.57 (t, 2H). <sup>13</sup>C{<sup>1</sup>H} NMR (600 MHz, CDCl<sub>3</sub>): 158.64, 109.19, 107.54, 78.09, 76.30, 72.08, 70.71, 69.30, 64.66, 56.28.

**(sPP)<sub>2</sub>-block-PEG.** An oven-dried Schlenk tube was cooled under vacuum and charged with sPP-(CH<sub>2</sub>)<sub>3</sub>N<sub>3</sub> (0.26 g, 0.044 mmol), PEG-OC(O)C<sub>6</sub>H<sub>3</sub>(OCH<sub>2</sub>CCH)<sub>2</sub> (0.10 g, 0.020 mmol) and copper iodide (1.0 mg, 0.006 mmol). Toluene (4 mL) and DMSO (1.3 mL) were syringed into the tube and heated to 80 °C. After 36 hours, the mixture was cooled to room temperature and the solution was poured into copious cold diethyl ether. The polymer was filtered and dried in vacuo to constant weight

(0.20 g, 88% yield).  $M_n(\text{GPC}) = 10,000$  g/mol,  $M_w/M_n = 1.46$ ,  $M_n(^1\text{H NMR}) = 28,000$  g/mol.  $^1\text{H NMR}$  (500 MHz,  $\text{C}_2\text{D}_2\text{Cl}_4$ , 75 °C):  $\delta$  7.62 (s, 2H), 7.33 (s, 2H), 6.94 (s, 1H), 5.23 (s, 4H), 4.46 (t, 2H), 4.33 (t, 4H), 3.63 (s, 800H) 0.68-1.72 (m, 2700H).

**$(\text{CH}=\text{CCH}_2\text{O})_2\text{C}_6\text{H}_3(\text{O})\text{CO-PEG-OC}(\text{O})\text{C}_6\text{H}_3(\text{OCH}_2\text{C}=\text{CH})_2$ .** An oven dried Schlenk tube was cooled under vacuum and charged with 3,5-bis(prop-2-yn-1-yloxy)benzoic acid (0.10 g, 0.44 mmol) and toluene (10 mL). Oxalyl chloride (0.10 mL, 1.11 mmol) was syringed into the flask and the mixture was warmed to 70 °C. After 4 hours, the solvent was removed and the residual solid was dried in vacuo. Poly(ethylene glycol) (0.70 g, 0.09 mmol) was added to the flask followed by toluene (10 mL) and triethylamine (0.06 mL, 0.44 mmol). After stirring at 100 °C for 18 hours, the mixture was cooled to room temperature, washed with water (100 mL) and extracted with chloroform (3 x 100 mL). The combined organic layers were dried with  $\text{Na}_2\text{SO}_4$ , filtered and dried in vacuo to constant weight (0.92 g, 97% yield).  $^1\text{H NMR}$  (300 MHz,  $\text{CDCl}_3$ ):  $\delta$  7.29 (d, 2H), 6.80 (t, 1H), 4.71 (d, 8H), 4.43 (t, 4H), 3.63 (s, 1400H), 2.57 (t, 4H).  $^{13}\text{C NMR}$  (600 MHz,  $\text{CDCl}_3$ ): 166.05, 158.63, 132.27, 109.19, 107.54, 78.10, 76.30, 70.70, 69.30, 64.65, 56.28, 45.90.

**$(\text{sPP})_2\text{-block-PEG-block-(sPP)}_2$ .** An oven-dried Schlenk tube was cooled under vacuum and charged with sPP- $(\text{CH}_2)_3\text{N}_3$  (0.33 g, 0.055 mmol),  $(\text{CHCCH}_2\text{O})_2\text{C}_6\text{H}_3(\text{O})\text{CO-PEG-OC}(\text{O})\text{C}_6\text{H}_3(\text{OCH}_2\text{CCH})_2$  (0.10 g, 0.0125 mmol) and copper iodide (1.0 mg, 0.006 mmol). Toluene (6 mL) and DMSO (2 mL) were syringed into the tube and heated to 80 °C. After 36 hours, the mixture was cooled to room temperature and the solution was poured into copious cold diethyl ether. The polymer was filtered and dried in vacuo to constant weight (0.20 g, 98% yield).  $M_n(\text{GPC}) = 9,100$  g/mol,  $M_w/M_n = 1.51$ ,  $M_n(^1\text{H NMR}) = 75,000$  g/mol.  $^1\text{H NMR}$  (500 MHz,  $\text{C}_2\text{D}_2\text{Cl}_4$ , 75 °C):  $\delta$  7.62 (s, 4H), 7.37 (s, 4H), 6.98 (s, 2H), 5.27 (s, 8H), 4.49 (t, 4H), 4.35 (t, 8H), 3.63 (s, 1800H), 0.68-1.72 (m, 7900H).

## REFERENCES

- (1) Coates, G. W. *Chem. Rev.* **2000**, 100, 1223-1252.
- (2) Resconi, L.; Cavallo, L.; Fait, A.; Piemontesi, F. *Chem. Rev.* **2000**, 100, 1253-1345.
- (3) Vasile, C., General Survey of the Properties of Polyolefins. In *Handbook of Polyolefins*, Second Ed. ed.; Vasile, C., Ed. Marcel Dekker Inc.: New York, 2000; pp 401-412.
- (4) Kennedy, J. P. *J. Poly. Sci., Part A: Poly. Chem.* **1999**, 37, 2285.
- (5) Aoshima, S.; Yoshida, T.; Kanazawa, A.; Kanaoka, S. *J. Poly. Sci., Part A: Poly. Chem.* **2007**, 45, 1801-1813.
- (6) Hadjichristidis, N.; Pitsikalis, M.; Pispas, S.; Iatrou, H. *Chem. Rev.* **2001**, 101, 3747-3792.
- (7) Bisht, H. S.; Chatterjee, A. K. *J. Macromol. Sci., Poly. Rev.* **2001**, 41, 139-173.
- (8) Hawker, C. J.; Bosman, A. W.; Harth, E. *Chem. Rev.* **2001**, 101, 3661-3688.
- (9) Matyjaszewski, K.; Tsarevsky, N. V. *Nature Chem.* **2009**, 1, 276-288.
- (10) Coates, G. W.; Hustad, P. D.; Reinartz, S. *Angew. Chem., Int. Ed.* **2002**, 41, 2236-2257.
- (11) Domski, G. J.; Rose, J. M.; Coates, G. W.; Bolig, A. D.; Brookhart, M. *Prog. Polym. Sci.* **2007**, 32, 30-92.
- (12) Inoue, K. *Prog. Polym. Sci.* **2000**, 25, 453-511.
- (13) Iha, R. K.; Wooley, K. L.; Nystrom, A. M.; Burke, D. J.; Kade, M. J.; Hawker, C. J. *Chem. Rev.* **2009**, 109, 5620-5686.
- (14) Gao, H.; Matyjaszewski, K. *Prog. Polym. Sci.* **2009**, 34, 317-350.
- (15) Peleshanko, S.; Tsukruk, V. V. *Prog. Polym. Sci.* **2008**, 33, 523-580.
- (16) Mihaies, M.; Olaru, A., Mechanical Properties and Parameters of Polyolefins. In *Handbook of Polyolefins*, 2nd ed.; Vasile, C., Ed. Marcel Dekker, Inc.: New York, 2000; pp 267-308.
- (17) Peacock, A. J., *Handbook of Polyethylene*. 1st ed.; Marcel Dekker, Inc.: New York, 2000.

- (18) Doeringhaus, P. J.; Baird, D. G. *J. Rheol.* **2003**, *47*, 717-736.
- (19) Lohse, D. J.; Milner, S. T.; Fetters, L. J.; Xenidou, M.; Hadjichristidis, N.; Mendelson, R. A.; Garcia-Franco, C. A.; Lyon, M. K. *Macromolecules* **2002**, *35*, 3066-3075.
- (20) Tian, J.; Wei, Y.; Zhou, C. *Polymer* **2006**, *47*, 7962-7969.
- (21) Su, F.-H.; Huang, H.-X. *J. Appl. Poly. Sci.* **2009**, *113*, 2126-2135.
- (22) Gotsis, A. D.; Zeevenhoven, B. L. F. *J. Rheol.* **2004**, *48*, 895-914.
- (23) Ye, Z.; Zhu, S. *J. Poly. Sci., Part A: Poly. Chem.* **2003**, *41*, 1152-1159.
- (24) Weng, W.; Markel, E. J.; Dekmezian, A. H. *Macromol. Rapid Commun.* **2001**, *22*, 1488-1492.
- (25) Lagendijk, R. P.; Hogt, A. H.; Buijtenhuijs, A.; Gotsis, A. D. *Polymer* **2001**, *42*, 10035-10043.
- (26) Fetters, L. J.; Kiss, A. D.; Pearson, D. S. *Macromolecules* **1993**, *26*, 647-654.
- (27) Tezel, A. K.; Leal, G. L. *Macromolecules* **2006**, *39*, 4605-4614.
- (28) Kapnistos, M.; Koutalas, G.; Hadjichristidis, N.; Roovers, J.; Lohse, D. J.; Vlassopoulos, D. *Rheol. Acta* **2006**, *46*, 273-286.
- (29) Hepperle, J.; Munstedt, H.; Haug, P. K.; Eisenbach, C. D. *Rheol. Acta* **2005**, *45*, 151-163.
- (30) Watanabe, H.; Matsumiya, Y.; Ishida, S.; Takigawa, T.; Yamamoto, T.; Vlassopoulos, D.; Roovers, J. *Macromolecules* **2005**, *38*, 7404-7415.
- (31) Daniels, R. D.; McLeish, T. C. B.; Kant, R.; Crosby, B. J.; Young, R. N.; Pryke, A.; Allgaier, J.; Groves, D. J.; Hawkins, R. J. *Rheol. Acta* **2001**, *40*, 403-415.
- (32) Jabbarzadeh, A.; Atkinson, J. D.; Tanner, R. I. *Macromolecules* **2003**, *36*, 5020-5031.
- (33) Pakula, T. *Macromol. Symp.* **2004**, *214*, 307-315.
- (34) Auhl, D.; Stange, J.; Munstedt, H.; Krause, B.; Voigt, D.; Lederer, A.; Lappan, U.; Lunkwitz, K. *Macromolecules* **2004**, *37*, 9465-9472.
- (35) Vega, D. A.; Sebastian, J. M.; Russel, W. B.; Register, R. A. *Macromolecules* **2002**, *35*, 169-177.

- (36) McLeish, T. C. B.; Allgaier, J.; Bick, D. K.; Bishko, G.; Biswas, P.; Blackwell, R.; Blottiere, B.; Clarke, N.; Gibbs, B.; Groves, D. J.; Hakiki, A.; Heenan, R. K.; Johnson, J. M.; Kant, R.; Read, D. J.; Young, R. N. *Macromolecules* **1999**, *32*, 6734-6758.
- (37) Blottiere, B.; McLeish, T. C. B.; Hakiki, A.; Young, R. N.; Milner, S. T. *Macromolecules* **1998**, *31*, 9295-9304.
- (38) Milner, S. T.; McLeish, T. C. B. *Macromolecules* **1998**, *31*, 7479-7482.
- (39) Hadjichristidis, N. *J. Poly. Sci., Part A: Poly. Chem.* **1999**, *37*, 857-871.
- (40) Schaeffgen, J. R.; Flory, P. J. *J. Am. Chem. Soc.* **1948**, *70*, 2709-2718.
- (41) Driva, P.; Lohse, D. J.; Hadjichristidis, N. *J. Poly. Sci., Part A: Poly. Chem.* **2008**, *46*, 1826-1842.
- (42) Fragouli, P.; Iatrou, H.; Hadjichristidis, N.; Sakurai, T.; Matsunaga, Y.; Hirao, A. *J. Poly. Sci., Part A: Poly. Chem.* **2006**, *44*, 6587-6599.
- (43) Avgeropoulos, A.; Hadjichristidis, N. *J. Poly. Sci., Part A: Poly. Chem.* **1997**, *35*, 813-816.
- (44) Adams, C. H.; Hutchings, L. R.; Klein, P. G.; McLeish, T. C. B.; Richards, R. W. *Macromolecules* **1996**, *29*, 5717-5722.
- (45) Hadjichristidis, N.; Xenidou, M.; Iatrou, H.; Pitsikalis, M.; Poulos, Y.; Avgeropoulos, A.; Sioula, S.; Paraskeva, S.; Velis, G.; Lohse, D. J.; Schulz, D. N.; Fetters, L. J.; Wright, P. J.; Mendelson, R. A.; Garcia-Franco, C. A.; Sun, T.; Ruff, C. J. *Macromolecules* **2000**, *33*, 2424-2436.
- (46) Bender, J. T.; Knauss, D. M. *J. Poly. Sci., Part A: Poly. Chem.* **2006**, *44*, 828-836.
- (47) Vazaios, A.; Lohse, D. J.; Hadjichristidis, N. *Macromolecules* **2005**, *38*, 5468-5474.
- (48) Sioula, S.; Tselikas, Y.; Hadjichristidis, N. *Macromolecules* **1997**, *30*, 1518-1520.
- (49) Zhongde, X.; Mays, J.; Xuexin, C.; Hadjichristidis, N.; Schilling, F. C.; Bair, H. E.; Pearson, D. S.; Fetters, L. J. *Macromolecules* **1985**, *18*, 2560-2566.
- (50) Mavroudis, A.; Avgeropoulos, A.; Hadjichristidis, N.; Thomas, E. L.; Lohse, D. J. *Chem. Mater.* **2003**, *15*, 1976-1983.

- (51) Mavroudis, A.; Avgeropoulos, A.; Hadjichristidis, N.; Thomas, E. L.; Lohse, D. J. *Chem. Mater.* **2006**, 18, 2164-2168.
- (52) Rose, J. M.; Mourey, T. H.; Slater, L. A.; Keresztes, I.; Fetters, L. J.; Coates, G. W. *Macromolecules* **2008**, 41, 559-567.
- (53) Kaneko, H.; Kojoh, S.-I.; Kawahara, N.; Matsuo, S.; Matsugi, T.; Kashiwa, N. *J. Poly. Sci., Part A: Poly. Chem.* **2005**, 43, 5103-5118.
- (54) Kaneko, H.; Kojoh, S.; Kawahara, N.; Matsuo, S.; Matsugi, T.; Kashiwa, N. *Macromol. Symp.* **2004**, 213, 335-345.
- (55) Zhang, K.; Ye, Z.; Subramanian, R. *Macromolecules* **2009**, 42, 2313-2316.
- (56) Kolb, H. C.; Finn, M. G.; Sharpless, B. K. *Angew. Chem., Int. Ed.* **2001**, 40, 2004-2021.
- (57) Moses, J. E.; Moorhouse, A. D. *Chem. Soc. Rev.* **2007**, 36, 1249-1262.
- (58) Hoyle, C. E.; Bowman, C. N. *Angew. Chem., Int. Ed.* **2010**, 49, 1540-1573.
- (59) Becer, C. R.; Hoogenboom, R.; Schubert, U. S. *Angew. Chem., Int. Ed.* **2009**, 48, 4900-4908.
- (60) Gil, M. V.; Arevalo, M. J.; Lopez, O. *Synthesis* **2007**, 11, 1589-1620.
- (61) Kolb, H. C.; Sharpless, B. K. *Drug Discovery Today* **2003**, 8, 1128-1137.
- (62) Hein, C. D.; Liu, X.-M.; Wang, D. *Pharmaceutical Research* **2008**, 25, 2216-2230.
- (63) Franc, G.; Kakkar, A. K. *Chem. Eur. J.* **2009**, 15, 5630-5639.
- (64) Golas, P. L.; Matyjaszewski, K. *Chem. Soc. Rev.* **2010**, 39, 1338-1354.
- (65) Sumerlin, B. S.; Vogt, A. P. *Macromolecules* **2010**, 43, 1-13.
- (66) Billiet, L.; Fournier, D.; Prez, F. D. *Polymer* **2009**, 50, 3877-3886.
- (67) Barner-Kowollik, C.; Inglis, A. J. *Macromol. Chem. Phys.* **2009**, 210, 987-992.
- (68) Carlmark, A.; Hawker, C.; Hult, A.; Malkoch, M. *Chem. Soc. Rev.* **2009**, 38, 352-362.
- (69) Le Droumaguet, B.; Velonia, K. *Macromol. Rapid Commun.* **2008**, 29, 1073-1089.

- (70) Johnson, J. A.; Finn, M. G.; Koberstein, J. T.; Turro, N. J. *Macromol. Rapid Commun.* **2008**, 29, 1052-1072.
- (71) Binder, W. H.; Sachsenhofer, R. *Macromol. Rapid Commun.* **2008**, 29, 952-981.
- (72) Lundberg, P.; Hawker, C. J.; Hult, A.; Malkoch, M. *Macromol. Rapid Commun.* **2008**, 29, 998-1015.
- (73) Nandivada, H.; Jiang, X.; Lahann, J. *Adv. Mater.* **2007**, 19, 2197-2208.
- (74) Fournier, D.; Hoogenboom, R.; Schubert, U. S. *Chem. Soc. Rev.* **2007**, 36, 1369-1380.
- (75) Roovers, J., *Encyclopedia of Polymer Science and Engineering*. 1985-1990; Vol. 2, p 478-499.
- (76) Schulz, G. V. *Z. Physik. Chem.* **1939**, B43, 25.
- (77) De Greef, T. F. A.; Smulders, M. M. J.; Wolffs, M.; Schenning, A. P. H.; Sijbesma, R. P.; Meijer, E. W. *Chem. Rev.* **2009**, 109, 5687-5754.
- (78) Stals, P. J. M.; Haveman, J. F.; Martin-Rapun, R.; Fitie, C. F. C.; Palmans, A. R. A.; Meijer, E. W. *J. Mater. Chem.* **2009**, 19, 124-130.
- (79) Smulders, M. M. J.; Schenning, A. P. H.; Meijer, E. W. *J. Am. Chem. Soc.* **2008**, 130, 606-611.
- (80) Roosma, J.; Mes, T.; Leclere, P.; Palmans, A. R. A.; Meijer, E. W. *J. Am. Chem. Soc.* **2008**, 130, 1120-1121.
- (81) Forster, S.; Antonietti, M. *Adv. Mater.* **1998**, 10, 195-217.
- (82) Rosler, A.; Vandermeulen, G. W. M.; Klok, H.-A. *Adv. Drug. Delivery Rev.* **2001**, 53, 95-108.
- (83) Letchford, K.; Burt, H. *Eur. J. Pharma. Biopharma.* **2007**, 65, 259-269.
- (84) Zhou, J.; Wang, L.; Ma, J. *Designed Monomers and Polymers* **2009**, 12, 19-41.
- (85) Hillmyer, M. A.; Lipic, P. M.; Hajduk, D. A.; Almdal, K.; Bates, F. S. *J. Am. Chem. Soc.* **1997**, 119, 2749-2750.
- (86) Dijkgraaf, I.; Rijnders, A. Y.; Soede, A.; Dechesne, A. C.; van Esse, G. W.; Brouwer, A. J.; Corstens, F. H. M.; Boerman, O. C.; Rijkers, D. T. S.; Liskamp, R. M. J. *Org. Biomol. Chem.* **2007**, 5, 935-944.

- (87) Mulders, S. J. E.; Brouwer, A. J.; van der Meer, P. G. J.; Liskamp, R. M. J. *Tet. Lett.* **1997**, 38, 631-634.
- (88) Brouwer, A. J.; Mulders, S. J. E.; Liskamp, R. M. J. *Eur. J. Org. Chem.* **2001**, 1903-1915.

# **Chapter 4**

Synthesis and Ring Opening Polymerization of  
Norbornene-Terminated Syndiotactic Polypropylene

## 4.1 Introduction

The ability to control bulk polymer properties through manipulation of molecular weight, stereochemistry and polymer structure remains an overarching goal in the field of polymer chemistry. Over the last few decades, the development of single-site transition metal olefin polymerization catalysts has resulted in polyolefin materials with well-defined structures.<sup>1-4</sup> Specifically, the production of polymers with high stereo- and regioregularity can give rise to materials with drastically improved properties.<sup>5</sup> Another way to modify the observed properties of a polymeric material is to control the amount of branching in the system. The presence of even a small amount of long-chain branching in a polyolefin significantly alters properties such as processability and melt strength.<sup>6-9</sup> For example, the incorporation of long-chain branches (Figure 4.1) in polypropylene has been shown to increase the melt strength of the polymer up to ten times that of its linear analog.<sup>10</sup> Even minimal incorporation of long-chain branches in polyolefin materials has an effect on observed properties, therefore, the investigation of highly branched polypropylene materials should be targeted.

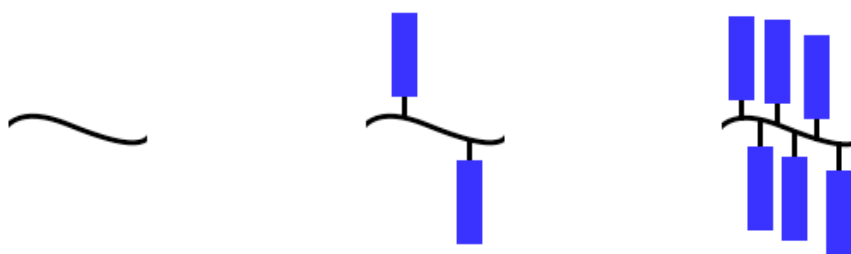


**Figure 4.1.** Representative structure of linear (left), long-chain branched (middle) and comb polymers (right).

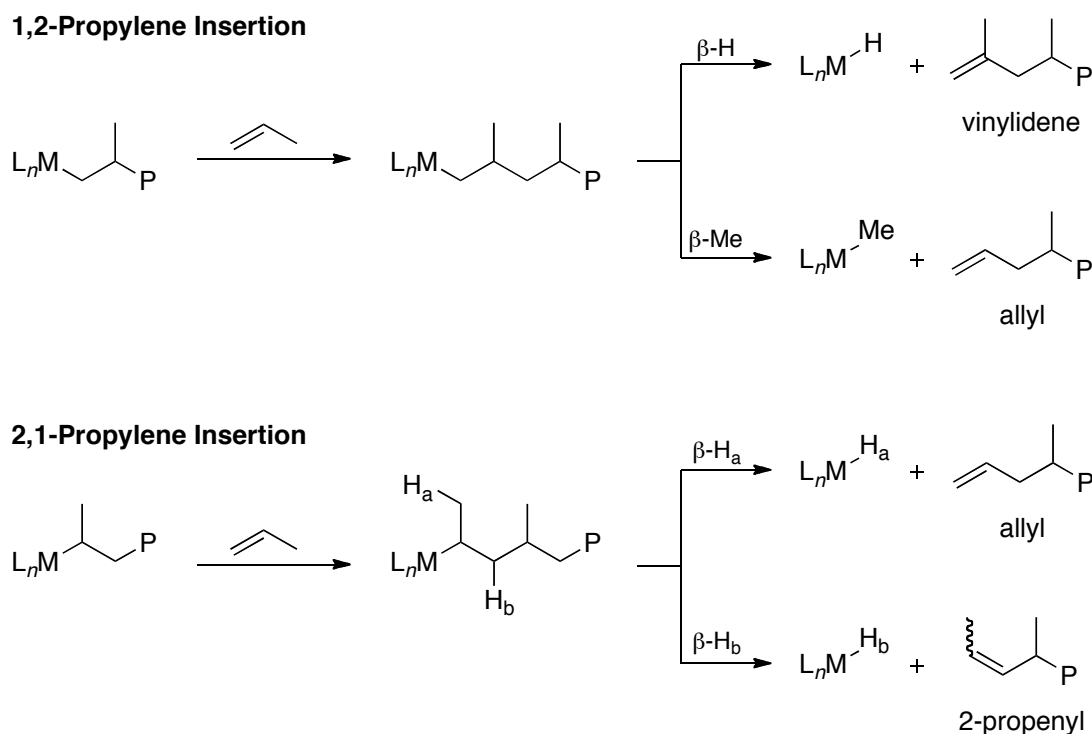
Comb polymers (Figure 4.1) are a type of hyperbranched material which contain one long-chain branch per repeat unit of the polymer backbone.<sup>11-15</sup> The high-

density of polymer arms along the backbone often results in the material adopting a compact cylindrical shape as opposed to the more commonly observed spherical shape.<sup>16-18</sup> Typical materials display lengths on the nanometer scale making the polymers useful in applications such as nanotubes,<sup>19</sup> nanocapsules<sup>20</sup> or templates for inorganic nanowires.<sup>21</sup> To synthesize comb polymers, one of three methods is typically employed.<sup>11,13,18</sup> In the “grafting onto” method, side-chains are prepared independently and then coupled to a functionalized polymer backbone.<sup>22-24</sup> Although properties such as molecular weight are easily characterized with this method, steric crowding often precludes formation of a comb-polymer with a high density of side-chains. Alternatively, the “grafting from” method employs a polymer backbone bearing initiating groups capable of polymerization as a basis for side-chain synthesis.<sup>16,25-28</sup> As with the previous method, a high density of side-chains is often difficult to obtain due to steric hindrance at the polymerization site. Furthermore, side-chain properties including molecular weight can be difficult to quantify. Finally, the “grafting through” or macromonomer method utilizes polymeric materials containing polymerizable functional groups.<sup>17,18,26,29</sup> With this approach, side-chains can be thoroughly characterized prior to polymerization. Additionally, each repeat unit is guaranteed to contain a polymer side-chain, so truly high-density comb polymers can be synthesized. Although a high degree of polymerization can be challenging to obtain, techniques including controlled/living radical<sup>16,22,25,27</sup> and ring-opening metathesis (ROMP)<sup>16-18,25-27,30</sup> have been employed in the synthesis of comb polymers. In particular, Bowden and coworkers have reported the successful production of several ultra-high molecular weight comb homo- and block copolymers containing polystyrene, polynorbornene and polylactide.<sup>16,25-27,30,31</sup> Therefore, we utilized the macromonomer method to produce branched, high molecular weight polypropylene comb polymers.

Despite a significant amount of research in this area,<sup>16-29</sup> there remain relatively few examples of comb polymers produced from the polymerization of polypropylene based macromonomers. In 2008, the homopolymerization of allyl-terminated poly(ethylene-*co*-propylene) using a living nickel  $\alpha$ -diimine catalyst, which resulted in star-like polymers containing up to 16 branches per sample, was reported.<sup>32</sup> Due to a low degree of polymerization, these polymers possessed star-like conformations in dilute solutions instead of the rigid rod structure that would be expected for higher molecular weight comb polymers. In another example employing end-functionalized polymers, Kaneko and coworkers utilized methacryloyl-terminated poly(ethylene-*co*-propylene) in free radical copolymerizations with methyl methacrylate.<sup>33,34</sup> With this method, graft and star copolymers were produced containing poly(methyl methacrylate) backbones and poly(ethylene-*co*-propylene) branches. Alternatively, the homopolymerization of semicrystalline polypropylene macromonomers (syndiotactic or isotactic) has been more difficult to achieve due in part to lower solubility compared with poly(ethylene-*co*-propylene) macromonomers. To synthesize semicrystalline polypropylene comb-polymers, syndiotactic polypropylene bearing a highly reactive, polymerizable functional group at the terminus was required. Specifically, a norbornene-terminated polypropylene was targeted due to previous reports of high reactivity with ring-opening metathesis polymerization catalysts for the synthesis of poly(macromonomer)s.<sup>16-18,25-27</sup>

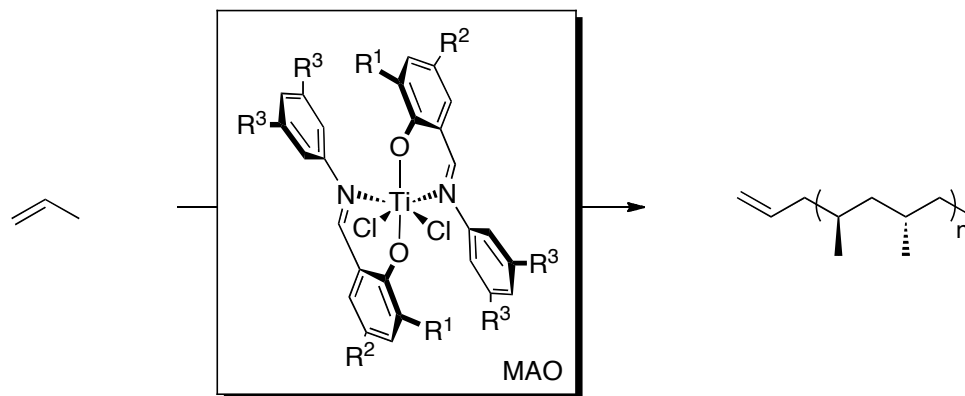
As was discussed extensively in chapter 2, end-functionalized polyolefins may be produced using a variety of different methods including thermal degradation<sup>35,36</sup> and chain transfer polymerization,<sup>37-43</sup> as well as living<sup>44-51</sup> and non-living<sup>52-64</sup> transition metal catalysis. Of particular interest are non-living transition metal olefin polymerization catalysts because of their ability to produce multiple polymer chains per metal center without the addition of a chain transfer agent (Scheme 4.1).<sup>2</sup> Non-

living olefin polymerization catalysts are known to undergo chain-release through  $\beta$ -hydrogen or  $\beta$ -methyl transfers, which result in a number of alkene-terminated polymers. Most commonly, a 1,2-insertion of propylene into the growing polymer chain followed by  $\beta$ -hydrogen transfer gives vinylidene-terminated polypropylene, which would be less desirable for further end-functionalization due to the steric bulk present at the alkene. Alternatively,  $\beta$ -methyl transfer from the same growing polymer chain results in allyl-terminated polypropylene, a much less sterically hindered macromonomer. A handful of metallocene catalysts have been observed to produce allyl end-groups following 1,2-propylene insertion, however, selectivities are at best 90% with vinylidenes making up the remaining chain-ends.<sup>63,65-67</sup> In systems that are capable of 2,1 propylene insertion,  $\beta$ -hydrogen transfer could result in two different



**Scheme 4.1.** Olefin polymerization chain-transfer pathways.

alkene-terminated polymers. Transfer of a  $\beta$ -hydrogen from the terminal methyl ( $\beta$ -H<sub>a</sub>) results in an allyl-terminated polypropylene, whereas  $\beta$ -hydrogen transfer from the internal methylene ( $\beta$ -H<sub>b</sub>) gives a polymer with a 2-propenyl end-group. Complexes of both titanium<sup>68</sup> and iron<sup>69-72</sup> have been shown to undergo propylene polymerization in a 2,1 fashion with subsequent  $\beta$ -hydrogen transfer resulting in polypropylene with terminal allyl groups. In fact, when 2,1-insertion dominates propylene polymerization, terminal allyl groups are almost exclusively observed.<sup>68</sup> Many alkene-terminated polypropylenes have served as useful synthetic intermediates in the production of polymers with alternative functional groups, such as alcohols and amines.<sup>52-64</sup> Furthermore, end-functionalized polymers are attractive building blocks for the synthesis of more complex architectures such as block copolymers<sup>73-77</sup> and star polymers.<sup>78-85</sup>



**Scheme 4.2.** Synthesis of allyl-terminated syndiotactic polypropylene using non-living bis(phenoxyimine)titanium catalysts.

Upon activation with methylaluminoxane (MAO), bis(phenoxyimine)titanium catalysts polymerize propylene in a 2,1 fashion to produce highly syndiotactic polypropylene (Scheme 4.2).<sup>68,86-101</sup> Extensive ligand modification has been carried

out, and studies have shown the fluorination pattern of the N-aryl ring has a significant effect on the nature of the polymerization.<sup>68,95,101</sup> With at least one fluorine present in the *ortho* position of the N-aryl ring, bis(phenoxyimine)titanium complexes catalyze the living polymerization of propylene resulting in polypropylene with completely saturated end-groups upon quenching with a protic electrophile. However, when all fluorines are removed from the *ortho* position of the N-aryl ring, the subsequent propylene polymerization is no longer living and the dominant chain termination pathway is  $\beta$ -hydrogen transfer.<sup>68</sup> The <sup>1</sup>H NMR spectrum of the polypropylene produced from non-living bis(phenoxyimine)titanium catalysts reveals only allyl-termination, with no vinylidene or internal alkenes observed. The syndiotactic polypropylene produced in this fashion is ideal for this study due to a low degree of steric hindrance at the chain-end.

Herein the synthesis and ring-opening metathesis polymerization of norbornene-terminated syndiotactic polypropylene macromonomers is reported. Polymers of varying molecular weights were produced from two different bis(phenoxyimine)titanium catalysts (**4.1** and **4.2**). Hydroxyl and norbornene end-functionalized polypropylene were obtained from the allyl-terminated polymer. Subsequent ring-opening metathesis polymerization reactions were carried out using ruthenium catalysts (**4.3** – **4.5**) resulting in the production of a new class of high molecular weight, syndiotactic comb polymers.

## **4.2 Results and Discussion**

### **4.2.1 Synthesis of Syndiotactic Polypropylene Macromonomer**

Activation of bis(phenoxyimine) titanium complexes **4.1** and **4.2** with MAO in the presence of propylene resulted in a polymer with modest molecular weight (Table 4.1,  $M_n = 3,600$  and  $5,600$  g/mol, respectively).<sup>68</sup> Bis(phenoxyimine) titanium

complexes bearing hydrogens in the *ortho*-positions of the N-aryl ring have previously been shown to insert propylene in a 2,1 fashion with subsequent chain transfer reactions resulting in alkene-terminated polypropylene.<sup>68</sup> Due to the 2,1-insertion mechanism (Scheme 4.1), propenyl- as well as allyl-terminated polymer could be produced from  $\beta$ -hydrogen transfer. Examination of the polypropylene <sup>1</sup>H NMR spectrum (Figure 4.2 and 4.5) revealed two resonances at  $\delta$  5.81 and 5.01 ppm, which have been assigned to the allyl functional group. Further analysis shows no resonance at  $\delta$  5.5, which would be indicative of the 2-propenyl end-group. Using <sup>13</sup>C NMR spectroscopy to analyze the polymer microstructure, a range of tacticities was observed from moderately ( $[rrrr] = 0.80$ ) for the polypropylene produced by **4.1** (MM-3600, Figure 4.3) to highly syndiotactic ( $[rrrr] = 0.94$ ) for the polymer obtained from **4.2** (MM-5600, Figure 4.4). As a result, the polymers displayed a range of melting temperatures ( $T_m = 113$  and  $145$  °C) as determined by differential scanning calorimetry. Fortunately, the semicrystalline allyl-terminated polypropylene produced by **4.1** and **4.2** are highly soluble in many solvents making a variety of organic transformations possible.

**Table 4.1.** Syndiotactic polypropylene macromonomer characterization.

MM	Cplx	R <sup>1</sup>	R <sup>2</sup>	$M_n$ (g/mol) <sup>a</sup>	$M_w/M_n$ <sup>a</sup>	$[rrrr]$ <sup>b</sup>	$T_c$ (°C) <sup>c</sup>	$T_m$ (°C) <sup>c</sup>	$\Delta H_m$ (J/g) <sup>c</sup>
MM-3600	<b>4.1</b>	<i>t</i> Bu	<i>t</i> Bu	3,600	1.87	0.80	72	113	40
MM-5600	<b>4.2</b>	SiMe <sub>3</sub>	H	5,600	1.75	0.94	109	145	42

<sup>a</sup> Molecular weight ( $M_n$ ) and molecular weight distribution ( $M_w/M_n$ ) were determined by gel permeation chromatography at  $140$  °C in 1,2,4-trichlorobenzene relative to polyethylene standards. <sup>b</sup> Syndiotacticity ( $[rrrr]$ ) was determined using <sup>13</sup>C NMR spectroscopy. <sup>c</sup> Melting temperature ( $T_m$ ), crystallization temperature ( $T_c$ ) and enthalpy ( $\Delta H$ ) were determined by differential scanning calorimetry (second heating run).

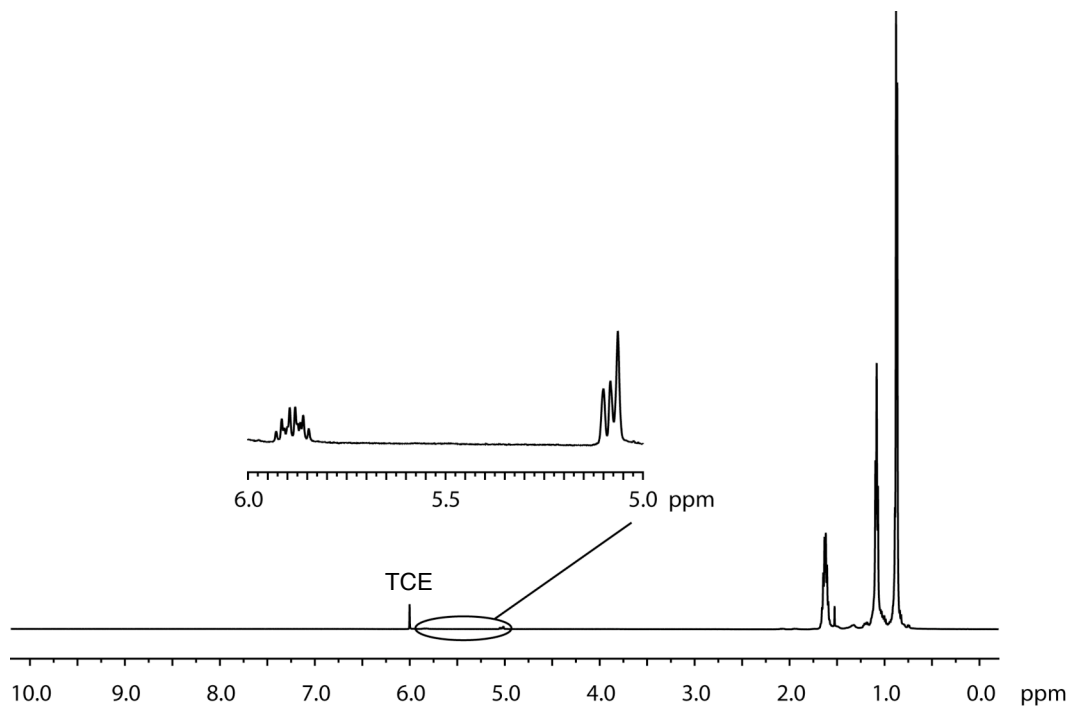


**Figure 4.2.**  $^1\text{H}$  NMR spectrum of sPP-allyl produced with **4.1** (Entry 1, Table 4.1, 600 MHz, 1,1,2,2-tetrachloroethane- $d_2$  (TCE), 135 °C).

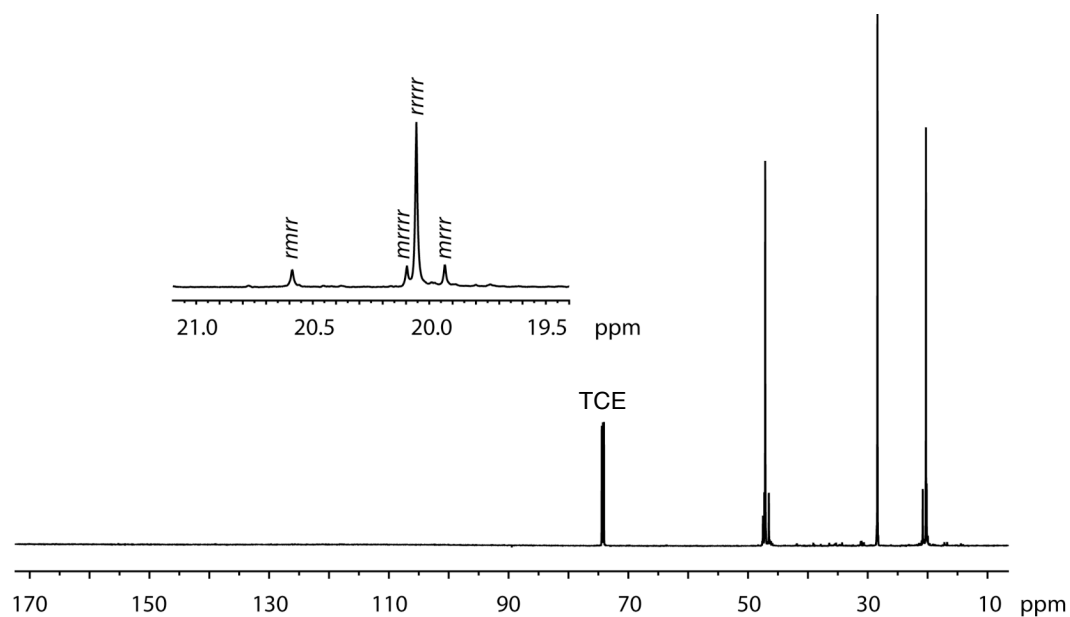


**Figure 4.3.**  $^{13}\text{C}\{^1\text{H}\}$  NMR spectrum of MM-3600 (Entry 1, Table 4.1, 600 MHz, 1,1,2,2-tetrachloroethane- $d_2$  (TCE), 135 °C).

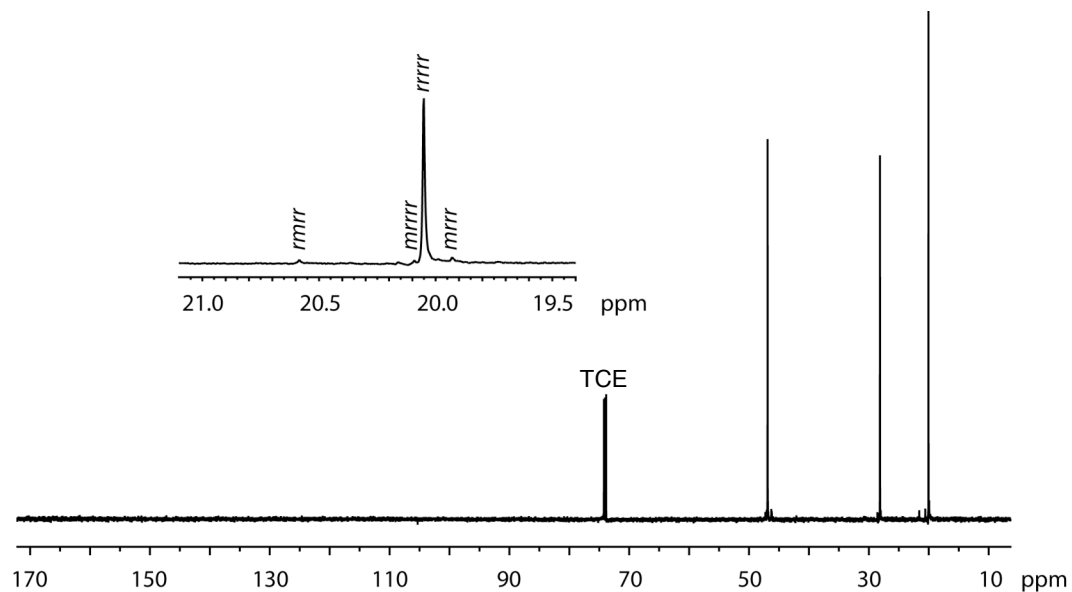


**Figure 4.4.**  $^{13}\text{C}\{\text{H}\}$  NMR spectrum of MM-5600 (Entry 2, Table 4.1, 600 MHz, 1,1,2,2-tetrachloroethane- $d_2$  (TCE), 135 °C).

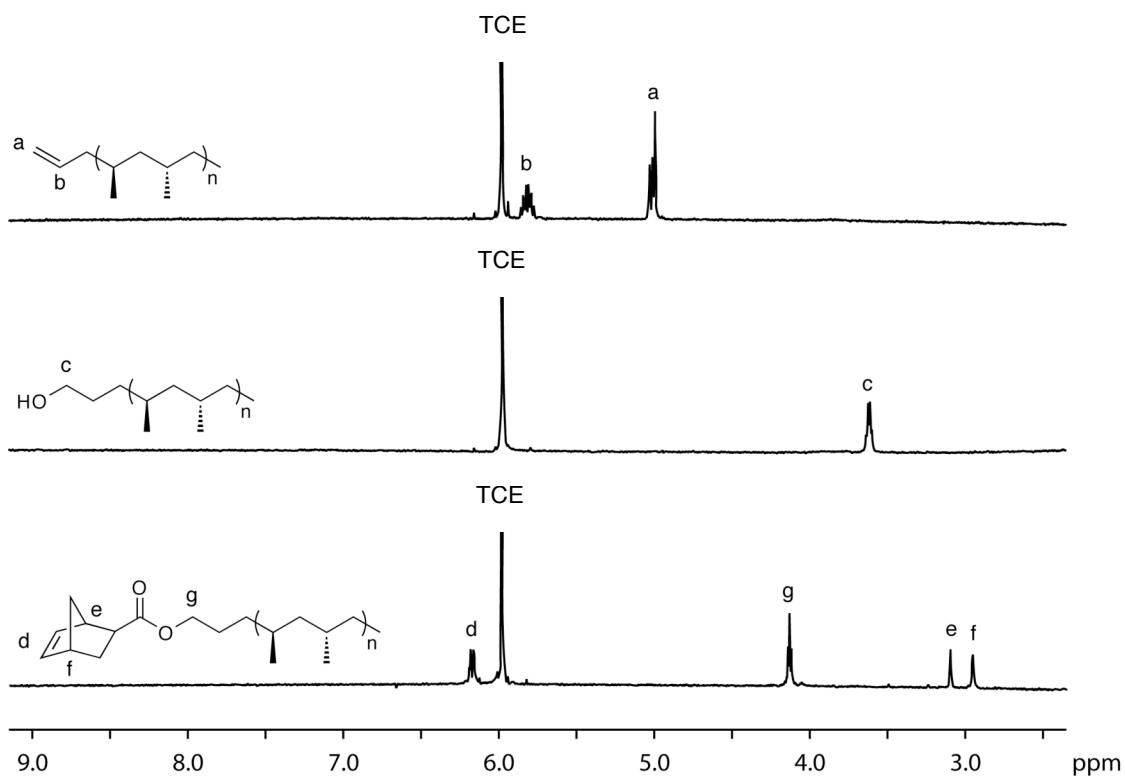
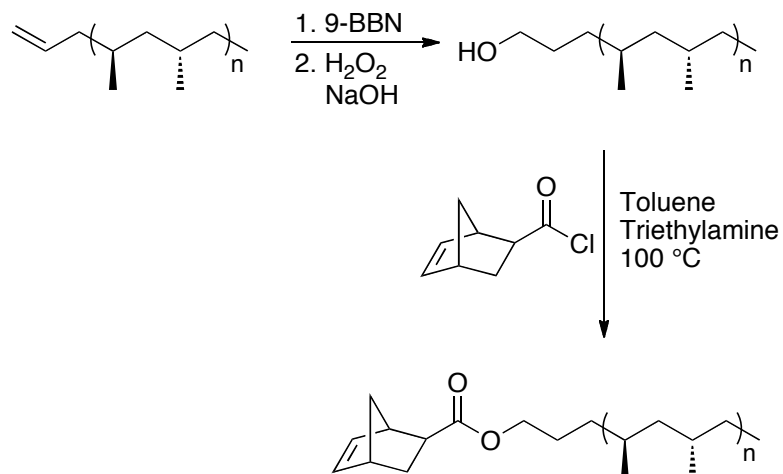


**Figure 4.5.**  $^1\text{H}$  NMR spectra of sPP-allyl, sPP-hydroxyl and sPP-norbornene (MM-3600, 600 MHz, 1,1,2,2-tetrachloroethane- $d_2$  (TCE), 135 °C).

The terminal alkene moiety was utilized as a synthetic handle for the production of end-functionalized polypropylene bearing functional groups with increased reactivity. The allyl-functionalized polypropylene can easily be converted to primary hydroxyl-terminated polypropylene using hydroboration-oxidation (Scheme 4.3). In 2005, Hagiwara and coworkers reported the conversion of vinylidene-terminated polypropylene formed through controlled thermal degradation to the primary alcohol using a borane-THF complex and subsequent hydrogen peroxide oxidation.<sup>36</sup> Conversion of the vinylidene to the hydroxyl end-group was achieved in greater than 90% yields for most of the polymers utilized in their study. Using a similar procedure, the allyl-terminated syndiotactic polypropylene produced with **4.1** and **4.2** was converted to the hydroxyl-functionalized polymer using 9-BBN at 65 °C followed by the addition of sodium hydroxide and hydrogen peroxide. Analysis of the <sup>1</sup>H NMR spectrum (Figures 4.5 and 4.6) showed complete disappearance of the alkene resonances and the appearance of a new resonance ( $\delta$  3.61) for the protons on the methylene adjacent to the hydroxyl and is consistent with literature reports for hydroxyl-terminated polymers.<sup>36</sup> Conversion to product was dependent on the solvent, time and temperature at which the oxidation was performed. For the allyl-terminated syndiotactic polypropylene produced from **4.1**, carrying the hydroboration out at 60 °C in THF followed by oxidation at 45 °C resulted in high conversion to hydroxyl-terminated polypropylene (92%). Due to lower solubility of the highly syndiotactic polymer produced from **4.2**, the hydroboration-oxidation was carried out in toluene, resulting in slightly lower conversion to hydroxyl-terminated polymer (60%). Installing the primary hydroxyl group on the end of the polypropylene chain resulted in an end-functionalized polymer, which was useful for the production of a syndiotactic polypropylene macromonomer.



**Scheme 4.3.** Synthesis of norbornene-terminated syndiotactic polypropylene.

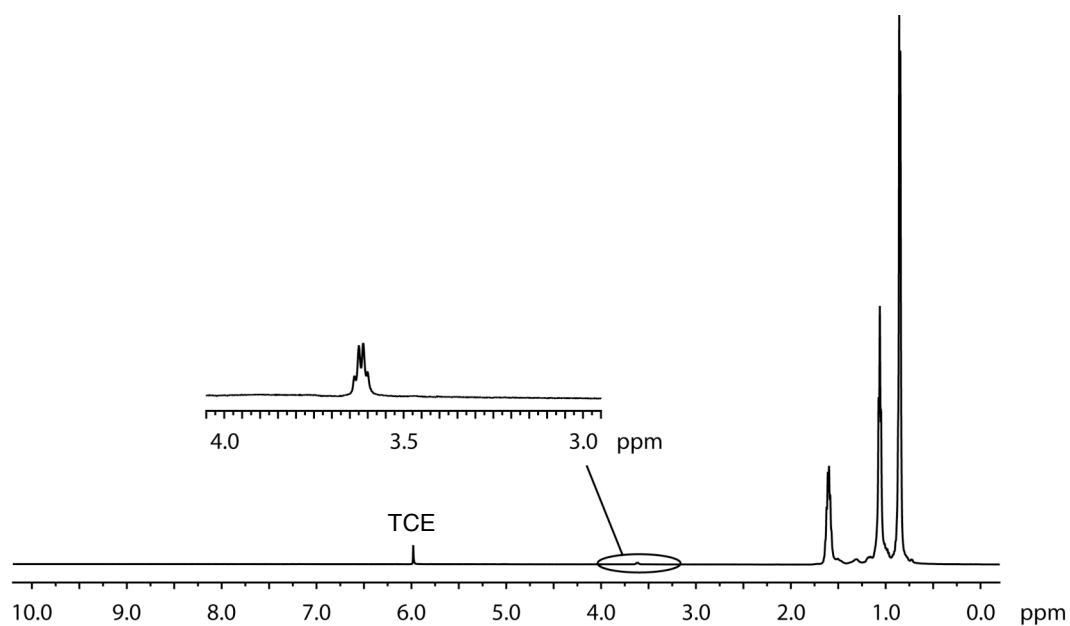


**Figure 4.6.** <sup>1</sup>H NMR spectrum of sPP-hydroxyl (MM-3600, 600 MHz, 1,1,2,2-tetrachloroethane-*d*<sub>2</sub> (TCE), 135 °C).

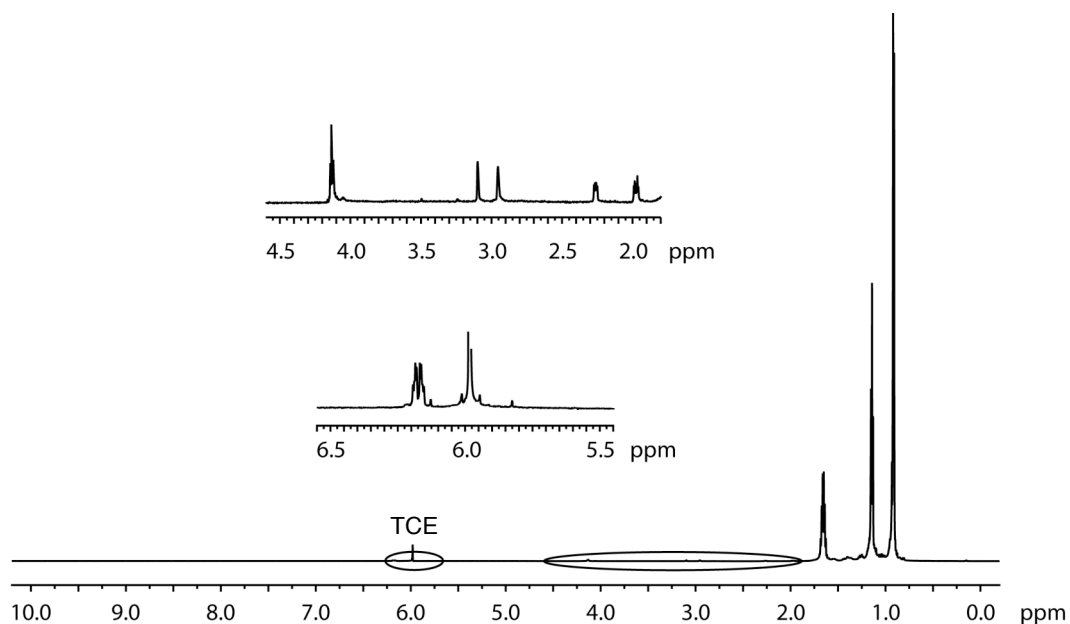


**Figure 4.7.**  $^1\text{H}$  NMR spectrum of *s*PP-norbornene (*exo*-MM-3600, 600 MHz, 1,1,2,2-tetrachloroethane- $d_2$  (TCE), 135 °C).

In particular, reaction of the hydroxyl-terminated polypropylene with acid chlorides was facile and was therefore utilized to produce polymerizable macromonomers. Ring opening metathesis polymerization of norbornene-terminated macromonomers has been achieved by a number of research groups to obtain high molecular weight poly(macromonomer)s.<sup>16-18,25-27,30</sup> Specifically, Bowden and coworkers observed decreased reaction rates, as well as molecular weights for the polymerization *endo/exo*-norbornene-terminated polylactide macromonomers compared with pure *exo*-norbornene-terminated polylactide macromonomers.<sup>26</sup> Therefore, the synthesis and subsequent polymerization behavior of *exo*-norbornene-terminated syndiotactic polypropylene was investigated. Starting from *exo*-5-norbornene-2-carboxylic acid, transformation of the carboxylic acid to the acid chloride was achieved with oxalyl chloride in toluene at 70 °C. The resultant acid chloride was combined with the hydroxyl-terminated syndiotactic polypropylene in

the presence of triethylamine and toluene at 100 °C. The *exo*-norbornene-terminated syndiotactic polypropylene macromonomers (*exo*-MM-3600 and *exo*-MM-5600) were produced utilizing the polymers obtained from catalyst **4.1** and **4.2**. <sup>1</sup>H NMR analysis of the *exo*-norbornene-terminated polymer (Figure 4.5 and 4.7) revealed a single resonance in the alkene region ( $\delta$  6.18), a signal attributed to the protons adjacent to the ester ( $\delta$  4.13) as well as four new resonances for the norbornene ring ( $\delta$  3.10, 2.95, 2.27 and 1.98 ppm).<sup>102,103</sup> Through facile organic transformations, syndiotactic polymers bearing norbornene groups at the terminus have been produced.

#### 4.2.2 Ruthenium Catalyst Screening for Metathesis Polymerization

Initial investigations into the polymerization behavior of the norbornene-terminated syndiotactic polypropylene were carried out with the lower tacticity, more soluble macromonomer, *exo*-MM-3600, and a series of metathesis catalysts (Figure 4.8). All three of the ruthenium complexes screened (**4.3** – **4.5**) resulted in high conversion of macromonomer to poly(macromonomer) (> 94%) in just two hours (Table 4.2, Scheme 4.4). The poly(macromonomer)s obtained from **4.4** and **4.5** both displayed high peak molecular weight ( $M_p$  = 73,000 and 64,000 g/mol, respectively),

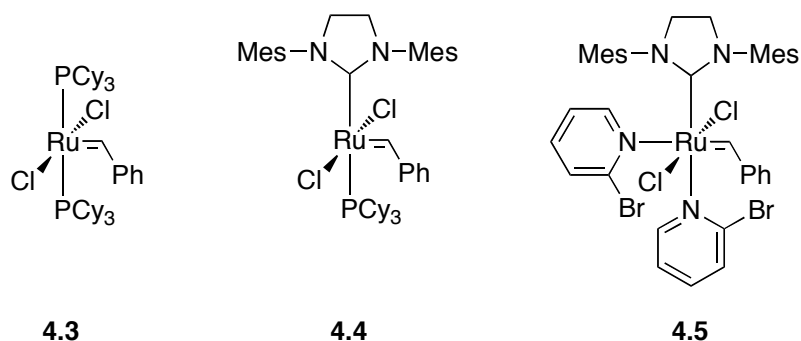


**Figure 4.8.** Grubbs' olefin metathesis polymerization catalysts for poly(macromonomer) preparation.

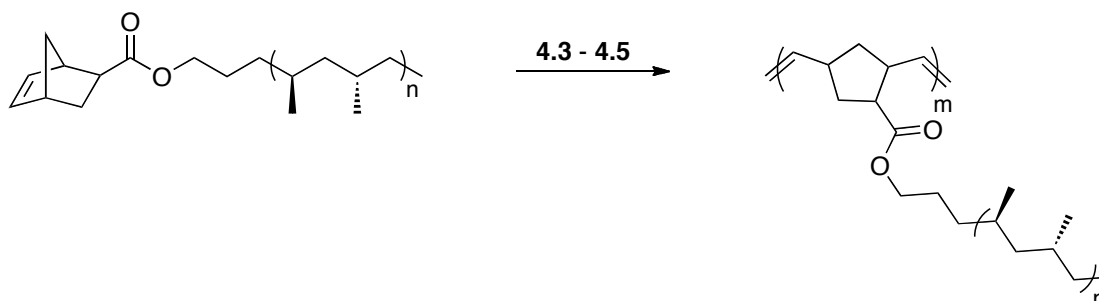
**Table 4.2.** Metathesis polymerization of *exo*-MM-3600 at 60 °C.

Entry	Cplx	$t_{\text{rxn}}$ (hr)	Conv. (%) <sup>c</sup>	$M_n$ (g/mol) <sup>d</sup>	$M_p$ (g/mol) <sup>d</sup>	$M_w/M_n$ <sup>d</sup>	$T_c$ (°C) <sup>e</sup>	$T_m$ (°C) <sup>e</sup>	$\Delta H_m$ (J/g) <sup>e</sup>
1 <sup>a</sup>	<b>4.3</b>	2	94	76,000	83,000	1.25	50	104	31
2 <sup>b</sup>	<b>4.4</b>	2	>99	35,000	73,000	2.00	42	105	36
3 <sup>a</sup>	<b>4.5</b>	2	>99	36,000	64,000	2.11	43	105	40

<sup>a</sup> General Conditions:  $[\textit{exo}\text{-MM-3600}]_0 = 0.083$  M,  $[\text{Ru}] = 1.65$  mM,  $[\textit{exo}\text{-MM-3600}]:[\text{Ru}] = 50:1$ . <sup>b</sup>  $[\textit{exo}\text{-MM-3600}]_0 = 0.0083$  M,  $[\text{Ru}] = 0.165$  mM,  $[\textit{exo}\text{-MM-3600}]:[\text{Ru}] = 50:1$ . <sup>c</sup> Determined using <sup>1</sup>H NMR spectroscopy in 1,1,2,2-tetrachloroethane at 135 °C. <sup>d</sup> Molecular weight ( $M_n$ ), peak molecular weight ( $M_p$ ) and molecular weight distribution ( $M_w/M_n$ ) were determined by gel permeation chromatography at 140 °C in 1,2,4-trichlorobenzene relative to polyethylene standards. <sup>e</sup> Melting temperature ( $T_m$ ), crystallization temperature ( $T_c$ ) and enthalpy ( $\Delta H$ ) were determined by differential scanning calorimetry (second heating run).

but, overall molecular weight ( $M_n = 35,000$  and  $36,000$  g/mol) was considerably lower. Furthermore, molecular weight distributions ( $M_w/M_n = 2.00$  and  $2.11$ ) were broader than those observed for the poly(macromonomer) ( $M_w/M_n = 1.25$ ) derived from **4.3**, which also displayed the highest molecular weight ( $M_n = 77,000$  g/mol). Additionally, molecular weight distribution of the poly(macromonomer) obtained from **4.3** was lower than the starting macromonomer ( $M_w/M_n = 1.87$ ). This is consistent with star polymer theory laid out by Schulz and Flory, which suggests that polymer molecular weight distribution will decrease as the number of arms linked together increases.<sup>104-106</sup> Analysis of the poly(macromonomer) by GPC reveals a very small low molecular weight shoulder, which can be attributed to a small amount of unfunctionalized polypropylene present in the starting macromonomer. This was confirmed by analysis of the <sup>1</sup>H NMR spectra, which showed the disappearance of the alkene resonances associated with the norbornene-terminated syndiotactic polypropylene. Homopolymerization of the norbornene-terminated polymer was

possible with the three different ruthenium metathesis catalysts that were screened. Based on these initial screening results, **4.3** was identified as the best catalyst for ring opening metathesis polymerization of the syndiotactic polypropylene macromonomers.



**Scheme 4.4.** Ring-opening metathesis polymerization (ROMP) of norbornene-terminated syndiotactic polypropylene.

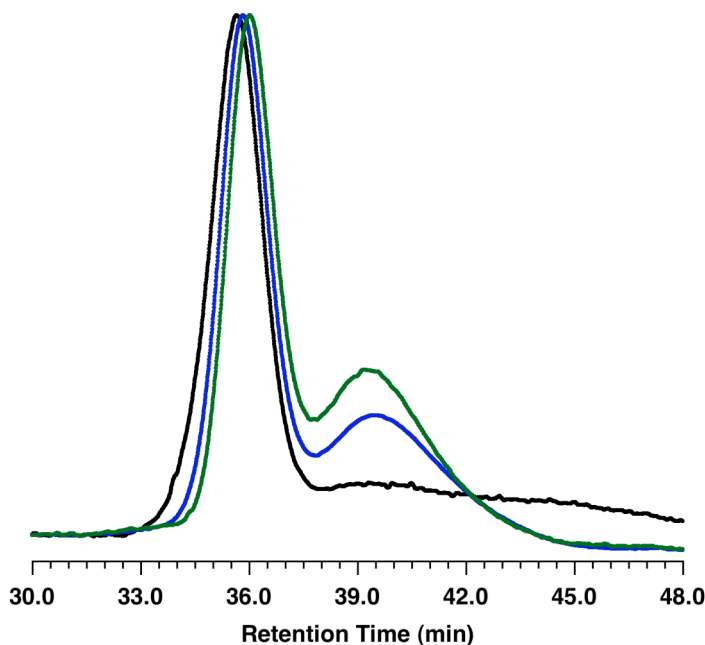
#### 4.2.3 Polymerization of Norbornene-Terminated sPP with 4.3

The polymerization rate of **4.3** (Table 4.3) was further investigated because of its ability to produce the highest molecular weight polymer with the narrowest polydispersity. After just three minutes, 59% conversion to comb polymer was observed through analysis of the poly(macromonomer)  $^1\text{H}$  NMR spectrum. In addition to the residual macromonomer, a higher molecular weight peak ( $M_p = 65,000$  g/mol) attributed to the poly(macromonomer) was observed (Figure 4.9). Due to overlapping macromonomer and poly(macromonomer) peaks in the GPC chromatogram, it is useful to compare peak molecular weights here. Upon increasing reaction time to six minutes, greater conversion (67%) and higher peak molecular weight ( $M_p = 73,000$  g/mol) was obtained in addition to residual macromonomer. After ten minutes, 87% conversion of macromonomer to comb polymer was observed ( $M_p = 75,000$  g/mol) along with a decreased amount of macromonomer. When reaction time was extended

**Table 4.3.** Metathesis polymerization of *exo*-MM-3600 with **4.3** at 60 °C.<sup>a</sup>

Entry	$t_{\text{rxn}}$ (min)	Conv. (%) <sup>b</sup>	$M_n$ (g/mol) <sup>c</sup>	$M_p$ (g/mol) <sup>c</sup>	$M_w/M_n$ <sup>c</sup>	$T_c$ (°C) <sup>d</sup>	$T_m$ (°C) <sup>d</sup>	$\Delta H_m$ (J/g) <sup>d</sup>
1	3	59	11,000	65,000	3.90 (bm) <sup>e</sup>	59	110	35
2	6	67	12,000	73,000	4.25 (bm) <sup>e</sup>	59	109	42
3	10	87	12,000	75,000	4.55 (bm) <sup>e</sup>	53	106	29
4	120	94	76,000	83,000	1.24	50	104	31
5	1440	>99	86,000	98,000	1.21	45	104	24

<sup>a</sup> General Conditions:  $[exo\text{-MM-3600}]_0 = 0.083$  M,  $[Ru] = 1.65$  mM,  $[exo\text{-MM-3600}]:[Ru] = 50:1$ . <sup>b</sup> Determined using  $^1\text{H}$  NMR spectroscopy in 1,1,2,2-tetrachloroethane at 135 °C. <sup>c</sup> Peak molecular weight ( $M_p$ ), molecular weight ( $M_n$ ) and molecular weight distribution ( $M_w/M_n$ ) were determined by gel permeation chromatography at 140 °C in 1,2,4-trichlorobenzene relative to polyethylene standards. <sup>d</sup> Melting temperature ( $T_m$ ), crystallization temperature ( $T_c$ ) and enthalpy ( $\Delta H$ ) were determined by differential scanning calorimetry (second heating run). <sup>e</sup> Bimodal due to presence of *exo*-MM-3600.

**Figure 4.9.** GPC chromatogram of ROMP polymerization of *exo*-MM-3600 using **4.3** after 3 (green, Entry 1, Table 4.3), 10 (blue, Entry 3, Table 4.3) and 120 minutes (black, Entry 4, Table 4.3).

to two hours, nearly complete conversion (94%) was obtained as evidenced by  $^1\text{H}$  NMR spectroscopy. Furthermore, molecular weight increased ( $M_p = 83,000$  g/mol,  $M_n = 76,000$  g/mol) and residual macromonomer was no longer present in the GPC chromatogram. Allowing the reaction to proceed for a full 24 hours resulted in quantitative conversion of macromonomer to poly(macromonomer) (>99 %) with the highest molecular weight ( $M_p = 98,000$  g/mol,  $M_n = 86,000$  g/mol) observed. Comparing the molecular weight data by GPC (Figure 4.9) reveals that the polymerization proceeds quickly up to ten minutes. Due to lower solubility and macromonomer concentration, extended reaction times are required to obtain higher conversions. Formation of comb polymer is also confirmed by comparison of the poly(macromonomer) alkene region of the  $^1\text{H}$  NMR spectra (Figure 4.10 and 4.11). After three minutes, macromonomer is observed, as evidenced by the multiplet at

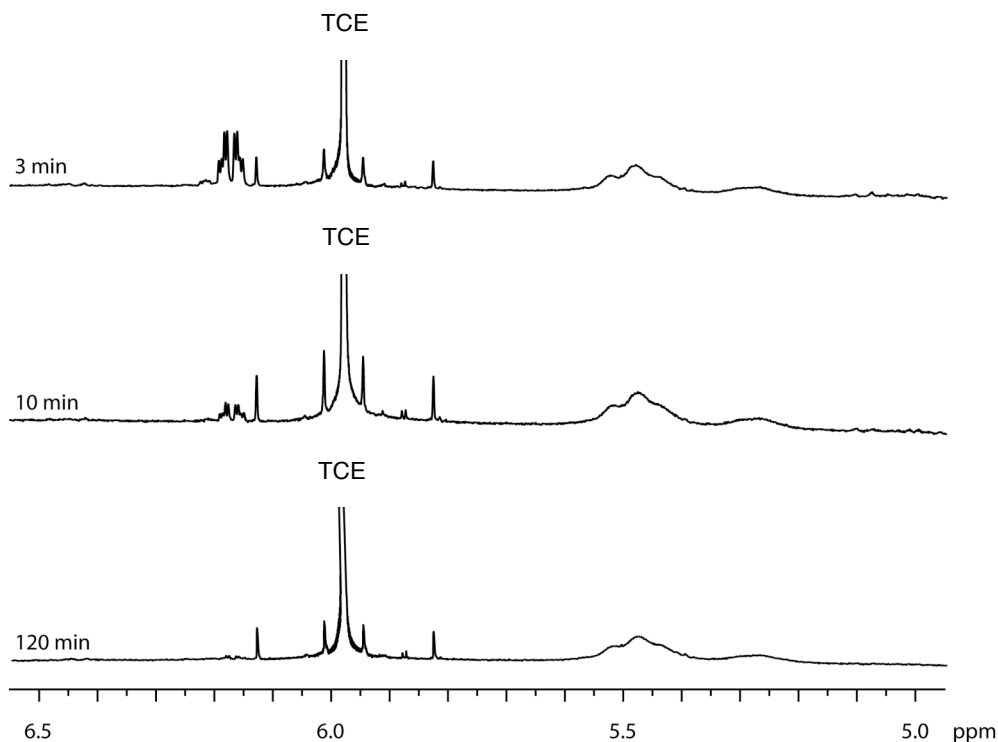


**Figure 4.10.**  $^1\text{H}$  NMR spectra of poly(*exo*-MM-3600) produced with **4.3** after 3 (Entry 1, Table 4.3), 10 (Entry 3, Table 4.3) and 120 (Entry 4, Table 4.3) minutes (600 MHz, 1,1,2,2-tetrachloroethane- $d_2$  (TCE), 135 °C).

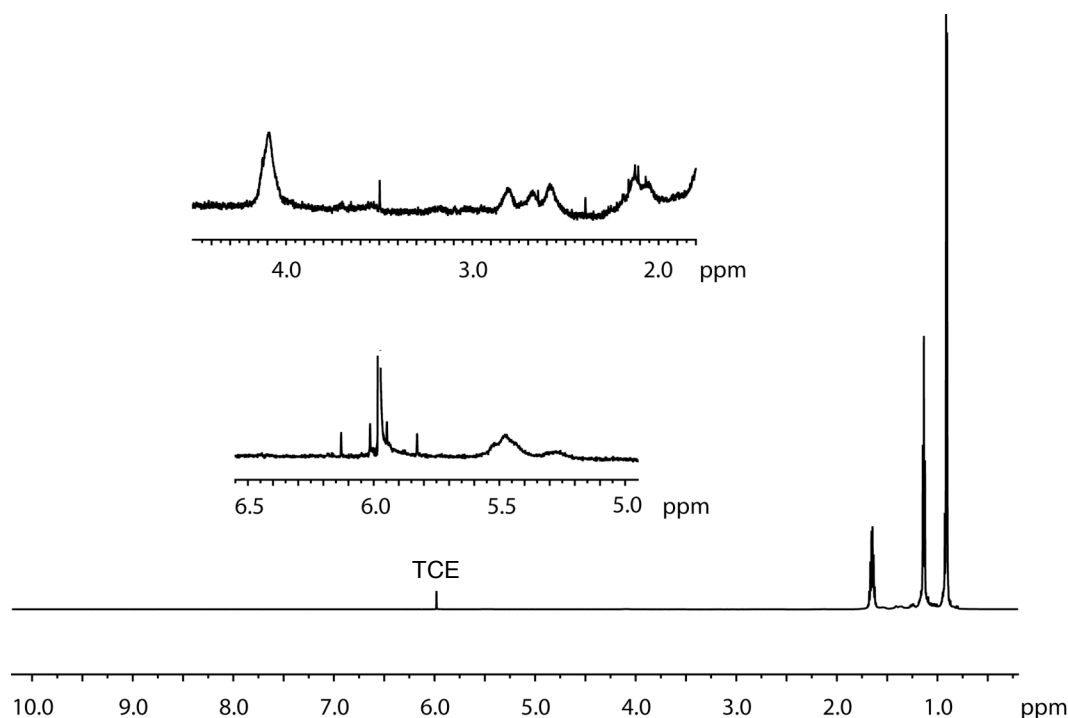


**Figure 4.11.** <sup>1</sup>H NMR spectrum of poly(*exo*-MM-3600) (Entry 4, Table 4.3) (600 MHz, 1,1,2,2-tetrachloroethane-*d*<sub>2</sub> (TCE), 135 °C).

$\delta$  6.18, and broad resonances at  $\delta$  5.58 – 5.19 ppm in the <sup>1</sup>H NMR spectrum are indicative of the comb-polymer. Increasing reaction time to ten minutes reveals further conversion to poly(macromonomer) with decreased macromonomer observed. At two hours, very little macromonomer is present in the <sup>1</sup>H NMR spectrum indicating nearly complete conversion to poly(macromonomer).

In addition to GPC and <sup>1</sup>H NMR spectroscopy, the extent of polymerization was also assessed through analysis of the comb-polymer thermal data (Table 4.3) obtained from differential scanning calorimetry. Compared with the starting the macromonomer ( $T_m = 113$  °C), a decrease in the melting temperature was observed for

poly(macromonomer) obtained after two hours ( $T_m = 104$  °C). Furthermore, melting temperature was also observed to decrease as a function of conversion with  $T_m = 110$ , 109 and 106 °C obtained after three, six and ten minutes, respectively. As with melting temperature, crystallization temperature was also observed to decrease with increasing conversion of macromonomer ( $T_c = 73$  °C) to comb-polymer ( $T_c = 59 - 45$  °C) with the lowest crystallization temperature observed for the highest conversion to poly(macromonomer). At varying reaction times, the polymerization of *exo*-MM-3600 with **4.3** resulted in poly(macromonomer) with molecular weights observed to increase over time while both melting temperature and crystallization temperature decreased with comb-polymer formation.

**Table 4.4.** Polymerization of *exo*-MM-3600 and *exo*-MM-5600 with **4.3**.<sup>a</sup>

Entry	<i>exo</i> -MM	[MM] <sub>0</sub> : [Ru]	Conv. (%) <sup>b</sup>	$M_n$ (g/mol) <sup>c</sup>	$M_w/M_n$ <sup>c</sup>	$T_c$ (°C) <sup>d</sup>	$T_m$ (°C) <sup>d</sup>	$\Delta H_m$ (J/g) <sup>d</sup>
1	MM-3600	50:1	>99	86,000	1.21	45	104	24
2	MM-3600	200:1	95	136,000	1.31	44	104	28
3	MM-3600	500:1	88	172,000	1.29	47	106	18
4	MM-5600	50:1	>99	46,000	1.89	104	135	59
5	MM-5600	200:1	>99	105,000	1.33	102	135	64
6	MM-5600	500:1	93	120,000	1.30	98	135	44

<sup>a</sup> General Conditions: [MM]<sub>0</sub> = 0.083 M, [Ru] = 1.65 mM, [MM]:[Ru] = 50:1. <sup>b</sup> Determined using <sup>1</sup>H NMR spectroscopy in 1,1,2,2-tetrachloroethane at 135 °C. <sup>c</sup> Peak molecular weight ( $M_p$ ), molecular weight ( $M_n$ ) and molecular weight distribution ( $M_w/M_n$ ) were determined by gel permeation chromatography at 140 °C in 1,2,4-trichlorobenzene relative to polyethylene standards. <sup>d</sup> Melting temperature ( $T_m$ ), crystallization temperature ( $T_c$ ) and enthalpy ( $\Delta H$ ) were determined by differential scanning calorimetry (second heating run).

#### 4.2.4. Metathesis Polymerization with Varied Catalyst Loadings

To test the limits of macromonomer polymerization, the two norbornene-terminated syndiotactic polypropylene macromonomers (*exo*-MM-3600 and *exo*-MM-5600) were polymerized with **4.3** at a variety of catalyst loadings (Table 4.4). Polymerization of *exo*-MM-3600 at low catalyst loadings (50:1, [MM]<sub>0</sub>:[Ru]) resulted in poly(macromonomer) ( $M_n = 86,000$  g/mol,  $M_w/M_n = 1.21$ ) with little residual macromonomer and high conversion (>99%) observed. Comparatively, poly(macromonomer) with modest molecular weight ( $M_n = 46,000$  g/mol,  $M_w/M_n = 1.89$ ) was obtained upon polymerization of *exo*-MM-5600 at low catalyst loadings (50:1, [MM]<sub>0</sub>:[Ru]). Tapering of the peaks observed by GPC (Figure 4.12) has been attributed to residual unfunctionalized macromonomer. This was confirmed through analysis of the <sup>1</sup>H NMR spectra, which revealed high conversion of the norbornene-terminated polymer to comb-polymer (>99%). Decreasing the catalyst loading (200:1,

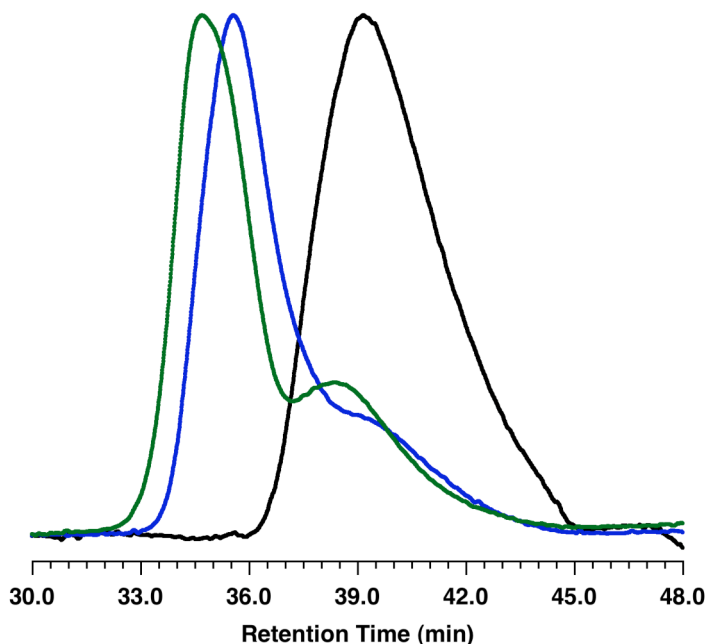


**Figure 4.12.** GPC chromatogram of *exo*-MM-5600 (black, Entry 2, Table 4.1) and poly(*exo*-MM-5600) produced using **4.3** with 50:1 (blue, Entry 4, Table 4.4) and 200:1 (green, Entry 5, Table 4.4) catalyst loadings.

[MM]<sub>o</sub>: [Ru]) resulted in the high conversion (95%) of *exo*-MM-3600 to comb polymer ( $M_n = 136,000$  g/mol) with very little low molecular weight polymer observed by GPC. Polymerization of *exo*-MM-5600 under the same conditions (200:1, [MM]<sub>o</sub>: [Ru]) also resulted in high conversion (>99%) to comb polypropylene ( $M_n = 105,000$  g/mol,  $M_w/M_n = 1.33$ ). In an attempt to obtain an even higher molecular weight, catalyst loadings (500:1, [MM]<sub>o</sub>: [Ru]) were decreased still further, and polymerization of *exo*-MM-3600 resulted in a poly(macromonomer) with  $M_n = 172,000$  g/mol and  $M_w/M_n = 1.29$ . An increased amount of residual macromonomer by GPC ( $M_n = 4,800$  g/mol) and lower conversion (88%) by <sup>1</sup>H NMR spectroscopy were observed compared with higher catalyst loadings. Using the same reaction conditions (500:1, [MM]<sub>o</sub>: [Ru]), poly(macromonomer) ( $M_n = 120,000$  g/mol,  $M_w/M_n = 1.30$ ) was obtained from the polymerization of *exo*-MM-5600. Similar to *exo*-MM-3600, an

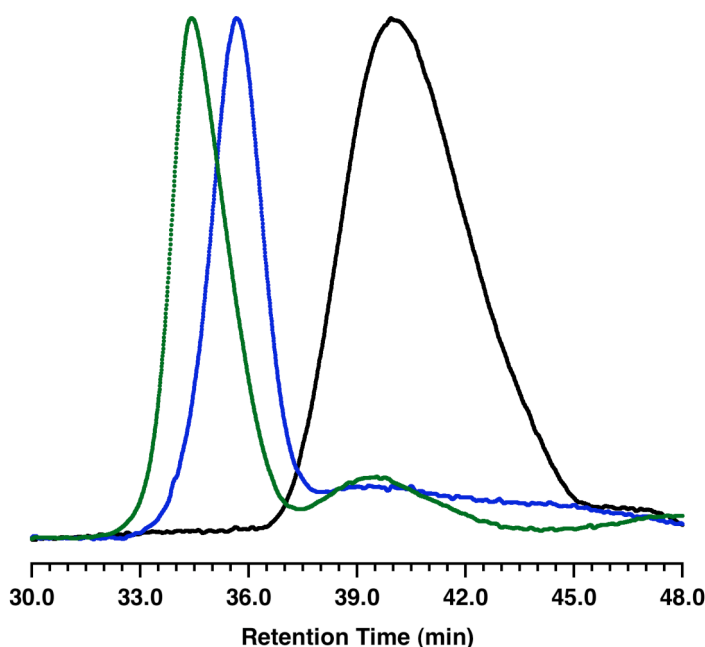


**Figure 4.13.** GPC chromatogram of *exo*-MM-3600 (black, Entry 1, Table 4.1) and poly(MM-3600) produced using **4.3** with 50:1 (blue, Entry 1, Table 4.4) and 200:1 (green, Entry 2, Table 4.4) [MM]<sub>o</sub>: [Ru].

increased amount of residual macromonomer was observed by GPC and decreased conversion (93%) was revealed through analysis of the  $^1\text{H}$  NMR spectrum. Attempts to decrease catalyst loadings further did not result in higher molecular weight poly(macromonomer) instead a considerable decrease in percent conversion was observed. Comparison of the GPC chromatograms of *exo*-MM-3600 (Figure 4.15) and *exo*-MM-5600 (Figure 4.17) with the chromatograms of the poly(macromonomer)s produced at 50:1 and 200:1 catalyst loadings shows a clear increase in molecular weight with decreased catalyst loading. In general, polymerization of *exo*-MM-3600 resulted in high conversion to poly(macromonomer) (>88%) with low molecular weight distributions ( $M_w/M_n = 1.21 - 1.31$ ) observed for a range of molecular weights ( $M_n = 86,000 - 172,000$  g/mol). Decreased molecular weights ( $M_n = 45,000 - 120,000$  g/mol,  $M_w/M_n = 1.30 - 1.89$ ) were observed for the polymerization of *exo*-MM-5600 due to an increased presence of unfunctionalized macromonomer compared with *exo*-MM-3600. However, the polymerization proceeded with good conversion (>93%) resulting in a highly syndiotactic polypropylene comb polymer.

The thermal properties (Table 4.4) of the syndiotactic macromonomers and the resultant comb-polymers were also investigated using differential scanning calorimetry. Decreased melting temperatures were observed for the poly(macromonomer)s ( $T_m = 104 - 106$  °C, Figure 4.14) compared with *exo*-MM-3600 ( $T_m = 112$  °C, Figure 4.15). Similar to the *exo*-MM-3600 series, the poly(macromonomer)s ( $T_m = 135$  °C, Figure 4.16) obtained from the polymerization of *exo*-MM-5600 ( $T_m = 145$  °C, Figure 4.17) display lower melting temperatures than the corresponding macromonomer. The DSC trace of *exo*-MM-5600 reveals a double melting endotherm with the second peak ( $T_m = 145$  °C) being more pronounced than the first. Previous reports for syndiotactic polypropylene suggest that initial melting is followed by an immediate recrystallization resulting in the observed peaks.<sup>107-112</sup>

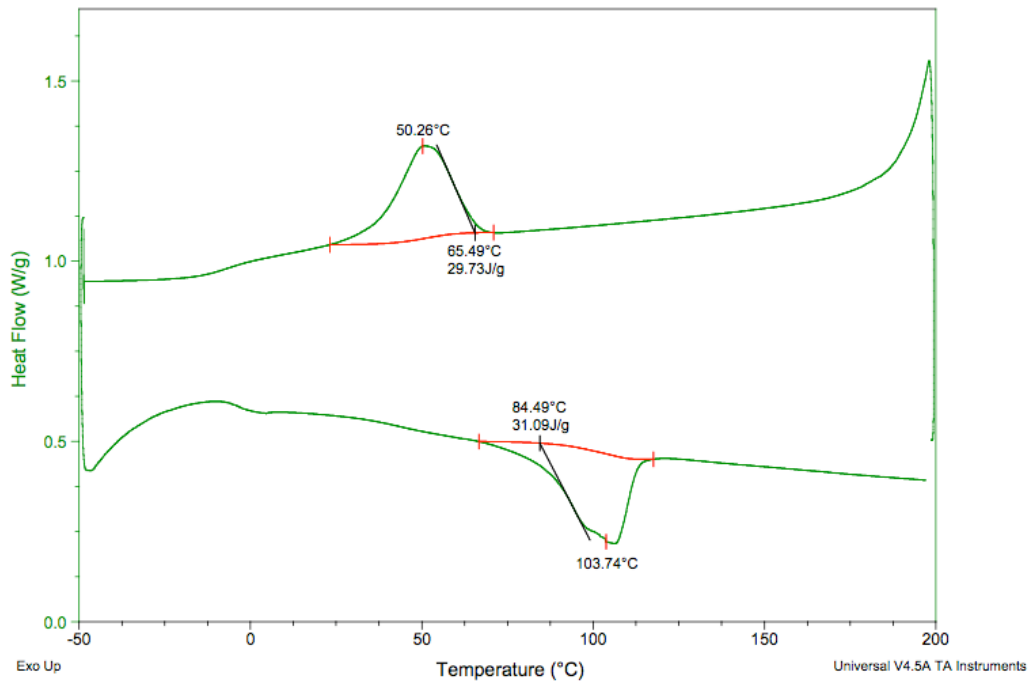


**Figure 4.14.** Differential scanning calorimetry (10 °C/min, second heat) thermogram of poly(*exo*-MM-3600) (Entry 4, Table 4.3).

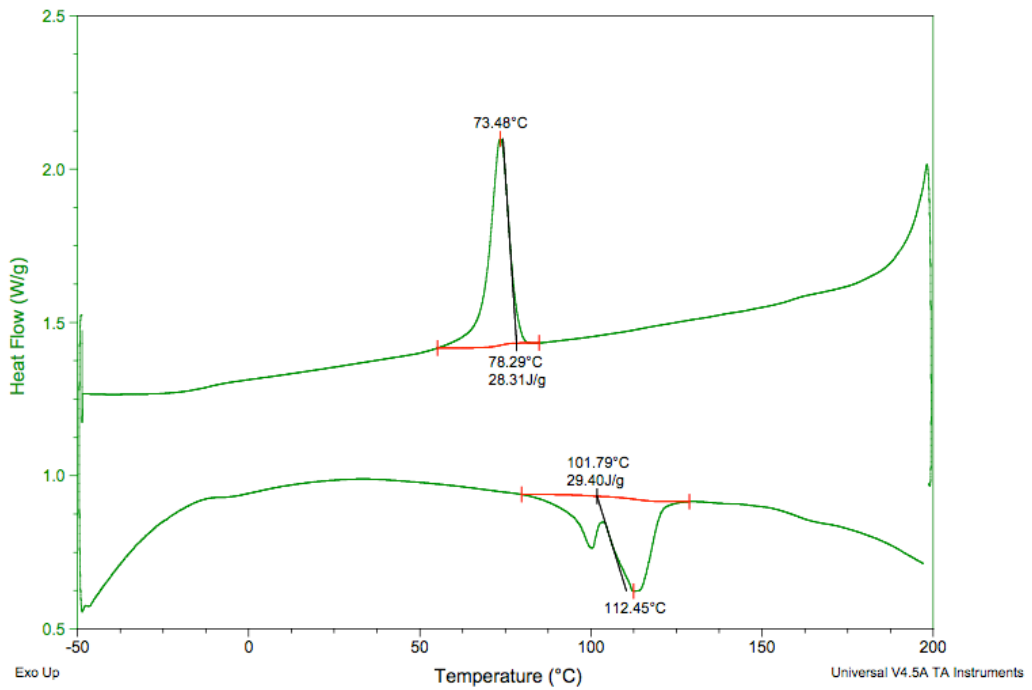


**Figure 4.15.** Differential scanning calorimetry (10 °C/min, second heat) thermogram of *exo*-MM-3600.

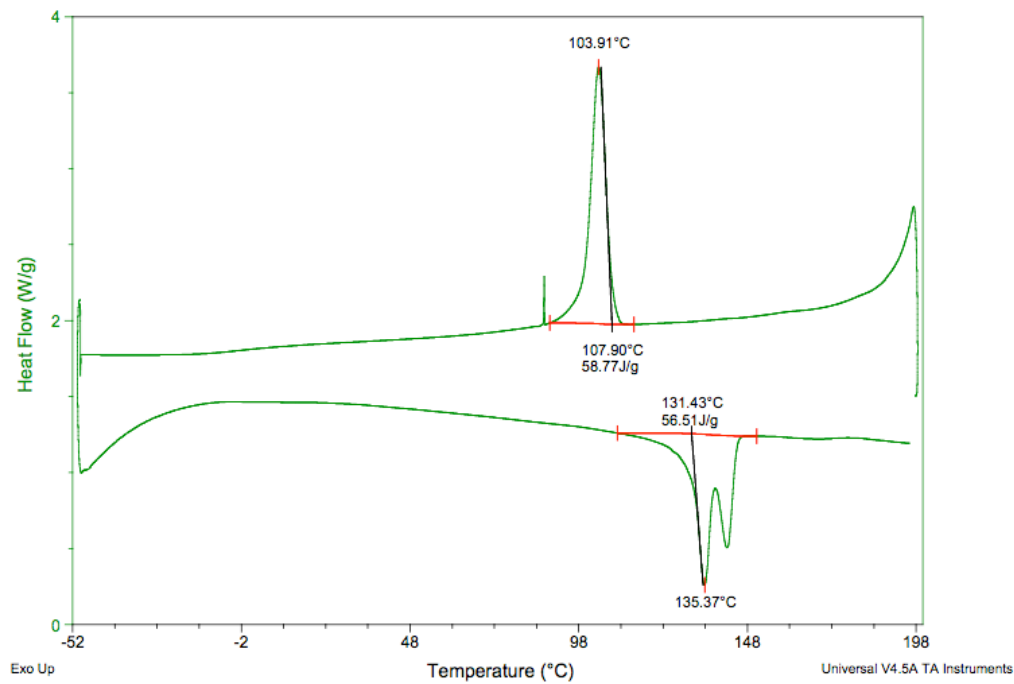


**Figure 4.16.** Differential scanning calorimetry (10 °C/min, second heat) thermogram of poly(*exo*-MM-5600) (Entry 4, Table 4.4).

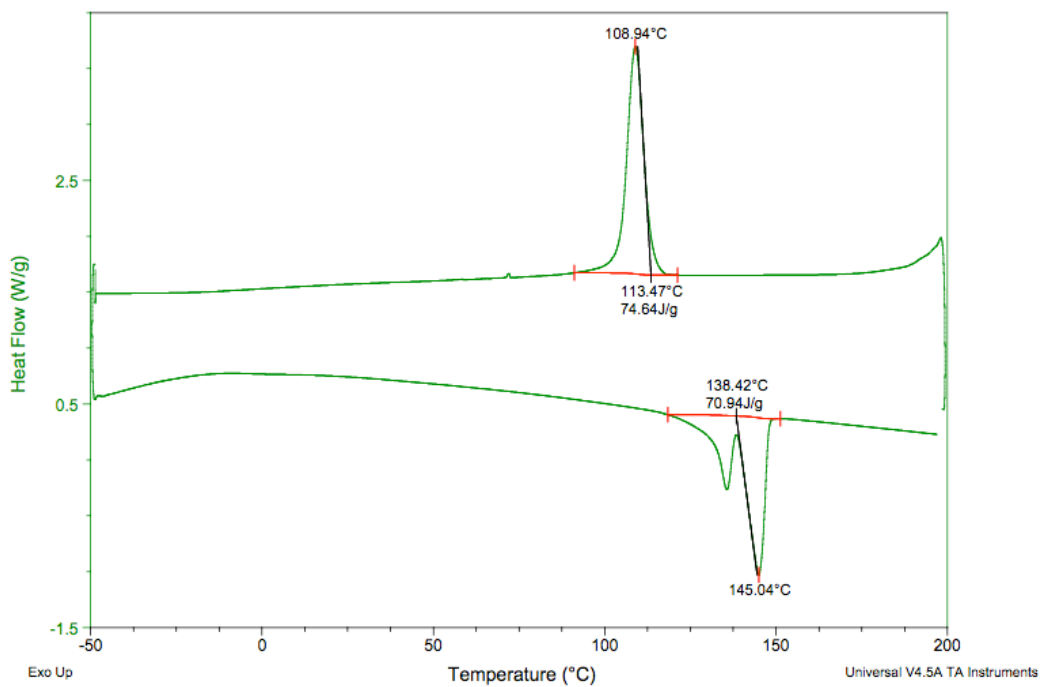


**Figure 4.17.** Differential scanning calorimetry (10 °C/min, second heat) thermogram of *exo*-MM-5600.

Interestingly, the poly(macromonomer) obtained from *exo*-MM-5600 also displays a double endotherm, however, the initial peak ( $T_m = 135\text{ }^\circ\text{C}$ ) is more prominent than the second endotherm for all poly(macromonomer)s studied suggesting that immediate recrystallization is suppressed with the formation of comb polymer. Further analysis of the DSC data reveals the crystallization temperature follows a similar trend. Formation of poly(*exo*-MM-3600) resulted in decreased crystallization temperatures ( $T_c = 44 - 47\text{ }^\circ\text{C}$ ) compared with *exo*-MM-3600 ( $T_c = 73\text{ }^\circ\text{C}$ ). Analogously, decreased crystallization temperatures ( $T_c = 98 - 104\text{ }^\circ\text{C}$ ) were observed for the poly(*exo*-MM-5600) compared with *exo*-MM-5600 ( $T_c = 109\text{ }^\circ\text{C}$ ). For both syndiotactic polypropylene macromonomers, melting temperature and crystallization temperature were found to decrease with the formation high molecular weight poly(macromonomer).

### 4.3. Conclusions

Ring-opening metathesis polymerization of norbornene-terminated syndiotactic polypropylene resulted in high molecular weight poly(macromonomer)s. To the best of our knowledge, this is the first report of a comb polymer from end-functionalized syndiotactic polypropylene. Utilizing allyl-terminated syndiotactic polypropylene obtained from bis(phenoxyimine)titanium catalysts, **4.1** and **4.2**, hydroxyl- and norbornene-terminated polymers of varying tacticity were obtained. The macromonomer was polymerized with ruthenium catalysts **4.3** – **4.5** to produce the poly(macromonomer)s. Reaction rate was investigated with catalyst **4.3** and initially the polymerization proceeded quickly, though longer reaction times were required to obtain high conversions. Poly(macromonomer)s with a range of molecular weights were obtained from *exo*-MM-3600 and *exo*-MM-5600 by varying catalyst loadings. The resultant comb polymers displayed interesting thermal properties with

both melting temperature and crystallization temperature decreasing upon formation of the poly(macromonomer). Further investigation to explain this behavior is currently underway.

#### 4.4 Experimental Section

**General.** All manipulations of air- and/or water-sensitive compounds were carried out under dry nitrogen using Braun UniLab drybox or standard Schlenk techniques. Toluene was purified over columns of alumina and copper (Q5). THF was purified over an alumina column and degassed by three freeze-pump-thaw cycles before use. Propylene (Airgas, research purity) was purified over columns (40 cm inner diameter x 120 cm long) of BASF catalyst R3-12, BASF catalyst R3-11, and 4Å molecular sieves. PMAO-IP (13 wt % Al in toluene, Akzo Nobel) was dried in vacuo to remove residual trimethyl aluminum and used as a solid white powder. Complexes **4.1** and **4.2** were prepared according to previously reported procedures.<sup>68</sup> Triethylamine was stirred over CaH<sub>2</sub> for several days and vacuum distilled. Oxalyl chloride, 0.5 M 9-borabicyclo[3.3.1]nonane (9-BBN) in THF, *exo*-5-norbornene-2-carboxylic acid, Cl<sub>2</sub>(Cy<sub>3</sub>P)<sub>2</sub>RuCHPh (**4.3**, Grubbs' first generation catalyst), Cl<sub>2</sub>(Cy<sub>3</sub>P)(H<sub>2</sub>IMes)RuCHPh (**4.4**, Grubbs' second generation catalyst), and Cl<sub>2</sub>(2-BrC<sub>5</sub>H<sub>5</sub>N)<sub>2</sub>(H<sub>2</sub>IMes)RuCHPh (**4.5**, Grubbs' third generation catalyst) were purchased from commercial sources and used as received.

**Polymer Characterization.** <sup>1</sup>H and <sup>13</sup>C{<sup>1</sup>H} NMR spectra of polymers were recorded using a Varian UnityInova (600 MHz) spectrometer equipped with a <sup>1</sup>H/BB switchable with Z-pulse field gradient probe operating and referenced versus residual non-deuterated solvent shifts. The polymer samples were dissolved in 1,1,2,2-tetrachloroethane-*d*<sub>2</sub> in a 5 mm O.D. tube, and spectra were collected at 135 °C. End-group analysis for molecular weight determination was achieved by relative

integration of the end-group vs alkyl peaks in the  $^1\text{H}$  NMR spectrum. Percent conversion was determined through relative integration of the macromonomer alkene resonance to the poly(macromonomer) alkene resonances in the  $^1\text{H}$  NMR spectrum. Syndiotacticity ( $[rrrr]$ ) was measured by Gaussian deconvolution of the methyl region of the  $^{13}\text{C}$  NMR spectrum. Molecular weights ( $M_n$  and  $M_w$ ) and polydispersities ( $M_w/M_n$ ) were determined by high temperature gel permeation chromatography (GPC). Analyses were performed with a Waters Alliance GPCV 2000 GPC equipped with a Waters DRI detector and viscometer. The column set (four Waters HT 6E and one Waters HT 2) was eluted with 1,2,4-trichlorobenzene containing 0.01 wt % di-*tert*-butyl-hydroxytoluene (BHT) at 1.0 mL/min at 140 °C. Data were calibrated using monomodal polyethylene standards (from Polymer Standards Service). Differential scanning calorimetric analyses were performed in crimped aluminum pans under nitrogen using a TA Instruments Q1000 calorimeter equipped with an automated sampler. Data were collected from the second heating run at a heating rate of 10 °C/min from -50 to 200 °C and were processed with the TA Q series software package.

#### 4.4.1 Macromonomer Synthesis

**sPP-CH<sub>2</sub>CH=CH<sub>2</sub>.** In a glovebox, a 12 oz Laboratory Crest reaction vessel (Andrews Glass) was charged with dried PMAO (1.15 g, 20 mmol) and toluene (300 mL). The vessel was purged with propylene gas three times and equilibrated at 0 °C and 30 psig propylene for 30 minutes. A solution of the Ti precatalyst (100  $\mu\text{mol}$ ,  $[\text{Al}]/[\text{Ti}] = 200$ ) in toluene (10 mL) was injected into the reactor. After 9 h, the reaction mixture was quenched with methanol (10 mL) and the polymer was precipitated into a copious amount of acidic methanol (5% HCl (aq)) and stirred overnight. The polymer was isolated and rinsed with methanol. To purify the sample,

the polymer was dissolved in hot toluene and filtered through a glass frit layered with silica, alumina, and Celite®. The toluene was removed and the polymer was dried in vacuo to constant weight. For MM-3600 from catalyst **1**, yield = 9.11 g,  $M_n(\text{GPC}) = 3,600$  g/mol,  $M_w/M_n = 1.87$ ,  $M_n(^1\text{H NMR}) = 5,800$  g/mol. For MM-5600 from catalyst **2**, yield = 8.5 g.  $M_n(\text{GPC}) = 5,600$  g/mol,  $M_w/M_n = 1.75$ ,  $M_n(^1\text{H NMR}) = 7,400$  g/mol.  $^1\text{H NMR}$  (600 MHz,  $\text{C}_2\text{D}_2\text{Cl}_4$ , 135 °C):  $\delta$  5.81 (dd, 1H), 5.01 (m, 2H), 1.72-0.68 (m, 800H (MM-3600), 1100H (MM-5600)).

**sPP-(CH<sub>2</sub>)<sub>3</sub>OH**. An oven-dried 1 L round bottom flask was cooled under vacuum and charged with allyl-terminated syndiotactic polypropylene (1 mmol). THF (500 mL, MM-3600) or toluene (500 mL, MM-5600) was cannulated into the flask and the mixture was heated to 45 °C. After 15 minutes, the 9-BBN (7 mL, 3.5 mmol) was added drop wise to the flask and the solution was heated to 65 °C. The mixture was cooled to 45 °C after 3 hours. A sodium hydroxide solution (1.5 M in H<sub>2</sub>O, 15 mmol) was added followed immediately by a hydrogen peroxide solution (1.22 M in THF, 11 mmol). After 2 hours, the mixture was poured into copious methanol. The polymer was collected, dissolved in hot toluene and filtered through a glass frit layered with silica, alumina, and Celite®. The toluene was removed and the polymer was dried in vacuo to constant weight. For MM-3600, yield = 5.8 g, conversion = 92%,  $M_n(\text{GPC}) = 3,700$  g/mol,  $M_w/M_n = 1.90$ ,  $M_n(^1\text{H NMR}) = 6,300$  g/mol. For MM-5600, yield = 7.0 g, conversion = 60%,  $M_n(\text{GPC}) = 5,600$  g/mol,  $M_w/M_n = 1.74$ ,  $M_n(^1\text{H NMR}) = 13,000$  g/mol.  $^1\text{H NMR}$  (600 MHz,  $\text{C}_2\text{D}_2\text{Cl}_4$ , 135 °C):  $\delta$  3.61 (q, 2H), 1.72-0.68 (m, 900H (MM-3600), 1850H (MM-5600)).

**exo-MM-3600 and exo-MM-5600**. An oven-dried Schlenk adapted round bottom flask was cooled under vacuum and charged with 5-norbornene-2-carboxylic acid (0.35 mL, 2.5 mmol) and toluene (10 mL). Oxalyl chloride (0.22 mL, 2.5 mmol) was slowly syringed into the tube at room temperature. The mixture was warmed to 70 °C

for 2 hours. The solution was then cooled to room temperature and the solvent was removed in vacuo. Additional dry toluene (250 mL), hydroxyl-terminated syndiotactic polypropylene (0.5 mmol) and triethylamine (0.35 mL, 2.5 mmol) were added to the flask and the mixture was heated to 70 °C. After 12 hours, the solution was cooled to room temperature and the polymer was precipitated with copious methanol. The polymer was collected, dissolved in hot toluene and filtered through a glass frit layered with silica, alumina, and Celite®. The toluene was removed and the polymer was dried in vacuo to constant weight. For MM-3600, yield = 2.8 g, conversion = 75%,  $M_n(\text{GPC}) = 3,600 \text{ g/mol}$ ,  $M_w/M_n = 1.87$ ,  $M_n(^1\text{H NMR}) = 8,400 \text{ g/mol}$ . For MM-5600, yield = 3.4 g, conversion = 93%,  $M_n(\text{GPC}) = 5,600 \text{ g/mol}$ ,  $M_w/M_n = 1.75$ ,  $M_n(^1\text{H NMR}) = 14,000 \text{ g/mol}$ .  $^1\text{H NMR}$  (600 MHz,  $\text{C}_2\text{D}_2\text{Cl}_4$ , 135 °C):  $\delta$  6.18 (m, 2H), 4.13 (t, 2H), 3.10 (s, 1H), 2.95 (s, 1H), 2.27 (m, 1H), 1.98 (m, 2H), 1.72-0.80 (m, 1200H (MM-3600), 2000H (MM-5600)).

#### 4.4.2 Poly(macromonomer) Synthesis

**Polymerization of *exo*-MM-3600 and *exo*-MM-5600 with 4.3 and 4.5.** A 20 mL scintillation vial was charged with norbornene-terminated polypropylene (0.042 mmol). A prescribed amount of 4.3 or 4.5 in toluene (1.65 – 0.42 mM) was syringed into the vial. The mixture was diluted with toluene until the total volume was 0.5 mL and heated to 60 °C or 80 °C for a given amount of time. Ethyl vinyl ether and additional toluene were added to the vial and the mixture was reheated to quench the polymerization and dissolve the poly(macromonomer). After one hour, the polymer was precipitated with copious methanol, collected. The resultant poly(*exo*-MM-3600) was dissolved in hot THF, cooled to -30 °C for 24 hours, filtered, collected and dried in vacuo to constant weight. Poly(*exo*-MM-5600) was dissolved in hot toluene, filtered

hot, collected and dried in vacuo to constant weight.  $^1\text{H}$  NMR (600 MHz,  $\text{C}_2\text{D}_2\text{Cl}_4$ , 135 °C):  $\delta$  5.58-5.19 (m), 4.21-3.98 (m), 2.89-2.46 (m), 2.21-1.98 (m), 1.72-0.68 (m).

**Polymerization of *exo*-MM-3600 with 4.4.** A 20 mL scintillation vial was charged with norbornene-terminated polypropylene (0.25 g, 0.042 mmol). A solution of **4.4** (0.5 mL, 1.65 mM) in toluene was syringed into the vial. The mixture was diluted with toluene until the total volume was 5 mL and heated to 60 °C for two hours. Ethyl vinyl ether and additional toluene were added to the vial and the mixture was reheated to quench the polymerization and dissolve the poly(macromonomer). After one hour, the polymer was precipitated with copious methanol, collected and dried in vacuo to constant weight.  $^1\text{H}$  NMR (600 MHz,  $\text{C}_2\text{D}_2\text{Cl}_4$ , 135 °C):  $\delta$  5.58-5.19 (m), 4.21-3.98 (m), 2.89-2.46 (m), 2.21-1.98 (m), 1.72-0.68 (m).

## REFERENCES

- (1) Coates, G. W. *Chem. Rev.* **2000**, *100*, 1223-1252.
- (2) Resconi, L.; Cavallo, L.; Fait, A.; Piemontesi, F. *Chem. Rev.* **2000**, *100*, 1253-1345.
- (3) Domski, G. J.; Rose, J. M.; Coates, G. W.; Bolig, A. D.; Brookhart, M. *Prog. Polym. Sci.* **2007**, *32*, 30-92.
- (4) Lopez, R. G.; D'Agosto, F.; Boisson, C. *Prog. Polym. Sci.* **2007**, *32*, 419-454.
- (5) Vasile, C., General survey of the properties of polyolefins. In *Handbook of Polyolefins*, 2nd ed.; C., V., Ed. Marcel Dekker Inc: New York, 2000; pp 401-412.
- (6) Chum, S.; Swogger, K. W. *Prog. Polym. Sci.* **2008**, *33*, 797-819.
- (7) Rojas, G.; Berda, E. B.; Wagener, K. B. *Polymer* **2008**, *49*, 2985-2995.
- (8) Gahleitner, M. *Prog. Polym. Sci.* **2001**, *26*, 895-944.
- (9) Doerpinghaus, P. J.; Baird, D. G. *J. Rheol.* **2003**, *47*, 717-736.
- (10) Lagendijk, R. P.; Hogt, A. H.; Buijtenhuijs, A.; Gotsis, A. D. *Polymer* **2001**, *42*, 10035-10043.
- (11) Hadjichristidis, N.; Pitsikalis, M.; Pispas, S.; Iatrou, H. *Chem. Rev.* **2001**, *101*, 3747-3792.
- (12) Sheiko, S. S.; Möller, M. *Chem. Rev.* **2001**, *101*, 4099-4123.
- (13) Zhang, M.; Müller, A. H. E. *J. Poly Sci., Part A: Poly. Chem.* **2005**, *43*, 3461-3481.
- (14) Voit, B. I.; Lederer, A. *Chem. Rev.* **2009**, *109*, 5924-5973.
- (15) Peleshanko, S.; Tsukruk, V. V. *Prog. Polym. Sci.* **2008**, *33*, 523-580.

- (16) Runge, M. B.; Dutta, S.; Bowden, N. B. *Macromolecules* **2006**, *39*, 498-508.
- (17) Xia, Y.; Olsen, B. D.; Kornfield, J. A.; Grubbs, R. H. *J. Am. Chem. Soc.* **2009**, *131*, 18525-18532.
- (18) Xia, Y.; Kornfield, J. A.; Grubbs, R. H. *Macromolecules* **2009**, *42*, 3761-3766.
- (19) Huang, K.; Rzyayev, J. *J. Am. Chem. Soc.* **2009**, *131*, 6880-6885.
- (20) Sarkar, D.; El Khoury, J. M.; Lopina, S. T.; Hu, J. *J. Appl. Poly. Sci.* **2007**, *104*, 1905-1911.
- (21) Yuan, J.; Lu, Y.; Schacher, F.; Lunkenbein, T.; Weiss, S.; Schmalz, H.; Müller, A. H. E. *Chem. Mater.* **2009**, *21*, 4146-4154.
- (22) Gao, H.; Matyjaszewski, K. *J. Am. Chem. Soc.* **2007**, *129*, 6633-6639.
- (23) Bousquet, A.; Barner-Kowollik, C.; Stenzel, M. H. *J. Poly Sci., Part A: Poly. Chem.* **2010**, *48*, 1773-1781.
- (24) Bao, H.; Hu, J.; Gan, L. H.; Li, L. *J. Poly Sci., Part A: Poly. Chem.* **2009**, *47*, 6682-6692.
- (25) Runge, M. B.; Bowden, N. B. *J. Am. Chem. Soc.* **2007**, *129*, 10551-10560.
- (26) Jha, S.; Dutta, S.; Bowden, N. B. *Macromolecules* **2004**, *37*, 4365-4374.
- (27) Runge, M. B.; Yoo, J.; Bowden, N. B. *Macromol. Rapid Commun.* **2009**, *30*, 1392-1398.
- (28) Zhang, N.; Steenackers, M.; Luxenhofer, R.; Jordan, R. *Macromolecules* **2009**, *42*, 5345-5351.
- (29) Cheng, X.; Ma, J.; Zhi, J.; Yang, X.; Hu, A. *Macromolecules* **2010**, *43*, 909-913.
- (30) Runge, M. B.; Lipscomb, C. E.; Ditzler, L. R.; Mahanthappa, M. K.; Tivanski, A. V.; Bowden, N. B. *Macromolecules* **2008**, *41*, 7687-7694.
- (31) Zhao, L.; Goodman, M. D.; Bowden, N. B.; Lin, Z. *Soft Matter* **2009**, *5*, 4698-4703.

- (32) Rose, J. M.; Mourey, T. H.; Slater, L. A.; Keresztes, I.; Fetters, L. J.; Coates, G. W. *Macromolecules* **2008**, *41*, 559-567.
- (33) Kaneko, H.; Kojoh, S.-I.; Kawahara, N.; Matsuo, S.; Matsugi, T.; Kashiwa, N. *J. Poly Sci., Part A: Poly. Chem.* **2005**, *43*, 5103-5118.
- (34) Kaneko, H.; Kojoh, S.; Kawahara, N.; Matsuo, S.; Matsugi, T.; Kashiwa, N. *Macromol. Symp.* **2004**, *213*, 335-345.
- (35) Mowery, D. M.; Assink, R. A.; Derzon, D. K.; Klamo, S. B.; Clough, R. L.; Bernstein, R. *Macromolecules* **2005**, *38*, 5035-5046.
- (36) Hagiwara, T.; Saitoh, H.; Tobe, A.; Sasaki, D.; Yano, S.; Sawaguchi, T. *Macromolecules* **2005**, *38*, 10373-10378.
- (37) Shiono, T.; Hiroki, K.; Soga, K. *Macromolecules* **1994**, *27*, 2635-2637.
- (38) Chung, T. C.; Xu, G.; Lu, Y.; Hu, Y. *Macromolecules* **2001**, *34*, 8040-8050.
- (39) Kaneyoshi, H.; Inoue, Y.; Matyjaszewski, K. *Macromolecules* **2005**, *38*, 5425-5435.
- (40) Hagihara, H.; Ishihara, T.; Ban, H. T.; Shiono, T. *J. Poly Sci., Part A: Poly. Chem.* **2008**, *46*, 1738-1747.
- (41) Lin, W.; Dong, J.; Chung, T. C. M. *Macromolecules* **2008**, *41*, 8452-8457.
- (42) Yi, Q.; Fan, G.; Wen, X.; Dong, J.-Y.; Han, C. C. *Macromol. React. Eng.* **2009**, *3*, 91-100.
- (43) Briquel, R.; Mazzolini, J.; Le Bris, T.; Boyron, O.; Boisson, F.; Delolme, F.; D'Agosto, F.; Boisson, C.; Spitz, R. *Angew. Chem. Int. Ed.* **2008**, *47*, 9311-9313.
- (44) Doi, Y.; Hizal, G.; Soga, K. *Makromol. Chem.* **1987**, *188*, 1273-1279.
- (45) Doi, Y.; Keii, T. *Adv. Polym. Sci.* **1986**, *73/74*, 201.
- (46) Doi, Y.; Murata, M.; Soga, K. *Makromol. Chem. Rapid Commun.* **1984**, *5*, 811-814.
- (47) Doi, Y.; Tokuhiko, N.; Suzuki, S.; Soga, K. *Makromol. Chem. Rapid Commun.* **1987**, *8*, 285-290.

- (48) Doi, Y.; Watanabe, Y.; Ueki, S.; Soga, K. *Makromol. Chem. Rapid Commun.* **1983**, *4*, 533-537.
- (49) Gottfried, A. C.; Brookhart, M. *Macromolecules* **2003**, *36*, 3085-3100.
- (50) Ueki, S.; Furuhashi, H.; Murakami, N.; Murata, M.; Doi, Y. *Science and Technology in Catalysis* **1995**, *92*, 359-362.
- (51) Makio, H.; Fujita, T. *Macromol. Rapid Commun.* **2007**, *28*, 698-703.
- (52) Kuo, J.-C.; Lin, W.-F.; Yu, C.-H.; Tsai, J.-C.; Wang, T.-C.; Chung, T.-M.; Ho, R.-M. *Macromolecules* **2008**, *41*, 7967-7977.
- (53) Lin, W.-F.; Tsai, J.-C. *J. Poly Sci., Part A: Poly. Chem.* **2008**, *46*, 2167-2176.
- (54) Lin, W.-F.; Hsiao, T.-J.; Tsai, J.-C.; Chung, T. M.; Ho, R.-M. *J. Poly Sci., Part A: Poly. Chem.* **2008**, *46*, 4843-4856.
- (55) Reddy, K. R.; Kumar, B.; Rana, S.; Tevtia, A. K.; Singh, R. P. *J. Appl. Poly. Sci.* **2007**, *104*, 1596-1602.
- (56) Lehmus, P.; Kokko, E.; Leino, R.; Luttikhedde, H. J. G.; Rieger, B.; Seppala, J. V. *Macromolecules* **2000**, *33*, 8534-8540.
- (57) Kojoh, S.; Tsutsui, T.; Kiola, M.; Kashiwa, N. *Polym. Journal* **1999**, *31*, 332-335.
- (58) Koo, K.; Marks, T. J. *J. Am. Chem. Soc.* **1999**, *121*, 8791-8802.
- (59) Kaneyoshi, H.; Matyjaszewski, K. *J. Appl. Poly. Sci.* **2007**, *105*, 3-13.
- (60) Shiono, T.; Kurosawa, H.; Ishida, O.; Soga, K. *Macromolecules* **1993**, *26*, 2085-2089.
- (61) Shiono, T.; Soga, K. *Macromolecules* **1992**, *25*, 3356-3361.
- (62) Kaneko, H.; Matsugi, T.; Kawahara, N.; Matsuo, S.; Kojoh, S.; Kashiwa, N. *Kinetics and Catalysis* **2006**, *47*, 227-233.
- (63) Weng, W.; Markel, E. J.; Dekmezian, A. H. *Macromol. Rapid Commun.* **2000**, *21*, 1103-1107.

- (64) Kawahara, N.; Kojoh, S.; Matsuo, S.; Kaneko, H.; Matsugi, T.; Toda, Y.; Mizuno, A.; Kashiwa, N. *Polymer* **2004**, *45*, 2883-2888.
- (65) Resconi, L.; Camurati, I.; Sudmeijer, O. *Top. Catal.* **1999**, *7*, 145-163.
- (66) Lahelin, M.; Kokko, E.; Lehmus, P.; Pitkänen, P.; Löfgren, B.; Seppälä, J. *Macromol. Chem. Phys.* **2003**, *204*, 1323-1337.
- (67) Resconi, L.; Jones, R. L.; Rheingold, A. L.; Yap, G. P. A. *Organometallics* **1996**, *15*, 998-1005.
- (68) Cherian, A. E.; Lobkovsky, E. B.; Coates, G. W. *Macromolecules* **2005**, *38*, 6259-6268.
- (69) Ye, Z.; Zhu, S. *J. Poly Sci., Part A: Poly. Chem.* **2003**, *41*, 1152-1159.
- (70) Britovsek, G. J. P.; Gibson, V. C.; Kimberley, B. S.; Maddox, P. J.; McTavish, S. J.; Solan, G. A.; White, A. J. P.; Williams, D. J. *Chem. Commun.* **1998**, 849-850.
- (71) Pellicchia, C.; Mazzeo, M.; Pappalardo, D. *Macromol. Rapid Commun.* **1998**, *19*, 651-655.
- (72) Small, B. L.; Brookhart, M. *Macromolecules* **1999**, *32*, 2120-2130.
- (73) Iha, R. K.; Wooley, K. L.; Nyström, A. M.; Burke, D. J.; Kade, M. J.; Hawker, C. J. *Chem. Rev.* **2009**, *109*, 5620-5686.
- (74) Petzetakis, N.; Pitsikalis, M.; Hadjichristidis, N. *J. Poly Sci., Part A: Poly. Chem.* **2010**, *48*, 1092-1103.
- (75) Inglis, A. J.; Paulöhr, T.; Barner-Kowollik, C. *Macromolecules* **2010**, *43*, 33-36.
- (76) Bellas, V.; Rehahn, M. *Macromol. Chem. Phys.* **2009**, *210*, 320-330.
- (77) Li, M.; De, P.; Gondi, S. R.; Sumerlin, B. S. *J. Poly Sci., Part A: Poly. Chem.* **2008**, *46*, 5093-5100.
- (78) Dag, A.; Durmaz, H.; Sirkecioglu, O.; Hizal, G.; Tunca, U. *J. Poly Sci., Part A: Poly. Chem.* **2009**, *47*, 2344-2351.
- (79) Ohno, S.; Gao, H.; Cusick, B.; Kowalewski, T.; Matyjaszewski, K. *Macromol. Chem. Phys.* **2009**, *210*, 421-430.

- (80) Dag, A.; Durmaz, H.; Tunca, U.; Hizal, G. *J. Poly Sci., Part A: Poly. Chem.* **2009**, *47*, 178-187.
- (81) Gao, H.; Matyjaszewski, K. *J. Am. Chem. Soc.* **2007**, *129*, 11828-11834.
- (82) Urbani, C. N.; Bell, C. A.; Lonsdale, D. E.; Whittaker, M. R.; Monteiro, M. J. *Macromolecules* **2007**, *40*, 7056-7059.
- (83) Hirao, A.; Hayashi, M.; Loykulant, S.; Sugiyama, K.; Ryu, S. W.; Haraguchi, N.; Matsuo, A.; Higashihara, T. *Prog. Polym. Sci.* **2005**, *30*, 111-182.
- (84) Hirao, A.; Tokuda, Y. *Macromolecules* **2003**, *36*, 6081-6086.
- (85) Lammens, M.; Fournier, D.; Fijten, M. W. M.; Hoogenboom, R.; Prez, F. D. *Macromol. Rapid Commun.* **2009**, *30*, 2049-2055.
- (86) Hustad, P. D.; Tian, J.; Coates, G. W. *J. Am. Chem. Soc.* **2002**, *124*, 3614-3621.
- (87) Makio, H.; Kashiwa, N.; Fujita, T. *Adv. Synth. Catal* **2002**, *344*, 477-493.
- (88) Mitani, M.; Saito, J.; Ishii, S.; Nakayama, Y.; Makio, H.; Matsukawa, N.; Matsui, S.; Mohri, J.; Furuyama, R.; Terao, H.; Bando, H.; Tanaka, H.; Fujita, T. *Chem. Rec.* **2004**, *4*, 137-158.
- (89) Tian, J.; Coates, G. W. *Angew. Chem. Int. Ed.* **2000**, *39*, 3626-3629.
- (90) Milano, G.; Fiorello, G.; Guerra, G.; Cavallo, L. *Macromol. Chem. Phys.* **2002**, *203*, 1564-1572.
- (91) Lamberti, M.; Gliubizzi, R.; Mazzeo, M.; Tedesco, C.; Pellicchia, C. *Macromolecules* **2004**, *37*, 276-282.
- (92) Talarico, G.; Busico, V.; Cavallo, L. *J. Am. Chem. Soc.* **2003**, *125*, 7172-7173.
- (93) Saito, J.; Mitani, M.; Onda, M.; Mohri, J.; Ishi, J. I.; Yoshida, Y.; Nakano, T.; Tanaka, H.; Matsugi, T.; Kojoh, S. I.; Kashiwa, N.; Fujita, T. *Macromol. Rapid Commun.* **2001**, *22*, 1072-1075.
- (94) Tian, J.; Hustad, P. D.; Coates, G. W. *J. Am. Chem. Soc.* **2001**, *123*, 5134-5135.
- (95) Mason, A. F.; Tian, J.; Hustad, P. D.; Lobkovsky, E. B.; Coates, G. W. *Isr. J. Chem.* **2002**, *42*, 301-306.

- (96) Mitani, M.; Mohri, J.; Yoshida, Y.; Saito, J.; Tsuru, K.; Matsui, S.; Furuyama, R.; Nakano, T.; Tanaka, H.; Kojoh, S.; Matsugi, T.; Kashiwa, N.; Fujita, T. *J. Am. Chem. Soc.* **2002**, *124*, 3327-3336.
- (97) Mitani, M.; Furuyama, R.; Mohri, J.; Saito, J.; Ishii, S.; Terao, H.; Nakano, T.; Tanaka, H.; Fujita, T. *J. Am. Chem. Soc.* **2003**, *125*, 4293-4305.
- (98) Talarico, G.; Busico, V.; Cavallo, L. *Organometallics* **2004**, *23*, 5989-5993.
- (99) Mitani, M.; Nakano, T.; Fujita, T. *Chem. Eur. J.* **2003**, *9*, 2396-2403.
- (100) Lamberti, M.; Pappalardo, D.; Zambelli, A.; Pellicchia, C. *Macromolecules* **2002**, *35*, 658-663.
- (101) Mason, A. F.; Coates, G. W. *J. Am. Chem. Soc.* **2004**, *126*, 10798-10799.
- (102) Stammen, B.; Berlage, U.; Kindermann, R.; Kaiser, M.; Günther, B.; Scheldrick, W. S.; Welzel, P.; Roth, W. R. *J. Org. Chem.* **1992**, *57*, 6566-6575.
- (103) Liaw, D.-J.; Huang, C.-C.; Fu, C.-W. *J. Poly Sci., Part A: Poly. Chem.* **2006**, *44*, 4428-4434.
- (104) Schaeffgen, J. R.; Flory, P. J. *J. Am. Chem. Soc.* **1948**, *70*, 2709-2718.
- (105) Roovers, J., Encyclopedia of Polymer Science and Engineering. In 1985-1990; Vol. 2, pp 478-499.
- (106) Schulz, G. V. *Z. Physik. Chem.* **1939**, *B43*, 25.
- (107) Ruokolainen, J.; Mezzenga, R.; Fredrickson, G. H.; Kramer, E. J.; Hustad, P. D.; Coates, G. W. *Macromolecules* **2005**, *38*, 851-860.
- (108) Schmidtke, J.; Strobl, G.; Thurn-Albrecht, T. *Macromolecules* **1997**, *30*, 5804-5821.
- (109) Supaphol, P.; Spruiell, J. E. *J. Appl. Poly. Sci.* **2000**, *75*, 44-59.
- (110) De Rosa, C.; Auriemma, F. *Prog. Polym. Sci.* **2006**, *31*, 145-237.
- (111) De Rosa, C.; Auriemma, F.; Vinti, V.; Galimberti, M. *Macromolecules* **1998**, *31*, 6206-6210.

- (112) De Rosa, C.; Circelli, T.; Auriemma, F.; Mathers, R. T.; Coates, G. W.  
*Macromolecules* **2004**, *37*, 9034-9047.

# Chapter 5

Polymerization of Propylene and Ureidopyrimidinone-  
Functionalized Olefins Using Ni(II)  $\alpha$ -Diimine Catalysts

## 5.1 Introduction

With worldwide production exceeding 100 million tons per year, polyolefins represent one of the most important classes of commercial polymers on the market today.<sup>1</sup> The materials obtained from olefin polymerization are useful in a variety of applications from automotive to food packaging and beyond, due in part to their robust chemical and physical properties combined with low cost.<sup>2</sup> However, the non-polar nature of polyolefin materials often results in poor adhesion properties and low compatibility with polar additives, which inhibits printability, dyeability and adhesion.<sup>3,4</sup> Incorporation of even small amounts of polar functional groups into a polyolefin chain can significantly improve these properties.<sup>5</sup> Polyolefins containing functional groups are currently produced commercially via radical polymerization methods, limiting the scope of materials produced.<sup>6</sup> In recent years, transition-metal catalyzed coordination-insertion polymerization has been targeted as a synthetic method to afford new functionalized polyolefin materials.<sup>6-11</sup>

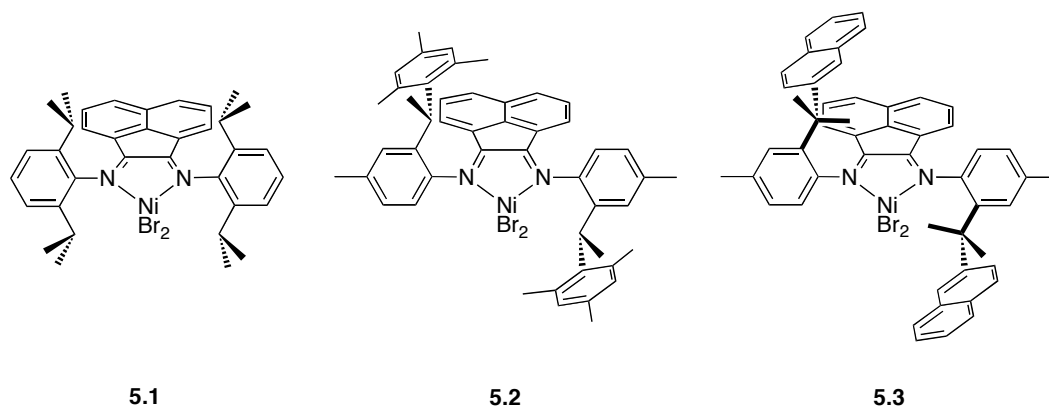
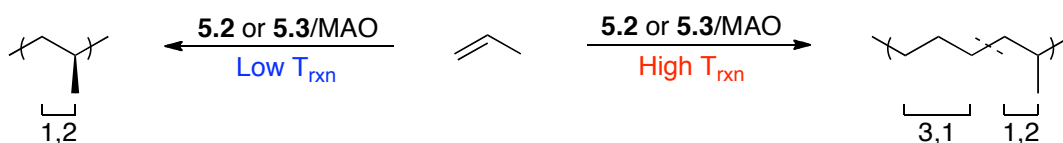


**Figure 5.1.**  $\alpha$ -Diimine Ni(II) olefin polymerization precatalysts.

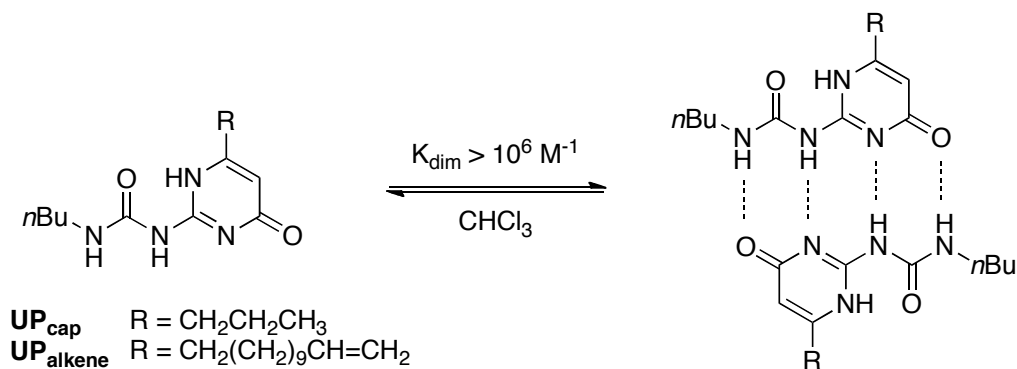
Although early metals are capable of catalyzing the copolymerization of olefins with polar comonomers,<sup>12-15</sup> late metal catalysts are generally more tolerant to polar functional groups due to their low oxophilicity.<sup>9,16-20</sup> In particular, nickel and

palladium olefin polymerization catalysts bearing  $\alpha$ -diimine ligands (Figure 5.1) have been utilized in the polymerization of olefins with a variety of comonomers including acrylates,<sup>16,20-30</sup> silyl vinyl ethers<sup>31</sup> and methyl vinyl ketones.<sup>20,21</sup> Brookhart and coworkers reported the  $\alpha$ -diimine class of catalysts in 1995 as the first late metal catalysts capable of converting  $\alpha$ -olefins to high molecular weight polymers.<sup>32</sup> Subsequent reports showed the Ni(II)  $\alpha$ -diimine catalysts polymerized  $\alpha$ -olefins in a living fashion making the production of block copolymers possible.<sup>33</sup> During propylene polymerization with **5.1**/MAO, chain walking following a 2,1-insertion of propylene ultimately results in 3,1-enchainments as well as the commonly observed 1,2-enchainment. As a result, the polypropylene produced by **5.1** at 0 °C is regioirregular and amorphous with only moderate syndiotacticity observed upon decreasing the reaction temperature to -78 °C.<sup>34</sup> In an effort to improve regio- and stereochemistry, Coates and coworkers developed a series of  $\alpha$ -diimine catalysts derived from chiral anilines.<sup>35-38</sup> At low reaction temperatures, complex **5.2** forms highly isotactic, regioregular polypropylene while regioirregular, amorphous polypropylene is formed at high reaction temperatures (Scheme 5.1). The living nature of the polymerization allowed for the production of elastomeric block copolymers from a single monomer.<sup>36</sup> Subsequent modifications to the aniline moiety resulted in a series of olefin polymerization catalysts (e.g. **3**) that displayed higher polymerization activity than **5.2** while maintaining stereoregularity at low temperatures.<sup>39</sup> Given the high functional group tolerance of late metal catalysts, we evaluated **5.2** and **5.3** as potential catalysts for the copolymerization of propylene and polar comonomers.



**Scheme 5.1.** Propylene polymerization using **5.2** or **5.3**/MAO.

Polar monomers bearing hydrogen bonding moieties represent a particularly intriguing class of functionalized olefins. Many polymers, both natural and synthetic, derive unique structure and function from the ability to form hydrogen bonded networks. This includes natural materials such as DNA and proteins, as well as synthetic materials such as polyamides, polyurethanes and nylon polymers.<sup>40-45</sup> In 1997, Meijer and coworkers described the first synthesis of high molecular weight polymers containing pendant ureidopyrimidinones (Scheme 5.2), which are capable of hydrogen bonding.<sup>46</sup> The strong, highly directional interaction between ureidopyrimidinones is due to the complementary DDAA (donor-donor-acceptor-acceptor) arrangement of the four hydrogen bonds and is evidenced by the dimerization constant ( $K_{\text{dim}} > 10^6 \text{ M}^{-1}$  in  $\text{CHCl}_3$ ). Since this seminal discovery, polymeric materials bearing hydrogen bonding groups have been produced using a variety of methods including radical,<sup>47-55</sup> anionic,<sup>56-62</sup> metathesis<sup>63-65</sup> and coordination-insertion polymerization.<sup>66</sup>



**Scheme 5.2.** Hydrogen bonding in 2-ureido-4[1H]-pyrimidinones.

Linear arrays, like those reported by Meijer and coworkers, produced through the dimerization of bifunctional hydrogen bonding monomers represent just one type

of supramolecular polymer.<sup>40,46</sup> Covalent incorporation of monomers bearing hydrogen bonding moieties into polymer main-chains, such as polybutadiene,<sup>56-62</sup> polystyrene,<sup>48,50,67</sup> and polybutylmethacrylate,<sup>47-49,51,53,55</sup> represent another type of supramolecular material which forms reversibly cross-linked networks that can effect bulk polymer properties.<sup>40</sup> For example, coordination-insertion polymerization of 1-hexene and a ureidopyrimidinone-functionalized olefin with **5.1**/Et<sub>2</sub>AlCl results in regioirregular poly(1-hexene) containing 2% of the hydrogen bonding moiety.<sup>66</sup> The resultant copolymer displayed increased solution viscosity compared with the homopolymer and mechanical testing of the functionalized poly(1-hexene) showed that the bulk polymer exhibits elastomeric properties at room temperature due to the presence of non-covalent cross-links.

Based on the improved mechanical properties obtained for poly(1-hexene) containing hydrogen bonding groups, we targeted propylene polymerization with **5.2** and **5.3** in the presence of the ureidopyrimidinone-functionalized olefin (UP<sub>alkene</sub>). A range of reaction temperatures were explored with **5.2** and **5.3** to obtain both regioirregular and regioregular polypropylene bearing hydrogen bonding moieties. Herein the synthesis and properties of the ureidopyrimidinone-functionalized polypropylene is reported.

## **5.2 Results and Discussion**

### **5.2.1 Homopolymerization of Propylene with 5.2 and 5.3**

A series of polypropylene homopolymers with varying regio-defects were produced using complexes **5.2** and **5.3**/MMAO-3A (Table 5.1). In collaboration with Dr. Rufina Alamo and Carolina Ruiz of Florida State University as well as industrial scientists at Exxon Mobil Research, detailed structural analysis of the polymers was carried out. By varying the reaction temperature (-55 °C to -30 °C), the effect of

polymerization temperature on the resultant polymer microstructure was investigated using catalysts **5.2** (2.9 – 15.5%, Entries 1 - 8, Table 5.1) and **5.3** (3.1 – 15.0%, Entries 9 - 15, Table 5.1). For both complexes, regio-defects increased with increasing polymerization temperature as evidenced by  $^{13}\text{C}\{^1\text{H}\}$  NMR spectroscopy.

Upon combining precatalysts **5.2** and **5.3** with MMAO-3A in the presence of propylene, an active olefin polymerization catalyst ( $\text{L}_n\text{Ni}^+\text{-Me}$ , Scheme 5.3) is produced and subsequently polypropylene is formed. At low reaction temperature (-55 °C), 1,2-insertion of propylene dominates the polymerization with the same propylene enantioface coordinating each time resulting in the formation of isotactic polypropylene upon insertion. However, even at low reaction temperature (-55 °C), some regio-defects are present in the polypropylene samples produced with **5.2** and **5.3**. These defects occur when propylene is inserted into the growing polymer chain in a 2,1 fashion. One of the most commonly observed defects in the polypropylene produced for this study was the isolated (3,1)-defect (Scheme 5.3a). Following a 2,1-insertion of propylene into the growing polymer chain,  $\beta$ -hydrogen elimination and reinsertion of the olefin coordinated polymer produces a primary Ni-polymer bond. A 1,2-propylene insertion following this event results in observed, isolated (3,1)-defect. Both **5.2** and **5.3** produce the isolated (3,1)-defect at all temperatures studied with an increasing amount of the defect observed with increasing reaction temperature. In general, the polypropylene produced by **5.3** contained fewer isolated (3,1)-defects than the polypropylene produced by **5.2**.

Defects occurring very near one another in the polypropylene chain can also be observed by  $^{13}\text{C}\{^1\text{H}\}$  NMR spectroscopy in addition to the isolated regio-defects. When a 3,1-insertion is followed by a single 1,2-insertion as well as another 3,1-insertion, the alternating (3,1)(1,2)(3,1)-defect (Scheme 5.3b) is obtained. Relative to the isolated (3,1)-defect fewer alternating (3,1)(1,2)(3,1)-defects are observed in the

polypropylene produced by **5.2** and **5.3** at all reaction temperatures. The polypropylene obtained from **5.2** typically contains more alternating (3,1)(1,2)(3,1)-defects than the polymers produced with **5.3**. If the first 3,1-insertion is instead followed by another 2,1-insertion and chain walking occurs, then the successive (3,1)(3,1)-defect (Scheme 5.3c) is observed. Both **5.2** and **5.3** produce very few successive (3,1)(3,1)-defects, even at high reactions temperatures (~1% at -30 °C). Interestingly, a 3,1-insertion of propylene followed by a 2,1-insertion resulting in the (2,1)(3,1)-defect does not occur as evidenced by  $^{13}\text{C}\{^1\text{H}\}$  NMR spectroscopy.

In addition to these defects, a number of other regioerrors are possible when a 2,1-insertion occurs without chain walking taking place. If normal 1,2-insertion of propylene resumes following a 2,1-insertion, then the isolated (2,1)-defect (Scheme 5.4f) is observed. Both **5.2** and **5.3** produce this defect during propylene polymerization, however, polymerization with **5.3** results in far fewer isolated (2,1)-defects at low reaction temperatures than **5.2**. Alternatively, following the 2,1-insertion by another 2,1-insertion would result in a (2,1)(2,1)-defect; however, this error was not observed by  $^{13}\text{C}\{^1\text{H}\}$  NMR spectroscopy. When subsequent 2,1-insertions occur, chain walking always takes place in the case of the second insertion resulting in a (3,1)(2,1)-defect (Scheme 5.3d). The polypropylene produced with **5.3** contains a significant amount of the (3,1)(2,1)-defect at all reaction temperatures studied, whereas **5.2** results in smaller amounts of this defect only at higher reaction temperatures.

A series of polypropylene samples with varying regiochemistry have been produced from the Ni(II)  $\alpha$ -diimine catalysts **5.2** and **5.3**. Because of the ability of late metal catalyst to chain-walk, (3,1)-defects are present in the polypropylene in addition to (2,1)-defects and may be combined in a number of different ways to produce regio-defects. Observed defects were low at low reaction temperature (-55



**Table 5.1** Propylene Polymerization with **5.2** and **5.3**/MMAO-3A.<sup>a</sup>

Entry	Cplx	$T_{\text{rxn}}$ (°C)	$t_{\text{rxn}}$ (hr)	$M_n$ (kg/mol) <sup>b</sup>	$M_w/M_n$ <sup>b</sup>	total defects mol% <sup>c</sup>	stereo mol% <sup>c</sup>	(3,1) mol% <sup>c</sup>	(3,1)(1,2)(3,1) mol% <sup>c</sup>	(3,1)(3,1) mol% <sup>c</sup>	(2,1)(3,1) mol% <sup>c</sup>	(2,1) mol% <sup>c</sup>
1	<b>5.2</b>	-55	48	13	1.46	2.9	0.4	2.5	0.0	0.0	0.0	0.0
2	<b>5.2</b>	-50	48	14	1.34	4.6	0.4	2.4	0.5	0.0	0.0	1.3
3	<b>5.2</b>	-48	42	24	1.25	6.8	0.4	4.1	0.8	0.1	0.0	1.4
4	<b>5.2</b>	-46	47	36	1.21	8.4	0.4	5.0	1.0	0.1	0.0	1.9
5	<b>5.2</b>	-45	46	38	1.15	10.2	0.4	7.2	1.4	0.2	0.0	1.0
6	<b>5.2</b>	-43	44	70	1.15	11.8	0.4	6.2	2.1	0.5	1.2	1.4
7	<b>5.2</b>	-40	24	53	1.14	13.8	0.4	7.3	3.0	0.0	2.7	0.4
8	<b>5.2</b>	-35	20	58	1.14	15.5	0.4	9.0	3.3	1.1	1.7	0.0
9	<b>5.3</b>	-55	48	58	1.23	3.1	0.4	1.1	0.2	0.1	0.9	0.4
10	<b>5.3</b>	-55	6	35	1.18	3.4	0.4	1.4	0.3	0.0	1.3	0.0
11	<b>5.3</b>	-55	48	72	1.29	3.4	0.5	0.9	0.5	0.0	1.5	0.0
12	<b>5.3</b>	-50	48	155	1.35	3.8	0.7	1.3	0.3	0.1	1.1	0.3
13	<b>5.3</b>	-40	48	164	1.32	5.8	0.4	3.1	0.6	0.0	1.7	0.0
14	<b>5.3</b>	-35	48	210	1.32	7.9	0.4	3.3	0.6	0.2	3.2	0.2
15	<b>5.3</b>	-30	24	221	1.33	15.0	0.4	4.6	2.2	1.3	5.7	0.8

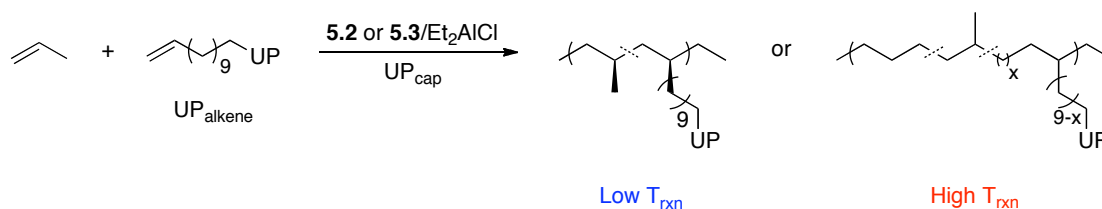
<sup>a</sup> General Conditions: Ni = 17  $\mu\text{mol}$ , [Al]/[Ni] = 270, 25 mL toluene, 5 or 15 g propylene. <sup>b</sup> Molecular weight ( $M_n$ ) and molecular weight distribution ( $M_w/M_n$ ) were determined by gel permeation chromatography at 140 °C in 1,2,4-trichlorobenzene relative to polyethylene standards. <sup>c</sup> Determined using  $^{13}\text{C}\{^1\text{H}\}$  NMR spectroscopy in 1,1,2,2-tetrachloroethane- $d_2$  at 135 °C.

°C) and increased with increasing reaction temperature. Using catalyst **5.2**, polypropylene with a range of regio-defects was produced (2.9 – 15.5%, Entries 1 - 8, Table 5.1). At all temperatures studied, the isolated (3,1)-defect was the predominant error. The alternating (3,1)(1,2)(3,1) was also observed in significant amounts as reaction temperature increased. The low isolated (2,1)-defects coupled with significant isolated (3,1)-defects suggests **5.2** is likely to chain walk to the primary position when a 2,1-misinsertion occurs. The polypropylene produced with **5.3** also displayed a wide range of regio-defects (3.1 – 15.0%, Entries 9 - 15, Table 5.1). The isolated (3,1)-defect was again one of the dominant errors, however, nearly equal amounts of the (2,1)(3,1)-defect were observed. Therefore, **5.3** is much more likely than **5.2** to follow a (3,1)-defect with a 2,1-misinsertion.

### 5.2.2 Copolymerization of UP<sub>alkene</sub> and Propylene using **5.2**/Et<sub>2</sub>AlCl

Initial investigations into the copolymerization behavior of propylene and UP<sub>alkene</sub> were carried out with catalyst **5.2** (Scheme 5.4, Table 5.2). Although a number of successful cocatalysts (MMAO-3A, MMAO-7 and Et<sub>2</sub>AlCl) were identified at 0 °C, propylene polymerization with **5.2**/Et<sub>2</sub>AlCl resulted in the highest molecular weight polymer and was therefore used as the activator for the remainder of the study. In addition to serving as an activator, Et<sub>2</sub>AlCl reacts with any acidic groups on the ureidopyrimidinone, acting as a protecting group. Previous reports found that the addition of a non-olefinic ureidopyrimidinone (UP<sub>cap</sub>) was necessary to prevent the formation of an insoluble network through reaction of the Al and UP functionalized polymer.<sup>66</sup> The addition of UP<sub>cap</sub> was also found to be necessary for the polymerizations carried out in this study. Three copolymerizations of propylene and UP<sub>alkene</sub> were carried out with **5.2**/Et<sub>2</sub>AlCl at 0 °C. The molecular weight of the resultant polypropylene ( $M_n = 15,000 - 59,000$  g/mol) was observed to increase with

conversion (0.48 g – 1.99 g). Based on these results, it is believed that **5.2** maintains its living behavior even in the presence of the functionalized monomer. Molecular weight distributions ( $M_w/M_n = 1.38 - 1.86$ ) are broader than what would normally be obtained from a living catalyst, which may be attributed to intermolecular hydrogen bonding between ureidopyrimidinones. For comparison, polymerization of propylene without UP<sub>alkene</sub> in the presence of **5.2**/Et<sub>2</sub>AlCl was carried out, yielding a polymer with a narrow molecular weight distribution ( $M_w/M_n = 1.11$ ) as well as an increased molecular weight ( $M_n = 53,000$  g/mol, Entry 1, Table 5.2), however, yield was nearly identical to the functionalized polymer. Intermolecular hydrogen bonding in the UP containing materials results in polypropylene with a smaller hydrodynamic radius, and therefore a smaller observed molecular weight than non-UP containing polymers.



**Scheme 5.4.** Copolymerization of propylene and UP<sub>alkene</sub> with **5.2** or **5.3**/Et<sub>2</sub>AlCl.

Over a range of temperatures (0 to -60 °C), molecular weight was observed to decrease with decreasing reaction temperature for both the UP ( $M_n = 8,900 - 59,000$  g/mol) and non-UP containing polymers ( $M_n = 17,000 - 53,000$  g/mol). Yield was found to be nearly identical for polymerization with and without the polar monomer, suggesting that the presence of UP<sub>alkene</sub> does not significantly alter the polymerization. Comparison of the <sup>1</sup>H NMR spectra of UP<sub>alkene</sub> and the resultant functionalized polypropylene (Figure 5.2, 5.4 and 5.5) shows the disappearance of the alkene

**Table 5.2.** Polymerization of propylene and UP<sub>alkene</sub> with **5.2**/Et<sub>2</sub>AlCl.

Entry	$T_{\text{rxn}}$ (°C)	$t_{\text{rxn}}$ (hr)	Yield (g)	$M_n$ (kg/mol) <sup>c</sup>	$M_n^{\text{theo}}$ (kg/mol)	$M_w/M_n^c$	UP (%) <sup>d</sup>	3,1 (%) <sup>d</sup>	$T_g$ <sup>e</sup> (°C)	$T_m$ <sup>e</sup> (°C)
1 <sup>a</sup>	0	1	0.48	15	28	1.79	0.91	44.5	-56	ND <sup>g</sup>
2 <sup>a</sup>	0	2	0.93	33	55	1.38	0.69	43.4	-55	ND <sup>g</sup>
3 <sup>b</sup>	0	2	0.89	53	52	1.11	--	48.4	-60	ND <sup>g</sup>
4 <sup>a</sup>	0	4	1.99	59	120	1.86	0.51	46.6	-56	ND <sup>g</sup>
5 <sup>a</sup>	-20	6	0.56	16	33	1.56	1.16	26.8	-44	ND <sup>g</sup>
6 <sup>b</sup>	-20	6	0.51	39	30	1.10	--	30.5	-50	ND <sup>g</sup>
7 <sup>a</sup>	-40	24	0.41	14	24	1.38	1.19	14.9	-28	ND <sup>g</sup>
8 <sup>b</sup>	-40	24	0.35	29	21	1.15	--	20.7	-36	ND <sup>g</sup>
9 <sup>a</sup>	-60	48	0.20	8.9	12	1.67	1.28	13.0	-17	104
10 <sup>b</sup>	-60	48	0.20	17	12	1.38	--	11.8	-26	112

<sup>a</sup> General Conditions: Ni = 17 μmol, [Al]/[Ni] = 530, UP<sub>cap</sub> = 1.2 mmol, UP<sub>alkene</sub> = 0.4 mmol, 25 mL toluene, 5 or 15 g propylene. <sup>b</sup> Ni = 17 μmol, [Al]/[Ni] = 530, 25 mL toluene, 5 or 15 g propylene. <sup>c</sup> Molecular weight ( $M_n$ ) and molecular weight distribution ( $M_w/M_n$ ) were determined by gel permeation chromatography at 140 °C in 1,2,4-trichlorobenzene relative to polyethylene standards. <sup>d</sup> Determined using <sup>1</sup>H NMR spectroscopy in 1,1,2,2-tetrachloroethane-*d*<sub>2</sub> at 135 °C. <sup>e</sup> Melting temperature ( $T_m$ ) and glass transition temperature ( $T_g$ ) were determined by differential scanning calorimetry (second heating run). <sup>g</sup> none detected.

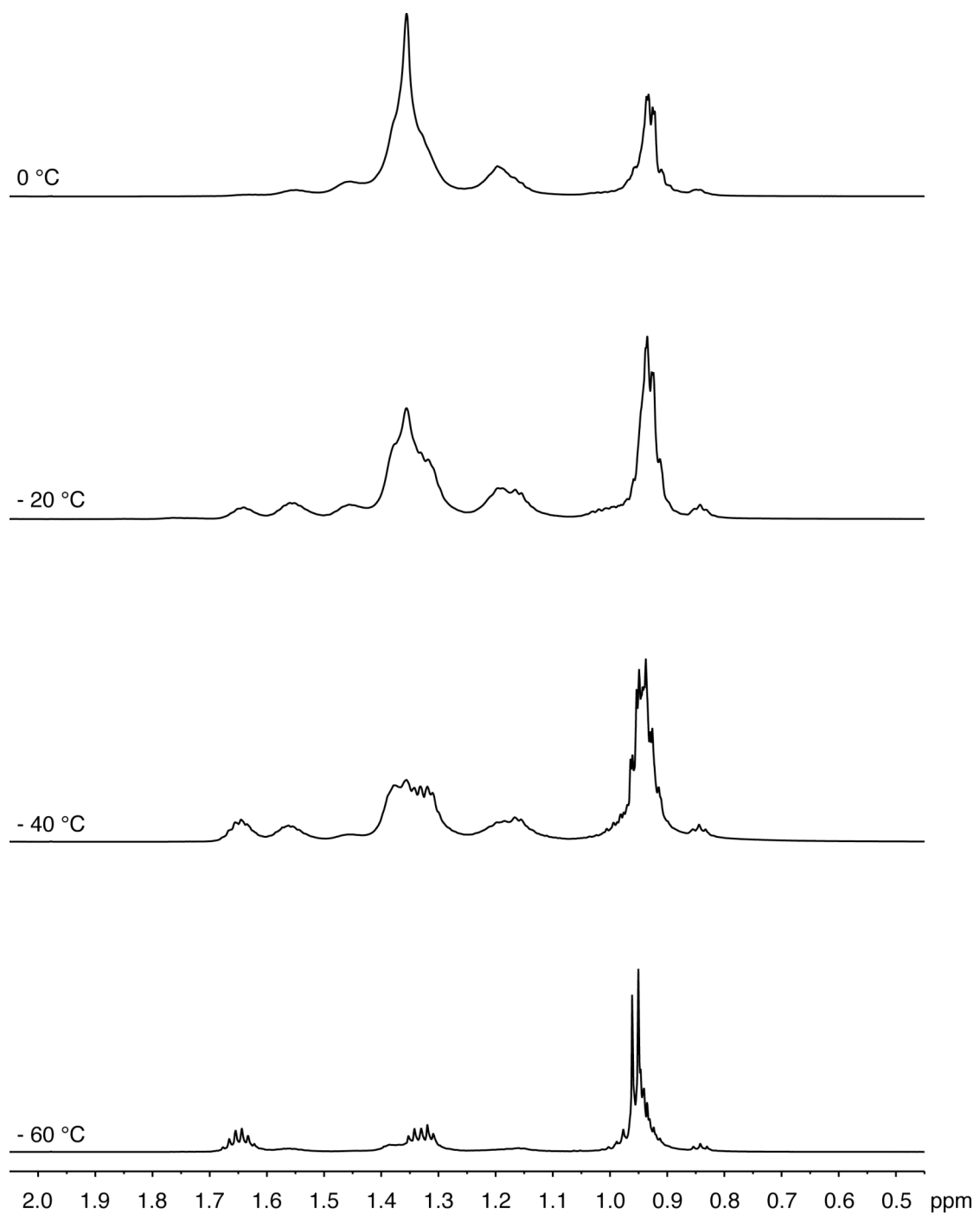


**Figure 5.2.**  $^1\text{H}$  NMR spectra of polypropylene produced with **5.2**/ $\text{Et}_2\text{AlCl}$  (600 MHz, 1,1,2,2-tetrachloroethane- $d_2$ , 135 °C).

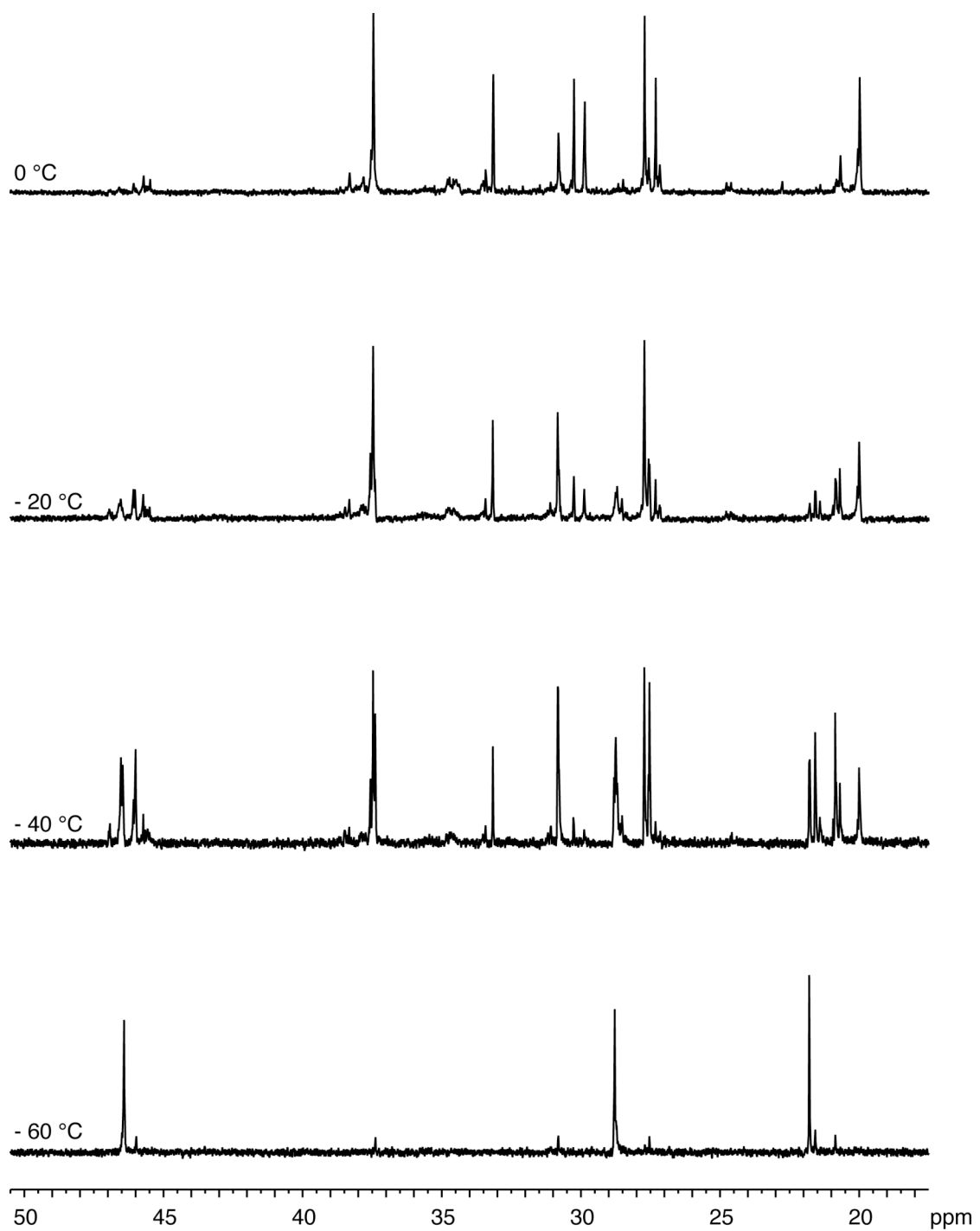


**Figure 5.3.**  $^{13}\text{C}\{^1\text{H}\}$  NMR spectra of polypropylene produced with 5.2/ $\text{Et}_2\text{AlCl}$  (600 MHz, 1,1,2,2-tetrachloroethane- $d_2$ , 135 °C).

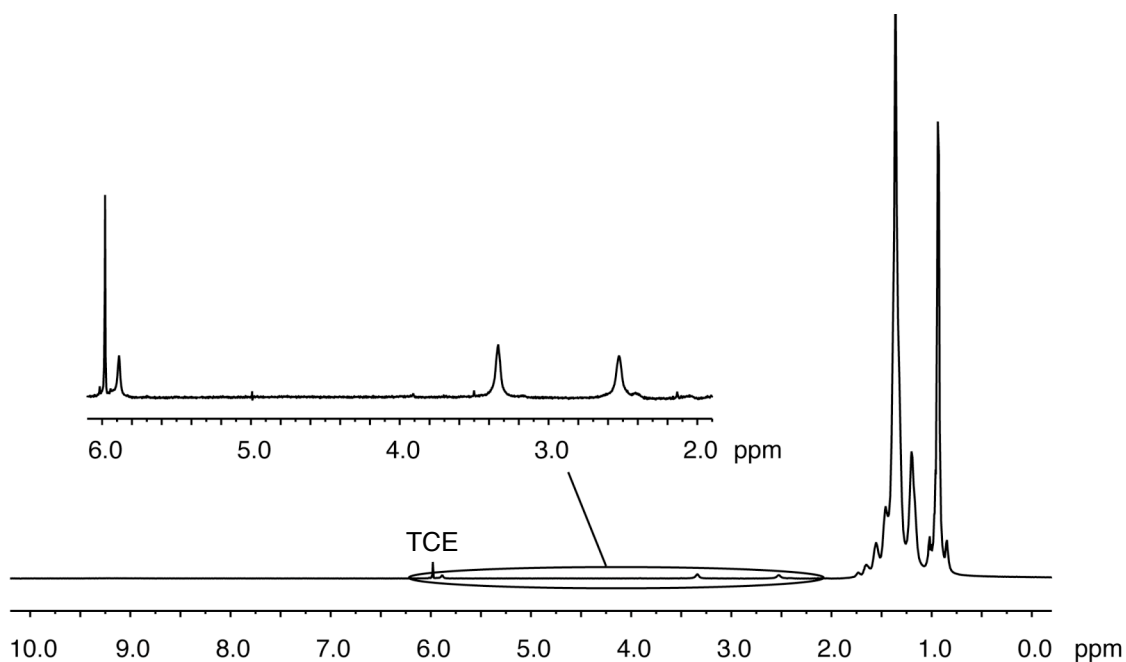


**Figure 5.4.**  $^1\text{H}$  NMR spectrum of poly(propylene-*co*-UP) produced at 0 °C using **5.2** (Entry 1, Table 5.2, 600 MHz, 1,1,2,2-tetrachloroethane- $d_2$  (TCE), 135 °C).

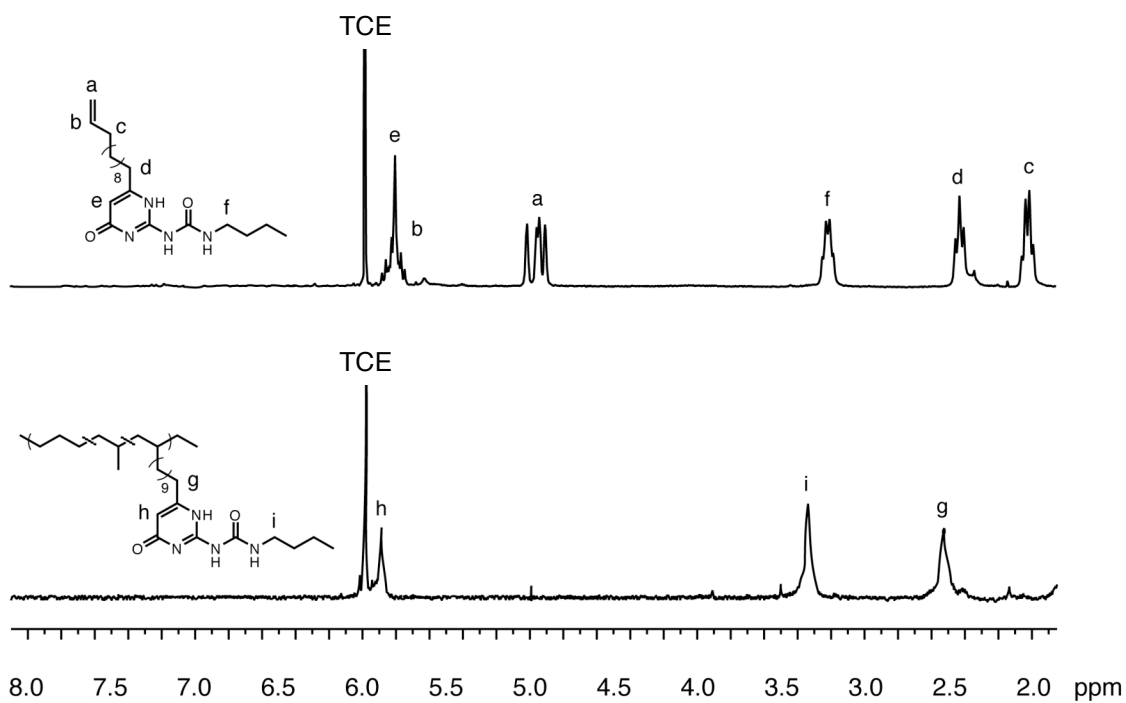


**Figure 5.5.**  $^1\text{H}$  NMR spectra in 1,1,2,2-tetrachloroethane- $d_2$  (TCE) of UP<sub>alkene</sub> and poly(UP-*co*-propylene) (Entry 1, Table 5.2) produced at 0 °C with **5.2**.

resonances ( $\delta$  5.81 and 4.94 ppm) and the signal for the protons adjacent to the alkene ( $\delta$  2.02) with only resonance attributed to the ureidopyrimidinone moiety ( $\delta$  5.88, 3.34 and 2.53 ppm) present in the functionalized polymer. Relative integration of the  $^1\text{H}$  NMR spectra showed 0.51 – 1.28 % incorporation of the functionalized monomer over a range of polymerization temperatures (0 to  $-60$   $^\circ\text{C}$ ). Further analysis of both the  $^1\text{H}$  and  $^{13}\text{C}\{^1\text{H}\}$  NMR spectra (Figure 5.3) for the polypropylene produced using **5.2**/ $\text{Et}_2\text{AlCl}$  shows an increase in both stereo- and regioregularity as reaction temperature decreased. For example, the polypropylene produced at  $0$   $^\circ\text{C}$  was regioirregular and displayed the highest percentage of 3,1-insertions (48.4%, Entry 3, Table 5.2) making this polymer more like an ethylene/propylene copolymer than polypropylene. Alternatively, polymerization at  $-60$   $^\circ\text{C}$  resulted in regioregular, isotactic polypropylene that displayed the lowest amount of 3,1-insertions (11.8% Entry 10, Table 5.2). Analysis of polypropylene thermal properties revealed an increase in the glass transition temperature ( $T_g = -60$   $^\circ\text{C}$  to  $-17$   $^\circ\text{C}$ ) with increasing stereoregularity as the reaction temperature was decreased. The UP containing polymers were generally found to exhibit higher glass transition temperatures than their non-UP containing counterparts. Melting temperatures ( $T_m = 104$  and  $112$   $^\circ\text{C}$ ) were only observed for the polymers produced at  $-60$   $^\circ\text{C}$ . Unlike the glass transition temperature, the melting temperature was observed to decrease upon incorporation of ureidopyrimidinone. Utilizing **5.2**/ $\text{Et}_2\text{AlCl}$ , polypropylene ranging from regioirregular, amorphous to regioregular, isotactic was produced containing hydrogen bonding moieties.

### 5.2.3 Copolymerization of $\text{UP}_{\text{alkene}}$ and Propylene using **5.3**/ $\text{Et}_2\text{AlCl}$

In an effort to increase both molecular weight and melting temperature of poly(propylene-*co*-UP), the copolymerization behavior of **5.3**/ $\text{Et}_2\text{AlCl}$  was also

investigated (Table 5.3). The cumyl-derived Ni(II) catalysts (e.g. **5.3**) had previously been shown to be more active for the polymerization of propylene as well as more selective at low reaction temperatures than **2**.<sup>39</sup> Increased polypropylene molecular weight was observed for the UP containing polymers ( $M_n = 12 - 267$  kg/mol) produced by **5.3**/Et<sub>2</sub>AlCl compared with the analogous polypropylene samples obtained from **5.2**/Et<sub>2</sub>AlCl ( $M_n = 8.9 - 33$  kg/mol). Utilizing **5.3**/Et<sub>2</sub>AlCl at 0 °C, an increase in yield was observed for UP containing polypropylene compared with the non-UP containing polymer suggesting that Et<sub>2</sub>AlCl has an adverse effect on the polymerization at this temperature. Significant difference between theoretical and actual molecular weights were also observed for the homopolymerization of propylene with **3**/Et<sub>2</sub>AlCl at 0 °C. Fortunately, improved polymerization behavior was achieved at lower reaction temperatures (-60, -40 and -20 °C) with good agreement between polymer yields as well as similar theoretical and actual molecular weights obtained for the unfunctionalized polymers. Analysis of the copolymers bearing hydrogen bonding moieties by <sup>1</sup>H NMR spectroscopy (Figure 5.6) revealed 0.18 – 0.69 % incorporation of the functionalized monomer. In general, the UP containing polymers produced with **5.3**/Et<sub>2</sub>AlCl resulted in higher molecular weights and lower overall functionalization than the polymers produced by **5.2**/Et<sub>2</sub>AlCl. Analysis of the polypropylene homo- and copolymers produced with **5.3**/Et<sub>2</sub>AlCl by <sup>1</sup>H and <sup>13</sup>C{<sup>1</sup>H} NMR spectroscopy (Figure 5.7) showed that regioirregular polypropylene (3,1 = 38.1%, Entry 1, Table 5.3) was produced at 0 °C and regioregular, isotactic polypropylene was obtained at -60 °C (3,1 = 10.8%, Entry 8, Table 5.3). The polymer series exhibited higher glass transition temperatures ( $T_g = -52$  to  $-19$  °C) as well as a lower melting temperature ( $T_m = 116$  °C) for the UP containing polymers compared with the non-functionalized polypropylene ( $T_g = -57$  to  $-19$  °C,  $T_m = 119$  °C). Overall, polymerization of propylene and UP<sub>alkene</sub> with **5.3**/Et<sub>2</sub>AlCl resulted in functionalized polypropylene with higher

molecular weights as well as similar stereo- and regiochemistry to the polymers produced by **5.2**/Et<sub>2</sub>AlCl.

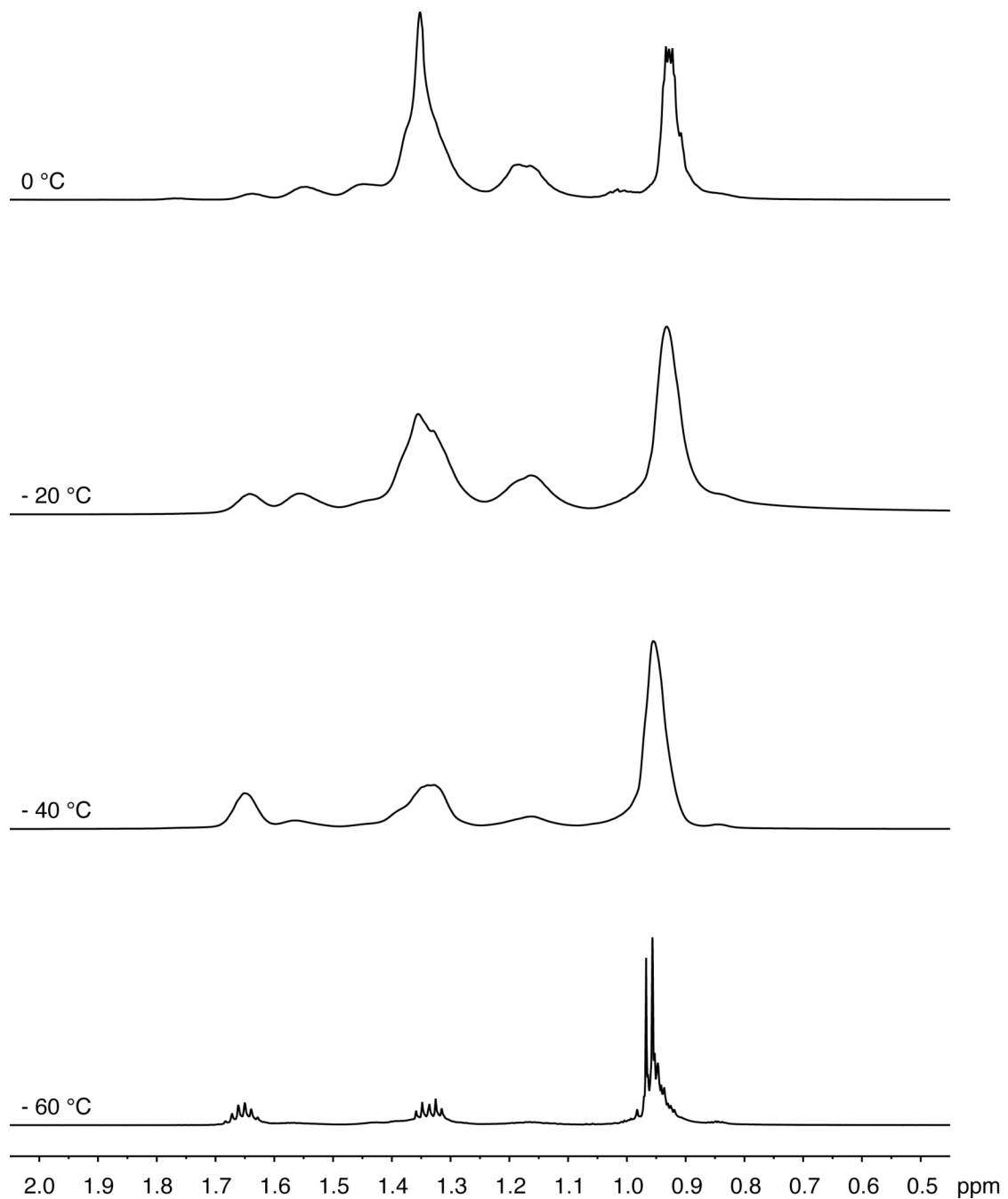


**Figure 5.6.** <sup>1</sup>H NMR spectra of polypropylene produced with **5.3**/Et<sub>2</sub>AlCl (600 MHz, 1,1,2,2-tetrachloroethane-*d*<sub>2</sub>, 135 °C).

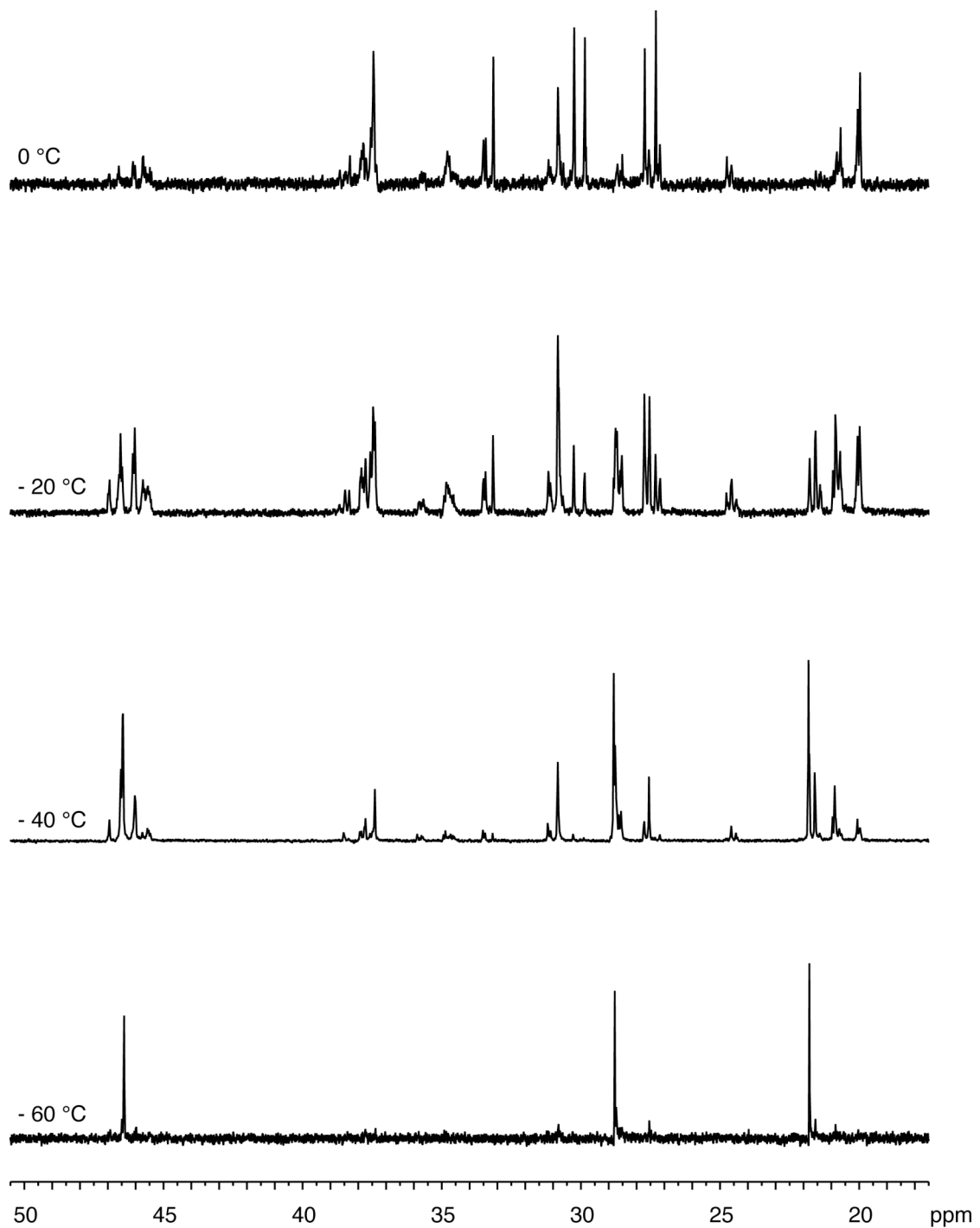


**Figure 5.7.**  $^{13}\text{C}\{^1\text{H}\}$  NMR spectra of polypropylene produced with **5.3**/ $\text{Et}_2\text{AlCl}$  (600 MHz, 1,1,2,2-tetrachloroethane- $d_2$ , 135 °C).

**Table 5.3.** Polymerization of propylene and UP<sub>alkene</sub> with **5.3**/Et<sub>2</sub>AlCl.

Entry	$T_{\text{rxn}}$ (°C)	$t_{\text{rxn}}$ (hr)	Yield (g)	$M_n$ (kg/mol) <sup>c</sup>	$M_n^{\text{theo}}$ (kg/mol)	$M_w/M_n^c$	UP (%) <sup>d</sup>	3,1 (%) <sup>d</sup>	$T_g$ (°C) <sup>e</sup>	$T_m$ (°C) <sup>e</sup>
1 <sup>a</sup>	0	2	0.76	63	45	7.19	0.69	38.1	-52	ND <sup>g</sup>
2 <sup>b</sup>	0	2	0.45	61	26	1.45	--	38.5	-57	ND <sup>g</sup>
3 <sup>a</sup>	-20	6	1.99	267	117	3.80	0.18	26.9	-38	ND <sup>g</sup>
4 <sup>b</sup>	-20	6	2.31	139	136	1.27	--	25.5	-39	ND <sup>g</sup>
5 <sup>a</sup>	-40	24	2.13	77	125	3.28	0.31	17.8	-23	ND <sup>g</sup>
6 <sup>b</sup>	-40	24	2.60	155	153	1.14	--	19.1	-27	ND <sup>g</sup>
7 <sup>a</sup>	-60	48	0.23	12	14	2.04	0.30	13.4	ND <sup>g</sup>	116
8 <sup>b</sup>	-60	48	0.16	16	9.4	1.59	--	10.8	-19	119

<sup>a</sup> General Conditions: Ni = 17 μmol, [Al]/[Ni] = 530, UP<sub>cap</sub> = 1.2 mmol, UP<sub>alkene</sub> = 0.4 mmol, 25 mL toluene, 5 or 15 g propylene. <sup>b</sup> Ni = 17 μmol, [Al]/[Ni] = 530, 25 mL toluene, 5 or 15 g propylene. <sup>c</sup> Molecular weight ( $M_n$ ) and molecular weight distribution ( $M_w/M_n$ ) were determined by gel permeation chromatography at 140 °C in 1,2,4-trichlorobenzene relative to polyethylene standards. <sup>d</sup> Determined using <sup>1</sup>H NMR spectroscopy in 1,1,2,2-tetrachloroethane-*d*<sub>2</sub> at 135 °C. <sup>e</sup> Melting temperature ( $T_m$ ) and glass transition temperature ( $T_g$ ) were determined by differential scanning calorimetry (second heating run). <sup>g</sup> none detected.

#### 5.2.4 Mechanical Testing of Poly(Propylene-co-UP).

The mechanical properties of the random copolymers were investigated by measuring the tensile stress and strain at break (Table 5.4, Figure 5.8, 5.9, 5.10 and 5.11). Even with only ~1% incorporation of the UP moiety, differences in mechanical properties were observed. For several of the unfunctionalized, regioirregular polymers produced by **5.2** and **5.3**, films were difficult to form due to low mechanical integrity and therefore tensile stress and strain were not measured. For the polypropylene produced by **5.2**, incorporation of UP resulted in polymeric materials with measurable mechanical properties (stress = 5.7 – 11 MPa, strain = 12 – 1000%) produced at all temperatures. For the regioregular, isotactic polypropylene produced at -60 °C mechanical properties were measurable for both the UP (stress = 11 MPa, strain = 12%, Entry 4, Table 5.3) and non-UP containing (stress = 6.4 MPa, strain = 25% Entry 5, Table 5.3) polymers. Higher stress and lower strain was observed for the hydrogen bonding polymer compared with the non-hydrogen bonding polymer.

Incorporation of the UP moiety into the polypropylene produced by **5.3** also resulted in polymeric materials with measurable mechanical properties (stress = 2.8 – 13 MPa, strain = 11 – 1200%). At -40 and -60 °C, both functionalized and unfunctionalized polymers produced by **5.3** were characterized and comparison of the polymers produced at identical temperatures reveals the effect the hydrogen bonding moiety. At -40 °C, the UP containing polymer exhibited higher tensile stress at break (13 MPa, Entry 8, Table 5.4) when compared with the non-functionalized polymer (8.1 MPa, Entry 9, Table 5.4) produced under identical reaction conditions. Further comparison of the polymers revealed that the functionalized polymer exhibits a dramatic decreased tensile strain at break (26%) relative to the non-UP containing polymer (1200%). Similarly at -60 °C, the UP containing polymer displayed an increased stress at break (13 MPa, Entry 10, Table 5.4) as well as decreased strain at

break (7.9%) compared with the non-UP containing polypropylene (5.5 MPa, 11%, Entry 11, Table 5.3). Differences in the observed mechanical properties confirm the incorporation of the hydrogen bonding moiety. Increased stress and decreased strain were observed in the functionalized polypropylene samples, which is consistent with cross-linking between polymer chains.

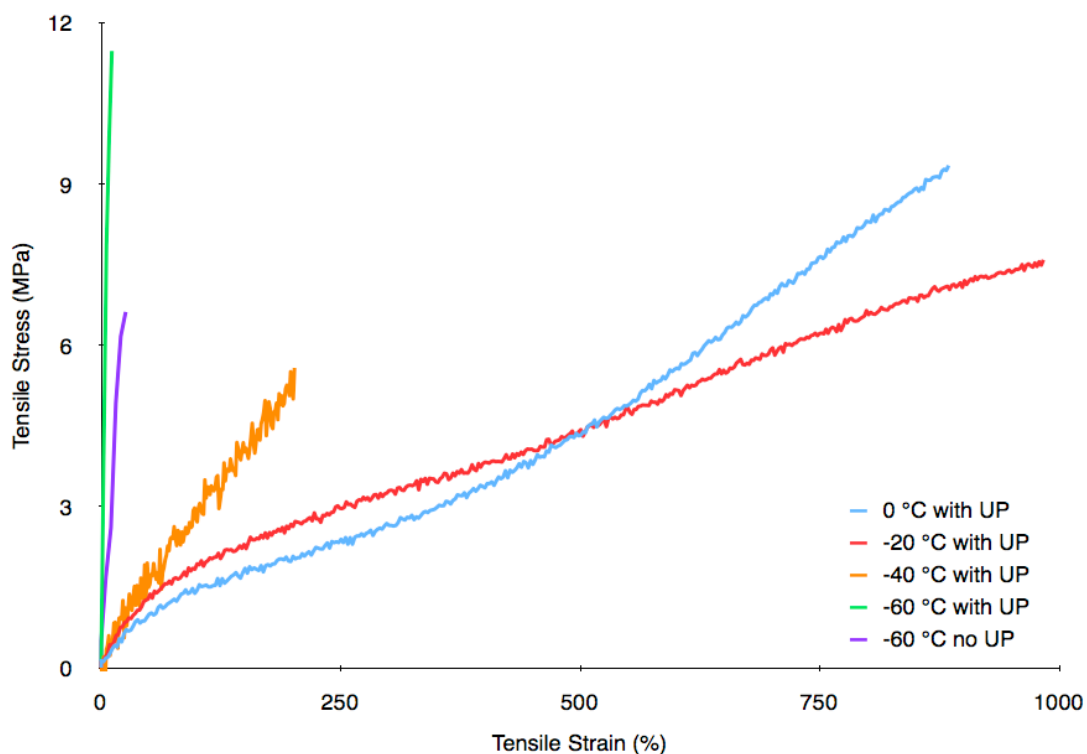


**Figure 5.8.** Tensile stress at break vs tensile strain at break of polypropylene produced with 5.2/Et<sub>2</sub>AlCl.

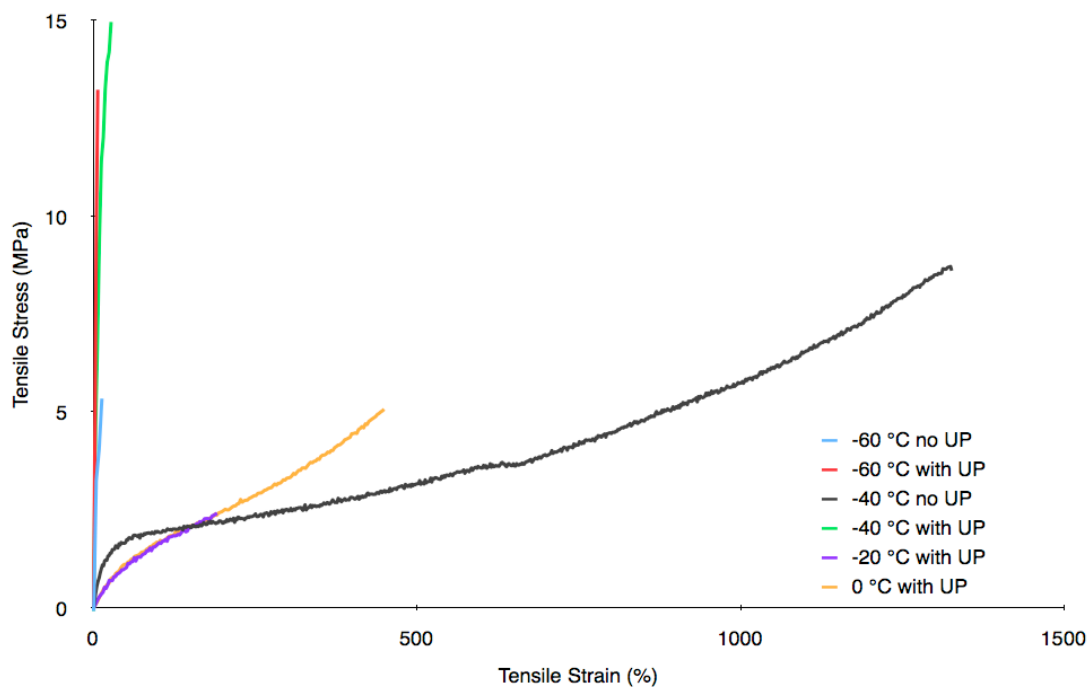


**Figure 5.9.** Tensile stress at break vs tensile strain at break of polypropylene produced with 5.3/Et<sub>2</sub>AlCl.

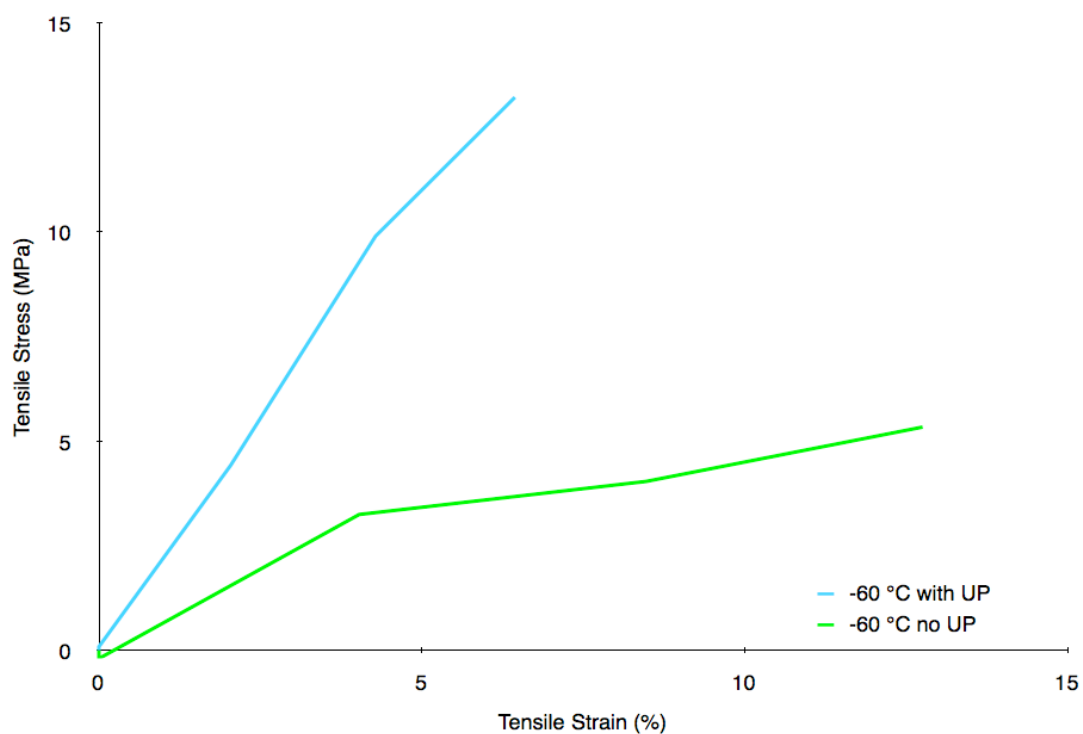


**Figure 5.10.** Tensile stress at break vs tensile strain at break of polypropylene produced with 5.3/Et<sub>2</sub>AlCl at -60 °C.

**Table 5.4.** Mechanical testing of polypropylene produced using **5.2** and **5.3**.

Entry	Complex	$T_{\text{rxn}}$ (°C)	$M_n$ (kg/mol) <sup>c</sup>	UP (%) <sup>d</sup>	Stress at Break (MPa) <sup>e</sup>	Strain at Break (%) <sup>e</sup>
1 <sup>a</sup>	<b>2</b>	0	33	0.69	9.7 ± 5	830 ± 390
2 <sup>a</sup>	<b>2</b>	-20	16	1.16	7.3 ± 0.6	1000 ± 180
3 <sup>a</sup>	<b>2</b>	-40	14	1.19	5.7 ± 0.5	200 ± 33
4 <sup>a</sup>	<b>2</b>	-60	8.9	1.28	11 ± 3	12 ± 5
5 <sup>b</sup>	<b>2</b>	-60	17	--	6.4 ± 2	25 ± 14
6 <sup>a</sup>	<b>3</b>	0	63	0.69	5.4 ± 2	400 ± 170
7 <sup>a</sup>	<b>3</b>	-20	267	0.18	2.8 ± 2	180 ± 84
8 <sup>a</sup>	<b>3</b>	-40	77	0.31	13 ± 2	26 ± 9
9 <sup>b</sup>	<b>3</b>	-40	155	--	8.1 ± 2	1200 ± 160
10 <sup>a</sup>	<b>3</b>	-60	12	0.30	13 ± 4	7.9 ± 3
11 <sup>b</sup>	<b>3</b>	-60	16	--	5.5 ± 3	11 ± 6

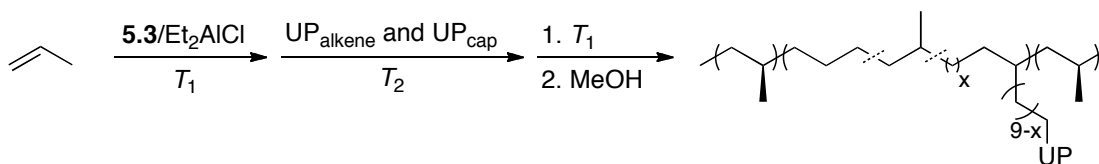
<sup>a</sup> General Conditions: Ni = 17 μmol, [Al]/[Ni] = 530, UP<sub>cap</sub> = 1.20 mmol, UP<sub>alkene</sub> = 0.4 mmol, 25 mL toluene, 5 or 15 g propylene. <sup>b</sup> Ni = 17 μmol, [Al]/[Ni] = 530, 25 mL toluene, 5 or 15 g propylene. <sup>c</sup> Molecular weight ( $M_n$ ) was determined by gel permeation chromatography at 140 °C in 1,2,4-trichlorobenzene relative to polyethylene standards. <sup>d</sup> Determined using <sup>1</sup>H NMR spectroscopy in 1,1,2,2-tetrachloroethane-*d*<sub>2</sub> at 135 °C. <sup>e</sup> Average of 5 trials using Instron mechanical testing machine.

### 5.2.5 Synthesis and Mechanical Properties of Triblock Copolymers.

Due to higher yields and molecular weights obtained for the copolymerization of UP<sub>alkene</sub> and propylene, **5.3**/Et<sub>2</sub>AlCl was utilized in the production of functionalized block copolymers. Triblock copolymers bearing regioregular, isotactic polypropylene endblocks and a regioirregular, amorphous polypropylene midblock have already been shown to exhibit good mechanical properties and behave as thermoplastic elastomers.<sup>36,39,68</sup> To obtain thermoplastic elastomers with enhanced mechanical properties, we targeted the formation of triblock copolymers bearing hydrogen bonding moieties. As discussed above, incorporation of even small amounts of ureidopyrimidinone into isotactic polypropylene results in a decrease in melting temperature. Therefore, addition of UP<sub>alkene</sub> into the amorphous midblock was investigated in an effort to maintain high crystallinity of the endblocks (Scheme 5.5, Table 5.5). Using **5.3**/Et<sub>2</sub>AlCl, regioregular, isotactic polypropylene endblocks were synthesized at -60 °C and triblock copolymers bearing both UP and non-UP containing midblocks were produced under identical reaction conditions with midblock production initially occurring at 0 °C. Obtaining aliquots after production of the first block at -60 °C revealed  $M_n = 20$  and 8 kg/mol for the UP and non-UP containing polymers (Entries 1 and 2, Table 5.5), respectively. Molecular weight was observed to increase with the formation of the second block for the functionalized ( $M_n = 32$  kg/mol) and unfunctionalized ( $M_n = 56$  kg/mol) polypropylene. Marginal increases in molecular weight were observed for the final blocks of both the UP ( $M_n = 36$  kg/mol) and non-UP containing polymers ( $M_n = 58$  kg/mol) suggesting that little to no polymer growth is achieved after the second block resulting in polymeric materials which are better described as diblock copolymers.

Observation of the functionalized block copolymer <sup>1</sup>H NMR spectrum (Figure 5.11, <sup>13</sup>C{<sup>1</sup>H} NMR Figure 5.13) revealed 0.26% incorporation of the hydrogen

bonding group when midblock synthesis was performed at 0 °C. Analysis of the thermal properties (Figure 5.15) showed melting temperatures for both the functionalized ( $T_m = 99$  °C) and unfunctionalized ( $T_m = 108$  °C) block copolymers. Glass transition temperature was observed to increase slightly for the UP ( $T_g = -48$  °C) vs non-UP containing ( $T_g = -55$  °C) block copolymers. Testing of the functionalized block copolymer mechanical properties (Figure 5.17) revealed a significant increase in tensile stress at break (17 MPa) and an increase in tensile strain at break (1100%) compared with the non-functionalized polypropylene (1 MPa, 90%). Despite the fact that the non-UP containing block copolymer did not display the expected mechanical properties, the UP containing polymer showed improved mechanical properties that can be attributed to the presence of the hydrogen bonding moieties.



**Scheme 5.5.** Synthesis of triblock copolymers using **5.3**/ $\text{Et}_2\text{AlCl}$ .

To obtain a true triblock copolymer with increased molecular weight, temperature of the midblock synthesis was decreased to -20 °C. Molecular weight was observed to increase with block formation for the functionalized ( $M_n = 7$  to 50 to 76 kg/mol, Entry 3, Table 5.5) as well as the unfunctionalized ( $M_n = 10$  to 162 to 190 kg/mol, Entry 4, Table 5.5) polymer confirming successful formation of the triblock copolymer. The  $^1\text{H}$  NMR spectrum (Figure 5.12,  $^{13}\text{C}\{^1\text{H}\}$  NMR Figure 5.14) of the UP containing triblock copolymer showed 0.13% incorporation of the ureidopyrimidinone. Melting temperatures (Figure 5.16) were observed for both the

functionalized ( $T_m = 108\text{ }^\circ\text{C}$ ) and unfunctionalized ( $T_m = 127\text{ }^\circ\text{C}$ ) polymers. Increased melting temperature for the unfunctionalized block copolymer compared with the unfunctionalized homopolymer produced at  $-60\text{ }^\circ\text{C}$  is attributed to decreased amounts of  $\text{Et}_2\text{AlCl}$  which appears to result in higher isotacticity endblocks. Mechanical properties (Figure 5.17) of both polymers were investigated with the functionalized block copolymer exhibiting improved stress at break (28 MPa) compared with the unfunctionalized polymer (18 MPa). The UP containing block copolymer exhibited a similar strain at break (2300%) to the non-UP containing triblock copolymer (2500%). Even though very small amounts of the hydrogen bonding ureidopyrimidinone were incorporated into the polypropylene triblock copolymer, differences in mechanical properties were observed.

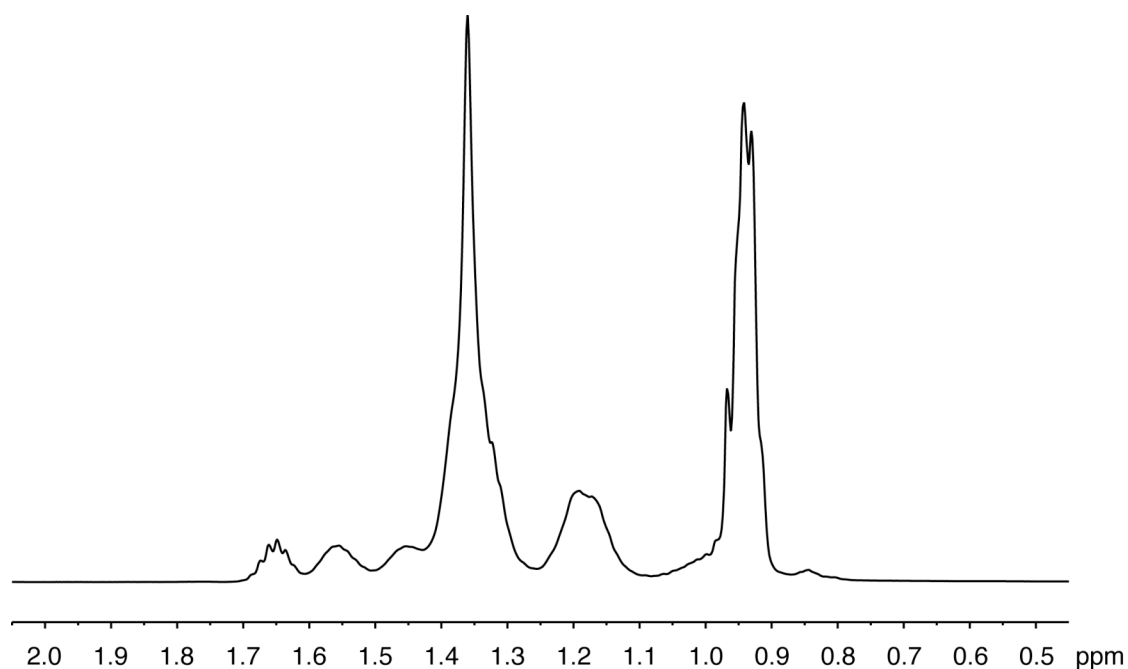


**Figure 5.11.**  $^1\text{H}$  NMR spectrum of triblock copolymer produced at  $-60$  to  $0$  to  $-60\text{ }^\circ$  with **5.3**/ $\text{Et}_2\text{AlCl}$  (600 MHz, 1,1,2,2-tetrachloroethane- $d_2$ ,  $135\text{ }^\circ\text{C}$ ).

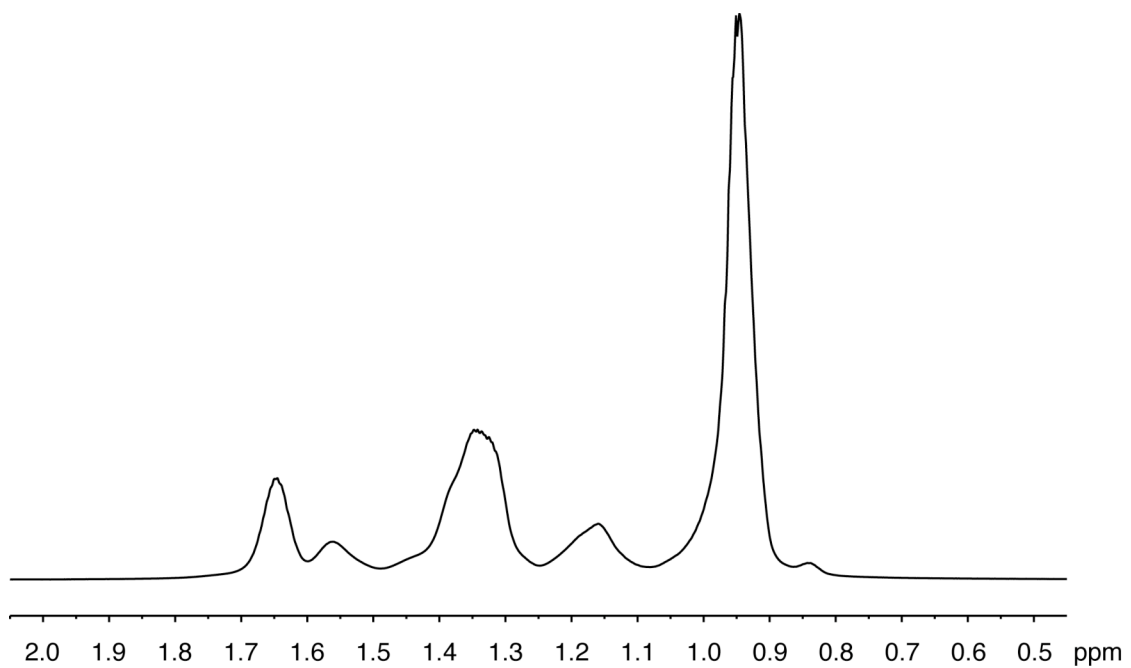


**Figure 5.12.**  $^1\text{H}$  NMR spectrum of triblock copolymer produced at  $-60$  to  $-20$  to  $-60$  ° with **5.3**/ $\text{Et}_2\text{AlCl}$  (600 MHz, 1,1,2,2-tetrachloroethane- $d_2$ ,  $135$  °C).

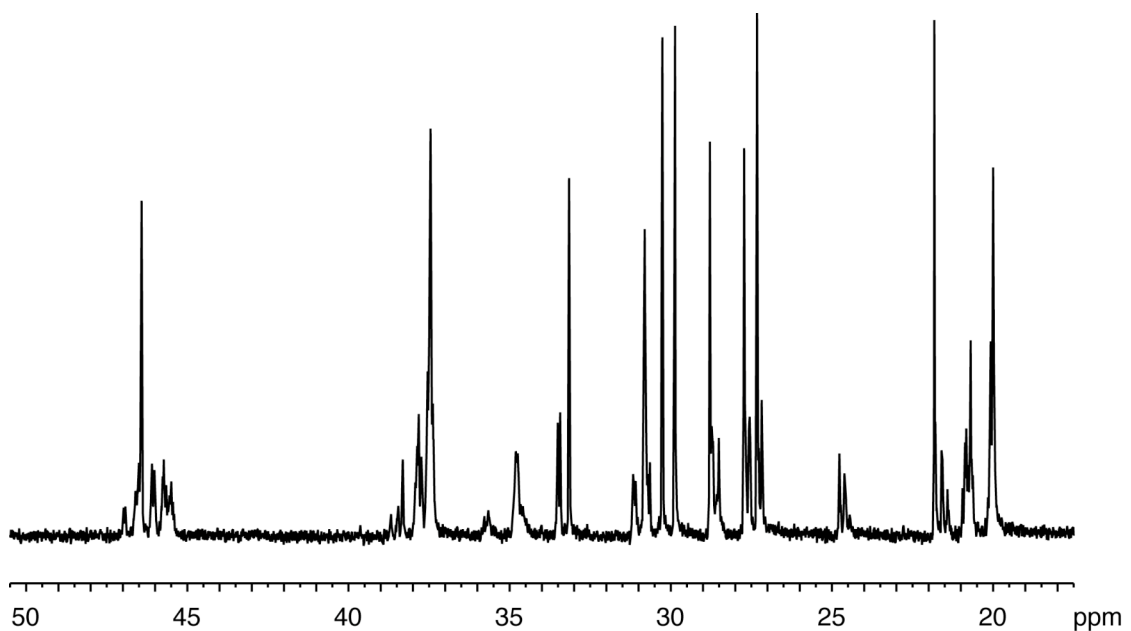


**Figure 5.13.**  $^{13}\text{C}\{^1\text{H}\}$  NMR spectrum of triblock copolymer produced at  $-60$  to  $0$  to  $-60$  °C with **5.3**/ $\text{Et}_2\text{AlCl}$  (600 MHz, 1,1,2,2-tetrachloroethane- $d_2$ ,  $135$  °C).

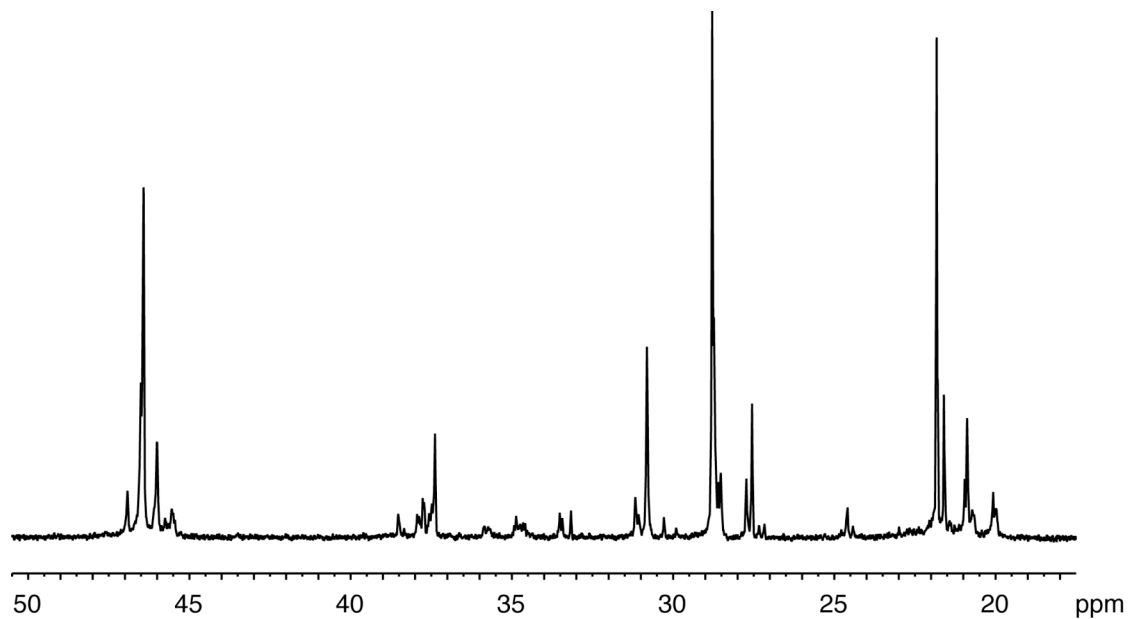


**Figure 5.14.**  $^{13}\text{C}\{^1\text{H}\}$  NMR spectrum of triblock copolymer produced at -60 to -20 to -60 °C with 5.3/Et<sub>2</sub>AlCl (600 MHz, 1,1,2,2-tetrachloroethane-*d*<sub>2</sub>, 135 °C).

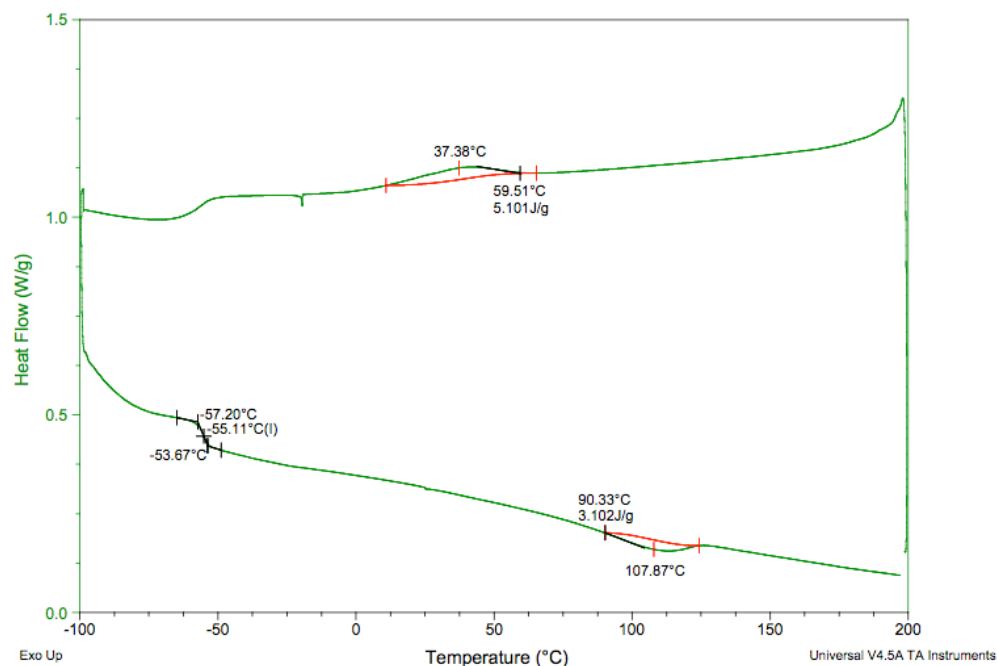


**Figure 5.15.** Differential scanning calorimetry (10 °C/min, second heat) thermogram of triblock copolymer produced at -60 to 0 to -60 °C (Entry 2, Table 5.5).

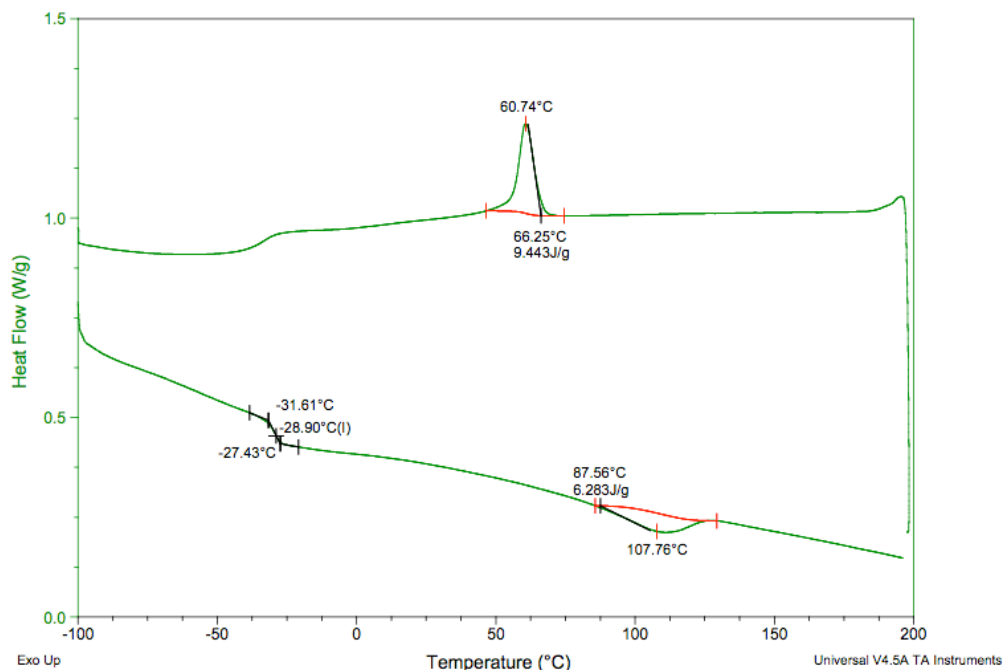


**Figure 5.16.** Differential scanning calorimetry (10 °C/min, second heat) thermograph of triblock copolymer produced at -60 to -20 to -60 °C (Entry 3, Table 5.5).

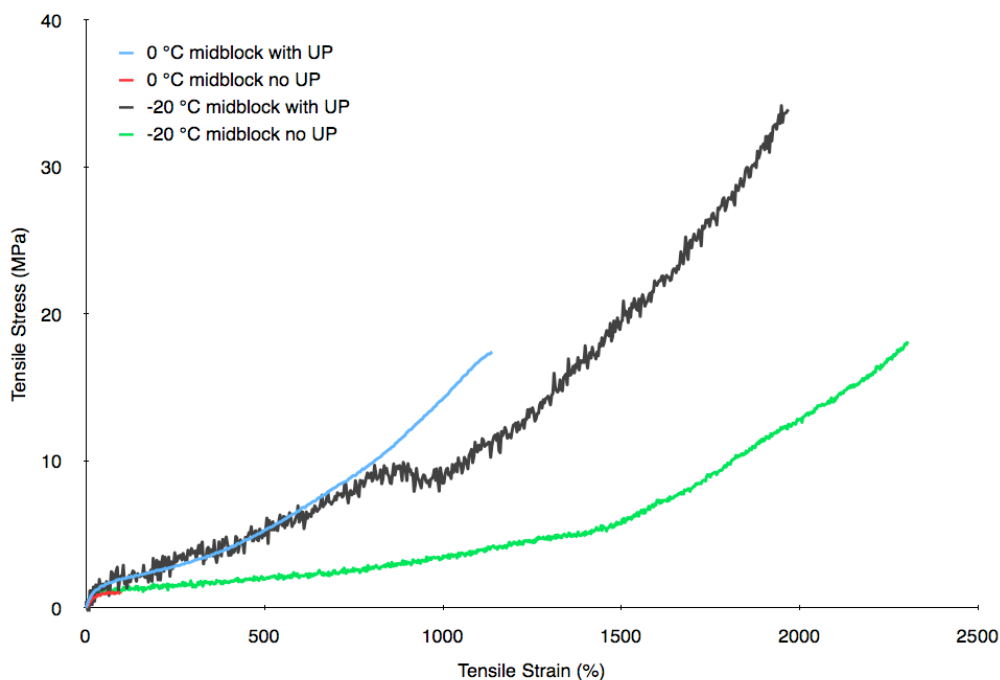


**Figure 5.17.** Tensile stress at break vs tensile strain at break of triblock copolymers produced with **5.3**/ $\text{Et}_2\text{AlCl}$ .

**Table 5.5.** Block copolymer synthesis using **5.3**/Et<sub>2</sub>AlCl.

Entry	$T_1$ (°C)	$T_2$ (°C)	Blocks (kg/mol) <sup>c</sup>	$M_n$ (kg/mol) <sup>c</sup>	$M_w/M_n$ <sup>c</sup>	UP (%) <sup>d</sup>	$T_g$ (°C) <sup>e</sup>	$T_m$ (°C) <sup>e</sup>	Stress at Break (MPa) <sup>f</sup>	Strain at Break (%) <sup>f</sup>
1 <sup>a</sup>	-60	0	20 - 12 - 4	36	1.51	0.26	-48	99	17 ± 5	1100 ± 100
2 <sup>b</sup>	-60	0	8 - 48 - 2	58	1.42	--	-55	108	1 ± 0.1	90 ± 20
3 <sup>a</sup>	-60	-20	7 - 43 - 26	76	2.00	0.13	-29	108	28 ± 7	2300 ± 500
4 <sup>b</sup>	-60	-20	10 - 152 - 28	190	1.18	--	-29	127	18 ± 4	2500 ± 300

<sup>a</sup> General Conditions: Ni = 20 μmol, [Al]/[Ni] = 270, UP<sub>cap</sub> = 1.2 mmol, UP<sub>alkene</sub> = 0.4 mmol, 30 mL toluene, 15 g propylene. <sup>b</sup> Ni = 20 μmol, [Al]/[Ni] = 270, 30 mL toluene, 15 g propylene. <sup>c</sup> Molecular weight ( $M_n$ ) and molecular weight distribution ( $M_w/M_n$ ) were determined by gel permeation chromatography at 140 °C in 1,2,4-trichlorobenzene relative to polyethylene standards. <sup>d</sup> Determined using <sup>1</sup>H NMR spectroscopy in 1,1,2,2-tetrachloroethane-*d*<sub>2</sub> at 135 °C. <sup>e</sup> Melting temperature ( $T_m$ ) and glass transition temperature ( $T_g$ ) were determined by differential scanning calorimetry (second heating run). <sup>f</sup> Average of 5 trials using Instron mechanical testing machine.

### 5.3 Conclusions

Utilizing an ureidopyrimidinone functionalized alkene, propylene copolymers were produced over a range of reaction temperatures with two  $\alpha$ -diimine Ni(II) catalysts. Polypropylene copolymers ranging from regioirregular, amorphous to regioregular, isotactic were obtained. Small amounts of the hydrogen bonding monomer incorporated into the polypropylene chain resulted in changes to the observed polymer properties. Analysis of the random copolymers mechanical behavior revealed increased tensile stress at break and decreased tensile strain at break upon functionalization with the hydrogen bonding moiety. Triblock copolymers bearing ureidopyrimidinone groups into the amorphous, midblock were produced and displayed increased tensile stress at break compared with the unfunctionalized block copolymers. UP containing block copolymers bearing amorphous midblocks produced at 0 and -20 °C showed mechanical properties that improved upon incorporation of the hydrogen bonding group.

### 5.4 Experimental Section

**General.** All manipulations of air- and/or water-sensitive compounds were carried out under dry nitrogen using Braun UniLab drybox or standard Schlenk techniques. Toluene was purified over columns of alumina and copper (Q5). Methylene chloride was purified over an alumina column and degassed by three freeze-pump-thaw cycles before use. Propylene (Airgas, research purity) was purified over columns (40 cm inner diameter x 120 cm long) of BASF catalyst R3-12, BASF catalyst R3-11, and 4Å molecular sieves. Et<sub>2</sub>AlCl (1.8 M, toluene) was purchased from Aldrich and used as received. Complexes **5.2** and **5.3** were prepared according to previously published procedures.<sup>36,39</sup> UP<sub>cap</sub> and UP<sub>alkene</sub> were also synthesized using previously reported methods.<sup>66</sup>

**Polymer Characterization.**  $^1\text{H}$  and  $^{13}\text{C}\{^1\text{H}\}$  NMR spectra of polymers were recorded using a Varian UnityInova (600 MHz) spectrometer equipped with a  $^1\text{H}/\text{BB}$  switchable with Z-pulse field gradient probe operating and referenced versus residual non-deuterated solvent shifts. The polymer samples were dissolved in 1,1,2,2-tetrachloroethane- $d_2$  in a 5 mm O.D. tube, and spectra were collected at 135 °C. From the  $^1\text{H}$  NMR spectra, %3,1 insertion was determined using relative integration of  $[\text{CH}_3]:[\text{CH}_2]$  and the equation:  $\%3,1 = (1-R)/(1 + 2R) \times 100$ , where  $R = [\text{CH}_3]/[\text{CH}_2]$ . The %UP incorporation was calculated using relative integration of  $[\text{UP}]:[\text{alkyl}]$  in the  $^1\text{H}$  NMR spectra. Molecular weights ( $M_n$  and  $M_w$ ) and polydispersities ( $M_w/M_n$ ) were determined by high temperature gel permeation chromatography (GPC). Analyses were performed with a Waters Alliance GPCV 2000 GPC equipped with a Waters DRI detector and viscometer. The column set (four Waters HT 6E and one Waters HT 2) was eluted with 1,2,4-trichlorobenzene containing 0.01 wt % di-*tert*-butylhydroxytoluene (BHT) at 1.0 mL/min at 140 °C. Data were calibrated using monomodal polyethylene standards (from Polymer Standards Service). Differential scanning calorimetric analyses were performed in aluminum pans under nitrogen using a TA Instruments Q1000 calorimeter equipped with an automated sampler. Data were collected from the second heating run at a heating rate of 10 °C/min from -80 to 150 °C and were processed with the TA Q series software package.

**Propylene Polymerization, General Procedure (Tables 5.1, Entries 1 - 9, 12 - 15).**

In a glove box, a 6 oz (180 mL) round-bottom Laboratory Crest reaction vessel (Andrews Glass) was charged with toluene (25 mL) and a solution of MMAO-3A (2.5 mL, 1.8 M in isoparE). An appropriate mass of propylene (15 g at -55 to -50 °C, 5 g at -48 to -30 °C) was condensed into the vessel at -78 °C. Following equilibration at the desired temperature for 10 minutes, the Ni(II) complex (17  $\mu\text{mol}$ ) was injected as a solution in 2 mL dry, degassed  $\text{CH}_2\text{Cl}_2$ . After an appropriate amount of time, the

polymerization was quenched with MeOH, the reaction mixture was precipitated in copious acidic MeOH (5% HCl (aq)) and stirred overnight. The polymer was dissolved in hot toluene, filtered over Celite®, silica and alumina. The polymer was reprecipitated with MeOH, filtered, rinsed and dried in vacuo to constant weight.

**Propylene Polymerization, General Procedure (Tables 5.1, Entries 10 - 11).** In a glove box, a 6 oz (180 mL) round-bottom Laboratory Crest reaction vessel (Andrews Glass) was charged with toluene (25 mL) and a solution of MMAO-3A (2.5 mL, 1.8 M in isoparE). An appropriate mass of propylene (15 g at -55 to -50 °C, 5 g at -48 to -30 °C) was condensed into the vessel at -78 °C. Following equilibration at the desired temperature for 10 minutes, complex **5.3** (17 μmol) was injected as a solution in 2 mL dry, degassed CH<sub>2</sub>Cl<sub>2</sub>. After 6 hours, an aliquot was taken from the reaction mixture using an overpressure of 30 psig propylene. The polymerization was quenched with MeOH after 48 hours, the reaction mixture was precipitated in copious acidic MeOH (5% HCl (aq)) and stirred overnight. The resultant polymers were dissolved in hot toluene, filtered over Celite®, silica and alumina. The polymer was reprecipitated with MeOH, filtered, rinsed and dried in vacuo to constant weight.

**Propylene Polymerization, General Procedure (Tables 5.2 – 5.3).** In a glove box, a 6 oz (180 mL) round-bottom Laboratory Crest reaction vessel (Andrews Glass) was charged with toluene (25 mL) and a solution of Et<sub>2</sub>AlCl (5.0 mL, 1.8 M in toluene) along with UP<sub>alkene</sub> (0.15 g, 0.40 mmol) and UP<sub>cap</sub> (0.30 g, 1.20 mmol) if necessary. An appropriate mass of propylene (15 g at -60 °C, 5 g at -40, -20 and 0 °C) was condensed into the vessel at -78 °C. Following equilibration at the desired temperature for 10 minutes, the Ni(II) complex (17 μmol) was injected as a solution in 2 mL dry, degassed CH<sub>2</sub>Cl<sub>2</sub>. After an appropriate amount of time, the polymerization was quenched with MeOH, the reaction mixture was precipitated in copious acidic MeOH (5% HCl (aq)) and stirred overnight. The polymer was isolated and redissolved in

toluene (300 mL). To remove any residual UP<sub>cap</sub>, acidic MeOH (50 mL, 5% HCl (aq)) was added and the solution was heated to 60 °C overnight. The polymer was precipitated with MeOH, filtered, rinsed and dried in vacuo to constant weight.

**Block Copolymer Synthesis, General Procedure (Table 5.5).** In a glove box, a 6 oz (180 mL) round-bottom Laboratory Crest reaction vessel (Andrews Glass) was charged with toluene (30 mL) and a solution of Et<sub>2</sub>AlCl (3.0 mL, 1.8 M in toluene). Propylene (15 g) was condensed into the vessel at -78 °C. Following equilibration at -60 °C for 10 minutes, the **5.3** (0.018 g, 20 μmol) was injected as a solution in 2 mL dry, degassed CH<sub>2</sub>Cl<sub>2</sub>. After 24 hours, an aliquot was taken from the reaction mixture using an overpressure of 30 psig propylene. If necessary, a solution of UP<sub>alkene</sub> (0.15 g, 0.40 mmol) and UP<sub>cap</sub> (0.30 g, 1.20 mmol) in 5 mL dry, degassed CH<sub>2</sub>Cl<sub>2</sub> was syringed into the vessel. The reactor was then transferred to a 0 or -20 °C bath and allowed to react for 3 or 6 hours, respectively. A second aliquot was taken via cannula with an overpressure of 30 psig propylene. The vessel was then transferred back to the -60 °C bath and allowed to react for an additional 48 hours. The polymerization was quenched with MeOH, the reaction mixture was precipitated in copious acidic MeOH (5% HCl (aq)) and stirred overnight. The polymer was isolated and redissolved in toluene (500 mL). To remove any residual UP<sub>cap</sub>, acidic MeOH (75 mL, 5% HCl (aq)) was added and the solution was heated to 60 °C overnight. The polymer was precipitated with MeOH, filtered, rinsed and dried in vacuo to constant weight.

**Mechanical Testing.** Polypropylene and poly(propylene-*co*-UP) samples were pressed into uniform films using a Carver press heated to 80 °C. Triblock copolymers were dissolved in toluene, transferred to an aluminum pan and films were obtained following evaporation of the solvent. The resultant films were cut into strips with a thickness of 0.05 – 0.25 mm and a width of 2.0 – 8.0 mm. Samples were stretched to fracture at room temperature using an Instron testing machine.

## REFERENCES

- (1) Lopez, R. G.; D'Agosto, F.; Boisson, C. *Prog. Polym. Sci.* **2007**, *32*, 419-454.
- (2) Chung, T. C. *Prog. Polym. Sci.* **2002**, *27*, 39-85.
- (3) Avella, M.; Laurienzon, P.; Malinconico, M.; Martuscelli, E.; Volpe, M. G., Functionalized Polyolefins: Synthesis and Application in Blends and Composites. In *Handbook of Polyolefins*, 2nd ed.; Vasile, C., Ed. Marcel Dekker, Inc.: New York, 2000; pp 723-771.
- (4) Zhou, X.; Dai, G.; Guo, W.; Lin, Q. *J. Appl. Poly. Sci.* **2000**, *76*, 1359-1365.
- (5) Vasile, C., General Survey of the Properties of Polyolefins. In *Handbook of Polyolefins*, 2nd ed.; Vasile, C., Ed. Marcel Dekker, Inc.: New York, 2000; pp 401-412.
- (6) Nakamura, A.; Ito, S.; Nozaki, K. *Chem. Rev.* **2009**, *109*, 5215-5244.
- (7) Boffa, L. S.; Novak, B. M. *Chem. Rev.* **2000**, *100*, 1479-1493.
- (8) Chen, E. Y.-X. *Chem. Rev.* **2009**, *109*, 5157-5214.
- (9) Guan, Z.; Popeney, C. S., Recent Progress in Late Transition Metal -Diimine Catalysts for Olefin Polymerization. In *Metal Catalysts in Olefin Polymerization*, Springer: Berlin/Heidelberg, 2008; Vol. 26, pp 179-220.
- (10) Goodall, B. L., Late Transition Metal Catalysts for Copolymerization of Olefins and Polar Monomers. In *Metal Catalysts in Olefin Polymerization*, Springer: Berlin/Heidelberg, 2009; Vol. 26, pp 159-178.
- (11) Sen, A.; Borkar, S. *J. Organomet. Chem.* **2007**, *692*, 3291-3299.
- (12) Yang, X.-H.; Liu, C.-R.; Wang, C.; Sun, X.-L.; Guo, Y.-H.; Wang, X.-K.; Wang, Z.; Xie, Z.; Tang, Y. *Angew. Chem. Int. Ed.* **2009**, *48*, 8099-8102.
- (13) Stojcevic, G.; Baird, M. C. *Dalton Trans.* **2009**, 8864-8877.
- (14) Sahre, K.; Schulze, U.; Eichhorn, K.-J.; Voit, B. *Macromol. Mater. Eng.* **2009**, *294*, 250-255.

- (15) Yasuda, H.; Desurmont, G. *Polym. Int.* **2004**, *53*, 1017-1024.
- (16) Popeney, C. S.; Camacho, D. H.; Guan, Z. *J. Am. Chem. Soc.* **2007**, *129*, 10062-10063.
- (17) Chen, G.; Ma, X. S.; Guan, Z. *J. Am. Chem. Soc.* **2003**, *125*, 6697-6704.
- (18) Deubel, D. V.; Ziegler, T. *Organometallics* **2002**, *21*, 4432-4441.
- (19) Ittel, S. D.; Johnson, L. K.; Brookhart, M. *Chem. Rev.* **2000**, *100*, 1169-1203.
- (20) Johnson, L. K.; Mecking, S.; Brookhart, M. *J. Am. Chem. Soc.* **1996**, *118*, 267-268.
- (21) Mecking, S.; Johnson, L. K.; Wang, L.; Brookhart, M. *J. Am. Chem. Soc.* **1998**, *120*, 888-899.
- (22) Johnson, L.; Bennett, A.; Dobbs, K.; Hauptman, E.; Ionkin, A.; Ittel, S.; McCord, E.; McLain, S.; Radzewich, C.; Yin, Z.; Wang, L.; Wang, Y.; Brookhart, M. *Polym. Mater. Sci. Eng* **2002**, *86*, 319.
- (23) McLain, S. J.; Sweetman, K. J.; Johnson, L. K.; McCord, E. *Polym. Mater. Sci. Eng* **2002**, *86*, 320.
- (24) Tian, G.; Boone, H. W.; Novak, B. M. *Macromolecules* **2001**, *34*, 7656-7663.
- (25) Heinemann, J.; Mulhaupt, R.; Brinkmann, P.; Luinstra, G. *Macromol. Chem. Phys.* **1999**, *200*, 384-389.
- (26) Meneghetti, S. P.; Kress, J.; Lutz, P. J. *Macromol. Chem. Phys.* **2000**, *201*, 1823-1832.
- (27) Michalak, A.; Ziegler, T. *Organometallics* **2003**, *22*, 2660-2665.
- (28) Marques, M. M.; Fernandes, S.; Correia, S. G.; Caroco, S.; Gomes, P. T.; Dias, A. R.; Mano, J.; Rausch, M. D.; Chien, J. C. W. *Polym. Int.* **2001**, *50*, 579-587.
- (29) Chien, J. C. W.; Fernandes, S.; Correia, S. G.; Rausch, M. D.; Dickson, L. C.; Marques, M. M. *Polym. Int.* **2002**, *51*, 729-737.
- (30) Borkar, S.; Yennawar, H.; Sen, A. *Organometallics* **2007**, *26*, 4711-4714.

- (31) Luo, S.; Jordan, R. F. *J. Am. Chem. Soc.* **2006**, *128*, 12072-12073.
- (32) Johnson, L.; Killian, C. M.; Brookhart, M. *J. Am. Chem. Soc.* **1995**, *117*, 6414.
- (33) Killian, C. M.; Tempel, D. J.; Johnson, L. K.; Brookhart, M. *J. Am. Chem. Soc.* **1996**, *118*, 11664-11665.
- (34) Pellecchia, C.; Zambelli, A. *Macromol. Rapid Commun.* **1996**, *17*, 333-338.
- (35) Cherian, A. E.; Lobkovsky, E. B.; Coates, G. W. *Chem. Commun.* **2003**, 2566-2567.
- (36) Cherian, A. E.; Rose, J. M.; Lobkovsky, E. B.; Coates, G. W. *J. Am. Chem. Soc.* **2005**, *127*, 13770-13771.
- (37) Cherian, A. E.; Domski, G. J.; Rose, J. M.; Lobkovsky, E. B.; Coates, G. W. *Org. Lett.* **2005**, *7*, 5135-5137.
- (38) Rose, J. M.; Cherian, A. E.; Coates, G. W. *J. Am. Chem. Soc.* **2006**, *128*, 4186-4187.
- (39) Rose, J. M.; Deplace, F.; Lynd, N. A.; Wang, Z.; Hotta, A.; Lobkovsky, E. B.; Kramer, E. J.; Coates, G. W. *Macromolecules* **2008**, *41*, 9548-9555.
- (40) Wilson, A. J. *Soft Matter* **2007**, *3*, 409-425.
- (41) Brunsveld, L.; Folmer, B. J. B.; Meijer, E. W.; Sijbesma, R. P. *Chem. Rev.* **2001**, *101*, 4071-4097.
- (42) Hofmeier, H.; Schubert, U. S. *Chem. Commun.* **2005**, 2423-2432.
- (43) Armstrong, G.; Buggy, M. *J. Mat. Sci.* **2005**, *40*, 547-559.
- (44) Gerhardt, W.; Crne, M.; Weck, M. *Chem. Eur. J.* **2004**, *10*, 6212-6221.
- (45) Bosman, A. W.; Brunsveld, L.; Folmer, B. J. B.; Sijbesma, R. P.; Meijer, E. W. *Macromol. Symp.* **2003**, *201*, 143-154.
- (46) Sijbesma, R. P.; Beijer, F. H.; Brunsveld, L.; Folmer, B. J. B.; Hirschber, J. H. K. K.; Lange, R. F. M.; Lowe, J. K. L.; Meijer, E. W. *Science* **1997**, *278*, 1601-1604.

- (47) Yamauchi, K.; Lizotte, J. R.; Long, T. E. *Macromolecules* **2003**, *36*, 1083-1088.
- (48) Park, T.; Zimmerman, S. C. *J. Am. Chem. Soc.* **2006**, *128*, 11582-11590.
- (49) Park, T.; Zimmerman, S. C. *J. Am. Chem. Soc.* **2006**, *128*, 14236-14237.
- (50) Park, T.; Zimmerman, S. C.; Nakashima, S. *J. Am. Chem. Soc.* **2005**, *127*, 6520-6521.
- (51) Feldman, K. E.; Kade, M. J.; Meijer, E. W.; Hawker, C. J.; Kramer, E. J. *Macromolecules* **2009**, *42*, 9072-9081.
- (52) Feldman, K. E.; Kade, M. J.; de Greef, T. F. A.; Meijer, E. W.; Kramer, E. J.; Hawker, C. J. *Macromolecules* **2008**, *41*, 4694-4700.
- (53) Li, J.; Viveros, J. A.; Wrue, M. H.; Anthamatten, M. *Adv. Mater.* **2007**, *19*, 2851-2855.
- (54) Kamps, A. C.; Magbitang, T.; Nelson, A. *Chem. Commun.* **2007**, 954-956.
- (55) El-ghayoury, A.; Hofmeier, H.; de Ruiter, B.; Schubert, U. S. *Macromolecules* **2003**, *36*, 3955-3959.
- (56) De Lucca Freitas, L. L.; Stadler, R. *Macromolecules* **1987**, *20*, 2478-2485.
- (57) Muller, M.; Dardin, A.; Seidel, U.; Balsamo, V.; Ivan, B.; Spiess, H. W.; Stadler, R. *Macromolecules* **1996**, *29*, 2577-2583.
- (58) Hilger, C.; Stadler, R. *Macromolecules* **1992**, *25*, 6670-6680.
- (59) Hilger, C.; Stadler, R.; de Lucca Freitas, L. L. *Polymer* **1990**, *31*, 818-823.
- (60) Hilger, C.; Stadler, R. *Polymer* **1991**, *32*, 3244-3249.
- (61) Hilger, C.; Drager, M.; Stadler, R. *Macromolecules* **1992**, *25*, 2498-2501.
- (62) Hilger, C.; Stadler, R. *Macromolecules* **1990**, *23*, 2095-2097.
- (63) Kushner, A. M.; Vossler, J. D.; Williams, G. A.; Guan, Z. *J. Am. Chem. Soc.* **2009**, *131*, 8766-8768.

- (64) Nair, K. P.; Breedveld, V.; Weck, M. *Macromolecules* **2008**, *41*, 3429-3438.
- (65) Scherman, O. A.; Ligthart, G. B. W. L.; Ohkawa, H.; Sijbesma, R. P.; Meijer, E. W. *Proc. Nat. Acad. Sci.* **2006**, *103*, 11850-11855.
- (66) Rieth, L. R.; Eaton, R. F.; Coates, G. W. *Angew. Chem. Int. Ed.* **2001**, *40*, 2153-2156.
- (67) Thibault, R. J.; Hotchkiss, P. J.; Gray, M.; Rotello, V. M. *J. Am. Chem. Soc.* **2003**, *125*, 11249-11252.
- (68) Hotta, A.; Cochran, E.; Ruokolainen, J.; Khanna, V.; Fredrickson, G. H.; Kramer, E. J.; Shin, Y.-W.; Shimizu, F.; Cherian, A. E.; Hustad, P. D.; Rose, J. M.; Coates, G. W. *Proc. Nat. Acad. Sci.* **2006**, *103*, 15327-15332.